



Investigation of ion channels involved in cholinergic activity in mouse bronchial smooth muscles

A thesis submitted to the
School of Health and Science,
Dundalk Institute of Technology

For the degree of **Doctor of Philosophy**

By

Ritu Dwivedi M.Res

August, 2022

Under the supervision of **Prof. Keith Thornbury**

and co-supervision of

Dr. Roddy Large and Dr. Bernard Drumm

Declaration

We, the undersigned declare that this thesis entitled “Investigation of ion channels involved in cholinergic activity in mouse bronchial smooth muscle” is entirely the author’s own work and has not been taken from the work of others, except as cited and acknowledged within the text.

The thesis has been prepared according to the regulations of Dundalk Institute of Technology and has not been submitted in whole or in part for an award in this or any other institution.

Author Name: Ritu Dwivedi

Author Signature: *Ritu Dwivedi*

Date: 1st September 2022

Supervisor Name: Prof. Keith Thornbury

Supervisor Signature: *K. Thornbury*

Date: 1st September 2022

Table of Contents

Acknowledgement	05
Abbreviations	06
Abstract	10
Publications	12
<u>Chapters</u>	
1. Literature Review	13
1.1 The respiratory system	14
1.2 Innervation of the lungs	18
1.3 Regulation of ASM contraction and relaxation	20
1.4 Receptors involved in smooth muscle contraction	23
1.5 Ion channels in airway smooth muscle	25
1.6 Calcium signalling in airway smooth muscle	41
1.7 Chronic respiratory diseases	43
1.8 Aims of the project	45
2. Materials and Method	46
2.1 Tissue extractions	47
2.2 Isometric tension recording	48
2.3 Isolation of mouse airway smooth muscle cells	49
2.4 Calcium imaging	51
2.5 Solutions and drugs	53

3. Effect of TMEM16A blockers on mouse bronchus smooth muscle contractions induced by CCh	59
3.1 Introduction	60
3.2 Results	62
3.2.1 <i>Effect of TMEM16A antagonists on CCh-induced contractions</i>	
3.2.2 <i>Effect of L-type Ca²⁺ channels blocker on CCh-induced contractions</i>	
3.2.3 <i>Effect of TMEM16A blockers on cholinergic-induced contractions in the presence of nifedipine</i>	
3.2.4 <i>Effect of TMEM16A inhibitors on KCl-induced contractions</i>	
3.2.5 <i>Effect of Ani9 on thromboxane agonist-induced contractions</i>	
3.2.6 <i>Effect of benzbromarone on cholinergic contractions after inhibiting BK channels</i>	
3.3 Discussion	91
4. Effect of TMEM16A blockers on intracellular Ca²⁺ signals in freshly isolated ASMCs	96
4.1 Introduction	97
4.2 Results	98
4.2.1 <i>Effect of TMEM16A antagonists on Ca²⁺ signals in ASMCs</i>	
4.2.2 <i>Effect of lower concentrations of benzbromarone and MONNA</i>	
4.2.3 <i>Effect of TMEM16A blockers on Ca²⁺ signals in the absence of extracellular Ca²⁺</i>	
4.2.4 <i>Effect of TMEM16A blockers on Ca²⁺ signals induced by caffeine</i>	
4.2.5 <i>Effect of caffeine on intracellular Ca²⁺ in the presence of the SERCA pump blocker, CPA</i>	
4.2.6 <i>Effect of caffeine on intracellular the Ca²⁺ level increase by benzbromarone</i>	
4.2.7 <i>Effect of a ryanodine receptor blocker on intracellular Ca²⁺ increased by benzbromarone</i>	
4.3 Discussion	117

5. Effect of blocking SOCE on cholinergic activity of mouse bronchi smooth muscles	121
5.1 Introduction	122
5.2 Results	125
5.2.1 <i>Effect of CRAC channels antagonist on CCh-induced contractions</i>	
5.2.2 <i>Effect of blocking of L-type Ca²⁺ channels and CRAC channels on cholinergic-induced contractions</i>	
5.2.3 <i>Effect of Ani9 on cholinergic contractions after blocking CRAC channels</i>	
5.2.4 <i>Effect of inhibiting Ca²⁺-induced Ca²⁺ release on cholinergic contractions</i>	
5.2.5 <i>Effect of benzbromarone after inhibition of cholinergic contractions with dantrolene</i>	
5.2.6 <i>Effect of 0.3 μM CCh on cytosolic Ca²⁺ levels in ASMCs</i>	
5.2.7 <i>Effect of CRAC channels blocker and L-type Ca²⁺ channels blocker on 0.3 μM CCh</i>	
5.2.8 <i>Effect of blocking of L-type Ca²⁺ channels and CRAC channels on CCh-induced Ca²⁺ signals</i>	
5.3 Discussion	152
6. General Discussion and Future Prospects	159
7. References	167
8. Appendix	199

Acknowledgements

Firstly, I would like to express my sincere gratitude to my supervisor Prof. Keith Thornbury for his consistent support and guidance during my PhD studies. His patience, continuous trust in me and in the project is key behind completion of this project. I would also like to extend my sincere thank you to Prof. Gerard Sergeant and Prof. Mark Hollywood for their keen insights, invaluable supervision and advice during this project.

I would like to thank Billie McIlveen for her support and encouragement throughout my time at SMRC. A special thank you to Dr. Eamonn Bradley, Dr. Roddy Large and Dr. Bernard Drumm for their help, support and encouraging me to think out of the box which really helped during the running of this project. I would also like to appreciate advice and guidance from Dr. Srikanth Dudem, Dr. Nicholas Mullins and Dr. Caoimhin Griffin. A deepest thank you to all the PhD students at SMRC past and present, specially the BREATH girls, Nicole and Vishakha. I will always appreciate all the emotional support, love and care I received especially during tough times. Thank you for making my time in the lab and outside enjoyable, and also for all the laughs and friendship. All the very best to all the PhD students and enjoy your time in the lab. Always remember dreams never come true overnight, it takes patience, determination and hard work.

Finally, my warmest and heartfelt thank you to my loving and caring family for their patience, help and support throughout my PhD journey.

Abbreviations

°C	Degree Celsius
[Ca ²⁺] _i	Intracellular calcium concentration
5-HT	5-hydroxytryptamine
ACh	Acetylcholine
ANO1	Anoctamin 1
ASM	Airway smooth muscle
ASMC	Airway smooth muscle cells
BK _{ca}	Large conductance calcium activated potassium channel
Ca ²⁺	Calcium ions
CaCC	Calcium activated chloride channel
cAMP	Cyclic adenosine monophosphate
Ca _v	Voltage dependent calcium channel
CCh	Carbachol
CLCA	Chloride channel accessory 1
CO ₂	Carbon dioxide
COPD	Chronic Obstructive Pulmonary Disease
COX	Cyclooxygenase enzyme
CRAC	Calcium release activated calcium channel
DAG	Diacylglycerol
DMSO	Dimethyl sulfoxide
DNA	Deoxyribonucleic acid
G	Gram

Gd ³⁺	Gadolinium
GFP	Green fluorescent protein
GTP	Guanosine triphosphate
IL	Interleukin
IP3R	Inositol-1,4,5-triphosphate
K ⁺	Potassium ion
KCl	Potassium chloride
M ₂ Receptor	Type 2 muscarinic receptor
M ₃ Receptor	Type 3 muscarinic receptor
mAChRs	Muscarinic acetylcholine receptors
MCh	Methacholine
Min	Minute
MLCK	Myosin Light Chain Kinase
mM	Millimolar
mN	Millinewton
mRNA	Messenger ribonucleic acid
ms	Millisecond
N	Animal numbers used
n	Number of samples
NANC	Non-adrenergic non-cholinergic
nM	Nanomolar
NO	Nitric oxide
NPY	Neuropeptide Y
O ₂	Oxygen
PCR	Polymerase chain reaction

PGD ₂	Prostaglandin D ₂
PGE ₂	Prostaglandin E ₂ , also known as dinoprost
PGF _{2α}	Prostaglandin F _{2α} , pharmaceutical term carboprost
PGI ₂	Prostacyclin
PHD	Pinhole disc
PIP ₂	Phosphatidylinositol 4,5-bisphosphate
PKC	Protein Kinase C
PLC	Phospholipase C
Pyr3	Pyrazole 3
RNA	Ribonucleic acid
RT-PCR	Reverse transcriptase PCR
RyR	Ryanodine receptor
S.E.M	Standard error of the mean
SDCLM	Spinning disc confocal laser microscope
Sec	Second
SERCA	Sarco/endoplasmic reticulum Ca ²⁺ -ATPase
SM	Smooth muscle
SMC	Smooth muscle cell
SOCC	Store operated calcium channel
SOCE	Store operated calcium entry
SR	Sarcoplasmic reticulum
STIC	Spontaneous transient inward current
STIM	Stromal interacting molecule
STOC	Spontaneous transient outward current
TGF-β	Transforming growth factor beta

TMEM16A	Transmembrane member 16A
TNF- α	Tumor necrosis factor alpha
TP receptor	Thromboxane-prostanoid receptor
TRP	Transient receptor potential
TRPA	Transient receptor potential ankyrin
TRPC	Transient receptor potential canonical
TRPM	Transient receptor potential melastatin
TRPML	Transient receptor potential mucolopin
TRPN	Transient receptor potential no mechanoreceptor potential C
TRPP	Transient receptor potential polycystin
TRPV	Transient receptor potential vanilloid
TRPY	Transient receptor potential yeast
TxA ₂	Thromboxane A ₂
UV	Ultra violet
VDCC	Voltage dependent Ca ²⁺ channel
VIP	Vasoactive intestinal peptide
WT	Wild-type
μ M	Micromolar

Abstract

Investigation of ion channels involved in cholinergic activity in mouse bronchial smooth muscles.

In airway smooth muscle cells (ASMCs), multiple ion channels are expressed, however their involvement in cholinergic contractions have been controversial. In the present study, using isometric tension and live cell- Ca^{2+} imaging, the role of ion channels for instance TMEM16A, and voltage-dependent and independent Ca^{2+} channels were investigated in murine bronchial smooth muscle. $\text{CaCC}_{\text{inh}}\text{-A01}$, benzbromarone and MONNA, three TMEM16A inhibitors inhibited sustained contractions rather than initial, suggesting involvement of TMEM16A on sustained part of cholinergic contractions. However, another TMEM16A inhibitor, Ani9 had little effect on cholinergic contractions. With the hypothesis that the other three inhibitors might be blocking L-type Ca^{2+} channels, their effects were tested after addition of nifedipine. Nifedipine (1 μM) itself reduced the effect of all of the concentrations of carbachol (CCh). However, TMEM16A inhibitors further reduced the responses when added in the presence of nifedipine. All three blockers increased intracellular Ca^{2+} concentration in calcium imaging experiments. With further investigation using 0 Ca^{2+} Hanks and caffeine, it was confirmed these blockers were causing Ca^{2+} release. Tetracaine (100 μM), ryanodine receptor blocker had an inhibitory effect on intracellular calcium increased by benzbromarone. Thus, confirming that TMEM16A blockers are causing Ca^{2+} release through ryanodine receptors.

Store operated calcium entry (SOCE) is a major pathway in Ca^{2+} signalling which is activated upon depletion of Ca^{2+} from the SR during excitation-contraction coupling. Apart from store refilling channels and L-type Ca^{2+} channels, a role in cholinergic activity for Ca^{2+} release channels on the SR has also been reported. Ca^{2+} release from SR in the smooth muscle occurs through IP_3Rs and RyRs (Kotlikoff & Wang, 1998). This project also investigated the involvement of calcium released activated calcium channel (CRAC; voltage independent Ca^{2+} channel) on cholinergic activity after inhibiting L-type Ca^{2+} channel (voltage

dependent Ca^{2+} channel). It was observed that blocking both the channels at the same time, completely inhibited CCh contractions of all concentrations. As similar effect was observed in Ca^{2+} signals induced by $0.3 \mu\text{M}$ CCh. It was also observed that after blocking CRAC channel using GSK-7975A, Ani9 has more of an inhibitory effect on cholinergic contractions. We have also found that in high KCl contractile activity in ASM, along with VDCC, Ca^{2+} release through RyR and CRAC channel are also actively involved.

The key findings of the project was that TMEM16A has minor role in cholinergic activator induced contractile activity in healthy murine bronchial smooth muscle. SOCE and Ca^{2+} release through RyR are majorly involved in maintaining contractile activity in ASM.

Publications

Data presented in the study has been communicated as posters and oral presentations in various scientific meetings:

Conference abstracts:

1. R Dwivedi, RJ Large, MA Hollywood, GP Sergeant, G Litherland & KD Thornbury. Effect of TRPC4/C5 channel antagonists in carbachol-induced contractions in murine airway. 2018, *Irish Journal of Medical Science*, Vol. 187, Suppl. 8, S252.
Irish Thoracic Society meeting, Belfast, Northern Ireland.
2. R Dwivedi, RJ Large, E Bradley, G Litherland, MA Hollywood, GP Sergeant & KD Thornbury (2019). The effect of inhibiting TMEM16A on carbachol-induced contractions in murine primary bronchial smooth muscle.
FASEB Smooth Muscle Conference, West Palm Beach, Florida, USA.
3. R Dwivedi, RJ Large, E Bradley, G Litherland, MA Hollywood, GP Sergeant & KD Thornbury (2019). The effect of inhibiting TMEM16A on carbachol-induced contractions in murine primary bronchial smooth muscle. *Irish Journal of Medical Science* 2019; 188 Suppl. 10, S269.
Irish Thoracic Society meeting, Galway, Republic of Ireland.

1. Literature Review

1.1 The respiratory system

The mammalian respiratory system is mainly built up of muscles and specific organs which function to bring oxygen into the body in exchange for carbon dioxide.

1.1.1 Anatomy

The respiratory system consists of the nose, mouth, pharynx, larynx, trachea, bronchi, bronchioles, alveolar ducts, alveolar sacs and alveoli. The bronchi, bronchioles, alveolar ducts, alveolar sacs and alveoli are all enveloped by the lungs. The lungs are pyramid-shaped structures connected by the right and left bronchi to the trachea. These paired organs are bordered by a flat, dome shaped muscle known as the diaphragm, which is situated at the base of the lungs and thoracic cavity. Functionally, the respiratory system is divided into two zones known as conducting and respiratory zones (*figure 1.1*). The conducting zone is from the nose to bronchioles and its primary function is to transport inhaled air into lungs, whereas, the respiratory zone consists of the alveolar duct, alveolar sacs and tiny passageways that allow rapid gas exchange (Tu *et al.* 2013).

1.1.2 Airway cell composition and their role

Several types of cells are expressed in the airway which are actively involved in carrying out its vital functions; (*figure 1.2*). These include epithelial cells, fibroblasts, smooth muscle cells (SMCs), mast cells and endothelial cells (Breeze & Turk, 1984). Epithelial cells line the entire lower respiratory tract i.e., from the trachea to the alveoli sacs (Knight & Holgate, 2003). Airway epithelium, besides being involved in gas exchange, also functions to moisten and protect the airway tract from injury and pathogens (Leiva-Juárez *et al.* 2017). A single layer of pseudostratified ciliated epithelial cells is positioned along the basal lamina lining of the trachea and bronchi. It consists of goblet cells (secrete mucus), ciliated cells (passaging mucus out of airway system) and basal cells (maintaining healthy epithelial layer). The lung is enriched with fibroblasts which fundamentally work to maintain the core integrity of the lung by producing collagen, proteoglycans and elastin (White, 2015). They function against tissue scarring and wounding by tissue remodelling and repairing processes. A layer of SMCs

are present beneath the epithelial layer in the trachea, bronchial tree and bronchioles (Ebina *et al.* 1990). The key function of SMCs is to maintain muscle tone and alter airway resistance, though the exact reason for this is unclear. Airway resistance is the degree of resistance to air flow through the respiratory tract during inhaling and exhaling. It majorly depends on respiratory tract diameter which decreases in asthma and COPD airways thus increasing airway resistance.

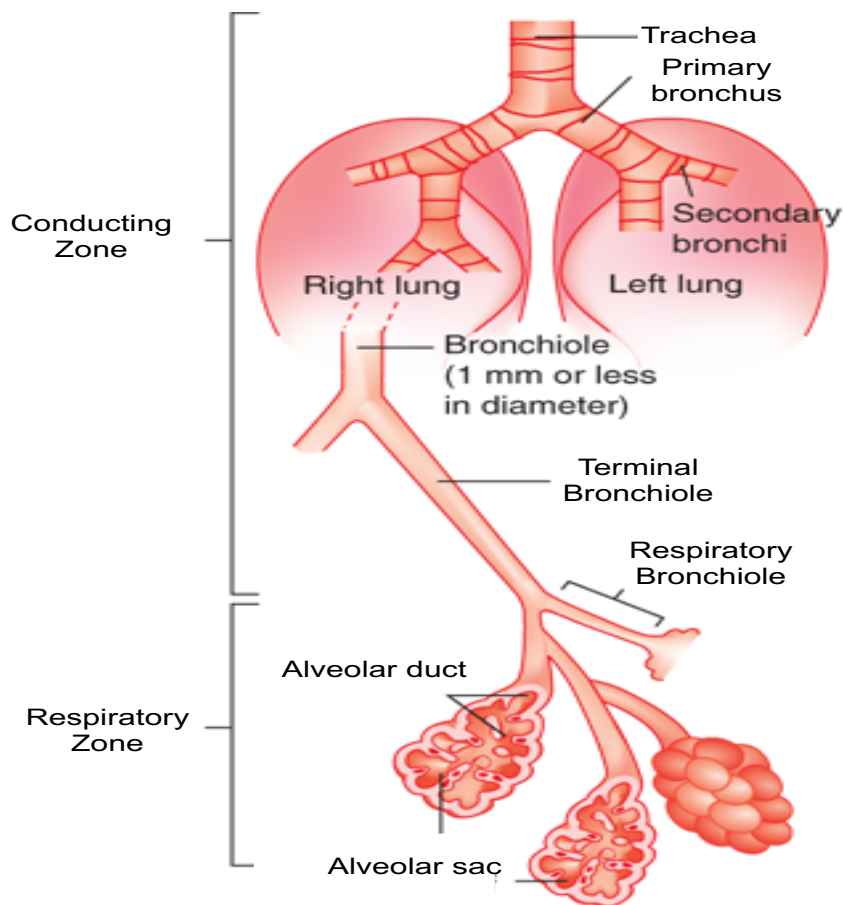


Figure 1.1:- Conducting and respiratory zones of the human respiratory system.

(Adapted from Lechner *et al.* 2011)

1.1.3 Airway smooth muscle cells

SMCs are defined as non-striated muscle with involuntary contractile activity. The cytoplasm of SMCs are rich in actin and myosin, the main proteins involved in the contractile activity (Fatigati & Murphy, 1984). The sarcoplasmic reticulum (SR) of SMCs is filled with calcium ions [Ca^{2+}], which help to sustain contractions. Airway smooth muscle cells (ASMCs) have been formerly described as the “appendix of the lung” by Mitzner, who stated that eradicating SMCs from the airways might result in increased airway size but without any major physiological changes (Mitzner, 2004). However, opponents to Mitzner’s view have proposed a pivotal role of ASM in pathogenesis of respiratory diseases such as asthma and Chronic Obstructive Pulmonary Disease (COPD) (Tliba & Panettieri, 2009). Airway hyperresponsiveness (AHR) and airway remodelling are two characteristic changes associated with both asthma and COPD. Studies have shown that ASMCs play a key role in modulating these changes (Tliba & Panettieri, 2009). Airway remodelling involves hyperplasia (a state of increased numbers of ASMCs) and hypertrophy (a state of increased ASMCs size) in the walls of the airway. The level of airway remodelling in ASM correlates with COPD severity (Panettieri *et al.* 2008; Hogg *et al.* 2004; Benayoun *et al.* 2003; Ebina *et al.* 1993). A trial study was carried out by Cox *et al.* (2007), where the effect of bronchial thermoplasty (bronchoscopic method to decrease the ASM mass and attenuate bronchoconstriction) was examined on moderate to severe asthma. Subjects with moderate to severe asthma showed that elimination of ASM improved asthma control (Cox *et al.* 2007). ASM has also been shown to contribute to inflammatory mechanisms of airway diseases by acting as a source of inflammatory mediators, enzymes and cytokines such as prostaglandin E₂ (PGE₂), nitric oxide, interleukin (IL) -8, IL-12, TNF- α and TGF- β (Tliba & Panettieri, 2009).

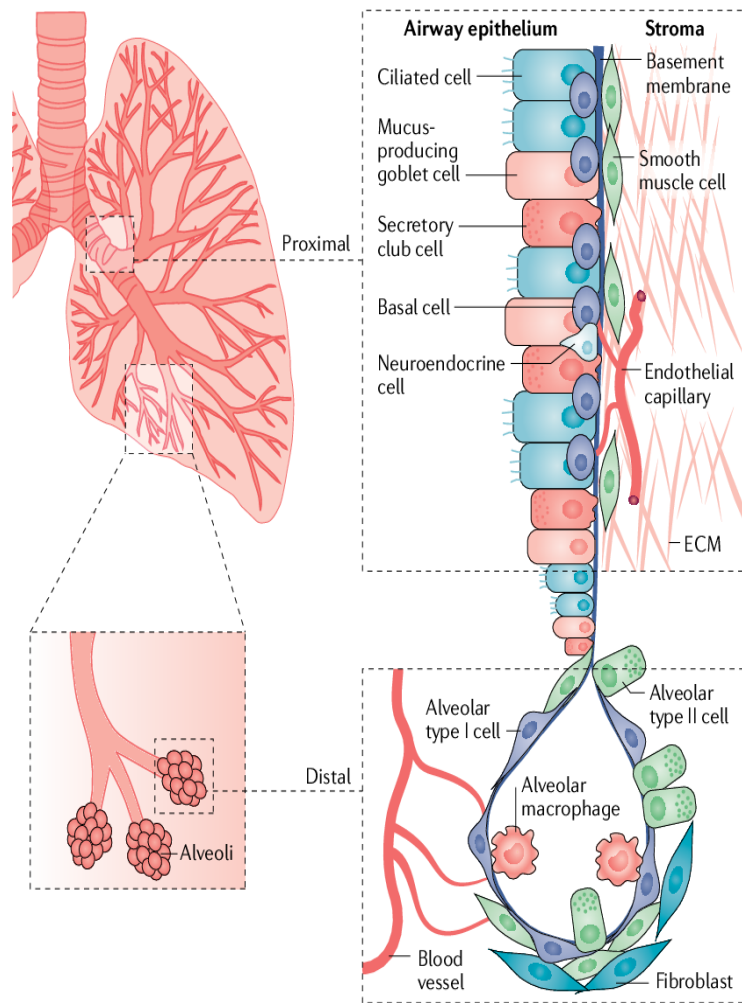


Figure 1.2: Schematic diagram showing types of cells expressed in healthy lungs

The figure above represents the heterogenous microenvironment of the lung. The various kinds of cell types present in mainstream airway and in alveoli. (Adapted from Altorki *et al.* 2019)

1.2 Innervation of the lungs

1.2.1 Parasympathetic-cholinergic system

The airway systems of almost all mammals are innervated by parasympathetic-cholinergic nerves (Barnes, 1988). Cholinergic nerves are found throughout the respiratory zone (trachea, bronchi, alveoli) and within the lungs; cholinergic nerves innervate smooth muscles (SMs) and secretory cells (Laitinen *et al.* 1987). They release the neurotransmitter acetylcholine (ACh) which acts on muscarinic receptors present on the target cell membrane. In the human lung, three subtypes of muscarinic receptors (M_1 , M_2 , M_3) have been pharmacologically recognised (White, 1995). An *in-vitro* study by Canning and Udem (1993) showed that a contraction was evoked in tracheal ASM by activation of cholinergic nerves. Widdicombe and Wells (1994) also concluded that cholinergic nerves are responsible for maintenance of ASM basal tone. In airway diseases, several mechanisms contributing to cholinergic bronchial constriction have been reported. In asthmatic patients, constriction mediators such as thromboxane, prostaglandin D_2 (PGD_2) (Inoue *et al.* 1985) and tachykinins (Hall *et al.* 1989) have been shown to assist in ACh release from parasympathetic nerves. Inflammatory mediators such as bradykinin and histamine stimulate sensory receptors in the airway and lead to a rise in reflex cholinergic bronchoconstriction (Kaufman *et al.* 1980; Coleridge & Coleridge, 1984). A study by Jongejan *et al.* (1990) demonstrated the effect of the inflammatory mediators histamine, thromboxane A_2 , prostaglandin D_4 , prostaglandin $F2\alpha$ and leukotriene C4 on cholinergic activity in human ASM. These inflammatory mediators directly increase SM sensitivity to cholinergic stimulation, enhancing bronchoconstriction (Jongejan *et al.* 1990).

1.2.2 Sympathetic-adrenergic system

Unlike cholinergic innervation, adrenergic innervation in ASM stimulates relaxation of the airway. It is either discrete or non-existent in species like rats, canine, bovine, guinea pig and humans (Doidge & Satchell, 1982). Daniel *et al.* (1986) suggested, through a study on human ASM, that the adrenergic system indirectly stimulates the airway by targeting parasympathetic ganglia (Daniel *et*

al. 1986). The main neurotransmitters involved in the sympathetic-adrenergic system are noradrenaline and neuropeptide Y (NPY) (Ind, 1994). The α - and β -adrenergic receptors are the two receptors in the sympathetic system activated by noradrenaline. Within human airways, the sympathetic system is less prominent than the parasympathetic system (Zaagsma *et al.* 1987), however β_2 -adrenoceptors are highly expressed in human ASM (Pack & Barnes, 1987) and have also been observed in rat airway (Hamid *et al.* 1991). There are contradictory reports, concerning the role of β_2 adrenoceptors in asthma. For example, de Jongste *et al.* (1987) and Bai *et al.* (1992) showed that in asthmatic ASM, β_2 adrenoceptors function normally, causing relaxation (de Jongste *et al.* 1987; Bai *et al.* 1992), while other studies reported a decrease in functional β_2 -adrenoceptors in asthmatic airways (Cerrina *et al.* 1986; Goldie *et al.* 1986). A study on guinea pig airway showed that NPY stimulates the release of prostaglandins, resulting in bronchoconstriction and in aggravated asthmatic airways, NPY serum levels are increased (Cadieux *et al.* 1989; Cardell *et al.* 1994). However, in contrast, Howarth *et al.* (1995) showed that there was no difference in the number of NPY-immunoreactive nerves in both healthy and asthmatic subjects.

1.2.3 Non-adrenergic non-cholinergic system

A third system, known as the non-adrenergic, non-cholinergic nervous system (NANC) was discovered in the 1960s (Burnstock & Holman, 1963). Firstly, NANC nerves were observed in the gastrointestinal system then later in the cardiovascular, reproductive and urinary systems (Burnstock & Holman, 1963; Burnstock, 1969). Later, Richardson & Beland (1976) discovered NANC nerves in human airways. Stimulation of NANC nerves may cause dilation or constriction of bronchi, mucus secretion, and activation of inflammatory cells. Thus, NANC nerves are sub-divided into excitatory (e-NANC) or inhibitory (i-NANC) categories. Neurotransmitters of the i-NANC system are mainly neuropeptides such as vasoactive intestinal peptide (VIP), pituitary adenylyl cyclase activating peptide and peptide histidine methionine (Ward *et al.* 1995). *In-vitro* studies performed on human, guinea pig and cat demonstrated relaxation caused by i-NANC nerves (Davis *et al.* 1982; de Jongste *et al.* 1987; Taylor *et al.* 1984; Altieri

et al. 1985). i-NANC innervation is co-localised with parasympathetic nerves (Lammers *et al.* 1988). The most potent relaxant neurotransmitter, VIP, is a 28-amino acid peptide, which acts by binding to VIP receptors (Barnes *et al.* 1991). It has been suggested by Belvisi *et al.* (1993) that VIP is released along with nitric oxide (NO), from cholinergic nerves (Belvisi *et al.* 1993). Both VIP and NO act prejunctionally to inhibit ACh release and also directly dilate the airways. VIP has been shown to potently stimulate mucus secretion in the trachea of the ferret (Peatfield *et al.* 1983). However, there is still a lack of convincing evidence of i-NANC dysfunction in an asthma model.

1.3 Regulation of ASM contraction and relaxation

Airway smooth muscle cells (ASMCs) have a network of actin and myosin filaments throughout their cytoplasm which are responsible for contractile activity (Meiss, 1997). In order for the contraction to occur, the 20-kDa light chain of myosin must be phosphorylated by myosin light chain kinase (MLCK), which enables interaction of myosin and actin. ASM contraction is the outcome of airway reactivity to external stimuli. In the absence of external stimuli, phosphorylation of myosin light chain is maintained at a low level causing basal tone (Bai & Sanderson, 2006). The obstruction of airflow caused by contraction is mild to moderate in healthy airways, however, increased constriction is a contributing factor in a number of pulmonary diseases such as asthma and chronic obstructive pulmonary disease (COPD) (James & Carroll, 2000).

ASM contractile activity is largely controlled by extracellular mediators acting on specific receptors present on the smooth muscle cell (SMC) membrane. *Figure 1.3* is a schematic diagram of the regulation of SM contraction. SM contractile activity starts with the activation of G-protein-coupled receptors by extracellular agonists such as histamine, thromboxane, acetylcholine and serotonin (Webb, 2003). This results in an increase in phospholipase C (PLC) activity *via* G-protein activation. PLC breaks down phosphatidylinositol 4,5 biphosphate (PIP₂), a membrane phospholipid, into two intracellular second messengers diacylglycerol (DAG) and inositol1,4,5 triphosphate (IP₃). IP₃ diffuses through the cytoplasm and binds to IP₃ receptors on the SR, resulting in the release of Ca²⁺ into the cytoplasm. DAG, the other product of PIP₂ hydrolysis, along with Ca²⁺ released

from store, activates protein kinase C (PKC), which further phosphorylates proteins and Ca^{2+} channels. Ca^{2+} also binds to calmodulin, which leads to MLCK activation. The activated MLCK phosphorylates the myosin light chain, which initiates contraction. In addition to the activation of PLC, a Ca^{2+} sensitising mechanism is initiated *via* activation of RhoA, a GTP-binding protein.

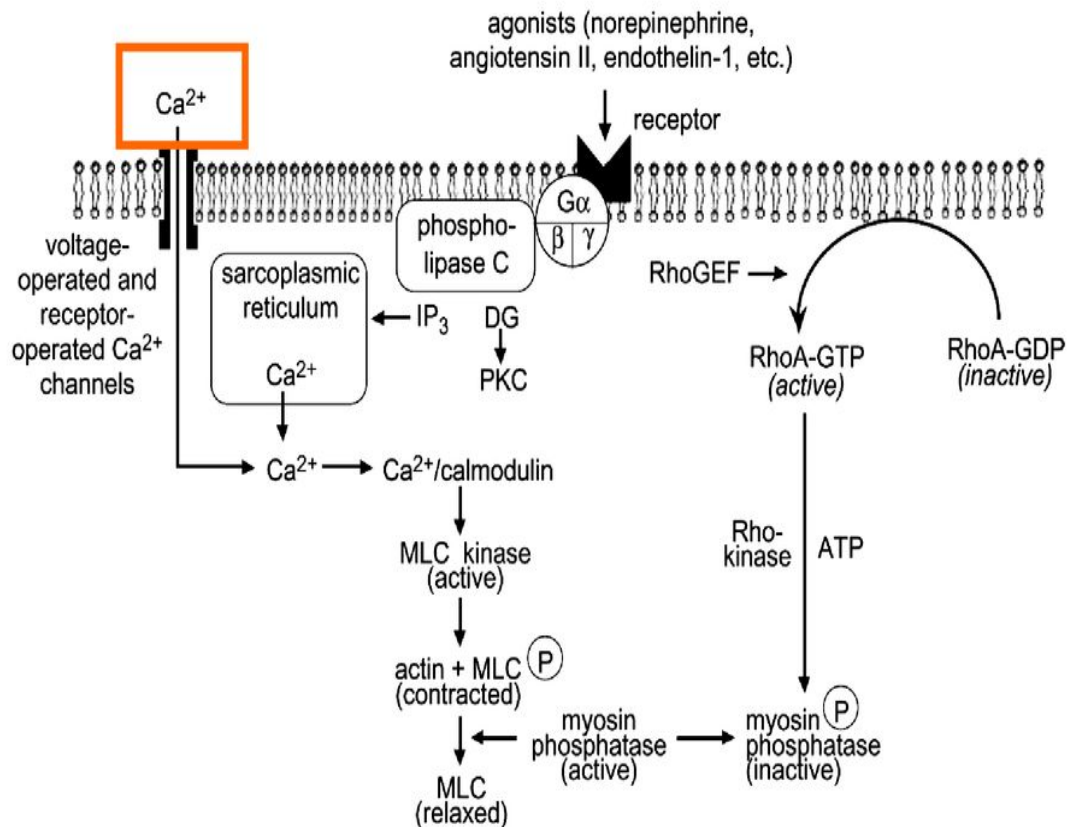


Figure 1.3. Schematic diagram of the regulation of SM contraction.
(Adapted from Webb, 2003)

Activated RhoA increases the activity of Rho kinase, which inhibits myosin phosphatase. The contractile state of the SMC is maintained by this Ca^{2+} -sensitising mechanism (Webb, 2003).

The regulation of ASM relaxation mainly results in the removal of external contractile stimuli. *Figure 1.4* depicts the pathways involved in SM relaxation. The process of relaxation requires a decrease in the concentration of cytosolic Ca^{2+} and an increase in the activity of MLCP. β_2 -adrenoceptors and prostaglandin E_2 receptors (EP2Rs) are the Gs-coupled receptors expressed in ASMCs (Hall *et al.* 1992; Hall *et al.* 1993). Subsequent to the activation of these receptors, Gs protein activates adenylyl cyclase which catalyses adenosine triphosphate to cyclic adenosine monophosphate (cAMP). cAMP then activates protein kinase A, which promotes an active state of MLCP, leading to SM relaxation.

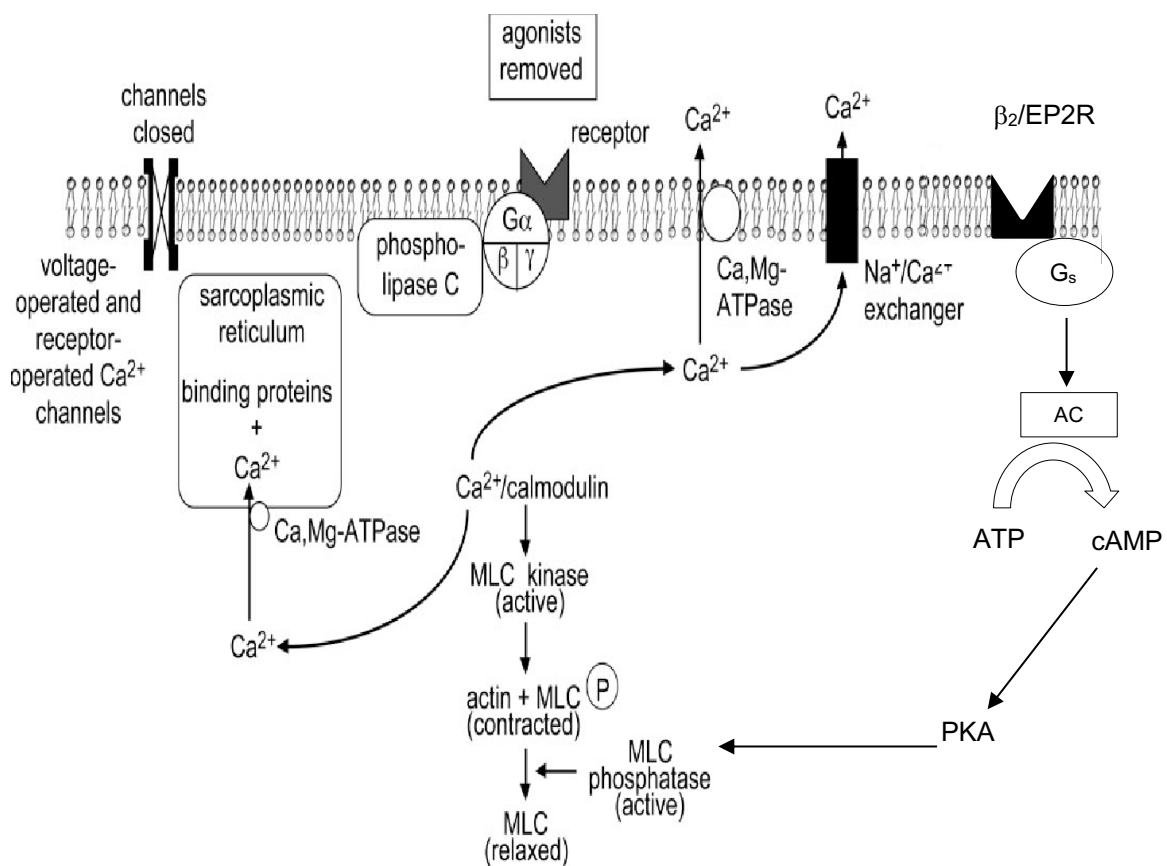


Figure 1.4:- Schematic diagram of the regulation of SM relaxation.
(Adapted from Webb, 2003)

1.4 Receptors involved in smooth muscle contraction

ASM contraction depends on external messengers acting on receptors present on the cell membrane. These messengers can be neurotransmitters, hormones or mediators released from epithelial and inflammatory cells (Pelaia *et al.* 2008). Wang *et al.* (2017) have shown that different inflammatory mediators such as histamine, U46619 (Thromboxane-A₂ synthetic analog), leukotriene D₄ and 5-hydroxytryptamine (5-HT) are able to induce contractile activity in mammalian ASM, all four of them are briefly described below.

Histamine is a well-known chemical mediator released by the body in response to allergic reaction (Criado *et al.* 2010). Four types of histamine receptors are expressed in the airway and pulmonary tissue. The bronchoconstrictor effect of histamine is mediated *via* H₁ receptor (Barnes, 1998). In 1946, John J. Curry had shown in patients with mild asthma, histamine induced bronchoconstriction (Curry, 1946). Histamine can induce constriction either by acting directly through stimulation of H₁ receptors on ASM or indirectly by stimulating afferent vagal fibers in airways (Leff, 1982). Besides smooth muscle contraction, histamine plays a vital role in airway obstruction *via* bronchial fluid secretion and airway mucosal edema (Yamauchi & Ogasawara, 2019).

Thromboxane-A₂ (TxA₂) is a lipid mediator that was discovered by Hamberg *et al.* (1975) as an unstable platelet-aggregated factor in human platelets and is one of the widely used mediators to study smooth muscle constriction acting *via* TP receptor. Thromboxane prostanoid receptors, widely known as TP-receptors, have been found in brain, kidney, liver, heart, lung and uterus (Huang *et al.* 2004). Studies have shown that TxA₂ acts as a bronchoconstrictor. In the human lungs, it is expressed in epithelial cells, SMCs and macrophages. The concentration of TxA₂ has shown to be increased in airway diseases such as asthma (Dogné *et al.* 2002). U-46619 is a chemically stable synthetic compound of TxA₂ that has been utilised extensively in TxA₂ experiments due to the instability of TxA₂ itself. U-46619 acts through TP-receptors, present on ASMCS, which activate G_{q/11} and G_{12/13} G-proteins, leading to contractile activity.

Cysteinyl Leukotrienes, are pro-inflammatory lipid mediators with an ability to induce bronchoconstriction in airways (Philleos *et al.* 2005). Three types of

cysteinyl leukotrienes are present in human airways; LTC₄, LTD₄ and LTE₄ which exerts their effect *via* activation of cys-LT₁ receptor (cysLT₁). A comparative study carried out in human airway demonstrated that, LTC₄ and LTD₄ are more potent bronchoconstrictors in comparison to histamine (Barnes *et al.* 1984). Various studies carried out in last four decades, confirmed that cysLT₁ are actively involved in airway remodelling observed in persistent asthma (Holgate *et al.* 2003). This remodelling includes smooth muscle hyperplasia, lung fibrosis, mucus hypersecretion, mucus gland hyperplasia and collagen deposition.

5-hydroxytryptamine (5-HT) or serotonin is a neurotransmitter that has been reported to be important in central nervous system and digestive tract. According to Takahashi *et al.* (1995), this inflammatory mediator has both relaxing and constricting effects on ASM tone depending on the concentration used and species. In humans, there are no reports of serotonergic fibers in respiratory system however they were reported to be present on mast and neuroendocrine cells (Campos-Bedolla *et al.* 2008). In asthmatic airways, plasma concentrations of free 5-HT were found to be increased and administration of tianeptine (drug used to lower plasma 5-HT) improved pulmonary function in asthmatic children.

1.4.1 Muscarinic acetylcholine receptors

In 1914, Dale had categorised ACh-activated receptors into nicotinic and muscarinic receptors. Muscarinic receptors (mAChRs) are expressed in brain, airway, stomach and bladder in a number of species including, mouse, rat, guinea pig and human (Ten Berge *et al.* 1995; Roffel *et al.* 1990; Struckmann *et al.* 2003; Higashida *et al.* 1997). mAChRs are subdivided into 5 subtypes, namely M₁₋₅. M₂ and M₃ are expressed in ASM and are actively involved in contractile activity *via* specific signalling pathways (Eglen *et al.* 1996). M₃R interacts with G_q to trigger PLC-activated contraction (Yang *et al.* 1991), whereas, M₂R interact with G_i to inhibit adenylyl cyclase, thus preventing relaxation (Ehlert, 2003).

M₂ and M₃ receptors are expressed in a 4:1 ratio in ASM (Roffel *et al.* 1988), however functional studies have indicated that M₃ are the primary G-protein coupled receptor responsible for ASM contraction in a diverse number of species including human (Roffel *et al.* 1990). Fryer and Jacoby (1998) reported that pre-junctional M₂R which are present on parasympathetic nerve terminals act as autoinhibitory receptors thus regulating cholinergic activities by repressing ACh

release. Dysfunctional neuronal M₂Rs and the increase in neuronal ACh release resulted in hyperresponsiveness of the airways isolated from antigen-challenged guinea pig (Fryer & Jacoby, 1998). The post-junctional M₂Rs role remained unclear however, a recent study by Alkawadri *et al.* (2021) on mouse bronchial smooth muscle has shown a novel role of post-junctional M₂Rs. Their detailed investigation provided strong evidence of M₂Rs-mediated hypersensitisation of M₃Rs-dependent contractions at lower frequency stimulus of 2 Hz. ACh and muscarinic receptors also play a significant part in ASM remodelling, mucus gland hypertrophy and goblet cell hyperplasia (Shimura *et al.* 1996). Kanefsky *et al.* (2006), demonstrated that muscarinic receptors expressed in ASMCs also regulate pro-inflammatory activity by increasing expression of cytokines IL-6, IL-1 β and chemokines IL-8, CCL (Kanefsky *et al.* 2006).

1.5 Ion channels in airway smooth muscle

Ion channels are defined as pore-forming proteins, which are located across the plasma membrane or intracellular membranes of cells and function as passageways, allowing the transport of cations and anions (Na⁺, Ca²⁺, K⁺, Cl⁻) from one side of the membrane to the other (Hille, 2001). Ion channels can be either be voltage-gated, ligand-gated or mechanosensitive. Voltage-gated ion channels open as a result of a change in voltage across the membrane whereas, ligand-gated ion channels are activated by binding of specific mediators or second messengers. Mechanosensitive ion channels, also known as Piezo channels act as mechanical sensors which are responsible for converting the extracellular mechanical stimulation into the biochemical signal. There are various ion channels present on ASMCs; activation of these ion channels facilitates cellular functions such as contractions. Voltage-dependent L-type and T-type Ca²⁺ channels activate following membrane depolarisation, subsequently increasing intracellular [Ca²⁺], thus leading to ASM contraction (Janssen *et al.* 1997). In ASMCs, multiple species of several ion channels are expressed, although their role in contraction is controversial (Perez-Zoghbi *et al.* 2009; Janssen, 2002). Calcium-activated potassium channels (K_{Ca}), calcium-activated chloride channels (TMEM16A), voltage-dependent calcium channels (Ca_v), calcium released-activated channels (CRAC), non-selective cation channels

(TRPs), voltage-dependent sodium channels (Na_v) and voltage-dependent potassium channels (K_v) have all been detected in ASM (Kume *et al.* 1994; Wang & Kotlikoff, 1997; Liu & Farley, 1996; Zhang *et al.* 2005; Kwong & Carr, 2015; Brueggemann *et al.* 2012; Bradley *et al.* 2014).

1.5.1 The Chloride channel family

Chloride channels are ion channels comprised of membrane proteins which allow passage of anions such as Cl^- , HCO_3^- , I^- , NO_3^- across the plasma membrane (Alexander *et al.* 2009). They play a key role in maintaining cell volume, pH and membrane potential. The chloride channel family is divided into subcategories based on regulation: ligand-gated ion channels (LGICs), voltage-gated chloride channels (CLCs), volume-regulated ion channels (VIC), cystic fibrosis transmembrane conductance regulator (CFTR) and calcium-activated chloride channels (CaCCs) (Verkman *et al.* 2009; Ferrera *et al.* 2019).

1.5.1.1 CaCCs

CaCCs were first discovered by Barish *et al.* in xenopus laevis oocyte in 1983. CaCCs are found in almost all tissues in both excitable and non-excitable cells, suggesting that they play an important role in physiological processes in a number of different tissues (Hartzell *et al.* 2005). When first discovered, several potential candidates of this channel were proposed. The first proposed candidate was a chloride channel calcium activated (CLCA), which had been isolated from bovine trachea (Cunningham *et al.* 1995). CLCA had been described as an asthma channel, since it is upregulated in allergic airway diseases (Erle & Zhen, 2006). In 2005, Gibson proposed CLCA as a cell adhesion molecule, which was involved in attachment of metastatic melanoma cells to endothelium layer of the lung (Gibson *et al.* 2005). Another argument against CLCA being a Cl^- channel was that many cell types which express CaCCs do not express CLCAs (Papassotiriou *et al.* 2001). Besides CLCA, bestrophin, a protein present in humans which acts as calcium-activated anion channel, was also suggested as a Cl^- channel (Sun *et al.* 2002). Suzuki *et al.* (2006) reported a *tweety* gene, which is located in drosophila and contains five or six transmembrane segments. A homologues of this gene in human, hTTYH3 has been suggested as the molecular basis for a Ca^{2+} -regulated maxi Cl^- channel (260 pS). However, in 2008

three different groups reported that a protein known as transmembrane 16A (TMEM16A), encoded by the ANO1 gene, as the molecular basis of CaCCs (Caputo *et al.* 2008; Yang *et al.* 2008; Schroeder *et al.* 2008).

1.5.1.2 TMEM16A

TMEM16A is also known as anoctamin 1 (ANO1) where “an” is for anion and “octa” for 8, as early studies proposed it had eight transmembrane domains (Duran *et al.* 2012). There are nine additional paralogs of TMEM16A (TMEM16B to TMEM16K), also known as ANO2 to ANO10. Anoctamins are expressed in various murine, rat, rabbit and human cell types. ANO 1,6,7,8,9 and 10 are expressed in epithelial cells of a variety of murine tissues, whereas ANO 2,3,4 and 5 are expressed in musculoskeletal and neuronal tissues (Schreiber *et al.* 2010). ANO1 and ANO2 are the only members of the TMEM16 family shown to be conclusively Ca²⁺-activated Cl⁻ channels. ANO3-7 have been shown to function as Ca²⁺-dependent phospholipid scramblases (Gyobu *et al.* 2016; Suzuki *et al.* 2013). ANO 8-10 are poorly expressed in the plasma membrane and are shown to be more retained in the cytosol (Tian *et al.* 2012). Brunner *et al.* (2014) have suggested that ANO 6 can be a nonspecific ion channel as well as acting as a lipid scramblase.

TMEM16A is reported to be expressed in murine epithelial cells, SMCs, vascular endothelial cells, cardiac muscles cells, olfactory sensory neurons, somatosensory neurons, interstitial cajal cells and hepatocytes (Rock *et al.* 2009; Ousingsawat *et al.* 2009; Romanenko *et al.* 2010; Oh & Jung, 2016; Ma *et al.* 2017; Wang *et al.* 2017). Several groups have reported the involvement of TMEM16A in mucus secretion in the airway and intestine (Huang *et al.* 2012; Kondo *et al.* 2017; Kang *et al.* 2017; Benedetto *et al.* 2018) as its inhibition/knockout decreases the mucus secretion in these tissues (Ousingsawat *et al.* 2009; Romanenko *et al.* 2010).

1.5.1.2a TMEM16A in airway

ANO1 is reported as important in the normal development of murine trachea as ANO1 knockout mice presented with a defect in ASM development on the posterior wall of trachea and failure of airway epithelial stratification causing early

death (Rock *et al.* 2008). Huang *et al.* (2012) reported reduced contractility in human bronchi in the presence of benzbromarone, an antagonist of ANO1, this suggests TMEM16A channels are involved in contractile activity in humans (Huang *et al.* 2012). TMEM16A expression was upregulated in ovalbumin-sensitised mouse model of chronic asthma (Zhang *et al.* 2013). Zhang *et al.* (2013) also showed that methacholine-induced airway contraction was attenuated by treatment with benzbromarone or niflumic acid, another TMEM16A antagonist. This finding was confirmed in ASMCs isolated from neonatal TMEM16A knockout mice, where calcium spark-induced transient inward currents were absent. Janssen and Sims (1995) provided evidence that in isolated canine tracheal SMCs, Cl⁻ channels are activated by Ca²⁺ entry through LTCC in the absence of agonists (Janssen & Sims, 1995). They have also shown that Ca²⁺ induced Ca²⁺ release is not necessary for activation of Cl⁻ channels as inward tail currents were observed in the cells even after depleting internal Ca²⁺ stores by pre-treating canine tracheal cells with SR inhibitor, cyclopiazonic acid and repeated application of ACh. Hirota *et al.* (2006) proposed that Cl⁻ channels on the SR might play a key role in modulating charge balance across SR membrane thus helping the release of Ca²⁺ and refilling of the stores (Hirota *et al.* 2006). These authors have also found that, in tracheal rings isolated from cows and pigs, inhibiting plasmalemmal Cl⁻ channels with Cl⁻ channel blockers niflumic acid and NPPB {(5-nitro-2-(3-phenylpropylamino)benzoic acid)} had a minor effect on cholinergic contractions, suggesting minor involvement of this channel in cholinergic contractile activity. Detailed work by Wang *et al.* (2017) investigated the involvement of TMEM16A in mice and guinea pig ASM on contractile activity induced by cholinergic agonist and by different inflammatory mediators such as thromboxane (U-46619), 5-HT, histamine and leukotriene D4. The study was carried out using TMEM16A inhibitor T16A_{inh}-A01 and TMEM16A knockout mice. Key results of their study were active involvement of TMEM16A channel in contractile activity induced by thromboxane (U-46619) and 5-HT in mice and histamine and leukotriene D4 in guinea pigs. However, in response to cholinergic agonist, methacholine-induced contractile activities there was minor or no inhibition observed in the contraction amplitude by T16A_{inh}-A01 and in TMEM16A^{-/-} ASM.

However, Hirota *et al.* (2006) and Wang *et al.* (2017) only tested the effect of TMEM16A blockers in experiments where the cholinergic agonist was applied for a short time (≤ 5 min). They failed to test a possible role for TMEM16A channels in mediating sustained cholinergic contractions. In this project, involvement of TMEM16A on cholinergic activity was re-investigated on CCh contractions which were applied for a longer duration of 10 minutes.

1.5.2 Voltage dependent calcium channel

Voltage gated calcium channels (VGCCs), also known as voltage dependent calcium channels (VDCCs) are a family of membrane proteins that are highly selective for calcium and activate on membrane depolarisation to allow Ca^{2+} influx into the cytosol (Catterall, 2011). VGCCs were initially classified based on their biophysical and pharmacological properties (Catterall, 2011). There are six main subtypes of VGCCS: L (Long-lasting), T (Transient), N (Neither T nor L, or Neuronal), P (Purkinje cells), Q (after P), and R (Resistant or Remaining). Based on the complexity of these channels, a gene-based nomenclature was established. L-type channels are now designated as $\text{Ca}_v1.1-1.4$, P/Q as $\text{Ca}_v 2.1$, N as $\text{Ca}_v 2.2$, R as $\text{Ca}_v 2.3$, and T-type channels as $\text{Ca}_v3.1-3.3$ (Ertel *et al.* 2000). VGCCs are found in the plasma membrane of all the excitable cell types; smooth muscles, cardiac muscles and skeletal muscles (McDonald *et al.* 1994), neurons (Dunlap *et al.* 1995). Different subtypes of VGCC are present in different cell types. L-type Ca^{2+} channels will be discussed in detail, as they are the most important type in smooth muscle cells. Apart from L-type Ca^{2+} channels, T-type Ca^{2+} channels are also expressed in airway smooth muscle cells (Wang *et al.* 2012). These channels were originally called low-voltage-activated channels and they are insensitive to dihydropyridines. T-type channels are expressed throughout the body, including neurons, heart, smooth muscle, reproductive organs (Perez-Reyes, 2003). Physiological processes they are involved in are smooth muscle contraction, neuronal firing, hormone secretion, myoblast fusion and fertilization.

1.5.2.1 L-type Ca²⁺ channel

L-type Ca²⁺ channel act as important way for Ca²⁺ influx into the cells, thus increasing intracellular concentration of free Ca²⁺. The L-type Ca²⁺ channel is the target of a large number of clinically important drugs such as dihydropyridines which are used as antihypertensive drugs. The common calcium channel blockers used are nifedipine (dihydropyridine), benzothiazepines (diltiazem) and verapamil (phenylalkylamine) (Hirota *et al.* 2003). Recently, it has been shown that some hereditary diseases such as hypokalemic periodic paralysis result from Ca²⁺ channelopathies (Lapie *et al.* 1997).

1.5.2.2 L-type Ca²⁺ channel in airway smooth muscles

L-type calcium channel expression in airway smooth muscle cells is well established, however there is extensive variation regarding its involvement in the bronchoconstriction and contraction (Hirota & Janssen. 2007). A number of studies have shown minor involvement of the channel in ASM contraction and constriction. For example, it has been claimed that the primary source for increasing cytosolic Ca²⁺ is Ca²⁺ stores in ASMCs (Perez-Zoghbi *et al.* 2009). Even with extracellular Ca²⁺ removed, agonist induced increase in cytosolic Ca²⁺ level and contraction still occurs mainly depending on internal Ca²⁺ stores. Also, Janssen (2009) suggested that all of calcium channel blockers (CCB) which are being used as hypertension drugs, have minimal effects on airway constriction in clinical trials. Although these are compelling points against a role of VGCC, there are a few studies that have shown reduction of agonist-induced contractions by CCB. These relaxing effects of CCB were largely dependent on concentration of constrictors used. For example, 10 nM CCh induced contraction was completely abolished by nifedipine, however the blocker had no effect on contraction induced by 10 µM CCh (Janssen, 2002). There are several other studies that have shown inhibitory effect of CCB on ASM but they were carried out in non physiological conditons either by depletion of the internal Ca²⁺ pool or by using high concentrations of CCB (Bourreau *et al.* 1991; Shen *et al.* 2000; Tao *et al.* 2000). Vannier *et al.* showed data on porcine trachea smooth muscle where 10 µM of nifedipine reduced 1 µM CCh contractions by 50% (Vannier *et al.* 1995). The relative contributions of Ca²⁺ influx and release of intracellular Ca²⁺ stores to agonist-induced ASMC contraction varies depending on agonist concentration.

Trachea smooth muscle isolated from dogs and human in two different studies carried out by Farley (1978) and Drazen *et al.* (1983) respectively, showed that CCB inhibited ACh (concentration less than 1 μ M) and histamine (10 μ M) - induced constriction. Byron *et al.* (2014) has shown in their study using precision cut lung slices obtained from rat, 230 nM of methacholine induces significant airway constriction which was fully reversed by application 10 μ M of verapamil. However in parallel experiments, the same concentration of verapamil had minor reversing effects on constriction induced by 10 μ M of methacholine (Byron *et al.* 2014). The available scientific literature suggests a key role of the channel in the ASMC constriction induced by agonists, mostly at submaximal concentrations.

1.5.3 Potassium Channel family

Plasmalemmal potassium channels mainly function to control efflux of K^+ ions from cells to the extracellular space. They are an important factor in smooth muscle excitability and force generation (Kotlikoff, 1993). Based on the structure and function, the channels are categorised into four major classes: voltage-gated (K_v), inwardly rectifying (K_{ir}), tandem pore domain (K_{2P}) and ligand-gated (K_{ligand}) channels (Kuang *et al.* 2015). Ca^{2+} -activated K^+ channels have been known for their important role in smooth muscle cell excitability by sensing and responding to the variation in intracellular Ca^{2+} concentration. The channel is further divided into 3 subtypes; small conductance (SK_{Ca} , 4-14 pS), intermediate conductance (IK_{Ca} , 32-40 pS), and large conductance (BK_{Ca} or Maxi K, 200-300 pS) (Berkefeld *et al.* 2010). Both SK_{Ca} and IK_{Ca} are intracellular Ca^{2+} -dependent and membrane potential-independent. However, BK_{Ca} are activated by both membrane potential and cytosolic Ca^{2+} concentration. The potassium channel that has been best described in the airway smooth muscle is the BK_{Ca} channel (Kotlikoff, 1993).

These are widely expressed in epithelial, endothelial cells, smooth muscle and in motor and sensory neurones but, curiously, are absent in the cardiac myocytes (Kshatri *et al.* 2018; Hughes *et al.* 2010; Contet *et al.* 2016; Kotlikoff, 1993; Zaidman *et al.* 2017; Adams *et al.* 1982). They have been found in abundance in the ASMCs of bovine, murine, canine, swine and human airways, where they are believed to regulate tone (Macmillan *et al.* 1995; Bradley *et al.* 2018; McCann & Welsh, 1985; Saunders & Farley, 1991; Martin *et al.* 2014). Activation of BK_{Ca}

leads to an efflux of K^+ ions thus resulting in repolarisation/hyperpolarisation of the membrane potential and this feeds back onto $[Ca^{2+}]_i$ by reducing Ca^{2+} influx either by deactivating voltage-gated Ca^{2+} channels or by increasing exchange activity of Na^+/Ca^{2+} exchanger (Berkefeld *et al.* 2010). BK_{Ca} currents have been documented in ASMCs isolated from mouse, guinea pig, dog, pig and rabbit and are believed to play an important role in membrane potential dynamics and in controlling ASM diameter (Bradley *et al.* 2018; ZhuGe *et al.* 1998; Murray *et al.* 1991; Saunders & Farley, 1991; McCann & Welsh, 1986). Bradley *et al.* (2018) have shown through their extensive study relaxing role of BK_{Ca} in bronchial rings isolated from rabbit and mouse. Histamine induced phasic contractions in rabbit bronchial rings were abolished by novel BK_{Ca} channels opener GoSlo-SR5-130. GoSlo-SR5-130 also abolished phasic contractions induced by CCh and U-46619 in mouse bronchial rings. ZhuGe *et al.* (2010) have shown that Ca^{2+} sparks activate nearby BK_{Ca} channels to generate spontaneous transient outward currents (STOCs) in mice ASM. STOCs hyperpolarised the plasma membrane and turned off VDCC. A recent study by Kume *et al.* (2018) showed BK_{Ca} channels blocker iberiotoxin reduced the relaxant effect of β_2 -AR agonists which was potentiated by muscarinic receptor antagonists.

Apart from BK_{Ca} channel, K_v7 plasmalemmal channels are known to be expressed in excitable cells and maintain membrane potential. They are a family of voltage-dependent K^+ channels encoded by KCNQ genes and there are 5 subtypes of the channels. In the lung tissues, K_v7 are expressed in pulmonary artery smooth muscle cells, airway smooth muscles cells, airway epithelial cells, and vagal airway C-fibers (Mondejar-Parreno *et al.* 2020). All five subtypes of K_v7 channel are confirmed to be expressed in guinea pig and human ASMCs (Brueggemann *et al.* 2012). In the same study, using patch-clamping technique, Brueggemann *et al.* have shown that K_v7 currents in guinea pig ASMCs were significantly reduced by histamine (30 μ M) and methacholine (0.1 μ M). K_v7 current amplitudes were increased by different channel activators such as flupirtine, retigabine, celecoxib and 2,5-dimethyl celecoxib. XE991, a K_v7 channel blocker reduced the channel currents in both guinea pig and human ASMCs. In human lung slices, XE991 led to constricted airways which was completely

reversed by verapamil and airway constriction was reduced in presence of K_v7 activator, suggesting an essential role of K_v7 in regulating airway diameter.

Adda *et al.* (1996) have shown that $K_v1.1$, $K_v1.2$ and $K_v1.5$ are expressed in airway smooth muscle. $K_v1.1$ and $K_v1.2$ did not seem to have any appreciable role in maintaining myocyte membrane potential. However, their study suggests that $K_v1.5$ does regulate resting membrane potential in human bronchial SMC and thus act as a potential important pharmacological target (Adda *et al.* 1996).

1.5.4 Calcium release activated calcium channel

Calcium Release Activated Calcium (CRAC) channel is a major Ca^{2+} influx pathway for calcium signalling, which is activated by depletion of Ca^{2+} from the ER, a process known as Store Operated Calcium Entry (SOCE). CRAC is important for different types of excitable and non-excitable cells; lymphocytes (Partiseti *et al.* 1994), pancreatic acinar cells (Zhu *et al.* 2018); vascular endothelial (Blatter, 2017) and smooth muscle cells (Spinelli & Trebak, 2016). Apart from their fundamental role in the human immune system, CRAC channels also have physiological importance in many other cellular types (Tian *et al.* 2016), hence aberrant CRAC channel activity is associated with disorders such as tumor growth and cancer metastasis as well as immune disorders i.e., Severe Combined Immunodeficiency (SCID). The CRAC channel is now well characterised with well-defined electrophysiological properties and molecular components. STIM and ORAI proteins are molecular components of the channel. ORAI acts as pore-forming extracellular subunit of the channel in the plasma membrane whereas STIMs (Stromal interaction molecule) are Ca^{2+} sensors localised in the ER membrane (Diercks & Guse, 2020). There are multiple forms of STIM proteins, two gene products, STIM1, STIM2, and STIM1L a long splice variant of STIM1 (Putney, 2018). There are three Orai gene products, Orai1, 2 and 3. Much less is known about the functions of Orai2 and 3. People with mutations in the genes encoding either Orai1 or STIM1 develop SCID, which is a life-threatening condition (Lacruz & Feske, 2016). Due to a lack of an effective immune system, SCID patients are at extreme risk of contracting life-threatening infections.

The STIM-Orai signalling is quite straightforward as shown in *figure 1.5*. Under normal Ca^{2+} levels in the ER, Ca^{2+} is bound to the EF hand domain of STIM, which is present on the lumen side. Upon Ca^{2+} store depletion, STIM proteins aggregate and are translocated within the ER to ER-plasma membrane junctions within close proximity of Orai and both components couple together.

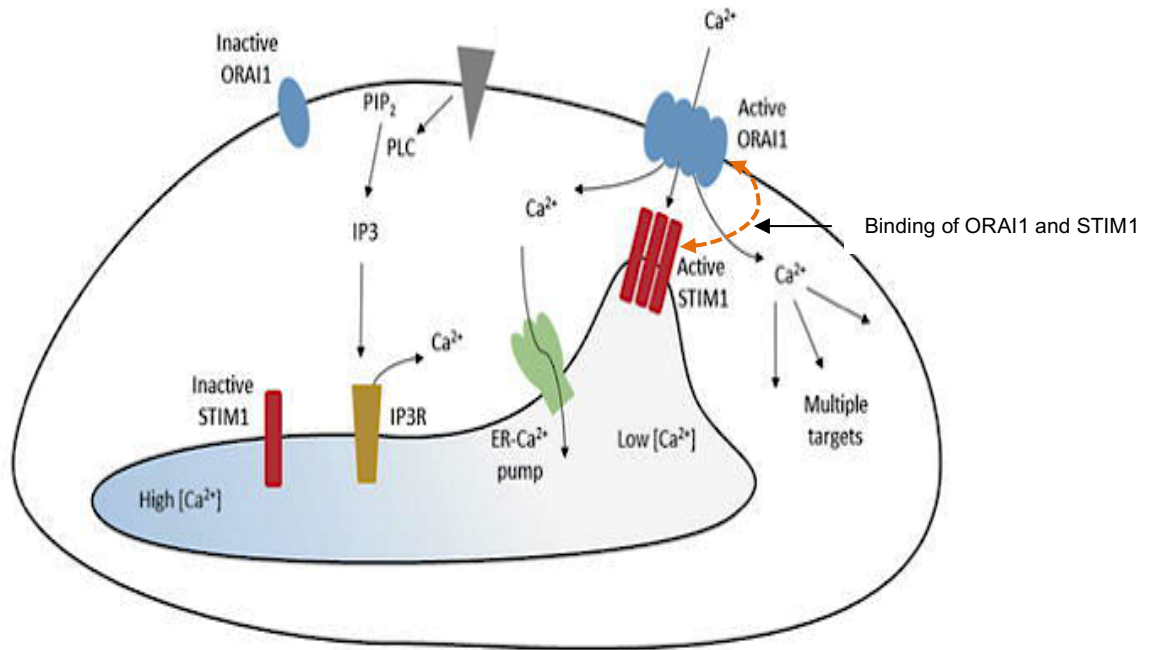


Figure 1.5:- Activation of store operated calcium entry (SOCE) or Ca^{2+} -released activated Ca^{2+} channel (CRAC) by STIM1/Orai1.
(Adapted from Martin-Romero *et al.* 2018)

This leads to opening of CRAC channel, which causes influx of Ca^{2+} into the cytoplasm. From the cytoplasm, Ca^{2+} ions are pumped back into the ER through the sarco/endoplasmic reticulum Ca^{2+} -ATPase pump (SERCA) which transports Ca^{2+} ions from the cytoplasm into the SR. As the Ca^{2+} concentration is restored in the ER, STIM disaggregates and Ca^{2+} binds again to the EF hand domains of STIM. Thus the channel is no longer activated.

1.5.4.1 CRAC in airway smooth muscle

The involvement of the CRAC channel to refill the ER stores in ASMCs has been previously studied by Chen and Sanderson (2017) and Peel *et al.* (2006, 2008). All three homologues of Orai (Orai1, 2, 3) and STIM1 and STIM2 are expressed in human ASMCs at mRNA level. Only Orai1 and STIM1 have been shown to express at protein level, due to a lack of antibodies available for the others. Peel

et al. (2006) have shown the potential role of STIM and Orai in the SOC influx in the human ASMCs. They have shown that STIM1 suppression reduced histamine-induced Ca^{2+} influx but it did not following application of bradykinin. STIM1 suppressed cells showed a reduced SOC inward current in comparison to the cells treated with scrambled or STIM2 siRNA sequences. SERCA pump blockers thapsigargin- and cyclopiazonic acid (CPA)-induced Ca^{2+} influx were reduced by suppression of Orai1 by siRNA. Additionally, Orai1 knockdown cells had less CPA-induced inward currents. A detailed study by Chen and Sanderson investigated the involvement of CRAC channels on Ca^{2+} oscillations and contractions induced by the cholinergic agonist, methacholine in PCLS of murine airways. In the study, they used, two different blockers of CRAC channels, GSK-7975A and GSK-5498A, and found that 100 μM of both blockers individually relaxed precontracted airway by around 85% as compared to partial relaxation caused by L-type channel blockers suggesting active involvement of CRAC channel in cholinergic activity. Spinelli and colleagues were the first to show upregulation of STIM1 and Orai1 expression in tracheobronchial ASMCs obtained from asthmatic mice (Spinelli *et al.* 2012). They also showed that knockdown of either STIM1 or Orai1 significantly reduced ASMC proliferation and chemotactic migration in response to platelet-derived growth factor (PDGF). Johnson *et al.* have also confirmed that STIM1 expression is increased in asthmatic mice (Johnson *et al.* 2021). They have shown that ASMCs isolated from house dust mite (HDM)-challenged mice have increased Ca^{2+} oscillation frequency and amplitude as compared to ASMCs isolated from saline challenged mice. ASMCs from smooth muscle specific STIM1^{-/-} HDM challenged mice have dramatically fewer Ca^{2+} oscillations than ASM cells isolated from HDM challenged tamoxifen-inducible smooth muscle Cre (Myh11 Cre) mice.

1.5.5 The TRP family

The TRP family is a superfamily of cation channels which are known for their role as cellular sensors. They serve as sensors in mammals against external stimuli such as temperature, light, smell, pain sensation and taste (Clapham *et al.* 2001). They are expressed in almost all cell types and tissues. TRPs are also defined as non-selective cation (Na^+ , Ca^{2+} , K^+ , Mg^{2+}) permeable channels which are

expressed on the plasma membrane and intracellular membranes (Dong *et al.* 2010). This superfamily is subdivided into 31 TRP channels which are classified into 10 families according to structural similarity: TRPC (canonical), TRPV (vanilloid), TRPVL (vanilloid-like), TRPM (melastatin), TRPA (ankyrin), TRPP (polycystin), TRPN (no mechanoreceptor potential C), TRPML (mucolipin), TRPY (yeast) and TRPS (soromelastatin) (Himmel & Cox, 2020) as shown in the *figure* 1.6 below.

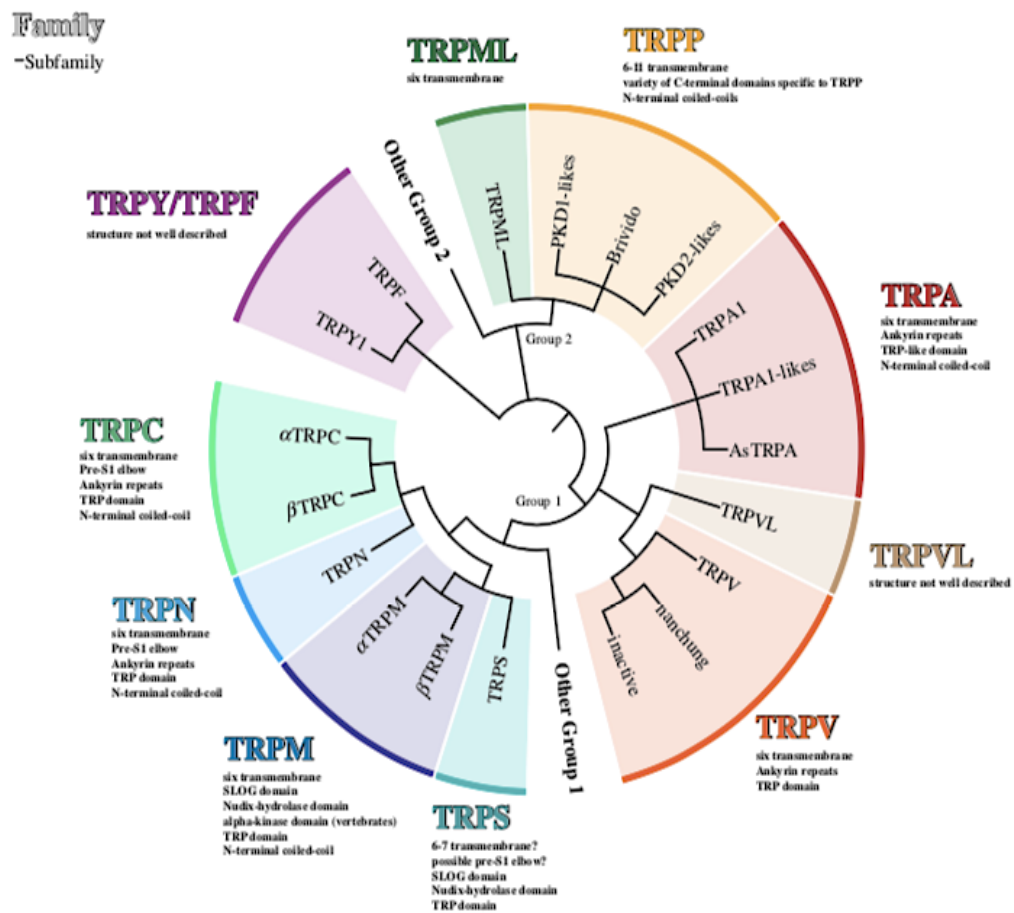


Figure 1.6:- Families and subfamilies of TRP channel.
(Adapted from Himmel & Cox, 2020)

1.5.5.1 TRPCs

Several studies have reported that TRPC channels are expressed in ASMCs (Nilius *et al.* 2007; Abramowitz & Birnbaumer, 2009). It has been shown that they are involved in the regulation of intracellular $[Ca^{2+}]$ and influx of extracellular Ca^{2+} . “Canonical” or “classical” TRP or TRPC share the most structural similarities to the *Drosophila* TRP channel (Dietrich *et al.* 2006). There are seven subunits of TRPC in mammals, TRPC1-7. These seven subunits are divided into four groups based on their functions and structural similarities: TRPC2, TRPC3/C6/C7, TRPC4/C5, TRPC1. TRPC2 is a pseudogene in humans and primates (Vannier *et al.* 1999). TRPCs are reported to be expressed in rat, mouse, guinea pig, pigs and human (Ong *et al.* 2002; Corteling *et al.* 2004; White *et al.* 2006). They are expressed in brain, kidney, liver, heart and lungs; although expression might differ for each subunit in different species (Godin & Rousseau, 2007; Ong *et al.* 2002; Ay *et al.* 2004). TRPC1, TRPC3 and TRPC4 are expressed in ASM of pigs and guinea pigs, whereas only TRPC1 and TRPC3 are expressed in mouse ASM (Ong *et al.* 2003; Ay *et al.* 2004). Isolated guinea pig ASMCs and passaged human ASMCs are able to express TRPC1, TRPC3, TRPC4 and TRPC6 (Ong *et al.* 2003; Corteling *et al.* 2004). In different species, expression of TRPC4 and TRPC5 in ASM varies. Corteling *et al.* (2004) found that TRPC5 are expressed in guinea pig ASMCs but not in passaged human ASMCs (Corteling *et al.* 2004). However, White *et al.* (2006) showed that TRPC5 are expressed in passaged human airway myocytes in a subsequent study (White *et al.* 2006).

Over the last few decades, the role of TRPC channels in ASM contraction and their involvement in airway diseases has been extensively studied. White *et al.* (2006) reported significant increase in TRPC3 mRNA and protein expression in TNF- α treated passaged human ASMCs compared to untreated controls. The same group also demonstrated that silencing of the TRPC3 gene inhibits ACh-evoked increase in intracellular Ca^{2+} in TNF- α treated human ASMCs. Xiao *et al.* (2010) demonstrated a threefold increase in protein expression of TRPC3 in an ovalbumin-challenged asthmatic mice model compared to controls, but no change in TRPC1 protein expression. They also showed at least a four-fold increase in non-selective cation channel activity in native asthmatic SMCs (Xiao *et al.* 2010). A study by Sweeney *et al.* (2002) suggested a major role of TRPC1

in ASMCs proliferation and airway remodelling, which is a contributing factor in a number of airway diseases including COPD and asthma. Additionally, Sweeney and co-workers reported a higher expression of TRPC1 mRNA in proliferating rat bronchial SMCs than in growth-arrested SMCs (Sweeney *et al.* 2002). Silencing of TRPC6 in primary ASMCs inhibited its protein expression, however, there was no effect on 1-oleoyl-2-acetyl-sn-glycerol (OAG, a TRPC activator)-evoked increase in intracellular concentration of Ca^{2+} (Godin & Rousseau, 2007).

Studies supporting a TRPC6 contribution to allergic airway inflammation and mucus secretion make TRPC6 a potential therapeutic target for COPD and asthma (Li *et al.* 2003; Sel *et al.* 2008). Sel *et al.* (2008) have shown that in comparison to wild type mice, TRPC6 deficient mice displayed a reduced response to allergen exposure, but no change in lung mucus production was observed. Intriguingly, agonist-induced contractile activity of tracheal rings was increased in TRPC6^{-/-} mice. This finding was contrary to previous reported findings by Godin & Rousseau (2007) that increases in intracellular Ca^{2+} evoked by OAG remained unaffected by TRPC6 silencing. Finney-Hayward *et al.* (2010) demonstrated that TRPC6 mRNA expression was elevated significantly in alveolar macrophages in COPD patients. However, there was no significant difference in the mRNA expression of TRPC3 or TRPC7 compared with control subjects.

In contrast, several studies have reported an active role of TRPC3 channels in ACh-induced contractions in ASM. Zhang *et al.* (2014) have shown that upon inhibition of the TRPC3 channel in epithelium denuded wild-type male murine tracheal rings using Pyr3 (a TRPC3 inhibitor), ACh-induced contractions were partially inhibited. Additionally, *in-vitro* studies demonstrated an increase in TRPC3 protein expression in murine ASMCs. (Chen *et al.* 2017; Chen *et al.* 2016). Chen *et al.* have shown that TRPC3-encoded nonselective cation channel currents were significantly increased when exposed to ACh. These increased currents were largely blocked by Gadolinium (Gd^{3+}). They also found that a major contributor of airway remodelling, lipopolysaccharide, was involved in up-regulation of TRPC3 protein, increasing resting intracellular calcium $[Ca^{2+}]_i$ and ACh invoked increase in $[Ca^{2+}]_i$. These studies suggest an essential role of TRPC3 in ACh-induced contraction and airway remodelling.

1.5.5.2 TRPVs

TRPVs are comprised of six members (TRPV1-6, Benham *et al.* 2002). On the basis of their structure and function, members of this family are subdivided into four groups: TRPV1/2, TRPV3, TRPV4 and TRPV5/6. TRPV1-4 are non-selective cation channels, which are activated by diverse stimuli such as heat and cold, chemical stress, mechanical stress and binding of intracellular and extracellular messengers (Nilius *et al.* 2003; Nilius *et al.* 2004). TRPV5 and TRPV6 are the most Ca²⁺-selective channels in the entire TRP family with a permeability ratio $P_{Ca}/P_{Na} > 100$ (Vennekens *et al.* 2000; Nilius *et al.* 2000). They are expressed in the bronchial SMCs of a number of species including human and guinea pig, TRPV2 and TRPV4 are also expressed in human bronchial SMCs (Jia *et al.* 2004).

Within the respiratory system, various exciting developments involving TRPV have been reported. TRPV1 and TRPV4 are the most extensively studied channel members. Watanabe *et al.* (2006) found expression of TRPV1 in the respiratory system of guinea pigs using immunohistochemistry (Watanabe *et al.* 2006; Watanabe *et al.* 2008). TRPV1-positive afferent fibers are expressed within ASM and epithelium layers, around blood vessels and in alveoli. A range of studies strongly suggests TRPV1 as a putative molecular target against airway diseases. Rehman *et al.* (2013) have shown that in a IL-13 induced asthmatic mice model, knockdown of TRPV1 not only attenuated inflammation and hyperresponsiveness of the airways, but also reduced metaplasia and fibrosis in asthmatic mice. Thomas *et al.* (2007) made an important finding in the context of lung inflammatory diseases; the TRPV1 agonist nonivamide induced stress to the endoplasmic reticulum (ER) in TRPV1-overexpressing alveolar cells and human bronchial epithelial cells (BEAS-2B) (Thomas *et al.* 2007). This increase in ER stress was measured by examining the expression of *GADD153* (growth arrest- and DNA-damage-inducible transcript 3), *GADD45 α* (growth arrest- and DNA-damage-inducible α), *ATF3* (activating transcription factor), *CCNG2* (cyclin G₂), and *BiP/GRP78* (glucose-regulated protein); which were increased after treatment with nonivamide. Although there has been less focus regarding their role in ASM contractility, there is evidence that TRPV1 expression is enhanced in asthmatic ASMCs and regulates ASM proliferation in rats (Zhao *et al.* 2013).

There is rising interest in the role of TRPV4 in asthma, cystic fibrosis and pulmonary fibrosis. TRPV4 is expressed in both non-neuronal and neuronal cells within the airway. TRPV4 is highly expressed in the epithelium and present in alveolar, bronchi and trachea, as well as in lung tissue, vessels, and the ASM of human, mice, guinea-pig (Jia *et al.* 2004; Alvarez *et al.* 2006; Dietrich *et al.* 2006; Yang *et al.* 2006; Fernández-Fernández, 2008). Groot-Kormenlink *et al.* (2012) reported that TRPV4 are highly expressed in macrophages while Zhao *et al.* (2014) have shown involvement of TRPV4 in proliferation of rat bronchial SMCs. The latter's findings suggest that TRPV4 stimulates proliferation of ASMCS *via* the calcineurin/NFAT-signalling pathway which transmits signals from receptors to the cell nucleus (Zhao *et al.* 2014). Interestingly, Bonvini *et al.* (2015) demonstrated that GSK1016790A, a TRPV4 agonist, induces bronchoconstriction in anaesthetised guinea pigs. GSK1016790A also caused contraction in human ASM, which was inhibited by the TRPV4 antagonist, GSK2193874.

Jia *et al.* (2004) investigated the functional role of TRPV4 in the regulation of airway myogenic tone in both guinea pig and isolated human airways (Jia *et al.* 2004). They demonstrated that hypotonic buffer, containing Ca^{2+} , induced SM contraction in human bronchus and guinea pig trachea. However, in Ca^{2+} deficient buffer, hypotonicity-induced contraction was significantly reduced in human bronchus rings and was completely abolished in guinea pig trachea. Gombedza *et al.* (2017) demonstrated through a house dust mite mouse model of asthma that TRPV4 mediates collagen expression, airway wall thickness, fibrotic airway remodelling and elevated expression of transforming growth factor- β . The same lab also demonstrated that *in-vitro* exposure to a hypotonic solution of tracheal rings and ASM caused SM contraction (Gombedza *et al.* 2017). Interesting pharmacological evidence, provided by McAlexander *et al.* (2014), showed that activation of TRPV4 with GSK1016790A caused constriction of human airway, which was due to cysteinyl leukotrienes, lipid inflammatory mediators (McAlexander *et al.* 2014). This study supports the findings of Gombedza *et al.* (2017) and Jia *et al.* (2004) indicating that the contractile response of SMCs to hypotonic saline involves interactions between the cysteinyl leukotriene and TRPV4.

1.6 Calcium signaling in airway smooth muscle

In airway smooth muscle, Ca^{2+} is known for its key part in various cellular responses such as excitation-contraction coupling, proliferation, migration and apoptosis. Ca^{2+} is often referred to as a “universal signaling molecule” in biology. To understand many human diseases and biological functions, Ca^{2+} signals have been studied in model organisms such as *Caenorhabditis elegans*, *Drosophila melanogaster* and zebrafish (Islam, 2020). Both extracellular Ca^{2+} influx and intracellular Ca^{2+} release are required to produce Ca^{2+} signals (Reyes-Garcia *et al.* 2018). Ca^{2+} influx occurs mainly due to ion channels and transporters such as VGCCs (L-type voltage gated Ca^{2+} channel), non selective cation channel (TRPs) and the $\text{Na}^+/\text{Ca}^{2+}$ exchanger (NCX). Ca^{2+} influx is also triggered by depletion of intracellular stores *via* the Ca^{2+} -release activated Ca^{2+} channel. Ca^{2+} release occurs in ASMC through stores present in the SR. To facilitate the Ca^{2+} release from intracellular Ca^{2+} stores, there are two channels on the SR; ryanodine receptors and inositol 1,4,5-trisphosphate receptors. Ca^{2+} signals are expressed in a variety of forms such as Ca^{2+} oscillations, Ca^{2+} sparks, Ca^{2+} puffs, Ca^{2+} ripples, Ca^{2+} flashes and global changes in intracellular Ca^{2+} concentration (Hill-Eubanks *et al.* 2011). Different types of physiological and pathological functions are regulated by these Ca^{2+} signals. In addition to contraction, Ca^{2+} signals are also involved in metabolism, transcription, migration and proliferation (Narayanan *et al.* 2012).

1.6.1 Ryanodine Receptors

Ryanodine receptors widely referred to as RyRs are intracellular Ca^{2+} release channels located on the sarcoplasmic reticulum membrane in the various types of smooth muscle cells (Guerrero-Hernandez *et al.* 2002). This receptor is well studied in skeletal muscle and cardiac muscle. Endo *et al.* were the first to suggest the presence of RyRs in smooth muscle as even in the absence of extracellular Ca^{2+} , caffeine induced transient contractures of smooth muscle (Endo *et al.* 1983). They exist as three isoforms RyR1, RyR2 and RyR3 in mammals and are named after the plant alkaloid ryanodine, which can both block and partially activate the channels (Takeshima, 1993; Lanner *et al.* 2010). RyRs

are homotetramers comprised of cytosolic N-terminal region, containing Ca^{2+} and regulatory protein binding sites, and a short SR-luminal carboxy terminus (Lanner *et al.* 2010). In smooth muscle, Ca^{2+} -release has been shown to be involved in contractions and relaxation (Berridge *et al.* 2000). Recently, RyR expression was established in ASM, but it varied in different species. All three isoforms are expressed in murine ASM (Du *et al.* 2005), whereas RyR1 and RyR2 are present in rat ASM (Du *et al.* 2006) and in human ASM, only RyR3 is expressed (Hyvelin *et al.* 2000). All three isoforms are suggested to be expressed in mouse ASMs at mRNA and protein level (Lifshitz *et al.* 2011). To regulate contractions, intracellular Ca^{2+} levels are increased globally across the entire cells. However, discrete and localised Ca^{2+} sparks arise from RyRs near plasma membrane and can activate nearby large conductance Ca^{2+} activated potassium channels (BK), causing spontaneous transient outward currents (STOCs) resulting in hyperpolarisation. This leads to inhibition of L-type Ca^{2+} channels, thus decreasing global Ca^{2+} levels and resulting in relaxation (Jaggar *et al.* 2000). Ca^{2+} sparks are also involved in initiating spontaneous transient inward currents (STICs) in tracheal myocytes isolated from guinea pig which is due to activation of TMEM16A (ZhuGe *et al.* 1998). ZhuGe and colleagues have shown that Ca^{2+} sparks could activate both STOCs and STICs, depending on the membrane potential. In their study, they showed that at more negative membrane potential, sparks caused STICs which were blocked by application of 100 μM ryanodine. Du *et al.* 2005 have shown that RyR are involved in bronchoconstriction caused by cholinergic agonists and can be potential therapeutic targets in asthma.

1.6.2 IP₃ Receptor (IP₃R)

IP₃Rs are tetramers, which are present on SR membrane and expressed in all types of SMCs. Three isoforms of IP₃R (IP₃R1, IP₃R2 and IP₃R3) have been identified in mammalian SMCs, however their expression levels vary, depending on the tissue of origin. All three isoforms are expressed in murine trachea myocytes (Wang *et al.* 2004). Following its activation through PLC-PIP₂-IP₃ pathway, IP₃R generates variety of Ca^{2+} signals including waves, sparks, oscillations, puffs and global $[\text{Ca}^{2+}]_i$ in ASMCs (Narayanan *et al.* 2012). It has been well established that the main function of IP₃ is to act as second messenger

to trigger Ca^{2+} release from the intracellular Ca^{2+} stores *via* IP_3R (Berridge, 1997). Bai and Sanderson had shown that in ASM, the ability of IP_3 to release Ca^{2+} from the stores is reduced in the presence of the adenylyl cyclase activator, forskolin (Bai & Sanderson, 2006). Additionally, Dale *et al.* (2018) reported that in the presence of isoproterenol, a β -adrenoreceptor agonist, histamine-induced IP_3R -dependent Ca^{2+} release was reduced in cultured human ASMCs (Dale *et al.* 2018). It has been suggested that cAMP-elevating agents can be used to mediate bronchodilation by reducing IP_3 receptor contribution to bronchoconstriction. Morgan *et al.* (2014) established that the inhibitory effects of β_2 -adrenoreceptor activation on calcium signals in cultured human ASMCs were mediated *via* cAMP-PKA. Saleem *et al.* (2014) has shown interaction of different antagonists of the IP_3 receptor with all three subtypes of the receptor. In their study, they measured IP_3 -evoked Ca^{2+} release by using a low affinity luminal Ca^{2+} indicator, Mag-Fluo-4AM, on permeabilised DT40 cells expressing single subtypes of mammalian IP_3R . The results indicated that 2-APB was able to inhibit Ca^{2+} evoked by the $\text{IP}_3\text{R}1$ receptor (Saleem *et al.* 2014). In contrast, $\text{IP}_3\text{R}2$ appeared to be resistant to 2-APB and when used at maximum concentration 100 μM , 2-APB caused some inhibition of $\text{IP}_3\text{R}3$. IP_3R involvement in asthma has been shown by Tao *et al.* (2000) in an asthmatic model of the Fischer rat. In the disease model, an increase in intracellular IP_3 signalling and Ca^{2+} release mediated by IP_3R were observed in ASMCs. This suggests that Ca^{2+} release through IP_3Rs could be an underlying mechanism for hyperresponsiveness in asthma. The study also showed that 2-APB inhibited remodelling of ASMCs induced by acidic pH, indicating IP_3Rs may also regulate extracellular matrix (ECM) formation and airway remodelling in asthma.

1.7. Chronic respiratory diseases

Chronic respiratory diseases are diseases of the lungs affecting function and structure. The major and common airway diseases are asthma and COPD. Asthma is a condition where patients' airways are inflamed resulting in swelling of airway tubes and production of extra mucus. According to WHO, asthma affected an estimated 262 million people in 2019 and caused 461,000 deaths (WHO, 2020). Currently available treatments effectively reduce inflammation and

acute airway narrowing, however they are less effective against structural changes in the airway (Bara *et al.* 2010). Whereas COPD is a group of progressive lung diseases characterised by a difficulty in expiration due to narrowing of airway tubes following structural changes. COPD is the third leading cause of death worldwide, causing 3.23 million deaths in 2019 (GBD, 2019). The pathology of COPD involves both the airways and the parenchyma of the lung and unfortunately, COPD patients respond poorly to bronchodilator or corticosteroid treatment (Woolcock *et al.* 1991). In both respiratory diseases, ASM has been viewed as an active responder to inflammatory mediators and neurotransmitters resulting in inflammation, hypercontractile activity, excessive mucus production and hyperresponsiveness (Howarth *et al.* 2004).

Ion channels have been extensively studied as potential therapeutic targets for the treatments of many diseases, including chronic respiratory diseases. As described earlier, several different ion channels are expressed in ASM of various mammalian species. CFTR, an ATP-gated anion channel associated with cystic fibrosis is the most intensively studied ion channel in lung disease. Cystic fibrosis is a lethal inherited disease caused by mutations in CFTR (Lopes-Pacheco, 2020). In last two decades, apart from CFTR, other ion channels have been extensively studied such as TMEM16A, various TRPs channels, VGCC, and BK channels in airway disease models. However, their exact involvement in physiological and pathological roles of ASM remains elusive. In most studies, their participation in cholinergic responses has been either investigated on a single concentration of cholinergic agonist or on transient cholinergic contractions. This project focuses on investigating the effect of blocking several ion channels using commercially available blockers on both sustained and transient components cholinergic agonist CCh induced transient and sustained contractile activities in ASM.

1.8. Aims of the project

This thesis aims to investigate involvement of ion channels such as TMEM16A channels, L-type Ca^{2+} channels, CRAC channels on cholinergic activity induced by CCh, cholinergic agonist. This project examined the effect of blocking ion channels on both transient and sustained components of contraction induced by different concentrations of the agonist unlike previous studies reported so far. Therefore, following are three main objective in this thesis:

- 1) Investigating the effect of inhibiting TMEM16A using different blockers of the channel on both sustained and transient components of contraction induced by cholinergic agonist CCh.
- 2) Examined the effect of TMEM16A blockers on Ca^{2+} signals evoked by CCh and caffeine in isolated ASM cells.
- 3) Exploring the role of SOCE through CRAC channel and Ca^{2+} release channel on cholinergic activity induced by CCh.

2. Materials and Methods

2.1 Tissue extractions

The experimental model for this study was freshly dissected lung tissues from adult male and female C57BL/6 mice aged between 10-14 weeks and GCaMP mice aged 14-17 weeks. Mice were humanely euthanized by intraperitoneal application of pentobarbital (100 mg/Kg) which is authorized process for euthanization. The process was carried out in accordance with EU Directive 2010/63/EU and approved by Dundalk Institute of Technology Animal Care and Use Committee. Composition of all the solutions used while carrying out experiments are mentioned in section 2.5.1 of this chapter. The lungs were dissected out from mice and placed in a SYLGARD™ coated petri dish filled with either Krebs solution or Ca²⁺ free solution. Under the microscope, surrounding blood vessels, connective tissue and fat were removed. Micro-dissection was carried out carefully to avoid any damage to the bronchial rings.

Fluo-4 AM

Fluo-4 AM is a cell permeable, fluorescent Ca²⁺ indicator which is commonly used to measure change in Ca²⁺ concentration inside live cells. It has K_d (dissociation constant) value of 345 nM and displays excitation (E_x) at ~ 488 nM and emission (E_m) at ~ 506 nM. Fluo-4 AM was used to perform live-cell Ca²⁺ imaging experiments for the study described in Chapter 4.

GCaMP Mice

GCaMP initially developed by Junichi Nakai in 2001, is a genetically encoded calcium indicator (Nakai *et al.* 2001). The main elements involved in designing GCaMP are calmodulin (CaM), the Ca²⁺-binding protein as the sensing element, M13 a peptide sequence from the calmodulin binding domain of myosin light-chain kinase and green fluorescent protein (GFP) (Yang *et al.* 2018). In the current study, GCaMP8.1 (Acta2-GCaMP8.1-mVermilion) transgenic mice were used which were obtained from the Jackson Laboratory. These genetically encoded Ca²⁺ indicator (GECI) mice have several advantages over cells loaded with Fluo-4AM, including reduced photobleaching, even distribution of fluorescent indicator throughout the cell, and the ability to perform longer experiments since the fluorescent indicator does not leave the cells. These

transgenic mice were available in the lab during the start of chapter 5 imaging study. Hence, ASMCs isolated from these mice were used to perform Ca^{2+} imaging experiments.

GCaMP8.1 is a sensitive variant of GCaMP range with high dynamic range and fast response kinetics as well as improved calcium-binding affinity. These transgenic mice express the GCaMP8.1/mVermilion fusion protein in smooth muscle cells of airways, gut, corpus cavernosum, vas deferens and bladder. mVermilion is a basic red fluorescent protein. mVermilion is a mCherry derivative with approximately a 2 fold brighter emission. It remains at a constant level, allowing for ratiometric measurements of calcium signalling in various smooth muscle. They were designed in the Kotlikoff laboratory in Cornell University. GCaMP8.1 consists of a polyHis plasmid leader sequence essential for thermal stability, a 20 residue peptide of chicken smooth muscle myosin light chain kinase (M13), a circularly permuted GFP (cpGFP) and a rat calmodulin DNA fragment (CaM). These transgenic mice express the GCaMP8.1/mVermilion fusion protein under control of the Acta2 locus promoter regions within the mouse bacterial artificial chromosome (BAC) transgene. With the use of homologous recombination engineering, the GCaMP8.1/mVermilion-SV40pA construct was inserted into the ATG start site of the BAC Acta2 gene (replacing the initiation codon of Acta2 in exon 2). These mice were used to isolate bronchial smooth muscle cells in order to carry out calcium imaging experiments described in chapter 5.

2.2 Isometric tension recording

Isometric tension recording can be defined as an experimental technique where the force generated by the muscle changes without changing the length of the muscle. In this study, either carbachol (muscarinic agonist) or 60 mM potassium chloride (KCl) were used in the medium to generate the muscle force. Bronchial rings of size 2-3 mm were cut off from the right or left main bronchus of a single mouse lung. The bronchial ring was hooked using two stainless steel hooks on a tension transducer. The hooked bronchial rings were then submerged in 14 ml jacketed-organ bath containing Krebs solution, which was continuously bubbled with 95% O_2 and 5% CO_2 gas mixture. Once mounted in the organ-bath, a

tension of 4 mN was applied to the rings. Tissues were incubated for an hour before starting experiments. A multi-channel Myobath system illustrated in *figure 2.1*, was used to measure the contractions and DataTrax2 software (World Precision Instruments, Europe) was used to acquire the data. LabScribe v4 (iWorx) was used to analyse the data.

Statistical analysis: Experimental data sets were performed on a minimum of six animals (N) for most of the experiments except for experiments described in figures 3.5, 3.6, 3.12, 3.18, 3.19, 4.2, 4.3, 4.4, 4.5, 4.9, 4.11, 4.12, 4.13 where a minimum four mice were used. Summarised data are presented as mean \pm standard error of the mean (SEM). All datasets were analysed using ANOVA (One-way or Two-way) or paired t-tests. The Bonferroni or Holm-Sidak methods were used for multiple comparisons within each dataset, if required. Paired t-test were used to test two data sets without variables. One-way ANOVA was used to test datasets with one variable and for datasets with two variables, two-way ANOVA was used. Data sets were considered as statistically significant if $p < 0.05$. Summarised data were plotted using GraphPad Prism software.

2.3 Isolation of mouse airway smooth muscle cells

Two methods of isolation of mouse bronchial smooth muscle cells were used. The first dispersal method was used to isolate ASMCS for chapter 4 imaging study and second dispersal method was used to isolate cells for chapter 5 imaging experiments. We found with second protocol of dispersal; cell gave reproducible response to lower concentration of CCh.

- Mouse ASMCS were isolated enzymatically using an enzyme mix containing 15 mg/ml of collagenase (type II, Sigma Aldrich), 10 mg/ml bovine serum albumin (Sigma Aldrich), 10 mg/ml trypsin inhibitor (Sigma Aldrich) and 1 mg/ml proteinase (Sigma Aldrich). Tissue dissection (Section 2.1) was performed in Ca^{2+} -free solution. Isolated bronchi (Section 2.1) were finely chopped into fragments and placed in a 35mm Nunclon dish containing Ca^{2+} -free solution, for 5-10 minutes at room temperature. Tissue fragments were then transferred to a glass test tube for enzymatic cell dispersal, which was performed in two steps. First, tissue fragments were incubated in the primary dispersal medium

comprising collagenase, bovine serum albumin and trypsin inhibitor dissolved in Ca^{2+} -free for 4 minutes at 37°C . Next, the secondary dispersal solution containing 1mg/ml proteinase dissolved in Ca^{2+} -free was added to the primary medium and incubated for a further 3 minutes at 37°C . During the dispersal, tissue fragments were mechanically stirred using a magnetic stir bar and gently titrated using a glass pipette to aid the release of single ASMCs. After 7 minutes of treatment with the enzyme mixture, the solution was centrifuged for 30 sec. The supernatant was discarded and Ca^{2+} -free was used to wash the enzyme treated tissue fragments. The glass tube containing tissue fragments and 4ml of Ca^{2+} -free was placed in a water bath (37°C) and the solution was gently titrated for 10 minutes to isolate ASMCs. Isolated cells were stored at 4°C and utilised within the same day.

- Mouse ASMCs were isolated enzymatically using 1 mg/ml of papain (Worthington), 1 mg/ml bovine serum albumin (BSA; Sigma), 1 mg/ml dithioerythritol (DTE; Sigma) and 1 mg/ml collagenase (type II; Sigma). Tissue dissection (Section 2.1) was performed in ice cold Dissection solution. Isolated bronchi (Section 2.1) were finely chopped into fragments and placed in a 35mm Nunclon dish containing Dissection solution, for 15-20 minutes at 4°C . Dissection solution was utilised throughout this protocol to ensure that the ASMCs were relaxed during the digestion process. Tissue fragments were then transferred to a 1.5 ml Eppendorf for enzymatic cell dispersion, which was completed in two steps. Firstly, tissue fragments were incubated in the primary dispersal medium comprising papain, BSA and DTE dissolved in Dissection solution for 30 minutes at 37°C . The suspension was then washed thoroughly with dissection solution before incubation in the second dispersal medium containing collagenase, BSA and $100\ \mu\text{M}\ \text{Ca}^{2+}$ dissolved in Dissection solution. This incubation was performed for 7 minutes at 37°C . After 10 minutes, the tissue was thoroughly rinsed again and allowed to rest on ice for 10 minutes. ASMCs were released from the tissue fragments by gentle trituration with three glass pipettes of decreasing diameter. Isolated cells were stored in Dissection solution at 4°C and were utilised within 8 hours.

2.4 Calcium imaging

A suspension of isolated ASMC (2 ml) was added to 2 ml Ca^{2+} -free with 100 μM added CaCl_2 in a WillCo-dish® glass bottom dish (35 x 10 mm), before being mounted on the stage of a Nikon Eclipse Ti microscope. Cells were allowed to stick to the bottom of the dish at room temperature for 40 minutes. Cells were then incubated with 1.5 μM Fluo-4AM (Molecular Probes) in a dark room for 7 minutes prior starting experiments.

After incubation with Fluo-4AM (for chapter 4 experiments), cells were continuously perfused with Hanks solution maintained at 37°C. Moreover, cells under examination were continuously superfused *via* a custom-built close delivery system as shown in *figure 2.2*. This gravity-fed system was comprised of multiple reservoirs (syringe bodies, containing pharmacological agents added to Hanks solution). A three-way tap at the bottom of the syringe body permitted the opening and closing of specific reservoirs. Silicon tubing was attached to the individual three-way taps which extended into a manifold with an outlet consisting of a glass micropipette, with a tip diameter of 200 μM . This micropipette was placed approximately 300 μM from the cell under examination.

Calcium activity in isolated cells was recorded using confocal microscopy. Confocal microscopy is a popular optical method that is widely used in many fields of biological science. It has several advantages over conventional widefield microscopy such as the elimination of out-of-focus signal, the ability to capture information from a reduced focus depth and imaging discrete optical regions in thicker samples. The most widely used confocal technique is confocal laser scanning microscopy (CLSM) in which single point of laser light is used to illuminate a sample.

In this study, a spinning disk confocal laser microscope (SDCLM) was utilised. In SDCLM, the sample is illuminated, and light detected simultaneously at multiple points. In SDCLM, an expanded beam illuminates an array of microlenses arranged on a disk. Each microlens has an associated pinhole laterally co-aligned on a second disk known as pinhole disk and axially positioned at the focal plane of the microlenses. The disks are fixed to a common shaft that is driven at high speed by an electric motor. When the disks spin, and the scanner is coupled

to a microscope with the pinhole disk located in its primary image plane, an array of focused laser beams scan across the specimen. The pinholes and microlenses are arranged in a pattern, which scans a field of view defined by the array aperture size and the microscope objective magnification. The scanning laser beams excite fluorescent labels in the specimen. Fluorescence emission will be most intense where this array is focused - the focal plane. Some fraction of this light will return along the excitation path where it will be preferentially selected by the same confocal pinholes. A dichroic mirror, which reflects emission wavelengths, is located between the two disks. This separates the laser emission from any excitation light reflected or scattered from the microscope optics. The geometry of the emission path results in a confocal fluorescence signal with extremely low background noise.

In the current study, cells were imaged using an iXon 887 electron multiplying charge coupled device (EMCCD) camera (Andor Technology, Belfast; 512 x 512 pixels, pixel size 16 x 16 μM), coupled to a dual Nipkow Spinning Disc (CSU22, Yokogawa, Japan), inclusive of a pinhole disk (PHD) attached to a micro lens disc (MLD). The MLD contains 20,000 micro lenses co-aligned to corresponding pinholes in the PHD, which focus light directly onto the pinholes as the disk revolves at high speed. Consequently, the emission of light reaches the specimen at multiple points simultaneously, resulting in improved light transmission, reduced light damage to the specimen and enhanced image clarity.

A Krypton-argon laser (Melles Griot, UK) was utilised at 488 nm to excite the Fluo-4AM and the resulting fluorescent emissions were detected at >510 nm. Experiments were completed using a x60 objective lens (Nikon Plan Apo VC, 1.4/NA). Images were captured at a frame rate of 15 frames per second (pixel size 0.266 x 0.266 μM).

2.4.1 Image analysis

Image recordings were performed on a desktop PC using Andor iQ software (Andor, Belfast), files were saved as a stack of TIFF (tagged image file format) images. Individual recording files were analysed using ImageJ software (version 1.48, National Institute of Health, MD, USA) for *post-hoc* analysis.

The initial analysis step involves subtraction of the background fluorescence, achieved by subtracting the mean fluorescence of a null frame from each frame to obtain 'F'. A pseudolinescan image was produced by drawing a single line within the cell or within region of interest in the cell and applying the 'reslice' function in ImageJ. This function displays the pixel intensity as a succession of lines, each representing a single frame from the movie stack. These are then arranged vertically, left to right so that the vertical axis of the line-scan represents the length of the cell (μM) and horizontal axis displays time (seconds). This allows for the spatial and temporal aspects of the calcium events to be viewed in a spacio-temporal map. The minimum or basal fluorescence measured between calcium events was defined as ' F_0 '. F/F_0 plots were derived from the entire *post hoc* line scan and plotting the intensity plot profile values in Microsoft Excel. The amplitude of calcium events was determined from the intensity profile by calculating the difference in calcium levels from basal to peak fluorescence, shown as $\Delta F/F_0$.

2.5. Solutions and drugs

2.5.1 Solutions (mM)

Concentrations of salts inside bracket are in millimolar (mM).

1. Krebs Solution

NaCl (120.0), KCl (5.9), NaHCO_3 (25.0), Glucose (5.5), NaH_2PO_4 (1.2), MgCl_2 (1.2), CaCl_2 (2.5).

The solution was bubbled with 95% O_2 and 5% CO_2 to maintain a pH of 7.4.

2. High potassium chloride (KCl) Krebs Solution

NaCl (65.8), KCl (60), NaHCO_3 (25.0), Glucose (5.5), NaH_2PO_4 (1.2), MgCl_2 (1.2), CaCl_2 (2.5).

The solution was bubbled with 95% O_2 and 5% CO_2 to maintain a pH of 7.4 and kept in a water bath at 37°C throughout the experiment.

3. *Ca²⁺ free Solution*

NaCl (125), KCl (5.36), Glucose (10), Sucrose (2.9), NaHCO₃ (15.5), Na₂HPO₄ (0.33), KH₂PO₄ (0.44), HEPES- free acid (10).

pH to 7.4 with NaOH.

4. *Hanks Solution*

NaCl (125), KCl (5.4), Glucose (10), Sucrose (2.9), NaHCO₃ (4.2), KH₂PO₄ (0.4), Na₂HPO₄ (0.3), MgCl₂.6H₂O (0.5), CaCl₂.2H₂O (1.8), MgSO₄.7H₂O (0.4), HEPES- free acid (10).

pH to 7.4 with NaOH.

5. *Dissection Solution*

MSG (80), NaCl (55), KCl (6), Glucose (10), MgCl₂.6H₂O (2), HEPES- free acid (10).

pH to 7.3 with NaOH.

6. *Ca²⁺ free Hanks superfusate Solution*

NaCl (125), KCl (5.36), Glucose (10), Sucrose (2.9), NaHCO₃ (4.17), KH₂PO₄ (0.44), Na₂HPO₄ (0.33), MgCl₂.6H₂O (2.3), EGTA (5.0), MgSO₄.7H₂O (0.4), HEPES-free acid (10).

pH to 7.4 with NaOH.

2.5.2 Drugs

Drug stock solutions were either made in dimethyl sulfoxide (DMSO), ethanol or distilled water (dH₂O) depending on their solvent solubility. All drug stock solutions were stored at 4°C or -20°C depending on the manufacturer's instructions.

<u>Drug</u>	<u>Supplier</u>
Carbachol (muscarinic agonist)	Sigma-Aldrich
Atropine (muscarinic antagonist)	Sigma-Aldrich
Indomethacin (COX-2 inhibitor)	Abcam
CaCC _{inh} -A01 (TMEM16A inhibitor)	Tocris
Benzbromarone (TMEM16A inhibitor)	Tocris
MONNA (TMEM16A inhibitor)	Tocris
Ani9 (TMEM16A inhibitor)	Tocris
Nifedipine (L-type Ca ²⁺ Channel inhibitor)	Ascent Scientific
Verapamil (L-type Ca ²⁺ Channel inhibitor)	Sigma-Aldrich
Tetracaine (Ryanodine inhibitor)	Sigma-Aldrich
GSK-7975A (CRAC channel inhibitor)	Merck
Dantrolene (Ryanodine inhibitor)	Sigma-Aldrich
2-Aminoethoxydiphenylborane (2-APB) (IP ₃ receptor inhibitor)	Sigma-Aldrich
Fluo-4AM (Fluorescent Ca ²⁺ indicator)	Molecular Probes
Caffeine (RyR Activator)	Sigma-Aldrich
Iberitoxin (IbTx) (BK channel inhibitor)	SMARTOX
U-46619 (Thromboxane agonist)	Abcam

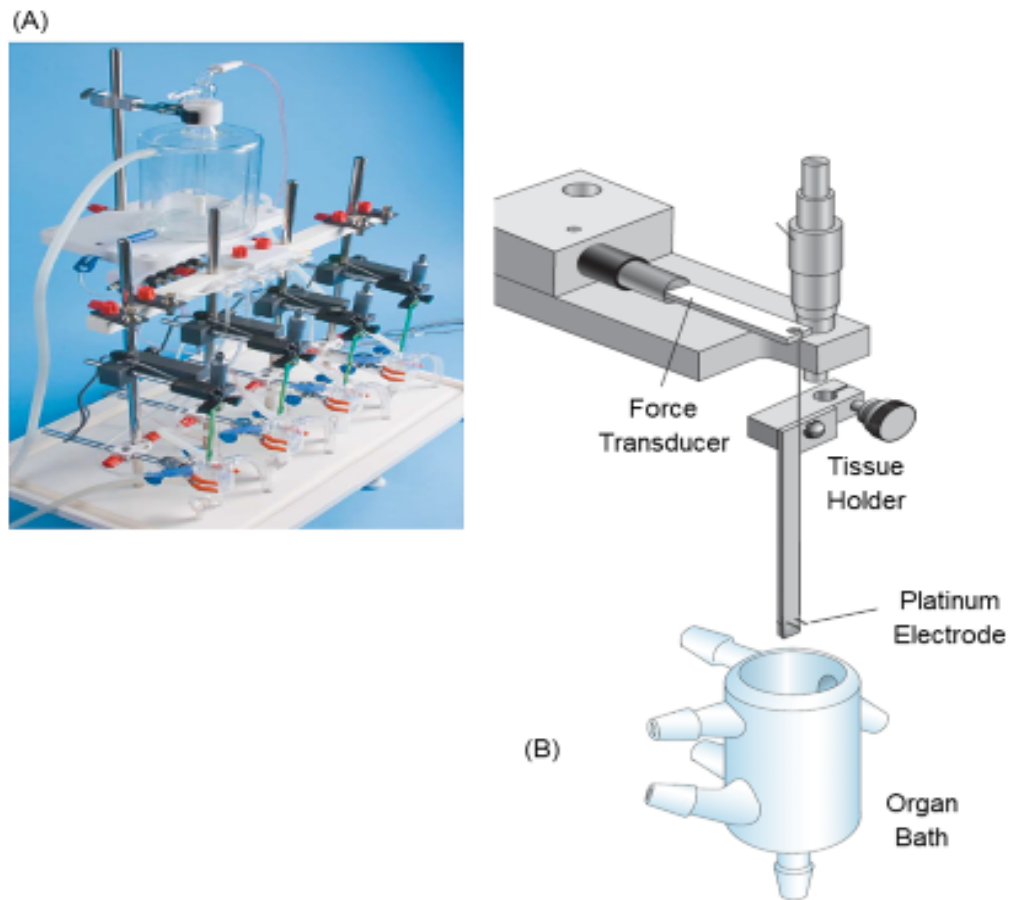


Figure 2.1 (A) A bench top four-channel Myobath system. (B) Illustration of the myobath tension setup. Bronchial ring was tied in between two electrodes on the tissue holder and connected to the force transducer. The tissue was then submerged in a water-jacketed organ bath during isometric tension recordings

(Image adapted from World Precision Instruments, WPI).

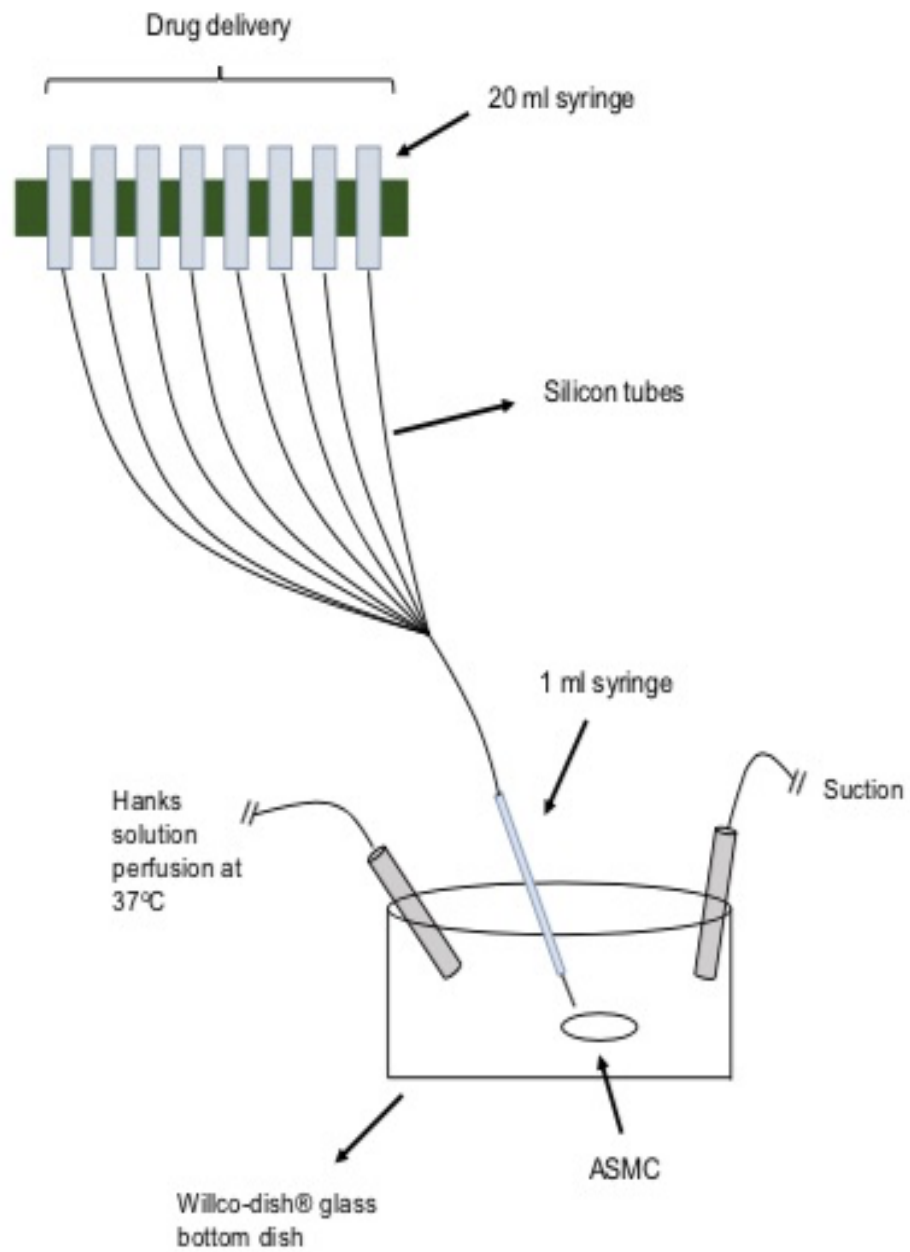


Figure 2.2 Schematic diagram of a custom built drug delivery system used during Ca^{2+} imaging. Drug solutions were administered through a gravity-fed system via capillary tubes to the ASMCs maintained at 35 ± 2 °C.

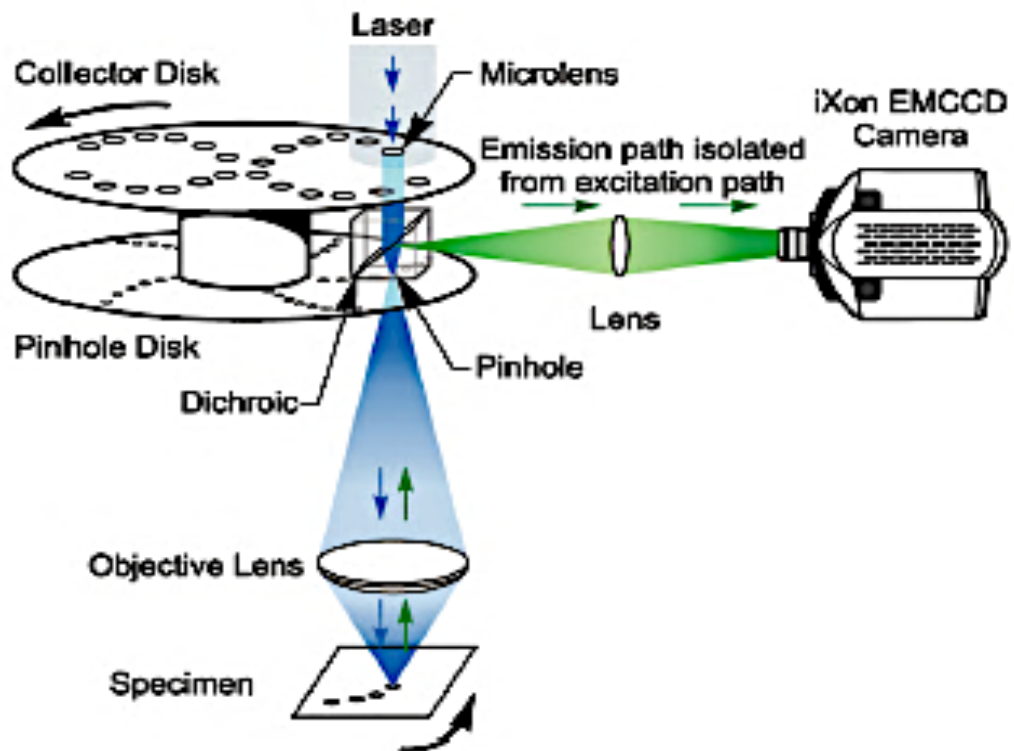


Figure 2.3. Representative image shows how spinning disk confocal laser microscope works.

(Image adapted from Andor Oxford Instruments)

3. Effect of TMEM16A blockers on mouse bronchus smooth muscle contractions induced by CCh

3.1 Introduction

CaCC are well studied anion channels in smooth muscle because of their role in excitation-contraction coupling. Following identification of the channel's molecular identity as TMEM16A (also known as ANO1) in 2008, its involvement in cell physiological functions have been studied. Apart from contributing in airway and vascular smooth muscle contractile activity (Huang *et al.* 2012; Davis *et al.* 2013), the channel is also involved in fluid secretion in epithelia of airways, salivary glands, intestines, renal tubules and sweat glands (Jang & Oh, 2014); inducing electrical pacemaker activity in interstitial cells of Cajal (Sanders *et al.* 2012); controlling cancer cells proliferation, survival and migration (Crottes & Jan, 2019); controlling acute and chronic pain sensation (Oh & Jung, 2016).

Contractions of ASMC are widely considered to amplify airways resistance in diseases like asthma and COPD, and available bronchodilators act on ASMC are basis for treating airways obstruction. In 2015, Danielsson *et al.* proposed a novel approach to bronchodilate the airways using TMEM16A antagonists. Haung *et al.* (2012) proposed that TMEM16A has dual role in epithelial mucin production and ASM contraction making it a potential target for treating airway diseases (Huang *et al.* 2012). In contrast, a recent study undertaken by Wang *et al.* (2017), showed only very minor changes in cholinergic agonist-induced contractions in the airway of TMEM16A deficient mice.

There are a few gaps in the studies done to date to examine TMEM16A involvement in cholinergic contractions in ASM. Key gaps are: i) lack of experimental details provided in studies such as how long cholinergic agonists were applied (Hirota *et al.* 2006); ii) use of only one concentration of cholinergic agonists to study the inhibitory effect of TMEM16A blockers (Hirota *et al.* 2006; Danielsson *et al.* 2015); iii) investigating the effect of TMEM16A blockers only on short applications of multiple concentrations of cholinergic agonist (Wang *et al.* 2017).

Thus, in this study we reinvestigated the effect of blocking TMEM16A channels for longer periods of time to inhibit cholinergic contractions in murine bronchial rings. The effect of four commercially available TMEM16A blockers, CaCC_{inh}-A01 (10 μ M), benzbromarone (1 μ M), MONNA (3 μ M) and Ani9 (10 μ M) were examined. CCh-induced contractions of murine bronchial rings were generated in increasing concentrations (0.1-10 μ M). The effect of TMEM16A blockers were studied on 3 different patterns of concentration-dependent contractions. Short (2 min/concentration) cumulative CCh dose-dependent response, long cumulative CCh dose-dependent response (10 min/concentration) and separate applications of CCh concentrations. In the separate applications of CCh, each concentration was applied for 10 minutes and washed out with Krebs, followed by 15 minutes of rest, before a higher concentration of CCh was applied. In all three patterns of CCh responses, control responses to CCh were obtained and, after wash out, TMEM16A antagonists were applied for 30 minutes before the concentration effect-response to CCh was repeated. The amplitude of the initial contraction and sustained contractions at each concentration were measured for the separate applications.

3.2 Results

3.2.1 Effect of TMEM16A antagonists on CCh-induced contractions

ASMC contractions were elicited by increasing concentration of CCh (0.1-10 μM) and the dose response relationship is shown in to the left of the panel in *figure 3.1A*. All the isometric tension experiments presented in this chapter were carried out in the presence of indomethacin (COX 1/2 inhibitor) to prevent spontaneous relaxations caused by the release of endogenous prostaglandins from epithelial cells. The first TMEM16A blocker examined on CCh-induced contractions was CaCC_{inh}-A01. As shown in panel A of *figure 3.1*, CaCC_{inh}-A01 (10 μM) had a significant effect when each concentration of CCh was applied for 2 min. It had more of an effect on contractions induced by higher concentrations of CCh in comparison to lower. At the lowest concentration of CCh (0.1 μM), mean amplitude of short-exposure contraction was reduced from 3.5 ± 1.1 mN to 2.04 ± 0.7 mN and at the highest CCh contraction (10 μM) mean amplitude of short-exposure was reduced from 7.6 ± 1.6 mN to 4.4 ± 1.0 mN. The summarized data of the experiment is presented as a line-graph in panel C of *figure 3.1*. However, CaCC_{inh}-A01 had a greater effect on longer CCh exposure (10 min) as displayed in panel B of *figure 3.1*. The mean amplitude of 0.1 μM CCh-induced contractions was decreased from 4.3 ± 0.7 mN to 1.1 ± 0.3 mN, whereas at 10 μM CCh-induced contractions mean amplitude was reduced from 8.8 ± 1.4 mN to 3.6 ± 0.5 mN as shown in the panel C of the same *figure*.

In our initial experiments, we applied increasing concentrations of CCh to ASM in a cumulative manner. In the next series of experiments, we evaluated the effect of CaCC_{inh}-A01 on ASM contraction by applying CCh of varying doses to the tissue and washing the tissue of agonist after 10 minutes in between applications, in both the absence and presence of the CaCC_{inh}-A01. The amplitude of CCh contraction at 2 minutes was labelled as the “initial component” and at 10 minutes as the “sustained component”. Panel A & B of *figure 3.2* shows the effect of CaCC_{inh}-A01 on 0.1-10 μM CCh-induced contractions. The inhibitory effects of CaCC_{inh}-A01 on the initial ASMC contraction was more pronounced at higher concentrations of agonist, whereas the sustained component was inhibited by the CaCC antagonist at all CCh doses tested (with the exception of 0.1 μM).The

mean amplitude of the initial contraction elicited by 0.1 μ M CCh was reduced from 2.2 ± 0.7 mN to 1.5 ± 0.3 mN by CaCC_{inh}-A01 as shown in summary data in panel C of *figure 3.2* and the sustained contraction at the same CCh concentration was reduced from 2.0 ± 0.7 mN to 1.5 ± 0.3 mN as shown in summary data in panel D of *figure 3.2*. However, at 10 μ M CCh, the initial component was reduced from 4.6 ± 0.8 mN to 2.8 ± 0.6 mN and mean amplitude of sustained component was reduced from 5.4 ± 0.9 mN to 2.0 ± 0.8 mN. Summarized data are represented in panel C and D of *figure 3.2*.

In a similar series of experiments, we examined effects of a second CaCC antagonist, benzbromarone on agonist induced ASMC contractions. Benzbromarone reduced the amplitude of contractions induced by cumulative CCh application (0.1-10 μ M) under conditions of both brief and long applications of CCh, and this effect was greater at higher CCh concentrations (*figure 3.3 A-D*). It had more inhibitory effect on contractions induced by CCh concentrations CaCC_{inh}-A01. At the lowest concentration of CCh (0.1 μ M), the mean contraction amplitude was reduced from 2.3 ± 0.8 mN to 1.3 ± 0.4 mN and at the highest concentration of CCh (10 μ M) the mean amplitude was reduced from 5.9 ± 1.0 mN to 3.1 ± 0.8 mN. The summarized data of the same experiment is presented in panel C of *figure 3.3*. Benzbromarone had more effect on the longer CCh response (10 min) as displayed in panel B of *figure 3.1*, similar to CaCC_{inh}-A01. The mean amplitude of contractions of long-exposure using 0.1 μ M CCh was decreased from 1.7 ± 0.6 mN before adding benzbromarone to 0.5 ± 0.2 mN in the presence of benzbromarone whereas at 10 μ M CCh-induced contractions, mean amplitude was reduced from 4.1 ± 1.1 mN to 0.7 ± 0.2 mN.

Figure 3.4, panel A displays the outcome of benzbromarone on the CCh-induced contractions at concentrations ranging from 0.1-10 μ M applied separately. The mean amplitude of the initial component at 0.1 μ M CCh-induced contractions was reduced from 3.0 ± 0.4 mN to 0.7 ± 0.4 mN and sustained component at the same concentration was reduced from 3.0 ± 0.5 mN to 0.6 ± 0.3 mN. However, at high CCh (10 μ M), the mean contraction amplitude of the initial component was reduced from 4.9 ± 0.6 mN to 3.5 ± 0.4 mN in the presence of benzbromarone and mean amplitude of the sustained contraction was reduced from 6.0 ± 0.7 mN to 1.1 ± 0.1 mN in the presence of benzbromarone. This suggests that

benzbromarone was more markedly effective at blocking the sustained components of contraction than the initial components and this was confirmed in the summary data in panels C & D of *figure 3.4*.

MONNA, another recently discovered TMEM16A blocker was also investigated. MONNA had greater effect on contractions evoked by longer exposure of CCh than short-exposure as is evident from panel A & B of *figure 3.5*. At the highest concentration of CCh (10 μ M) the mean contraction amplitude reduced from 5.4 ± 1.0 mN to 5.0 ± 0.8 mN in short-exposure as shown in summarized data in the *figure 3.5C*. MONNA had more inhibitory effect on the sustained response like benzbromarone and CaCC_{inh}-A01 as displayed in panel B&D of *figure 3.5*.

Panel A of *figure 3.6* shows the effect of MONNA on the cholinergic contractions induced by separate applications of CCh concentrations of 0.1-10 μ M. In this trace it is evident that the drug affected sustained contractions more than initial contractions, at least at the higher concentrations of CCh. Summary data are shown in panels C & D, where the greater effect on sustained versus initial contractions was confirmed. At 0.1 μ M CCh, the mean amplitude of the initial contraction component was reduced from 2.6 ± 0.6 mN to 1.1 ± 0.4 mN by MONNA and the sustained contraction at the same CCh concentration was reduced from 2.3 ± 0.7 mN to 0.9 ± 0.2 mN. At the highest CCh concentration of 10 μ M, the initial contraction component was reduced from 4.8 ± 0.9 mN to 3.4 ± 0.7 mN and the mean amplitude of sustained contraction component was reduced from 5.2 ± 1.1 mN to 1.9 ± 0.7 mN.

Lastly Ani9, a novel TMEM16A blocker was also examined. Ani9 is most potent and selective blocker of the TMEM16A channel compared to any other blockers tested (Seo *et al.* 2016). Overall, the drug had significant but small effect on cholinergic contractions, regardless of whether the exposure was for 2 mins or 10 mins, as shown in panel A and B of *figure 3.7*. The mean amplitude of the contractions in response to short exposures to CCh did not significantly change in the presence of Ani9, e.g., from 2.8 ± 0.6 mN to 3.1 ± 0.4 mN at 0.1 μ M CCh and from 7.2 ± 1.2 mN to 7.3 ± 1.4 mN at 10 μ M. The summarized data for a series of similar experiments is shown in panel C of *figure 3.6*. Similarly, for 10 mins cumulative dose response the mean amplitude at 0.1 μ M CCh-induced contractions decreased slightly from 3.5 ± 0.9 mN to 2.9 ± 0.9 mN, whereas at

10 μM CCh-induced contractions, the mean amplitude slightly increased from 6.5 ± 1.0 mN to 7.0 ± 1.1 mN, but neither change was significant.

In separate applications of CCh concentrations (0.1-10 μM), Ani9 had no effects on both initial and sustained components of agonist-induced contractions, unlike other CaCC antagonists tested in this study. Shown in panel A & B of *figure 3.8*, is the effect of Ani9 on CCh-induced contractions evoked by 0.1-10 μM . Ani9 had no inhibitory effect on contractions induced by all the CCh concentrations. However, in the next step, nifedipine was applied in the presence of Ani9, the amplitude of CCh contractions was significantly reduced. For instance, the mean amplitude of the initial contraction induced by 0.1 μM CCh remained unchanged in the presence Ani9 2.2 ± 0.5 mN to 2.3 ± 0.5 mN, next in the presence of both nifedipine and Ani9, contraction amplitude was significantly reduced from 2.3 ± 0.5 mN to 0.46 ± 0.2 mN. Similar inhibitory pattern was observed for all the other CCh concentrations and for both initial and sustained components as shown in summarized data in panel D & E of the same *figure*. This experiment result suggest that L-type Ca^{2+} channel can be activated in the absence of TMEM16A.

3.2.2 Effect of L-type Ca^{2+} channels blocker on CCh-induced contractions

Numerous studies have reported that CaCC channels mediate SM contraction by inducing depolarization and subsequently activating L-type Ca^{2+} channels (Wray *et al.* 2021, Brozovich *et al.* 2016). However, their role is more controversial in ASM (Janssen, 2002). With three CaCC blockers having similar inhibitory effect on cholinergic contraction raised a question about non specific effects of these blockers through blocking of L-type Ca^{2+} channels. Thus, we aimed at examining inhibitory effect of L-type Ca^{2+} channels on cholinergic contractions using dihydropyridine blocker.

The L-type Ca^{2+} blocker tested for this study was nifedipine. 1 μM of nifedipine significantly reduced the cholinergic contractions induced by CCh in the concentration range of 0.1-10 μM . In *figure 3.9*, the isometric tension recording in panel A shows the effect of nifedipine on short applications of CCh concentrations. At 0.1 μM , the lowest concentration of CCh, the mean amplitude of contractions were reduced from 1.9 ± 0.1 mN to 0.4 ± 0.1 mN and at the highest

CCh concentration (10 μM) mean amplitude of short-time application was reduced from 4.1 ± 0.4 mN to 2.8 ± 0.4 mN.

As shown in *figure 3.9B*, blocking L-type Ca^{2+} with nifedipine significantly reduced the amplitude of ASMC contractions induced by all CCh concentrations tested (0.1-10 μM), and this was true for both short and longer CCh applications (*figure 3.9 C&D*). At the lowest concentration of CCh 0.1 μM , the mean amplitude of contractions were reduced from 3.0 ± 0.5 mN to 0.7 ± 0.2 mN and at the highest CCh concentration (10 μM) mean amplitude of contraction was reduced from 6.0 ± 0.9 mN to 4.8 ± 0.6 mN. In conclusion, nifedipine reduced the effects of all concentrations of CCh and affected contractions in response to short (2 min) and long (10 min) applications of CCh approximately equally.

3.2.3 Effect of TMEM16A blockers on cholinergic-induced contractions in the presence of nifedipine

Experiments performed with CaCC blockers and L-type Ca^{2+} blocker suggest involvement of L-type Ca^{2+} channels following depolarization caused by activation of CaCC channels in cholinergic-mediated contractions in mice airway. Some TMEM16A blockers have been shown to block L-type Ca^{2+} channels (Hannigan *et al.* 2017; Fedigan *et al.* 2017). However, TMEM16A blockers except Ani9 in the present study had a greater effect on sustained than initial contractions and more of an effect on contractions induced by higher CCh concentrations than lower, whereas, L-type Ca^{2+} channels blockers had an overall similar effects on cholinergic contractions independent of CCh concentrations or duration of the applications. It was nevertheless puzzling that the effects of the TMEM16A blockers and nifedipine were not more similar, because the usual working hypothesis of how TMEM16A channels stimulate smooth muscle is due to depolarisation of the SMC (due to Cl^- efflux when TMEM16A channels open), followed by activation of L-type Ca^{2+} channels and Ca^{2+} influx across the plasma membrane. If the TMEM16A blockers in the present study were working this way, and not by a nonspecific mechanism (e.g. by L-type Ca^{2+} channels directly, or by yet another mechanism), we reasoned that, if we applied them in the presence of nifedipine, they should have no additional inhibitory effect than nifedipine. 1 μM of nifedipine completely blocked

high K⁺ contractures indicating used concentration of the blocker is sufficient to inhibit L-type Ca²⁺ channels in bronchial smooth muscle as shown in *figure 5.3*.

Cumulative CCh concentration-evoked contractions protocol with longer CCh application (10 min) for each concentration (0.1- 10 μM) was used to performed next series of experiment. Started with control cumulative CCh response, the tissue was then treated with the L-type Ca²⁺ channels blocker, nifedipine (1 μM) followed by repeated CCh responses. Next, after wash-out tissues were treated with nifedipine (1 μM) and a TMEM16A blocker together, after which the CCh responses were repeated again.

The effect of CaCC_{inh}-A01 in the presence of nifedipine was investigated first. The trace in panel 3.10A confirm that the effect of CaCC_{inh}-A01 on CCh-induced contractions of murine bronchial rings are independent of L-type Ca²⁺ channels. Like *figure 3.1B*, CaCC_{inh}-A01 had a greater effects on contractions induced by high CCh concentrations in this experiment. The summary data are presented in the panel B of *figure 3.10*.

Next, the effect of benzbromarone in the presence of L-type Ca²⁺ channels blocker was investigated. The trace in panel 3.11A shows that like CaCC_{inh}-A01, the effect of benzbromarone on CCh-induced contractions was not affected by L-type Ca²⁺ channels blockade and therefore mediates its effects independently of L-type Ca²⁺ channels. The effect of benzbromarone in this case was the same as observed when the tissue was treated with benzbromarone alone (*figure 3.3*; panel B). The summary data are presented in the panel B of *figure 3.11*.

Next, the effect of MONNA was examined in the presence of nifedipine. The trace in panel 3.12A shows that like CaCC_{inh}-A01 and benzbromarone, MONNA in the presence of nifedipine reduced the contraction amplitude. The summary data in the panel B of *figure 3.12* confirm this effect.

Lastly, the effect of Ani9 in the presence of nifedipine was examined. The representative isometric traces are shown in *figure 3.13*. Panel A shows that Ani9 made little difference, if applied in the presence of nifedipine. These results are summarized in panel B.

3.2.4 Effect of TMEM16A inhibitors on KCl-induced contractions

A series of experiments on high KCl-induced contractions were carried out in order to determine whether these TMEM16A blockers affect contractions which relies on membrane depolarisation. In normal isometric tension experiments, the concentration of K^+ was 5.9 mM in the extracellular solution. To induce KCl-mediated contractions, the molarity of KCl was increased to 60 mM in Krebs solution. The high concentration of K^+ depolarizes the SMC membrane and activates voltage-dependent Ca^{2+} channels which causes an influx of extracellular Ca^{2+} , thus increasing cytosolic free Ca^{2+} , resulting in contraction (Webb, 2003). To prevent spontaneous relaxations caused by the release of endogenous prostaglandins from epithelial cells, the COX 1/2 inhibitor, indomethacin (10 μ M) was present throughout.

Janssen *et al.* (2004) used 1 μ M atropine, a muscarinic receptor antagonist, in high K^+ experiments in porcine ASM with the objective to block constriction evoked by KCl-induced release of acetylcholine (Janssen *et al.* 2004). Control experiments were performed in the absence and presence of atropine to demonstrate what portion of the high K^+ -induced contraction was due to the release of ACh. A representative isometric trace in *figure 3.14A*, shows that atropine reduced the amplitude of high K^+ -induced contractions by more than two thirds. Summary data from experiments are plotted as a bar graph in panel B of *figure 3.14*, exhibiting mean amplitude of the peak of contraction in both cases. All four inhibitors CaCC_{inh}-A01, benzbromarone, MONNA and Ani9 were examined on high K^+ -induced contractions in the presence of indomethacin and atropine. The TMEM16A inhibitor, CaCC_{inh}-A01 had a minor relaxant effect on high K^+ -induced contractions. CaCC_{inh}-A01 (10 μ M), which was the same concentration used in the CCh experiments, significantly reduced the peak of high K^+ -induced contractions by 19% as shown in *figure 3.15A*. However, no significant change was observed in sustained component of high K^+ contracture by the blocker. Summarized data are shown as a bar-graph in panel B & C of *figure 3.15*.

Benzbromarone 1 μ M had a different effect on both components of high K^+ contractions, with only a 8% reduction in peak of high K^+ contraction amplitude recorded. Whereas, the sustained component of high K^+ contractions was

reduced by 37%. The representative isometric tension trace of the experiment is presented in the panel A in the *figure 3.16*. The mean amplitude of the peak of high K⁺-induced contractions was reduced from 1.18 ± 0.43 mN to 1.08 ± 0.45 mN following incubation with benzbromarone while mean amplitude of the sustained K⁺- contractions was reduced from 1.23 ± 0.4 mN to 0.77 ± 0.2 mN. The summarized data are displayed as a bar graph in panel B & C of *figure 3.16*. MONNA appeared to have a small effect on on high K⁺ induced contractions in some experiments, but overall this was not statistically significant, *figure 3.17*. Ani9 had minor effect on cholinergic contractions as shown in experiments presented in *figure 3.7 & 3.8*. Ani9 10 µM was investigated on high K⁺ contractures as shown in panel A of *figure 3.18*. Summarized data are displayed in panel B & C of *figure 3.18*. At the concentration of Ani9 tested (10 µM), there was no significant effects on KCl induced contractions.

3.2.5 Effect of Ani9 on thromboxane agonist-induced contractions

Ani9 had little to no effect on CCh-induced contractions in the present study, but we know that it is a potent blocker of TMEM16A currents in both HEK293 cells and native mouse smooth muscle cells from patch clamp experiments performed in the Smooth Muscle Research Centre laboratory in DkIT by Dr Eamonn Bradley. However, we hypothesized if Ani9 was breaking down in the bronchial tissue as it was not stable in blood plasma (Seo *et al.* 2018). Wang *et al.* 2017 showed that in TMEM16A knockout mice contractions induced by the thromboxane agonist, U-46619, were about 60% less than those in the wild-type, even though the cholinergic contractions were similar in each case. In the current study, Ani9 was applied to phasic contractions induced by 0.1 µM of U-46619 without indomethacin (COX1/2 blocker). Ani9 (3 µM) significantly inhibited 90% of phasic contraction as shown in panel A of *figure 3.19*. Mean contraction before and after treatment with Ani9 was compared by measuring the area. Area was reduced from 371.1 ± 83.1 to 38.8 ± 8.2 mN.s, as shown in the summary bar chart in *figure 3.19B*. This suggests that the Ani9 was able to work effectively in whole tissue.

3.2.6 Effect of benzbromarone on cholinergic contractions after inhibiting BK channels

Some CaCC blockers have been previously shown to activate BK channels (Srikanth Dudem, personal communication). We hypothesized that CaCC blockers might be having inhibitory effect on cholinergic contractions by activating BK channels. Therefore, separate CCh experiments were performed where benzbromarone was applied in the presence of iberiotoxin to inhibit BK channels. In *figure 3.20*, panel A, B and C represents a trace of an experiment where A is control, B is in the presence iberiotoxin and C is in the presence of iberiotoxin and benzbromarone. On treating with iberiotoxin, the amplitudes CCh-induced contractions increased at all concentrations, though much more markedly at the lower CCh concentrations. The mean amplitude of the initial contraction elicited by 0.1 μM CCh was increased from 0.45 ± 0.3 mN to 3.5 ± 0.8 mN and the sustained contraction at the same CCh concentration was increased from 0.35 ± 0.2 mN to 3.2 ± 0.7 mN. At highest CCh concentration of 10 μM , the initial component was amplified from 3.8 ± 1.0 mN to 4.1 ± 0.8 mN and mean amplitude of sustained component was amplified from 3.7 ± 0.8 mN to 5.2 ± 0.9 mN. However, when benzbromarone was applied the amplitudes of the contractions at all CCh concentrations were significantly reduced, as before. The mean amplitude for 0.1 μM CCh was reduced from 3.5 ± 0.8 mN to 0.8 ± 0.5 mN compared to iberiotoxin and the sustained contraction at the same CCh concentration was reduced from 3.2 ± 0.7 mN to 0.3 ± 0.09 mN. At 10 μM CCh concentration, the initial component was reduced from 4.1 ± 0.8 mN to 2.7 ± 0.7 mN and the sustained component was reduced from 5.2 ± 0.9 mN to 0.8 ± 0.2 mN. Thus the effects of benzbromarone were unlikely to have resulted from activation of BK channels.

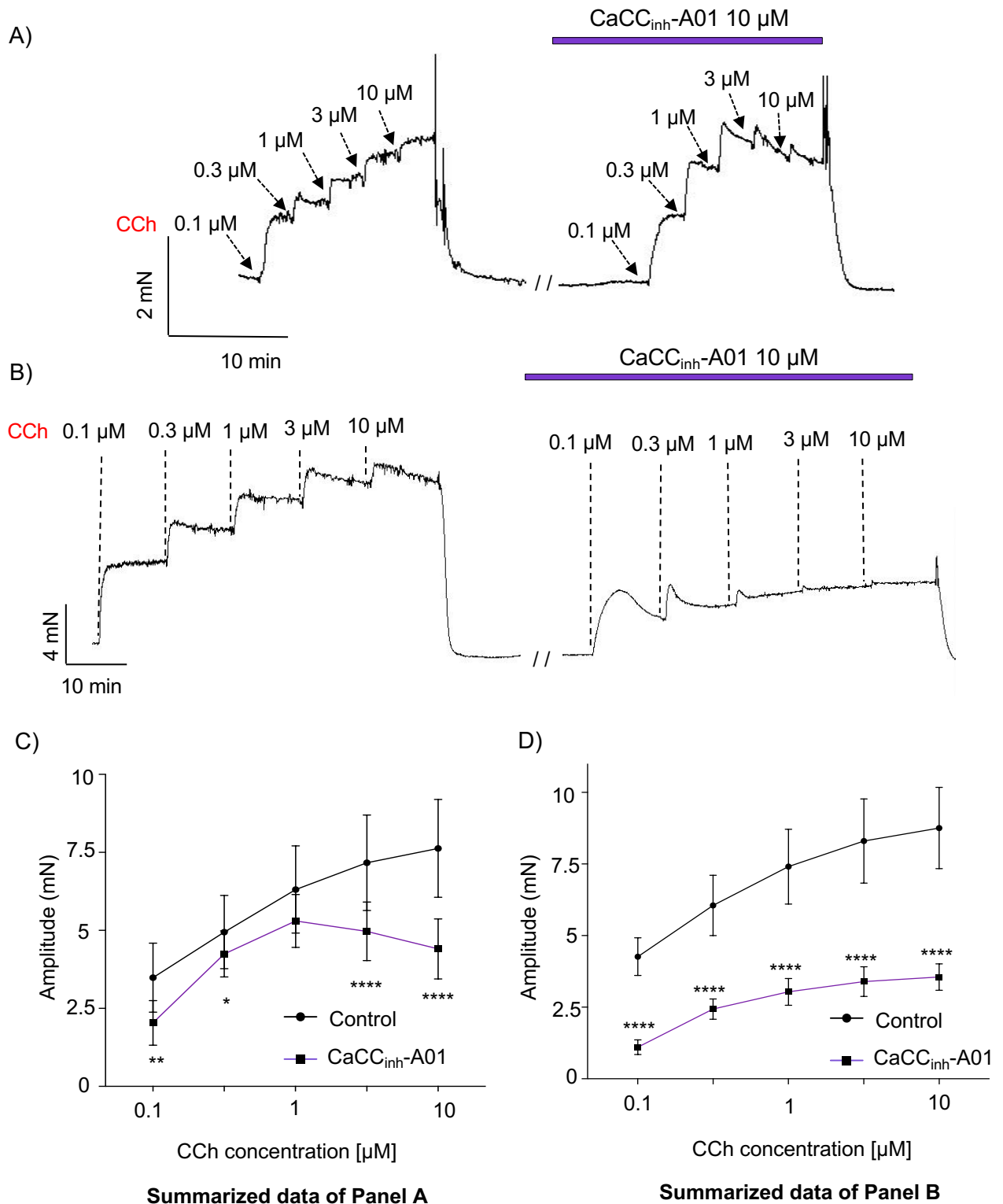


Figure 3.1. Effect of CaCC_{inh}-A01 on carbachol-induced contractions in mouse bronchial rings.

Panel A and B represents tension recording showing the effect of the TMEM16A blocker CaCC_{inh}-A01 (10 μM) on CCh-induced contraction (0.1, 0.3, 1, 3, 10 μM). Panel A) short (2 min/concentration); B) sustained (10 min/concentration). Panel C and D shows summarized data as line graph (n=6; N=6) of mean amplitude of short and sustained response C) and D) respectively for each CCh concentration.

ANOVA, *p<0.05, **p<0.005, ****p<0.0001 compared to control.

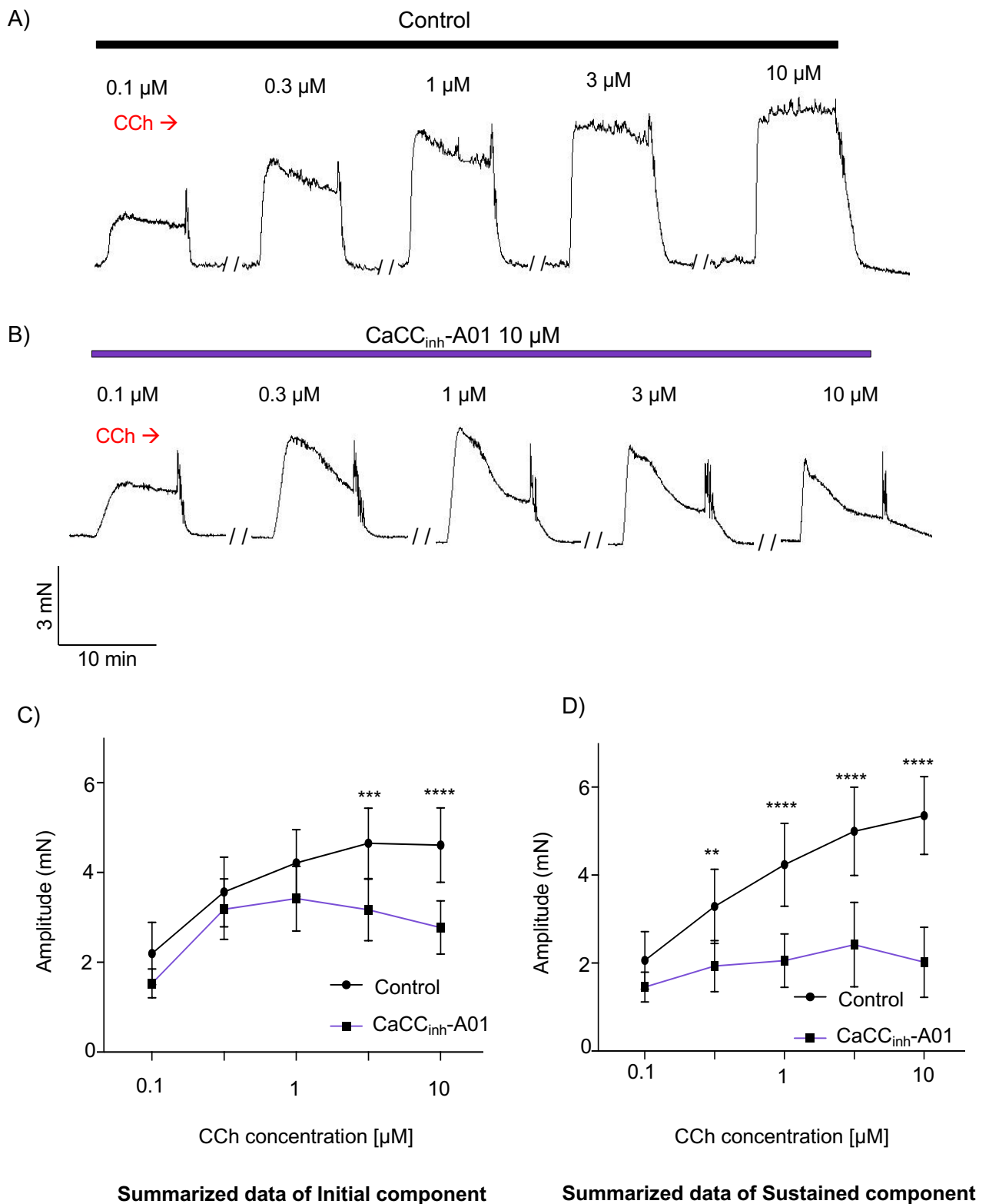


Figure 3.2. Effect of CaCC_{inh}-A01 on carbachol-induced contractions in mouse bronchial rings.

Representative isometric tension trace showing the effect of the TMEM16A blocker CaCC_{inh}-A01 (10 μM) on CCh-induced contraction (0.1, 0.3, 1, 3, 10 μM) separately; each concentration was applied for 10 minutes. Panel A and B represent before and after treatment with CaCC_{inh}-A01 respectively. Summarized data represented as line graph (n=6; N=6) of mean amplitude of initial (2 min) and sustained (10 min) response in panel C and D respectively of each CCh concentration.

ANOVA, **p<0.005, ***p<0.001, ****p<0.0001 compared to control.

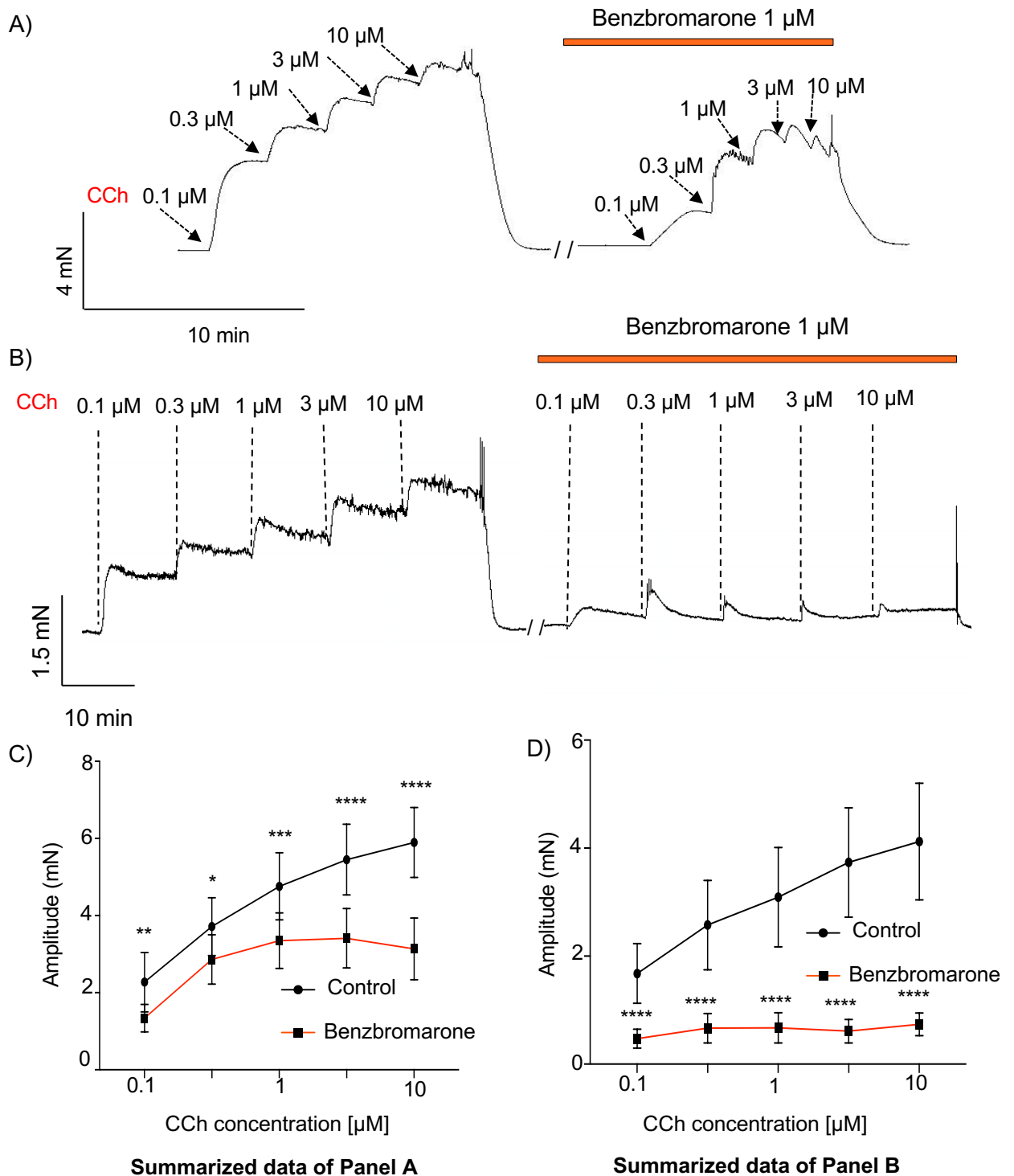


Figure 3.3. Effect of benzbromarone on carbachol-induced contractions in mouse bronchial rings.

Isometric tension traces in panel A and B represents the effect of TMEM16A blocker benzbromarone ($1 \mu\text{M}$) on CCh-induced ($0.1, 0.3, 1, 3, 10 \mu\text{M}$) short (2 min/concentration) and sustained (10 min/concentration) contractions, respectively. Panel C and D shows summarized data as line graph ($n=6; N=6$) of mean amplitude of initial and sustained CCh response for each CCh concentration, respectively.

ANOVA, $*p<0.05$, $**p<0.005$, $***p<0.001$, $****p<0.0001$ compared to control.

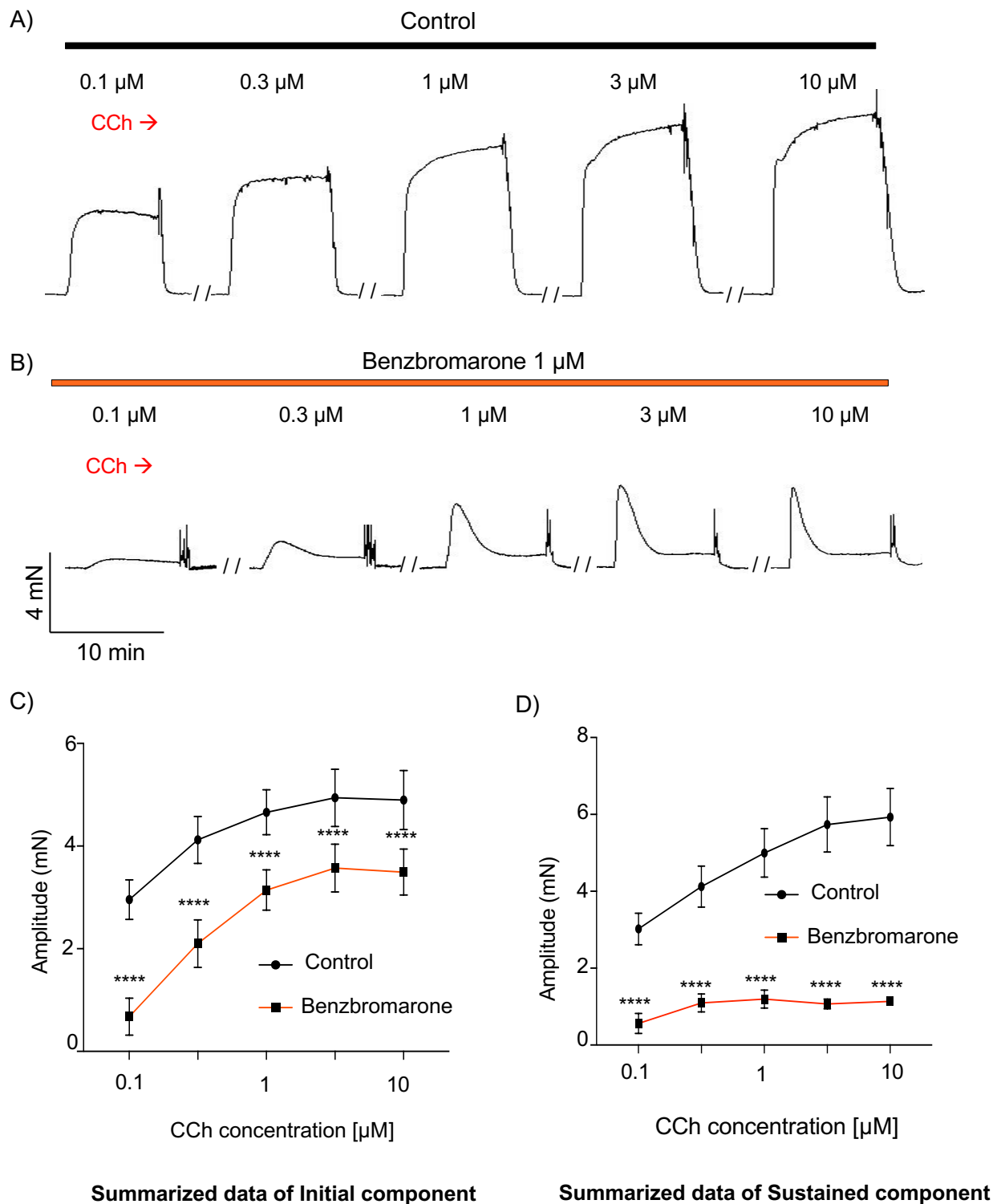


Figure 3.4. Effect of benzbromarone on carbachol-induced contractions in mouse bronchial rings.

Representative tension recording showing the effect of TMEM16A blocker benzbromarone (1 μM) on CCh-induced contraction (0.1, 0.3, 1, 3, 10 μM), with CCh concentrations added separately. Panel A and B represents before and after treatment of bronchial rings with benzbromarone, respectively. Summarized data represented as line graph (n=6; N=6) of mean amplitude of initial and sustained response in panel C and D respectively for each CCh concentration.

ANOVA, ****p<0.0001 compared to control.

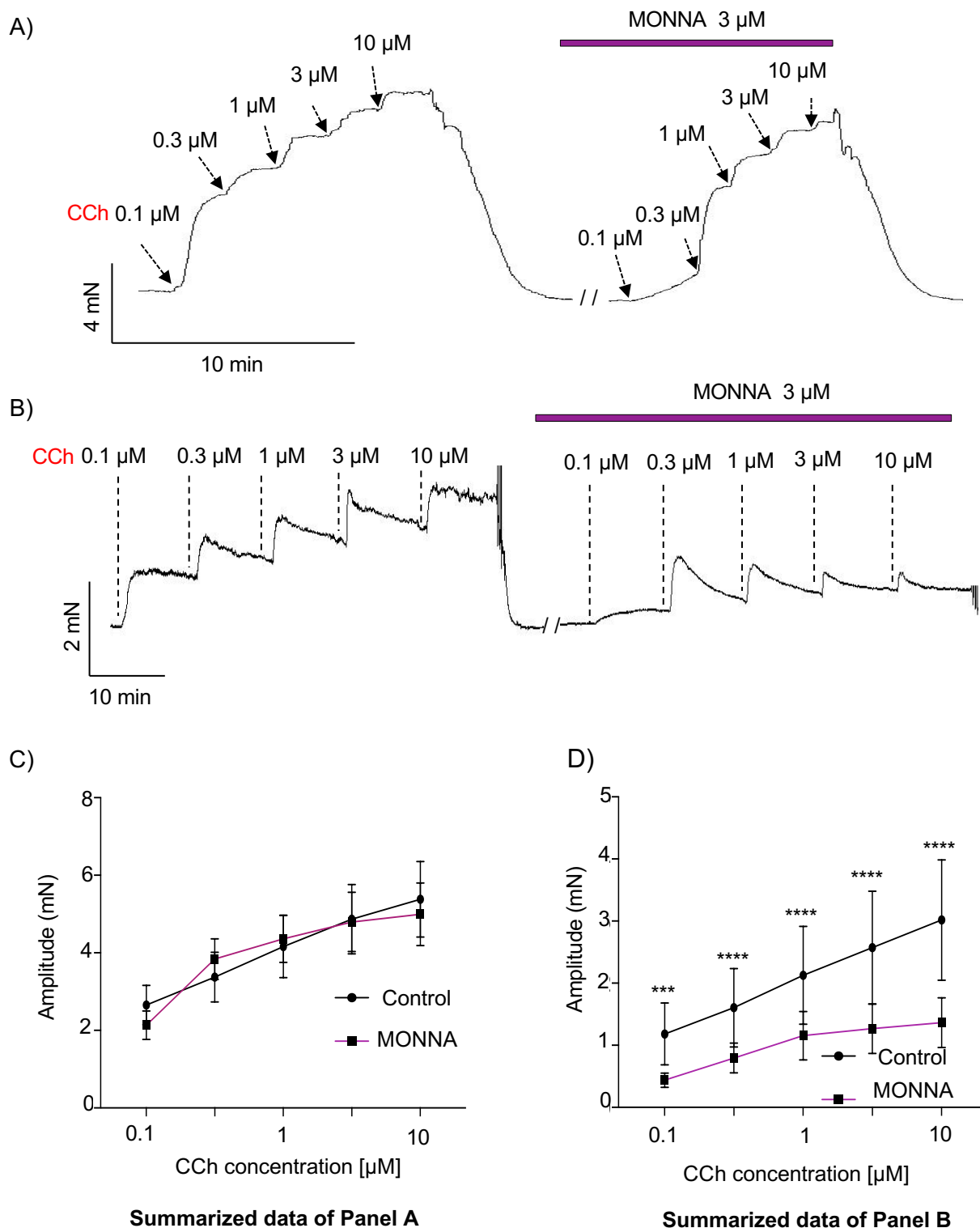


Figure 3.5. Effect of MONNA on carbachol-induced contractions in mouse bronchial rings.

Panel A and B represents tension recording showing the effect of TMEM16A blocker MONNA (3 μM) on CCh-induced contraction (0.1, 0.3, 1, 3, 10 μM). Panel A) short (2 min/concentration); B) sustained (10 min/concentration). Panel C and D shows summarized data as line graph (n=6; N=4) of mean amplitude of short (2 min) and sustained (10 min) response respectively for each CCh concentration. ANOVA, **p<0.005, ****p<0.0001 compared to control.

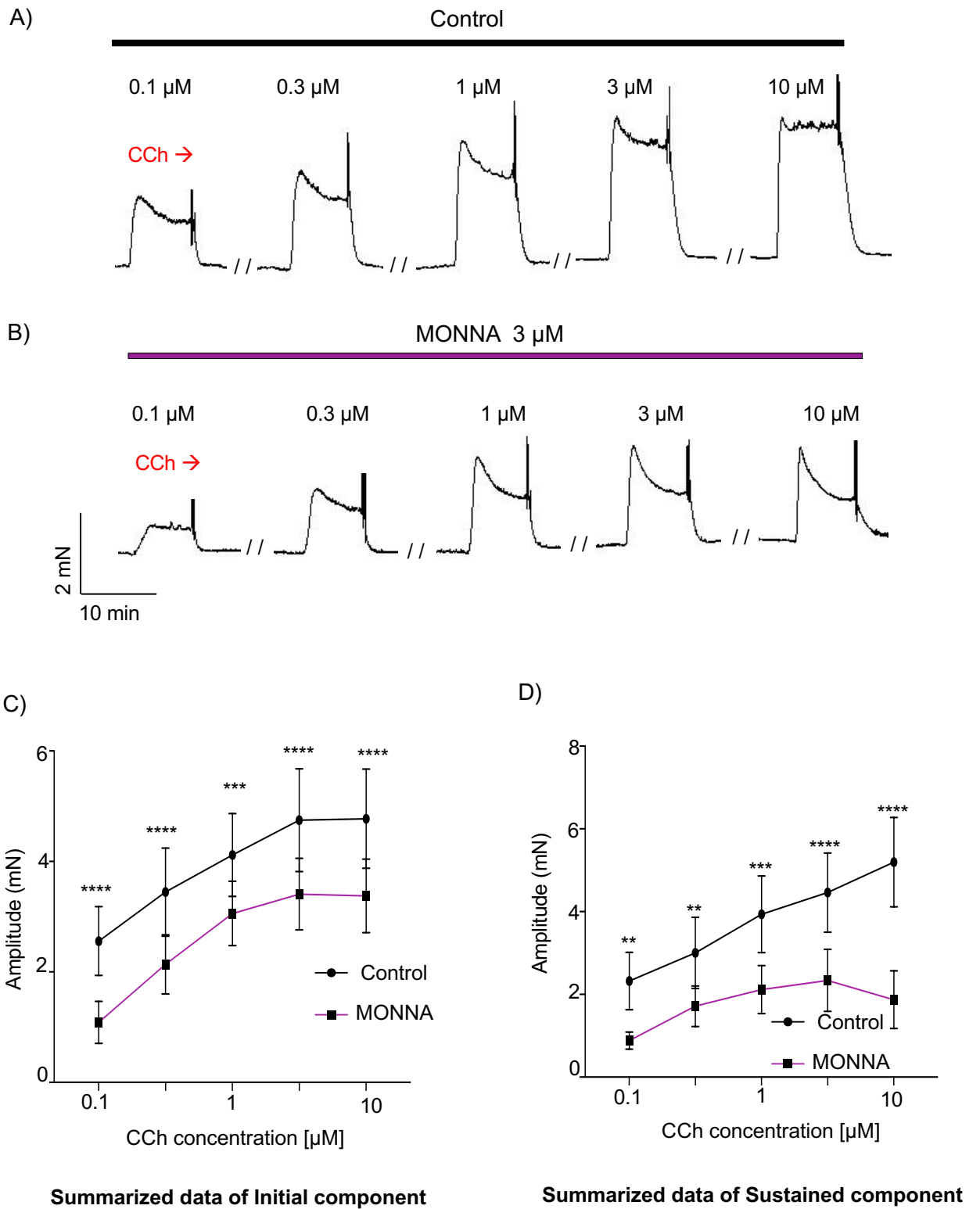


Figure 3.6. Effect of MONNA on carbachol-induced contractions in mouse bronchial rings.

Representative tension recording showing the effect of TMEM16A blocker MONNA (3 μM) on CCh-induced contraction (0.1, 0.3, 1, 3, 10 μM) separately. Panel A and B represent before and after treatment with MONNA respectively. Summarized data represented as line graph (n=6; N=4) of mean amplitude of initial and sustained response (C) and (D) respectively for each CCh concentration.

ANOVA, **p<0.005, ***p<0.001 ****p<0.0001 compared to control.

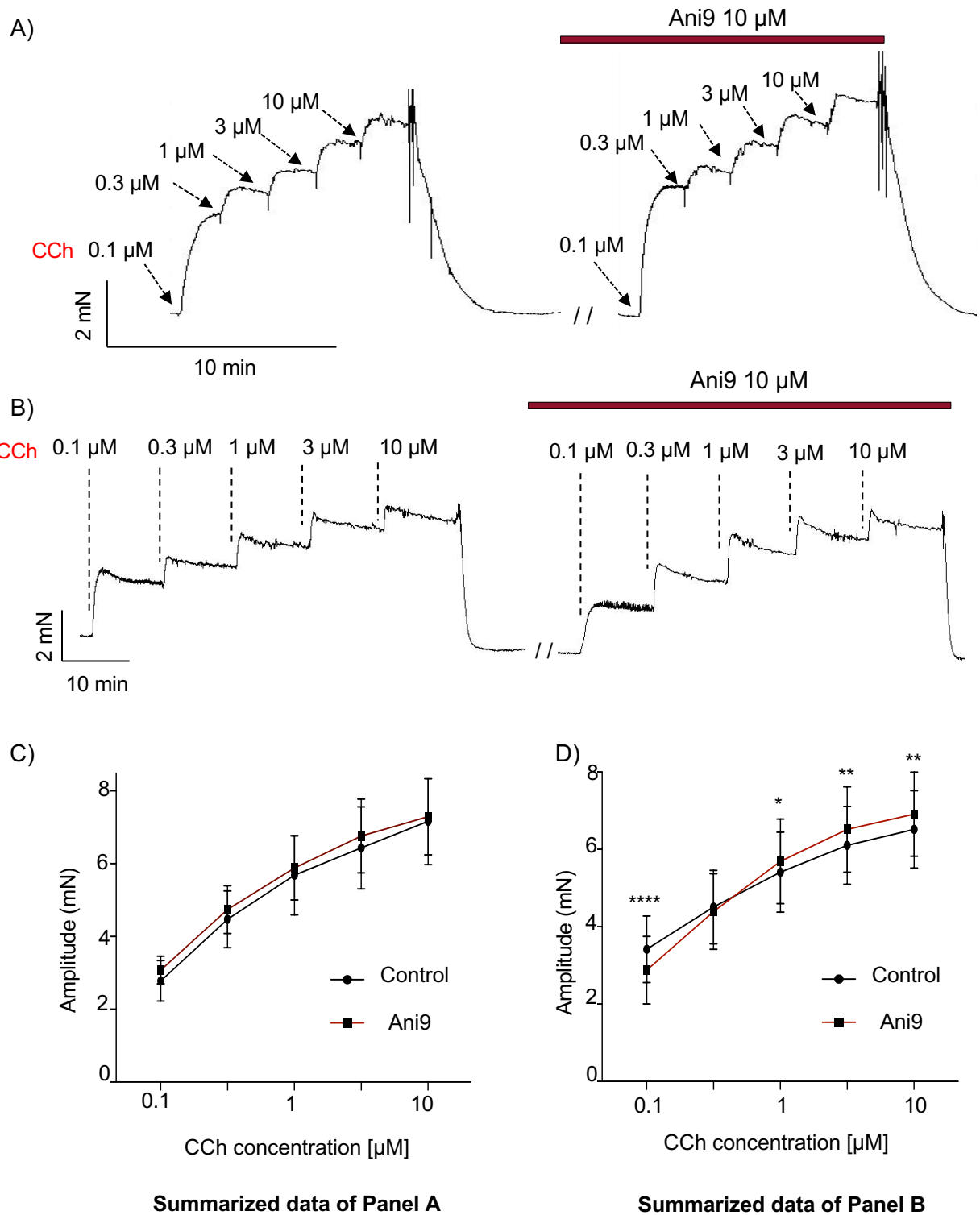


Figure 3.7. Effect of Ani9 on carbachol-induced contractions in mouse bronchial rings.

Representative tension recording showing the effect of a novel TMEM16A blocker Ani9 (10 μM) on CCh-induced contractions (0.1, 0.3, 1, 3, 10 μM) A) short (2 min/concentration) and B) sustained (10 min/concentration). Summarized data represented as line graph (n=6; N=6) of mean amplitude of short (2 min) and sustained (10 min) response as shown in C and D panel respectively for each CCh concentration.

ANOVA, * $p < 0.05$, ** $p < 0.005$, **** $p < 0.0001$ compared to control.

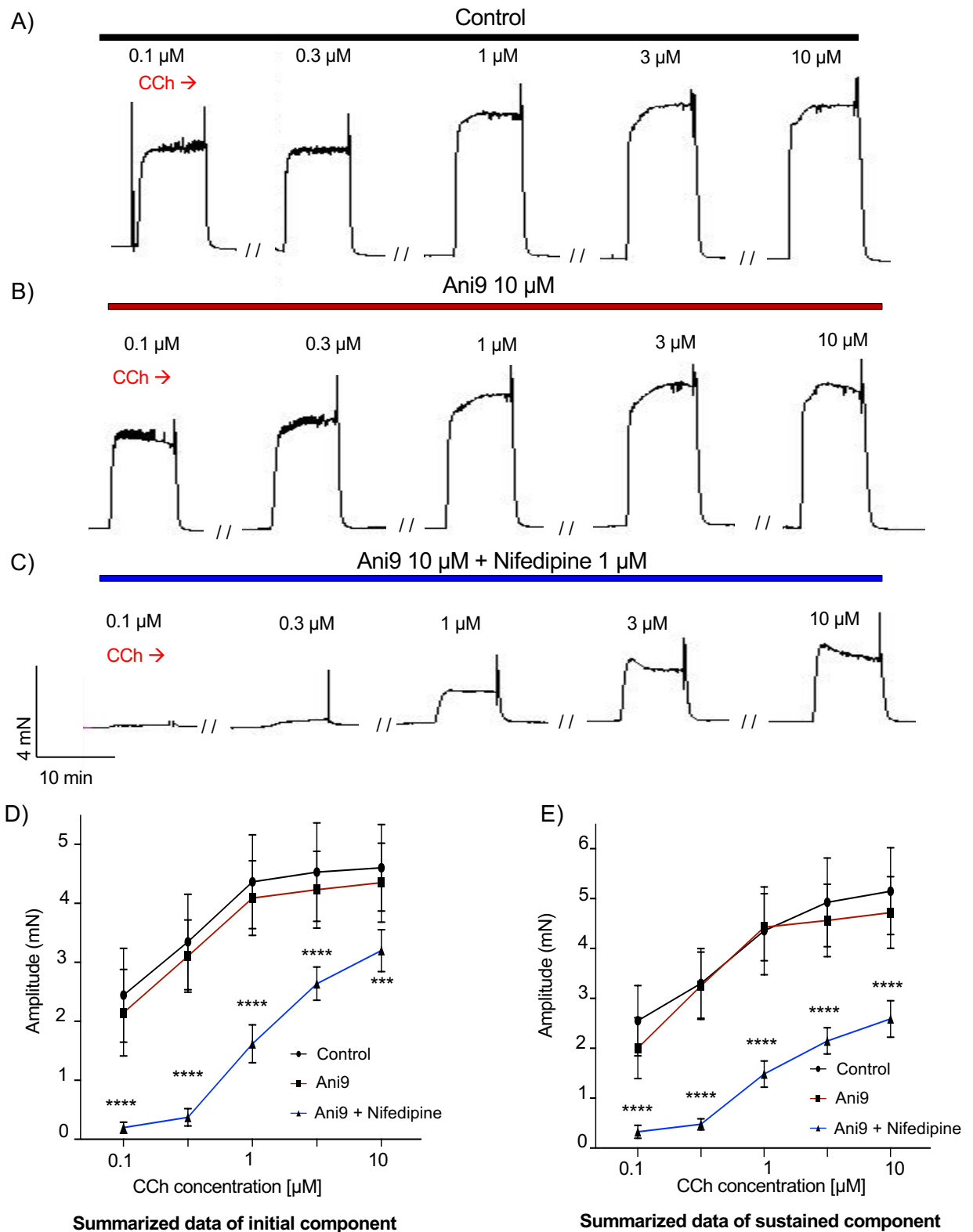


Figure 3.8. Effect of nifedipine on carbachol-induced contractions in presence of Ani9 in mouse bronchial rings.

Representative tension recording showing the effect of LTCC blocker nifedipine (1 μM) in presence of Ani9 (10 μM) on CCh-induced contraction (0.1, 0.3, 1, 3, 10 μM). Panel (A) control, (B) Ani9 (10 μM), (C) Ani9 (10 μM) with nifedipine (1 μM). Summarized data represented as line graph ($n=6$; $N=6$) of mean amplitude of initial (D) and sustained CCh responses (E) of all three sets; which were measured within 2nd and at 10th minutes for each CCh contractions, respectively. ANOVA, **** $p<0.0001$; comparing Ani9 + Nifedipine vs Ani9.

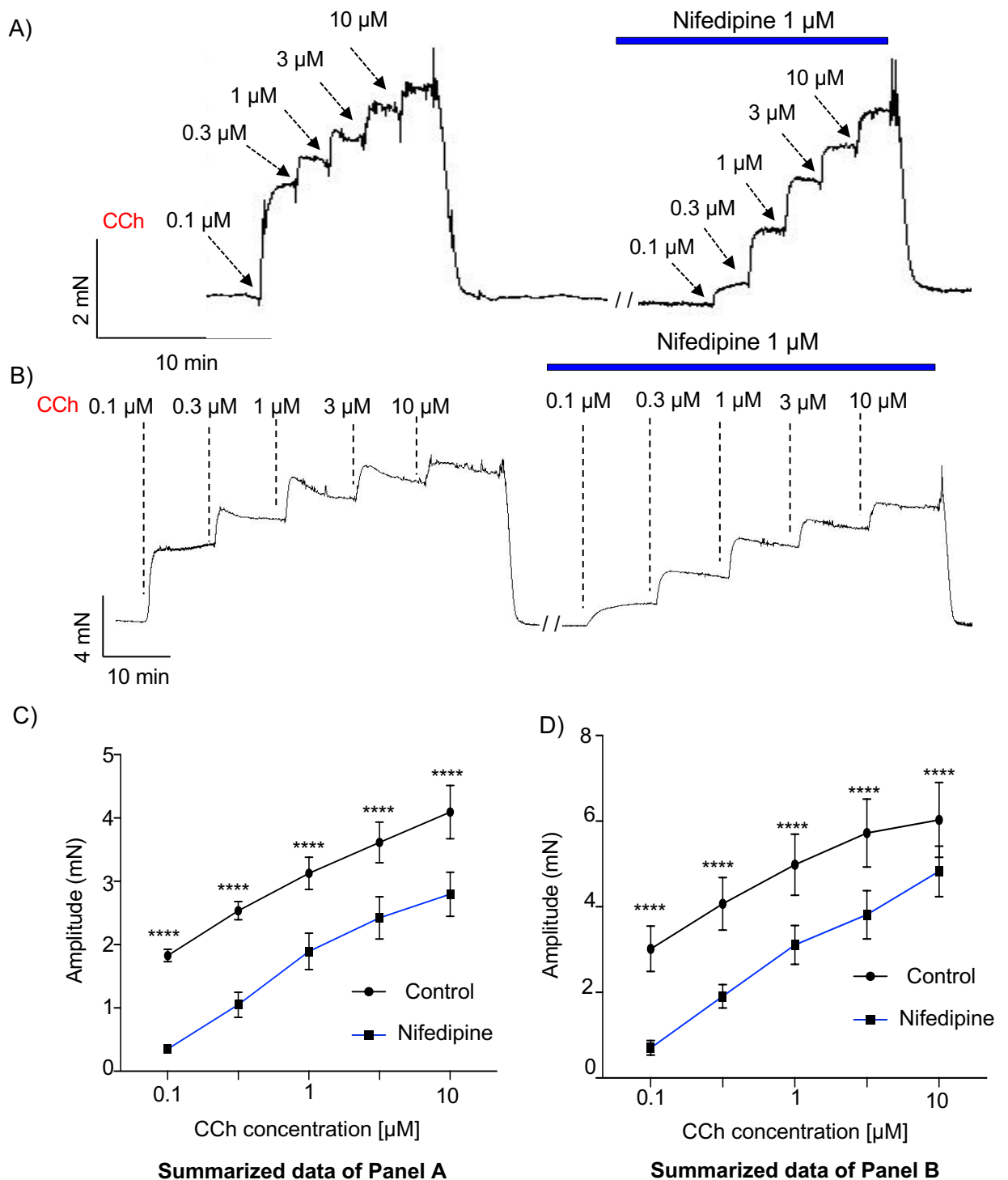


Figure 3.9. Effect of nifedipine on carbachol-induced contractions in mouse bronchial rings.

Isometric tension traces in panel A and B represents the effect of LTCC blocker nifedipine ($1 \mu\text{M}$) on CCh-induced ($0.1, 0.3, 1, 3, 10 \mu\text{M}$) short (2 min/concentration) and sustained (10 min/concentration) contractions, respectively. Panel C and D shows summarized data as line graph ($n=6$; $N=6$) of mean amplitude of short (2nd min) and sustained (10th min) CCh response for each CCh concentration, respectively.

ANOVA, **** $p < 0.0001$ compared to control.

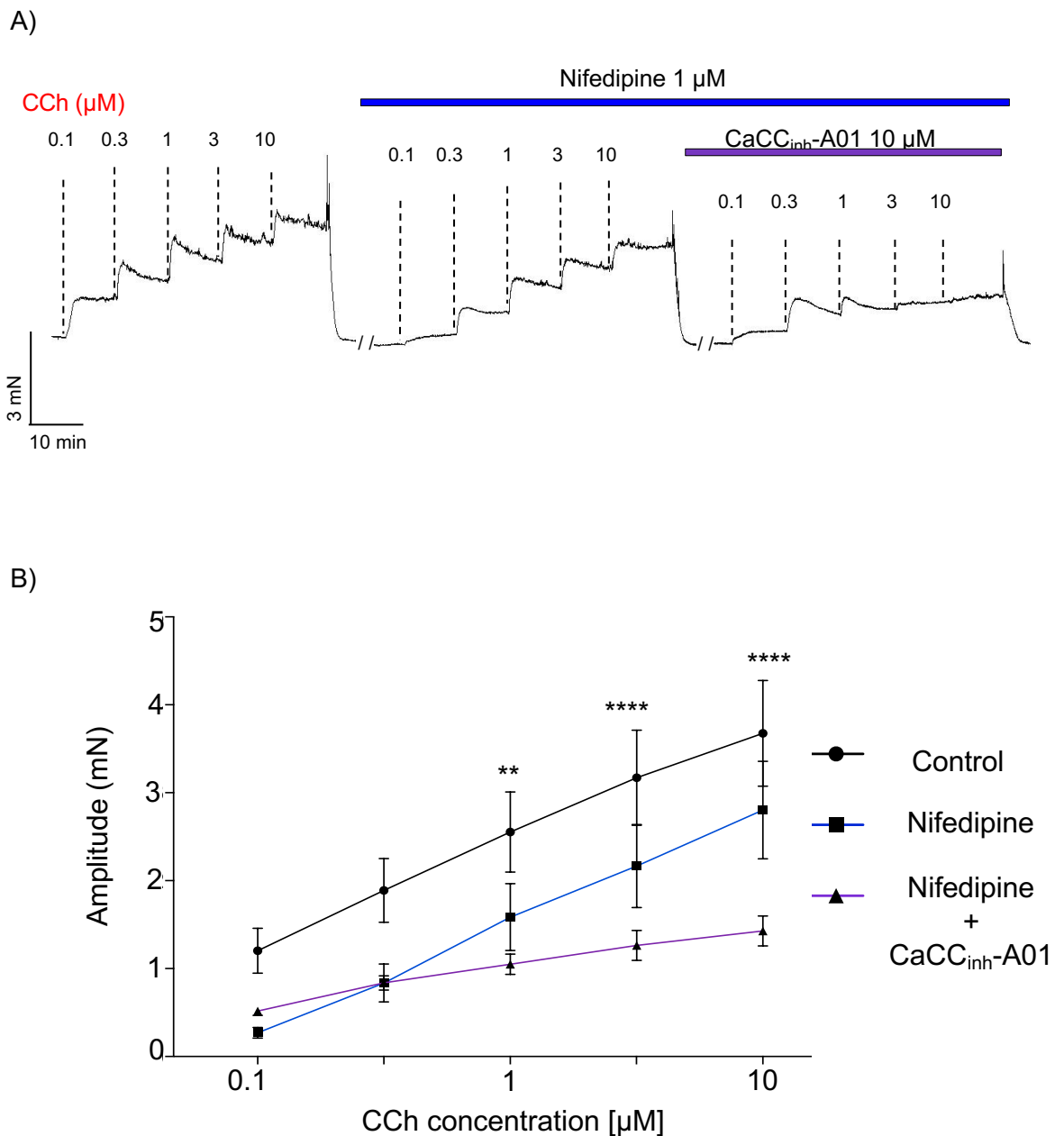
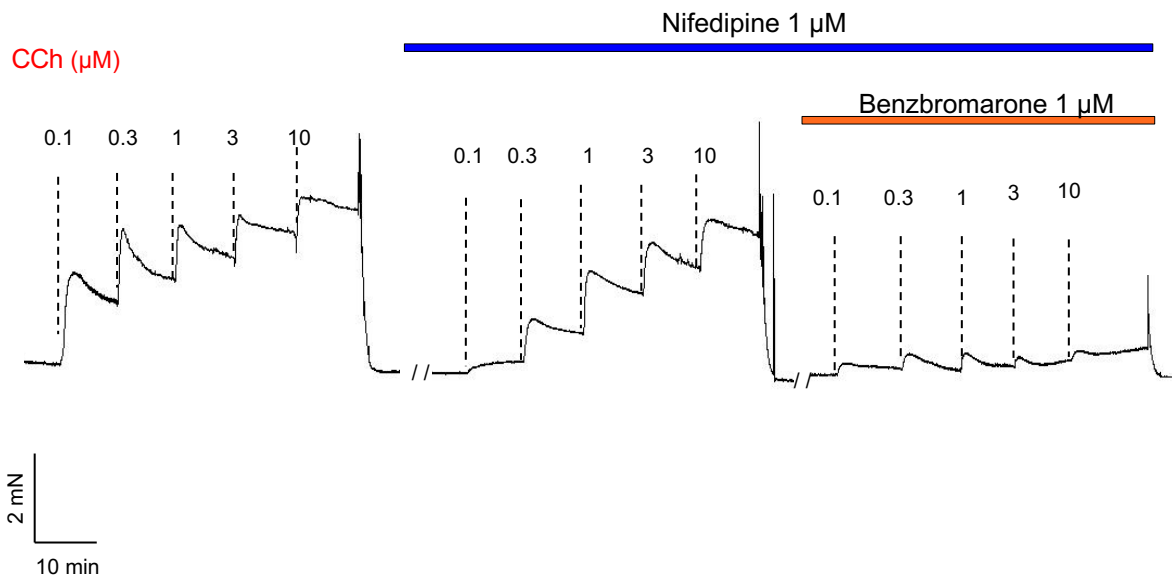


Figure 3.10. Effect of CaCC_{inh}-A01 on carbachol-induced contractions in presence of nifedipine in mouse bronchial rings.

Representative tension recording showing the effect of TMEM16A blocker CaCC_{inh}-A01 (10 μM) in presence of nifedipine (1 μM) on CCh-induced contraction (0.1, 0.3, 1, 3, 10 μM). Panel (A) shows CCh control, followed by CCh in presence of nifedipine (1 μM) and then CCh in presence of nifedipine (1 μM) with CaCC_{inh}-A01 (10 μM). Summarized data represented as line graph (n=6; N=6) of mean amplitude of sustained CCh responses (B) of all three sets; which were measured at 10th minutes for CCh concentration.

ANOVA, **p<0.005, ****p<0.0001; comparing Nifedipine + CaCC_{inh}-A01 vs Nifedipine.

A)



B)

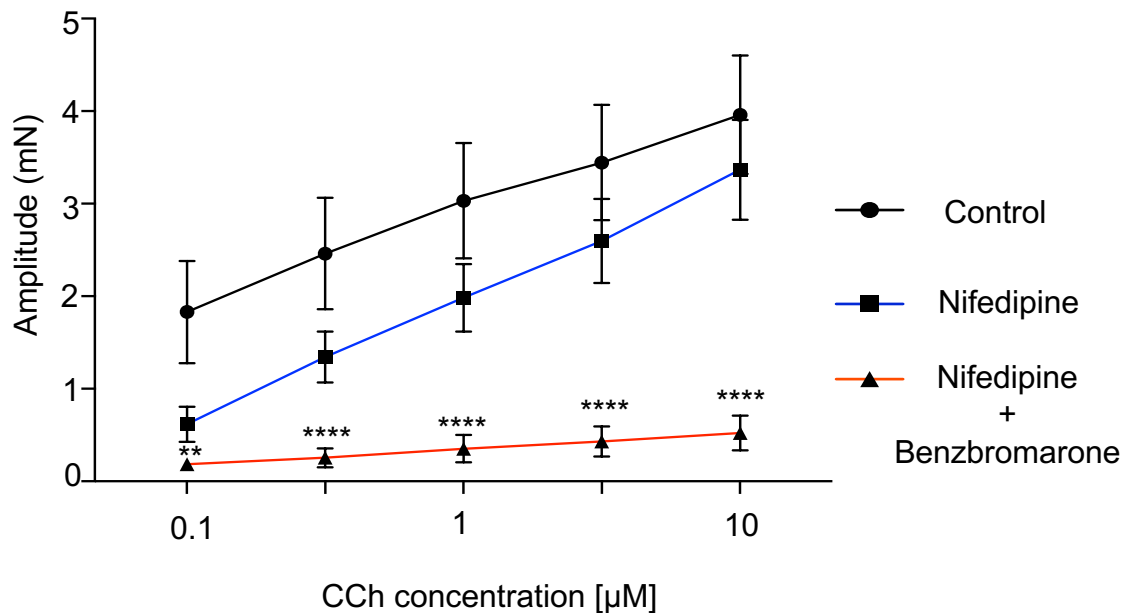


Figure 3.11. Effect of benzbromarone on carbachol-induced contractions in presence of nifedipine in mouse bronchial rings.

Isometric tension recording showing the effect of nifedipine (1 μM) with/without benzbromarone (1 μM), TMEM16A blocker on CCh-induced contractions (0.1, 0.3, 1, 3, 10 μM) is represented in Panel A. Panel (A) shows CCh control, followed by CCh in presence of nifedipine (1 μM) and then CCh in presence of nifedipine (1 μM) with benzbromarone (1 μM). Panel B shows summarized data as line graph (n=6; N=6) of mean amplitude, which were measured at 10th minutes for CCh concentration response of control, nifedipine, nifedipine + benzbromarone.

ANOVA, **p<0.005, ****p<0.0001; comparing Nifedipine + Benzbromarone vs Nifedipine.

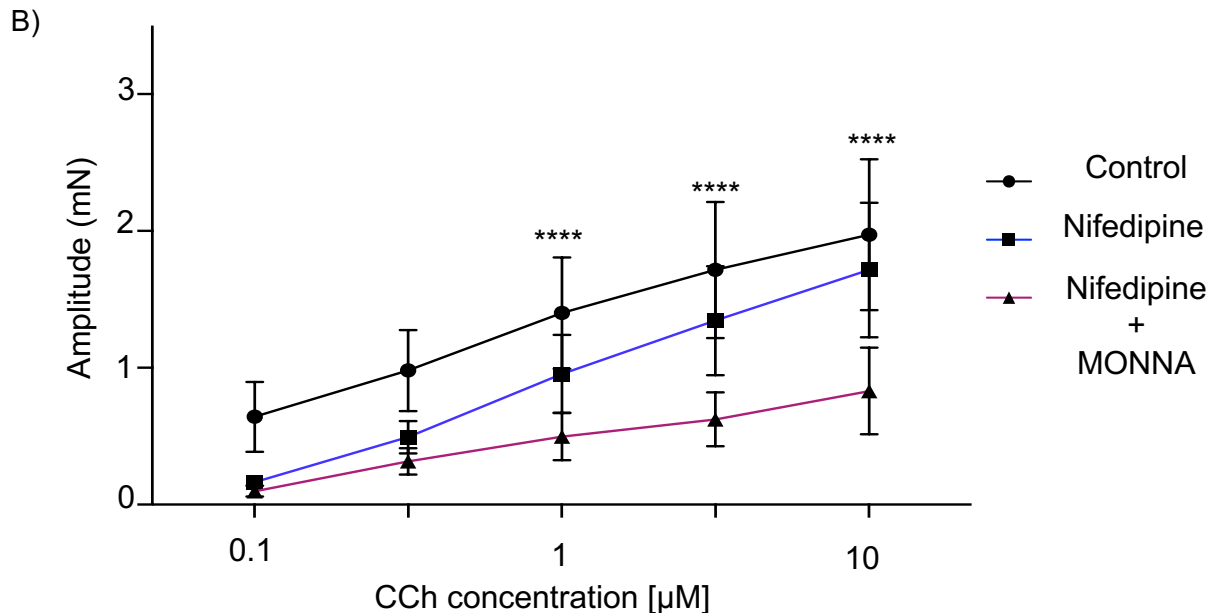
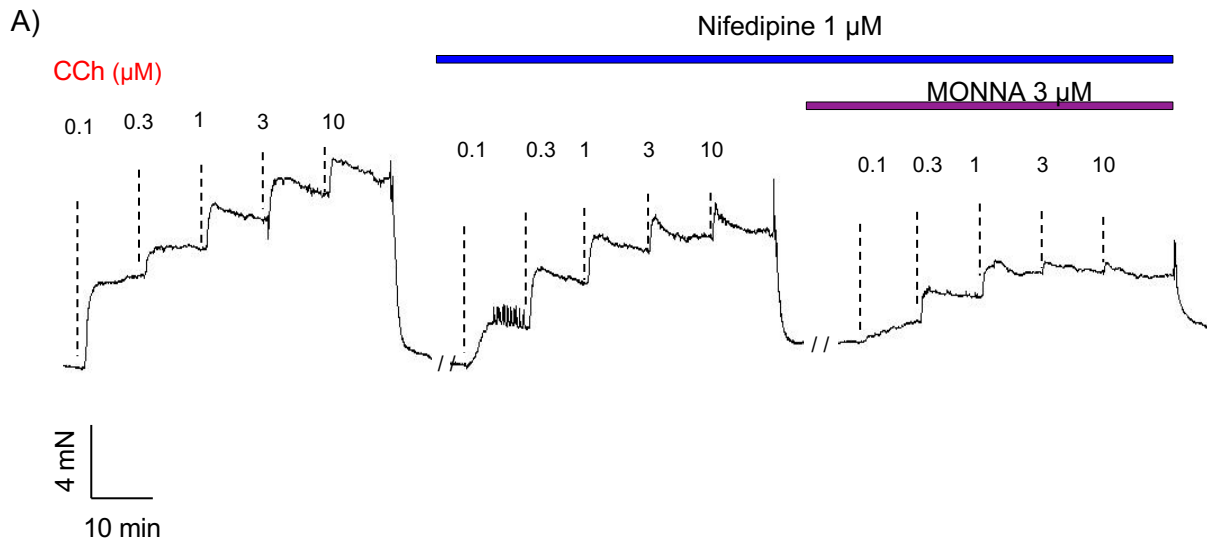


Figure 3.12. Effect of MONNA on carbachol-induced contractions in presence of nifedipine in mouse bronchial rings.

Representative isometric tension trace showing the effect of TMEM16A blocker MONNA ($3 \mu\text{M}$) in the presence of nifedipine ($1 \mu\text{M}$) on CCh-induced contractions ($0.1, 0.3, 1, 3, 10 \mu\text{M}$). Panel (A) shows CCh control, followed by CCh in presence of nifedipine ($1 \mu\text{M}$) and then CCh in presence of nifedipine ($1 \mu\text{M}$) with MONNA ($3 \mu\text{M}$). Panel B summarizes data-set as line graph ($n=6$; $N=4$) of mean amplitude of sustained response measured at 10th minutes of all three groups for each CCh concentration.

ANOVA, ** $p < 0.005$, **** $p < 0.0001$; comparing Nifedipine + MONNA vs Nifedipine.

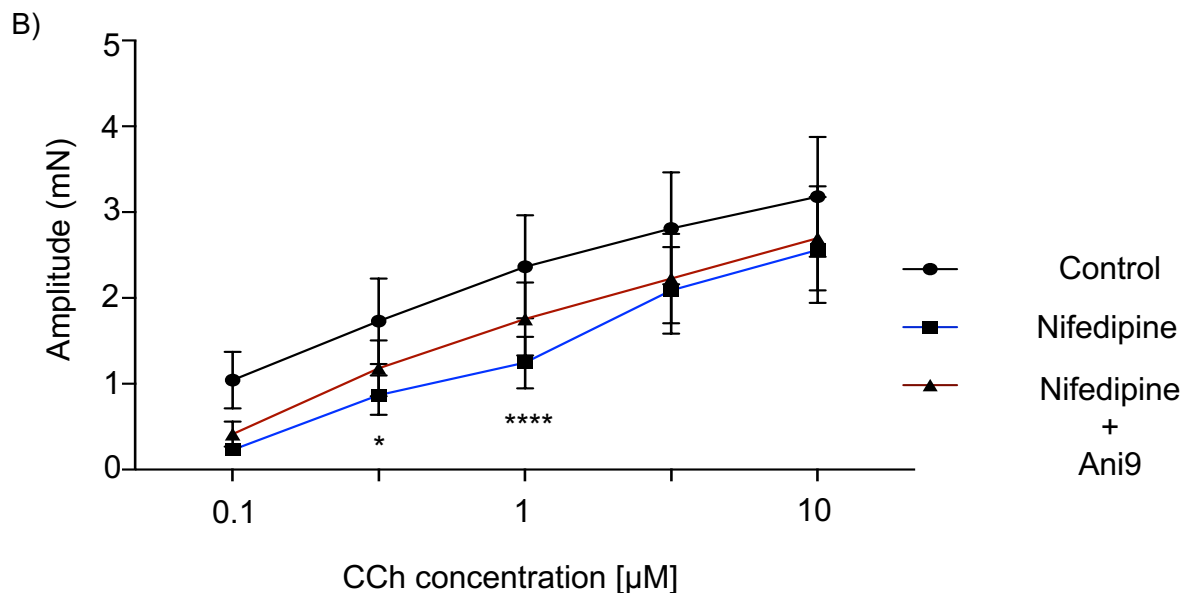
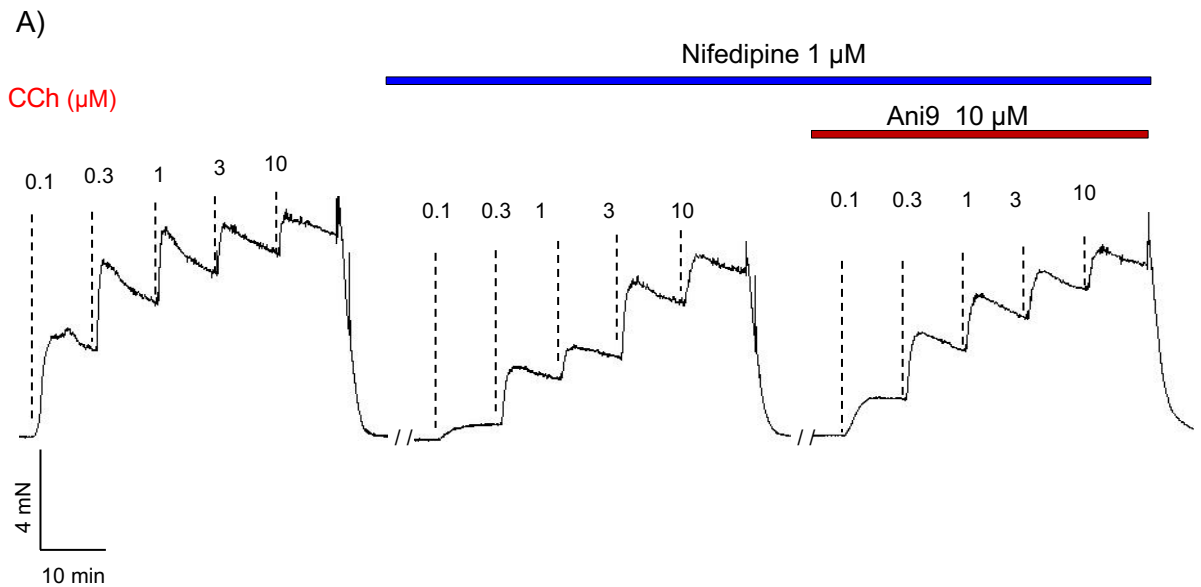


Figure 3.13. Effect of Ani9 on carbachol-induced contractions in presence of nifedipine in mouse bronchial rings.

Isometric tension recording showing the effect of TMEM16A blocker novel TMEM16A inhibitor, Ani9 (10 μM) in presence of nifedipine (1 μM) on CCh-induced cumulative contractions (0.1, 0.3, 1, 3, 10 μM); Panel (A) shows CCh control, followed by CCh in presence of nifedipine (1 μM) and then CCh in presence of nifedipine (1 μM) with Ani9 (10 μM). Summarized data represented in Panel B as line graph (n=6; N=6) of mean amplitude of CCh sustained contractions measured at 10th minutes for CCh concentration of all three test groups.

ANOVA, **p<0.005, ****p<0.0001; comparing Nifedipine + Ani9 vs Nifedipine.

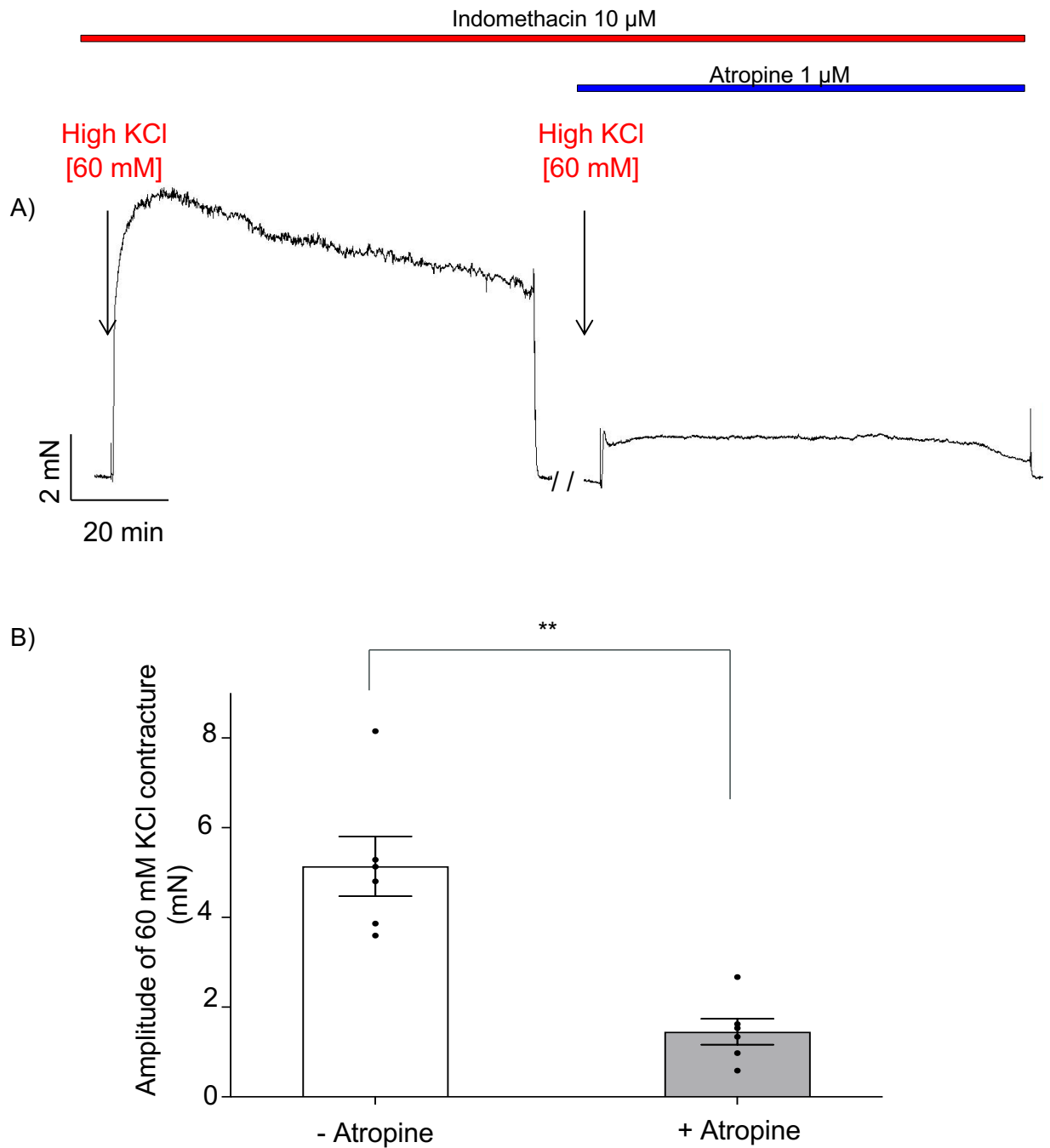
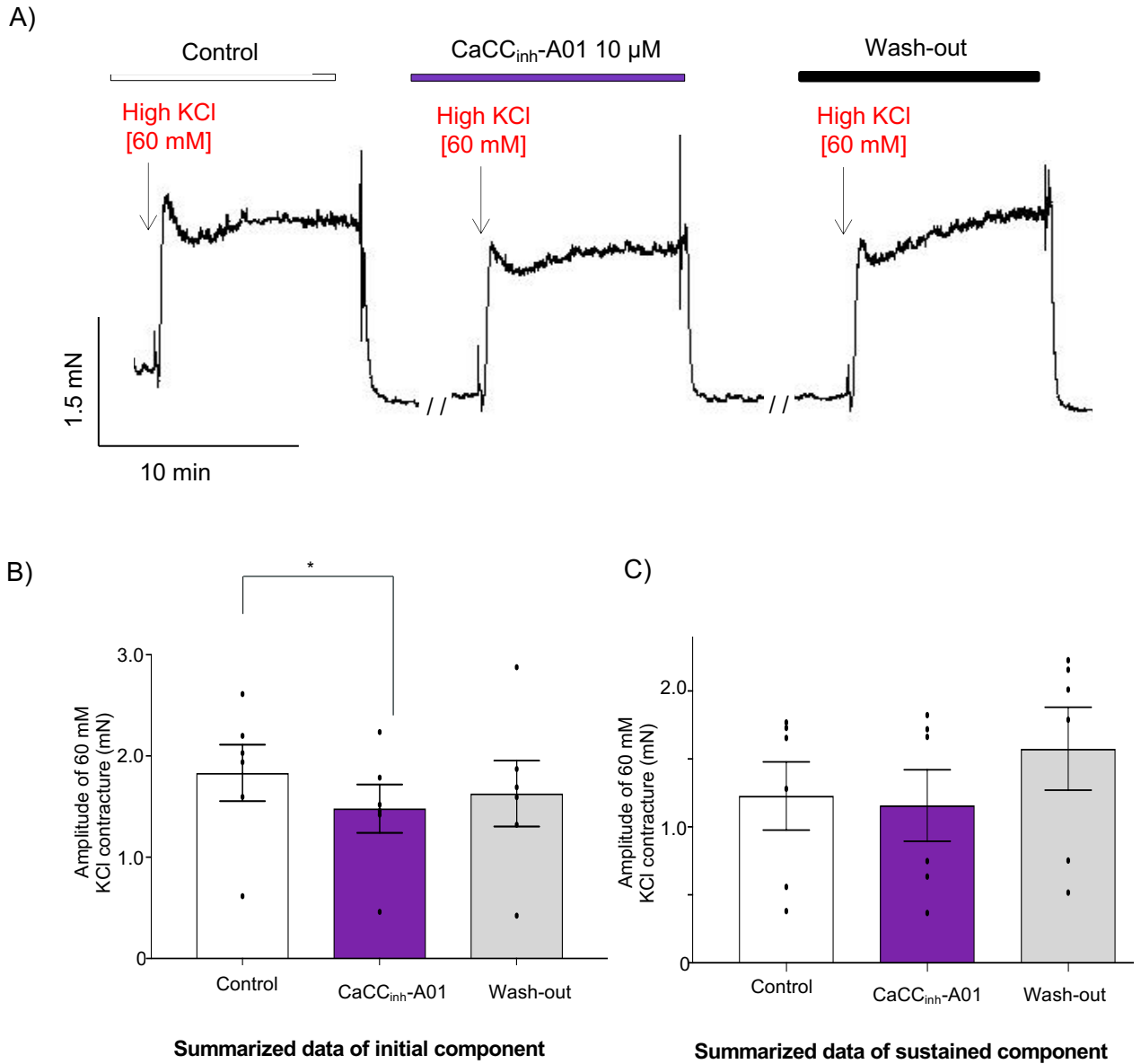


Figure 3.14. Effect of atropine on KCl [60 mM]-induced contraction of mouse bronchial smooth muscle.

A representative isometric tension recording of a bronchial ring showing on KCl [60 mM]-induced contractions in absence and presence of atropine 1 μM, as shown in panel A. Summarized data (n=6; N=4) showing the effect of atropine after 20 minutes treatment on peak of high KCl contractions.

Paired t-test; **p<0.005.

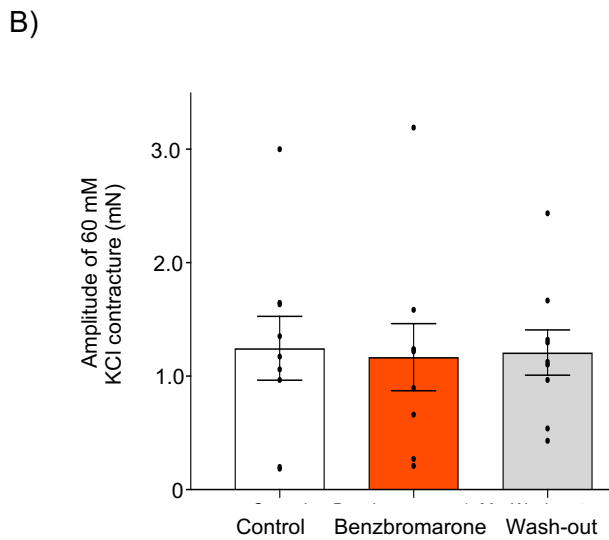
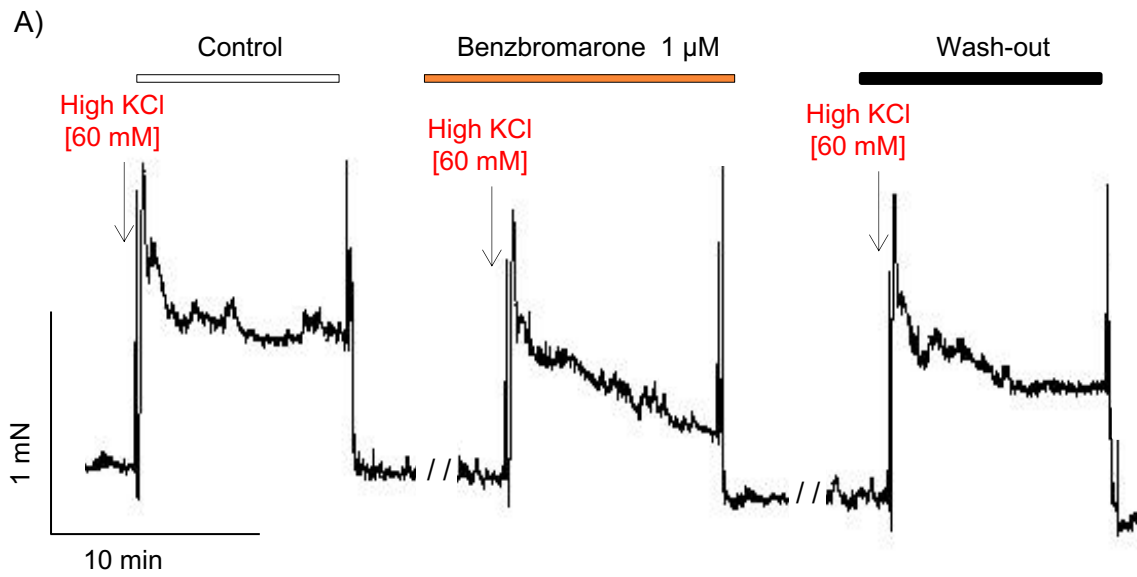


(Indomethacin 10 μM and Atropine 1 μM is present throughout the experiment)

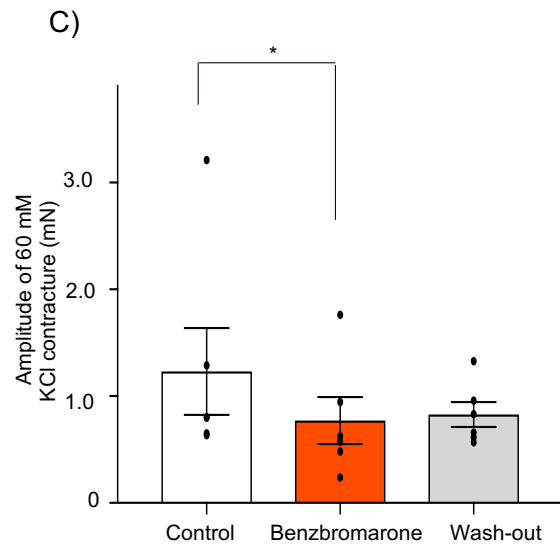
Figure 3.15. Effect of CaCC_{inh}-A01 on KCl [60 mM]- induced contraction of mouse bronchial smooth muscle.

Panel A represents an isometric tension recording showing the time-control and effect of CaCC_{inh}-A01(10 μM) on KCl [60 mM] contractions in presence of indomethacin 10 μM and atropine 1μM, respectively. Summary bar chart (n=6; N=6) in panel B and C represents peak and sustained amplitude of KCl [60 mM] contracture before and after treatment with CaCC_{inh}-A01 for 20 minutes, respectively.

Paired t-test, *p<0.05.



Summarized data of initial component



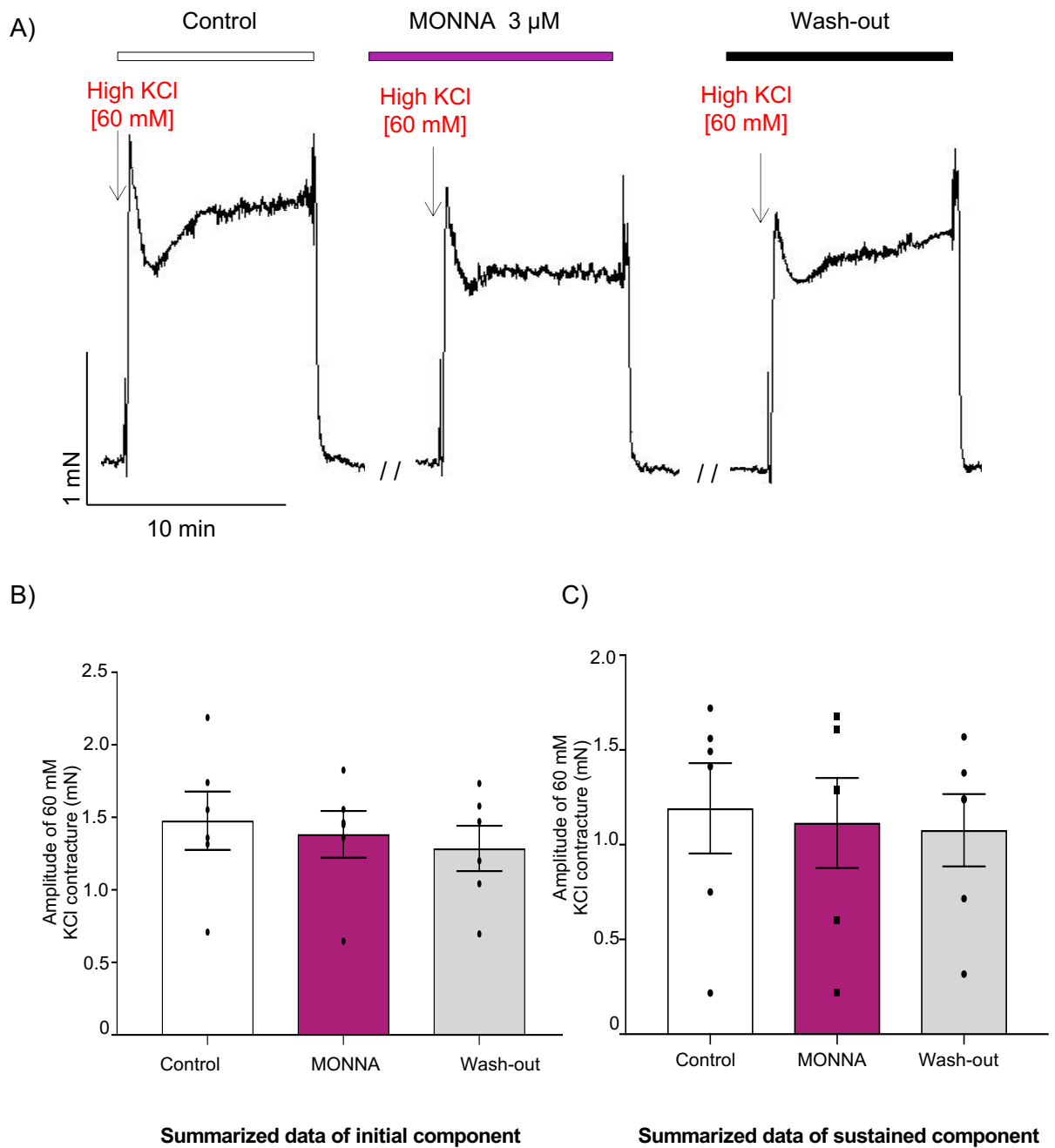
Summarized data of sustained component

(Indomethacin 10 μM and Atropine 1 μM is present throughout the experiment)

Figure 3.16. Effect of Benzbromarone on KCl [60 mM]- induced contraction of mouse bronchial smooth muscle.

Panel A represents an isometric tension recording showing the time-control and effect of benzbromarone (1 μM) on KCl [60 mM] contractions in presence of indomethacin 10 μM and atropine 1 μM, respectively. Summary bar chart (n=6; N=6) in panel B and C represents peak and sustained amplitude of KCl [60 mM] contracture before and after treatment with benzbromarone for 20 minutes, respectively.

Paired t-test, *p<0.05.

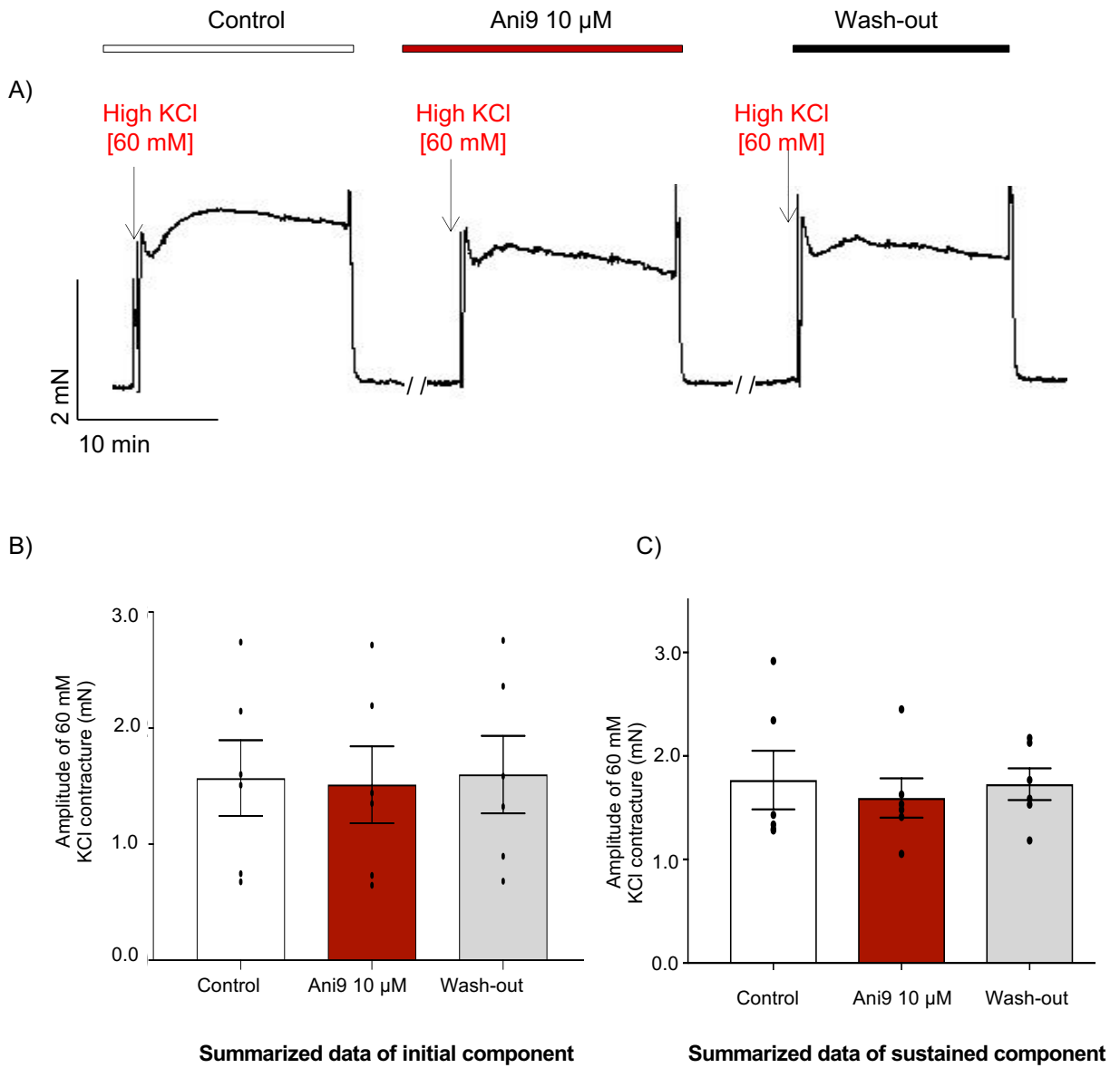


(Indomethacin 10 μ M and Atropine 1 μ M is present throughout the experiment)

Figure 3.17. Effect of MONNA on KCl [60 mM]- induced contraction of mouse bronchial smooth muscle.

Panel A represents an isometric tension recording showing the time-control and effect of MONNA (3 μ M) on KCl [60 mM] contractions in presence of indomethacin 10 μ M and atropine 1 μ M, respectively. Summary bar chart (n=6; N=6) in panel B and C represents peak and sustained amplitude of KCl [60 mM] contracture before and after treatment with MONNA for 20 minutes, respectively.

Paired t-test, $p > 0.05$.



(Indomethacin 10 µM and Atropine 1 µM is present throughout the experiment)

Figure 3.18. Effect of Ani9 on KCl [60 mM]- induced contraction of mouse bronchial smooth muscle.

Panel A represents an isometric tension recording showing the time-control and effect of Ani9 (10 µM) on KCl [60 mM] contractions in presence of indomethacin 10 µM and atropine 1 µM, respectively. Summary bar chart (n=6; N=5) in panel B and C represents peak and sustained amplitude of KCl [60 mM] contracture before and after treatment with Ani9 for 20 minutes, respectively.

Paired t-test, p>0.05.

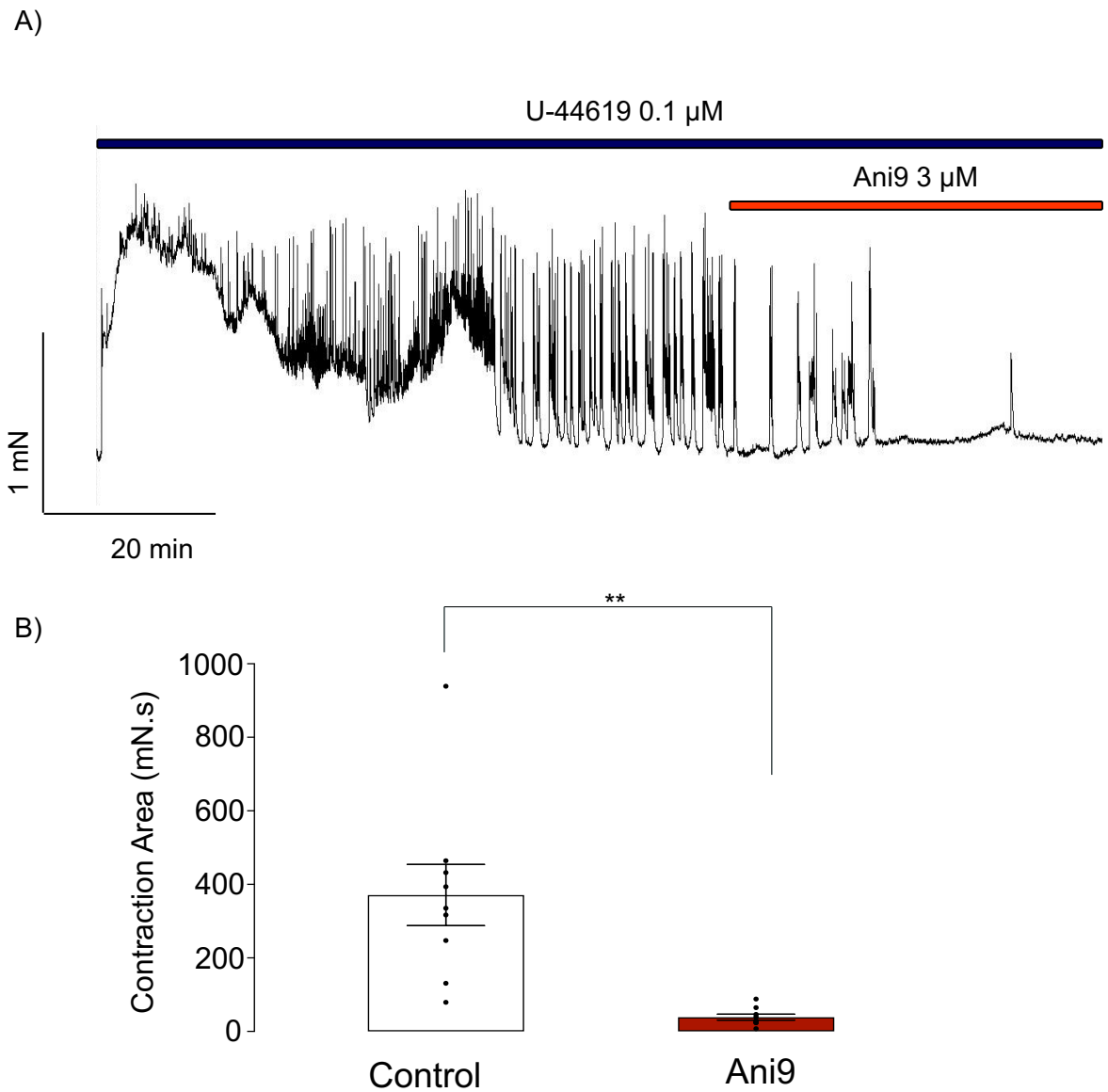


Figure 3.19. Ani9 significantly reduced phasic contractions induced by U-46619 in mouse bronchial rings.

Representative isometric tension recording in panel A showing the effect of Ani9 (3 μM) on phasic contractions induced by 0.1 μM U-46619 in bronchial rings. Panel B summarized (n=9; N=5) of contraction area of last 20 minutes of control contraction and last 20 mins after addition of Ani9 (3 μM).

Paired t- test, **p<0.005.

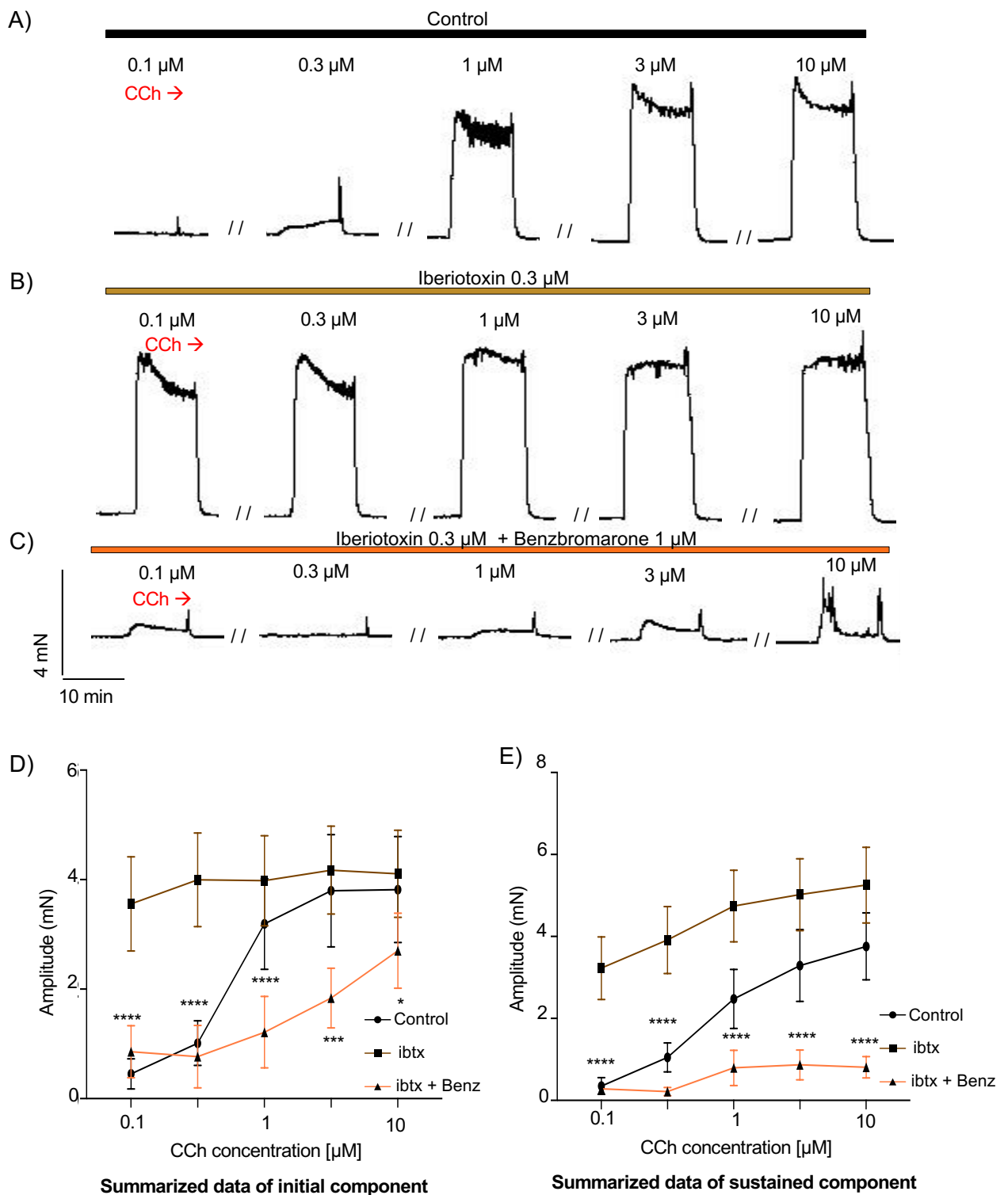


Figure 3.20. Effect of benzbromarone (Benz) on carbachol-induced contractions in presence of iberiotoxin (ibt) in mouse bronchial rings.

Representative tension recording showing the effect of TMEM16A blocker benzbromarone (1 μM) in presence of iberiotoxin (0.3 μM) on CCh-induced contraction (0.1, 0.3, 1, 3, 10 μM). Panel (A) control, (B) benzbromarone (1 μM), (C) benzbromarone (1 μM) with iberiotoxin (0.3 μM). Summarized data represented as line graph (n=6; N=6) of mean amplitude of initial (D) and sustained CCh responses (E) of all three sets; which were measured within 2nd and at 10th minutes for each CCh contractions, respectively. ANOVA, *p<0.05, ***p<0.001 ****p<0.0001; comparing ibtx + Benz vs ibtx.

3.3 Discussion

CaCC were originally found in tracheal smooth muscle cells isolated from dog and guinea pig by Janssen & Sims in 1992 (Janssen & Sims, 1992). This current could be evoked by ACh or caffeine, its reversal potential was sensitive to extracellular $[Cl^-]$ and it was antagonized by two Cl^- channel blockers, SITS (4-acetamido-4-isothiocyanatostilbene-2,2-disulfonic acid) and niflumic acid. Interestingly, even at this early stage, these authors showed that cells contracted in response to ACh when voltage was clamped at -60 mV, or when the ACh-sensitive Cl^- current was blocked with niflumic acid, indicating that the Cl^- current was not essential for ACh-evoked contractions. The presence of CaCC were confirmed in tracheal smooth muscle cells isolated from pigs and horses, when it was also demonstrated that the ACh-induced currents were activated by IP_3 -mediated Ca^{2+} -release (Liu & Farley, 1996; Kotlikoff & Wang, 1998). Besides activating in response to ACh, spontaneous Cl^- currents, termed 'spontaneous transient inward currents' (STICs) were observed in the original paper by Janssen & Sims in 1992 (Janssen & Sims, 1992). STICs were later studied in detail in mouse trachea by Zhuge and colleagues, by simultaneously measuring membrane currents and intracellular Ca^{2+} events using confocal microscopy (Zhuge *et al.* 1998; Bao *et al.* 2008; Zhuge *et al.* 2010). These studies concluded that a single Ca^{2+} spark, released from clusters of RyR, in close proximity to the plasma membrane, could simultaneously activate both STICs and STOCs (spontaneous transient outward currents) due to activation of BK_{Ca} channels. STOCs were predominant at depolarized membrane potentials (e.g. 0 mV), while STICs were evoked at hyperpolarized potentials (e.g. -80 mV) and mixed events (termed STOICs – spontaneous transient inward and outward currents) were observed at intermediate membrane potentials. These studies proposed a role for CaCC in depolarizing the membrane and activation L-type Ca^{2+} channels, thus causing contraction of ASM (Zhuge *et al.* 1998; Zhuge *et al.* 2010). However, it is important to realise that this idea has remained controversial as others have challenged not only the importance of CaCC, but also membrane potential and the role of L-type Ca^{2+} channels in excitation-contraction coupling in ASM (Janssen, 2002; Hirota *et al.* 2007)

Following identification of TMEM16A as the molecular identity of CaCC in 2008 (see Literature Review), there was renewed interest in the role of CaCC in ASM. Firstly, Huang *et al.* (2009) generated a polyclonal antibody against TMEM16A that enabled them to probe the expression of TMEM16A in airway and other tissues. They found higher levels of TMEM16A expression in ASM than in airway epithelium, in agreement with mRNA studies in a previous paper (Rock *et al.* 2008). Gallos *et al.* later provided immunohistochemical evidence of TMEM16A in both cultured and native human ASM (Gallos *et al.* 2013). These authors also showed that a TMEM16A antibody (as well as several pharmacological blockers of CaCC) reduced the amplitude of STICs in cultured human ASM and benzbromarone and tannic acid (another CaCC blocker) reduced the contractile response of guinea pig trachea to substance P. Two studies have shown that TMEM16A is upregulated in the airways of ovalbumin-sensitized mice, a commonly used model of asthma (Huang *et al.* 2012; Zhang *et al.* 2013). Huang *et al.* showed that TMEM16A was upregulated in the airway epithelium of the asthma model, while Zhang *et al.* confirmed this and also showed upregulation in ASM. Zhang *et al.* also cloned TMEM16A from mouse ASM and showed that it generated Cl⁻ currents when expressed in HEK293 cells.

Benzbromarone was first identified as a TMEM16A blocker using high throughput screening in the Huang study referred to above (Huang *et al.* 2012). They went on to show that benzbromarone was an effective blocker of TMEM16A expressed in HEK293 cells (IC₅₀ = 10 μM) and reported that pre-treatment with benzbromarone reduced the amplitude of methacholine-induced contractions in human bronchial rings from a single patient. However, they did not show any original tension records and the protocol they used was not specified, so it was not possible to determine the time course of the methacholine applications. The Zhang study also showed that benzbromarone blocked methacholine-induced contraction in both the normal and ovalbumin-sensitized mice, again without specifying the protocol (Zhang *et al.* 2013). Benzbromarone was also shown to block cholinergic-induced contractions in guinea pig tracheal rings, though 50 μM was required to abolish the responses (Danielsson *et al.* 2015). It also hyperpolarized human ASM cells and reduced cytosolic Ca²⁺ (however the manner in which it might have done this is discussed further in chapter 4). In

another study, the same group also showed that Eact, an opener of TMEM16A channels, increased tone in guinea pig tracheal rings and this effect was blocked by benzbromarone and T16A_{inh}-A01, another TMEM16A blocker.

Despite all of the above studies, which support a role for TMEM16A in mediating ASM contractions, including cholinergic contractions, a study by Wang *et al.* using smooth muscle selective TMEM16A knockout (KO) mice seemed to cast doubt on the its role in cholinergic contractions (Wang *et al.* 2017). Wang *et al.* (2017) found that contractions in response to methacholine were only minimally affected in the KO mice, though responses to other agonists such as 5-HT and U-46619 were impaired. In the Wang study, only short applications of cholinergic agonists were studied. We, therefore, wondered if this could account for the difference compared to the pharmacology experiments described above. We hypothesized that the early phase of cholinergic contractions might be due mainly to IP₃-induced Ca²⁺ release, while TMEM16A channels (activated by the released Ca²⁺) caused depolarization and activation of L-type Ca²⁺ channels which then sustained the cholinergic contractions. Therefore, we studied the effect of a range of TMEM16A blockers on both short and long applications of CCh.

In the present study, apart from benzbromarone, MONNA and CaCC_{inh}-A01 were also examined. CaCC_{inh}-A01 is one of the benchmark antagonists of TMEM16A which has been used in several cell types to block Cl⁻ currents. For instance, in rabbit urethra interstitial cells of Cajal (Fedigan *et al.* 2017), HEK cells overexpressing human TMEM16A. Bradley *et al.* (2018) showed that CaCC_{inh}-A01 (10 µM) was able to abolish phasic contractions induced by histamine (1 µM) in rabbit bronchial rings, suggesting that TMEM16A are involved in histamine-induced contractions.

In the present study, benzbromarone, MONNA and CaCC_{inh}-A01 had a greater inhibitory effect on the sustained component of cholinergic-induced contractions when compared to the initial component, at first appearing to confirm our hypothesis that TMEM16A might be involved in sustained component of cholinergic contractions. However, Ani9 had little effect, which contradicted the results obtained using other blockers. Ani9 is a potent TMEM16A blocker (Seo *et al.* 2016) and we confirmed this by using same batch of Ani9 to block TMEM16A-expressing HEK293 cells and in native CaCC currents in mouse ASMCs

(experiments were performed by Dr Eamonn Bradley). At first, we were worried that Ani9 might be breaking down in tissue, as it is unstable in blood plasma (Seo *et al.* 2018), although it should be stated that it has been used effectively to block contractions in gastro-intestinal muscles (Drumm *et al.* 2019; Drumm *et al.* 2022). However, we observed that same batch of Ani9 successfully inhibited phasic contractions induced by U-44619, thus confirming it worked in bronchial tissue. This led us to think that the other blockers might be having non-specific effects. In terms of other ion channels, benzbromarone was able to efficiently block TMEM16B but failed to block CFTR or ENaC (Huang *et al.* 2012), while MONNA did not block any other chloride channel members such as CLC, bestrophins or CFTR in specificity tests, suggesting MONNA is the most selective antagonist of TMEM16A (Oh *et al.* 2013; Hyuga *et al.* 2018).

It is also notable that the pattern of inhibiting cholinergic contractions by the TMEM16A blockers differed from that of nifedipine. Nifedipine did not differentiate between the initial and sustained response to CCh, while the TMEM16A blockers preferentially blocked the sustained phase. If TMEM16A really acts upstream of L-type Ca^{2+} channels by causing depolarisation, it might be expected that the effects of TMEM16A blockers and L-type Ca^{2+} channels blockers would be similar. The fact that this is not the case added to the suspicion the TMEM16A blockers had non-specific actions. Not only was the pattern of block different, but all three TMEM16A antagonists caused further block over and above that of L-type Ca^{2+} channel blockers. For example, nifedipine (1 μM) itself reduced CCh induced-contractions (0.1-10 μM) and $\text{CaCC}_{\text{inh}}\text{-A01}$ further reduced these responses. Similar results were obtained for benzbromarone and MONNA, suggesting that these TMEM16A antagonists have effects on cholinergic contractions that cannot be accounted for by blocking L-type Ca^{2+} channels. Interestingly, Ani9 had only a small further effect in the presence of nifedipine. Also, the TMEM16A blockers produced slight to moderate block of KCl contractions, though to a much lesser extent than the CCh-induced contractions. One reason may be that they had a slight blocking effect on L-type Ca^{2+} channels as this has been previously reported (Hannigan *et al.* 2017; Boedtkjer *et al.* 2015). However, the relative lack of effects on high KCl contractions suggest that they were not blocking L-type Ca^{2+} channels to any great extent (e.g., compare the

effect of nifedipine on high KCl contractions, *figure 5.3*), nor is it likely that they are affecting the contractile proteins directly.

In conclusion, the results of this chapter do not support a role for TMEM16A in mediating CCh-induced contractions, except perhaps at low concentrations of CCh (see Ani9, *figure 3.8*). Although Benzbromarone, MONNA and CaCC_{inh}-A01 strongly blocked CCh-induced contractions across the concentration range of CCh tested, the fact that the pattern of the block differed from that of nifedipine, that they had effects over and above nifedipine, and that Ani9 had much less effect, suggest that the other 3 drugs had off-target actions. The next chapter will investigate this further by examining the effects of these blockers on intracellular Ca²⁺.

4. Effect of TMEM16A blockers on intracellular Ca²⁺ signals in freshly isolated ASMCs

4.1 Introduction

In the previous chapter, it was observed that three different TMEM16A antagonists, CaCC_{inh}-A01, benzbromarone and MONNA had inhibitory effects, particularly on the sustained cholinergic contractions induced by CCh in mouse bronchial rings. These inhibitory effects were not mediated through L-type Ca²⁺ channels, as they were evident even in the presence of nifedipine. This was also inconsistent with the hypothesis that they inhibited TMEM16A channels and thus prevented membrane depolarisation, followed by activation of the L-type Ca²⁺ channels. These observations, and the fact that Ani9, another TMEM16A blocker, had very little effect on CCh-induced contractions suggested that the other three TMEM16A blockers had off-target effects. Any off-target effects were unlikely to be due to direct inhibition of the contractile mechanism by acting on the contractile proteins, as high K⁺-induced contractures were only slightly affected by the three blockers.

The aim of the experiments in this chapter was to investigate the effect of TMEM16A blockers CaCC_{inh}-A01, benzbromarone, MONNA and Ani9 on the intracellular Ca²⁺ signals induced by CCh or caffeine in the freshly isolated ASMCs. ASMCs which were not spontaneously oscillatory were used to carry out this study. We initially hypothesized that the three blockers were inhibiting Ca²⁺-release from the SR in response to CCh, or inhibiting Ca²⁺ influx induced by CCh *via* a pathway other than by L-type Ca²⁺ channels (e.g. TRPC3 or other non-voltage-dependent pathways). The cells under study were from wild-type mice and were loaded with fluo-4AM as described in the chapter 2.

4.2 Results

4.2.1 Effect of TMEM16A antagonists on Ca²⁺ signals in ASMCs

The initial aim of this chapter was to examine the effect of TMEM16A blockers on intracellular Ca²⁺ levels increased by CCh. However, while performing these experiments we observed that CaCC_{inh}-A01, benzbromarone and MONNA themselves increased cytosolic Ca²⁺ concentration. *Figure 4.1* shows the effect of 10 µM of CaCC_{inh}-A01 on ASMCs. The representative pseudolinescan in the *figure 4.1A* demonstrates a surprising and unexpected elevation of [Ca²⁺]_i recorded over a period of 5 minutes. An intensity plot for the same is plotted in panel B. In 9 cells, the mean F/F₀ was calculated at every 30 seconds and plotted as a line graph in panel C of *figure 4.1*. The mean F/F₀ remained elevated throughout the 5 minutes, for instance mean F/F₀ at the 1st minute was 1.46 ± 0.08 and was 1.52 ± 0.17 at the 5th minute.

Benzbromarone (1 µM) also caused an increase in intracellular Ca²⁺ as shown in *figure 4.2*. A representative pseudolinescan in panel A and intensity plot in panel B demonstrate that [Ca²⁺]_i increased and was sustained for the 6 minutes of recording. In 8 cells, the mean F/F₀ was calculated at every 30 seconds and line graph plot for the same is plotted in panel C of *figure 4.2*. The mean F/F₀ remained almost same throughout the experiments, for instance mean F/F₀ at 2 minutes was 2.2 ± 0.2 and was 2.4 ± 0.25 at the 6th minute.

MONNA had a similar effect to the other two blockers on intracellular Ca²⁺. *Figure 4.3* shows the effect of 3 µM of MONNA on ASMCs. A representative pseudolinescan in the *figure 4.3A* and intensity plot in panel B demonstrate that the increase in [Ca²⁺]_i lasted for approximately 6 minutes of the recording. In 7 cells, the mean F/F₀ was calculated at every 30 seconds and line graph plot for the same is plotted and represented in the panel C of *figure 4.3*. The mean F/F₀ remained roughly consistent throughout the experiments, for instance mean F/F₀ at the 1st minute was 1.4 ± 0.2 and at the 5th minute was 1.3 ± 0.2 .

Lastly, the novel TMEM16A blocker Ani9 (10 µM) was also examined and, unlike the other three blockers, it did not cause an increase in intracellular Ca²⁺. The pseudolinescan is represented in *figure 4.4A*, the intensity plot in panel B and

summary results for 7 cells in panel C. In the typical example shown, caffeine (10 mM) caused a sharp increase in Ca^{2+} level.

4.2.2 Effect of lower concentrations of benzbromarone and MONNA

It was found in the above experiments that the effects of high concentrations of drugs persisted after wash-out for 120-180s. The next aim was, therefore, to design a protocol that produced a reproducible effect of benzbromarone and MONNA, so that other interventions could be tested on the response. The next set of control experiments was done using lower concentrations of benzbromarone (0.3 μM) and MONNA (1 μM). The TMEM16A blockers were applied for 30 seconds with 120-180 seconds interval between each application. It was found that 3 reproducible responses were obtained for both drugs. In the pseudolinescan in *figure 4.5A* and corresponding intensity plot in panel B, benzbromarone 0.3 μM produced 3 clear cut increases in Ca^{2+} that reversed upon wash out. The summary bar chart with aligned dot-plot for 6 cells in panel C shows the mean amplitude of the peak Ca^{2+} increases following each application of the drug. $\Delta\text{F}/\text{F}_0$ for the 1st application was 1.36 ± 0.4 , this was slightly reduced at 1.24 ± 0.33 for 2nd application and remained unchanged for 3rd application at 1.24 ± 0.45 .

In the *figure 4.6*, similar to benzbromarone, MONNA 1 μM caused repeatable increases in intracellular Ca^{2+} . Again, a representative pseudolinescan is presented in panel A and corresponding intensity plot in panel B. The summarised bar chart for 7 cells in panel C, shows that the mean amplitude of the peak response was ($\Delta\text{F}/\text{F}_0$): 0.55 ± 0.07 for the 1st application, 0.52 ± 0.05 for the 2nd application and 0.53 ± 0.1 for the 3rd application.

4.2.3 Effect of TMEM16A blockers on Ca^{2+} signals in the absence of extracellular Ca^{2+} using EGTA-buffered Ca^{2+} free

The next aim of the study was to investigate whether this increase in intracellular Ca^{2+} was due to Ca^{2+} influx across the plasma membrane or Ca^{2+} release from the SR using the protocol developed in the previous section. First, extracellular Ca^{2+} was removed to eliminate the effect of Ca^{2+} influx. This was achieved by introducing EGTA-buffered Ca^{2+} free Hanks solution for 30 secs before applying

the TMEM16A blocker for a further 30 secs in Ca²⁺-free conditions. An example is shown in *figure 4.7A* and B, where benzbromarone was applied first in normal Ca²⁺ (1.8 mM, control), then in Ca²⁺-free and then again in normal Ca²⁺ (2nd control). The introduction of the Ca²⁺-free can be observed as a fall in the baseline in panel B (and a darkening of the background in panel A). In this particular example the response to benzbromarone appeared to be slightly larger under Ca²⁺-free conditions compared to control, but some of this difference persisted when the drug was applied again in 1.8 mM Ca²⁺ (wash-out of Ca²⁺-free). *Figure 4.7C* shows that the mean $\Delta F/F_0$ increases were similar for 6 cells under each condition with no significant differences between the responses.

Similarly, the EGTA-buffered Ca²⁺-free Hanks had no significant effect on the responses to MONNA (*figure 4.8*). However, in the example shown in *figure 4.8A* & B, drug response appeared to be slightly reduced in Ca²⁺-free conditions compared to both controls (1.8 mM Ca²⁺). $\Delta F/F_0$ reduced from 2.5 ± 0.6 to 2.1 ± 0.5 for 7 cells comparing 1st control to 0 Ca²⁺ Hanks.

The results of these experiments suggest that these pharmacological blockers of TMEM16A can cause Ca²⁺ release from the SR.

4.2.4 Effect of TMEM16A blockers on Ca²⁺ signals induced by caffeine

To further confirm this idea, these TMEM16A blockers were tested with caffeine. Caffeine triggers an increase in the intracellular Ca²⁺ level by causing Ca²⁺ release from the SR by opening RyR receptors. Caffeine responses were reproducible as shown in the pseudolinescan and intensity plot in the panels A & B of *figure 4.9* and in the summary data for 6 cells in panel C.

In the next experiments, the TMEM16A blockers were applied after caffeine to see if they could further increase the cytosolic Ca²⁺ after caffeine had caused Ca²⁺-release. An example is shown in *figure 4.10A* & B, where first was a control application of caffeine, then during second application of caffeine (after 15 sec) benzbromarone was applied with caffeine for 30 sec. There was no further increase in the Ca²⁺ level as a result of the addition of the benzbromarone. The summary bar chart for similar experiments on 6 cells is shown in panel C of the same figure, which shows the mean sustained responses (measured at 20 sec

for each application) for the first caffeine (Control Sustained), the second caffeine after benzbromarone was applied (+ Benzbromarone) and the third caffeine (Wash-out of Benzbromarone). There were no significant differences between these responses when compared by ANOVA.

A similar effect was observed when the same experiment was carried out with MONNA as shown in the *figure 4.11*, thus suggesting that the increase in the intracellular Ca^{2+} levels by benzbromarone and MONNA could be due to opening of RyR. Also, preliminary experiments with 2-APB, IP_3R blocker had shown no inhibitory effect on benzbromarone and MONNA evoked increase in intracellular Ca^{2+} levels.

4.2v Effect of caffeine on intracellular Ca^{2+} in the presence of the SERCA pump blocker, CPA

Next, we performed a control experiment with SERCA pump blocker cyclopiazonic acid (CPA), which inhibits refilling of Ca^{2+} stores. 10 μM of CPA caused a rapid increase in cytosolic Ca^{2+} levels as a result of unopposed Ca^{2+} leaks from the SR. In the experiment presented in *figure 4.12A*, after 60 sec application of CPA, caffeine (10 mM) was applied for 20 sec every 90 sec, 4 times. CPA was present throughout the experiment. The caffeine response reduced by 50% (1.6 ± 0.5 to $0.81 \pm 0.27 \Delta\text{F}/\text{F}_0$, $n=5$; $N=4$) between 1st and 4th application, however this failed to reach statistical significance. It is notable that even after the 4th caffeine application, Ca^{2+} stores were not completely depleted (panel C of *figure 4.12*).

4.2.6 Effect of caffeine on intracellular the Ca^{2+} level increased by benzbromarone

It was possible, that the TMEM16A blockers might be causing increased intracellular Ca^{2+} levels by blocking SERCA pump. Therefore, like CPA experiment, caffeine (10 mM) was applied for 20 sec every 90 sec in the presence of benzbromarone (1 μM) as displayed in line-scan in panel A of *figure 4.13*. However, unlike the previous experiment, caffeine caused a minor decline of 18% (1.76 ± 0.26 to $1.43 \pm 0.3 \Delta\text{F}/\text{F}_0$, $n=4$; $N=3$) in the benzbromarone response as shown in panel C of *figure 4.13*. It was an interesting observation and was

consistent through all four applications of caffeine. Despite the fact that it was not statistically significant in data collected from 4 cells, the effect was observed in all applications in all of the 4 cells. This inhibitory effect of caffeine could be because it is also a well-known phosphodiesterase inhibitor which results in elevated intracellular cAMP (Sato *et al.* 1988) and this could have stimulated the SERCA pump (see Discussion).

4.2.7 Effect of a ryanodine receptor blocker on intracellular Ca²⁺ increased by benzbromarone

In order to test the idea that benzbromarone might be opening RyR, the RyR blocker tetracaine (100 μ M) was used for the next experiment. The pseudolinescan in the panel A of the *figure 4.14* shows that during a sustained exposure to benzbromarone 0.3 μ M, tetracaine reduced the increase in Ca²⁺ induced by benzbromarone. This effect was reversible as shown by the fact that the Ca²⁺ returned to pre-tetracaine levels upon wash-out. As shown in the summary bar chart in the panel C, tetracaine significantly reduced intracellular Ca²⁺ level induced by benzbromarone by 81% (0.61 ± 0.1 to $0.11 \pm 0.04 \Delta F/F_0$, n=10; N=6).

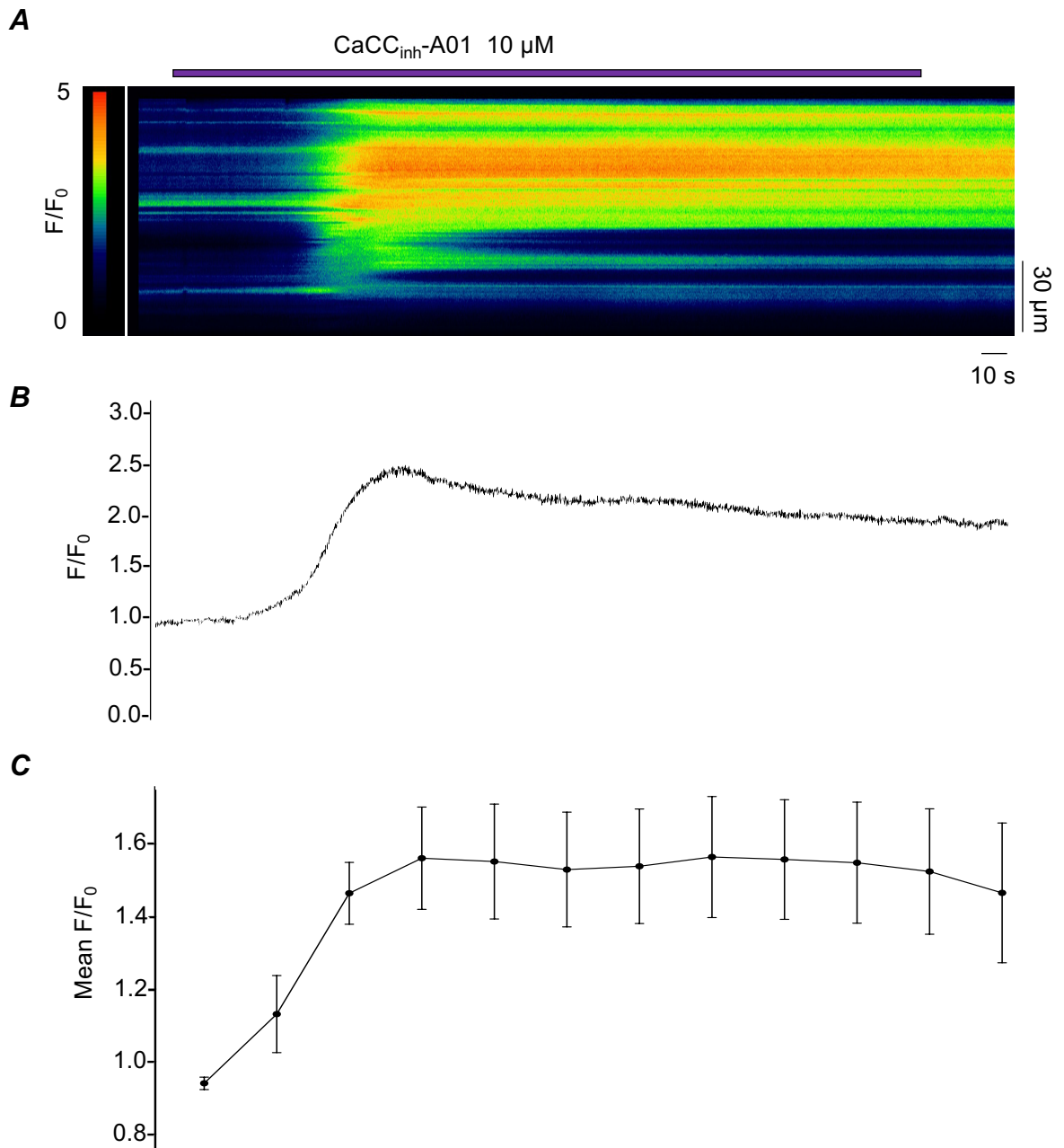


Figure 4.1. Effect of CaCC_{inh}-A01 on the intracellular Ca²⁺ concentration in freshly isolated ASMCs.

A) Representative pseudolinescan showing the effects of CaCC_{inh}-A01 (10 μ M) on basal Ca²⁺ level in ASMCs, and (B) the corresponding intensity profile plot. (C) Summary line-plot (measured every 30 sec) shows change in the mean intensity of Ca²⁺ concentration caused by CaCC_{inh}-A01 in 9 similar experiments. (n=9; N=7).

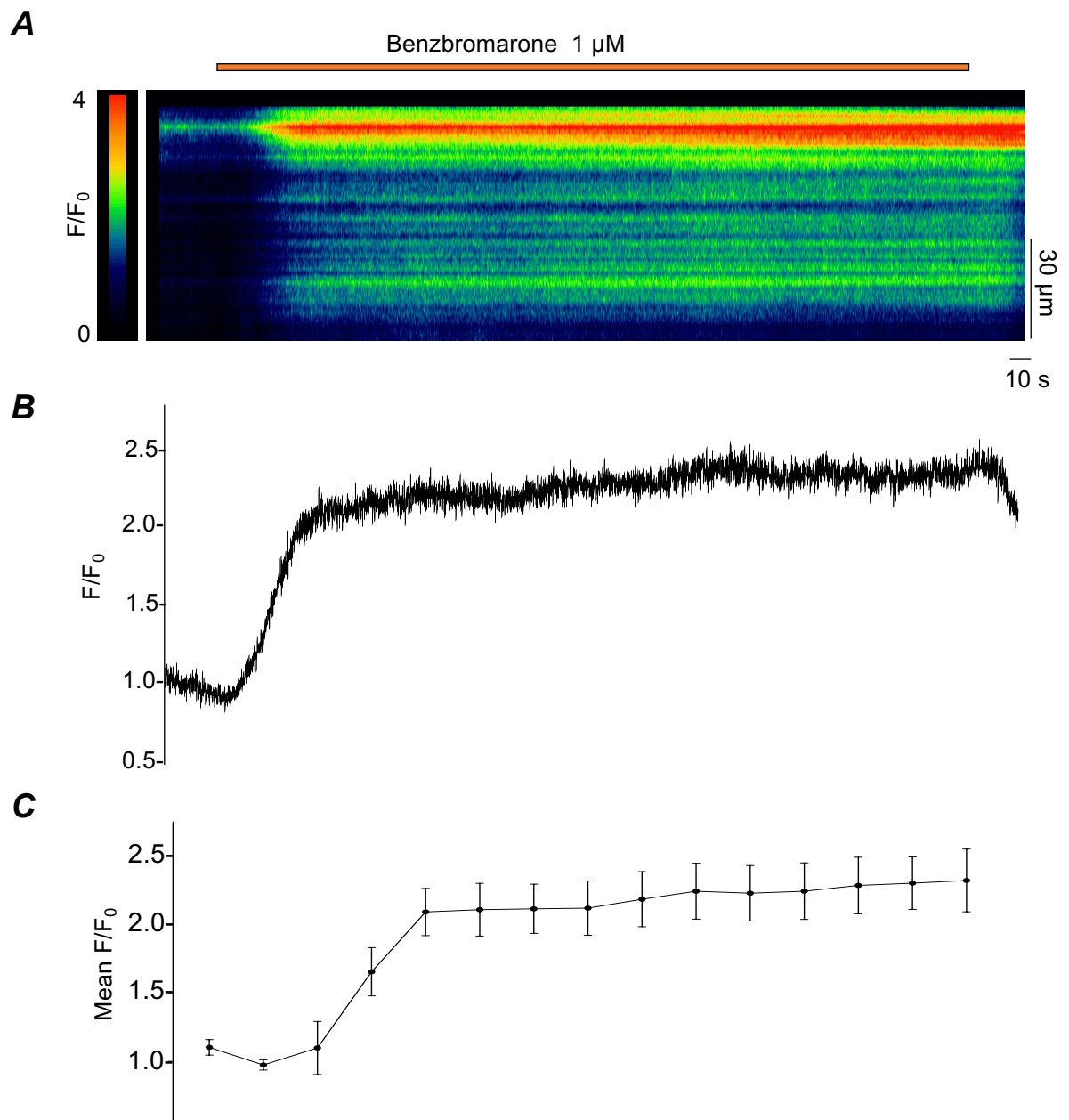


Figure 4.2. Effect of benzbromarone on the intracellular Ca^{2+} concentration in freshly isolated ASMCs.

(A) Representative pseudolinescan showing the effects of benzbromarone (1 μ M) on basal Ca^{2+} level in ASMCs, and (B) the corresponding intensity profile plot. (C) Summary line-plot (every 30 sec) shows change in the mean intensity of Ca^{2+} concentration caused by benzbromarone in 8 similar experiments. (n=8; N=5).

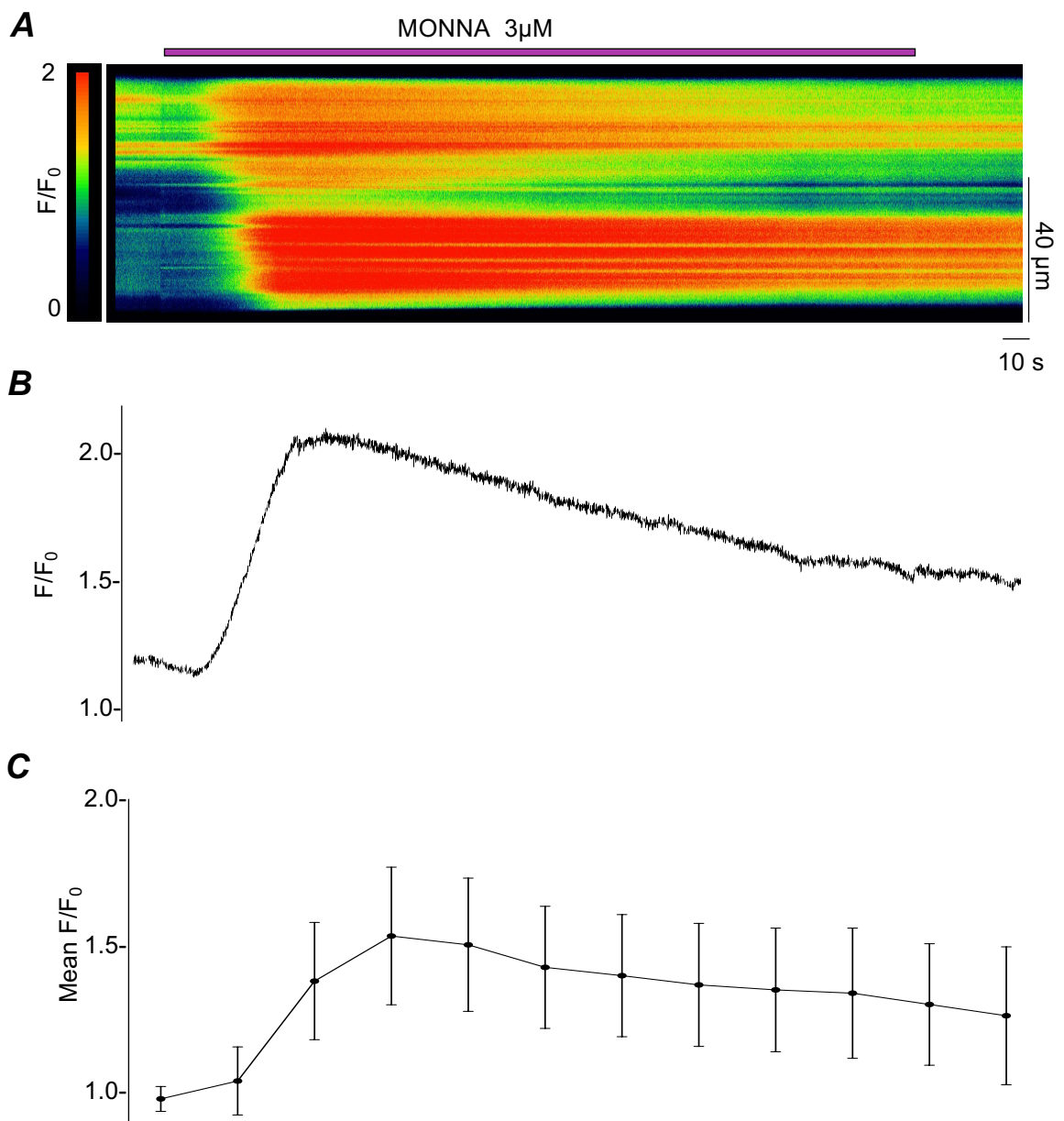


Figure 4.3. Effect of MONNA on the intracellular Ca²⁺ concentration in freshly isolated ASMCs.

(A) Representative pseudolinescan showing the effects of MONNA (3 μ M) on the basal Ca²⁺ level in ASMCs, and (B) the corresponding intensity profile plot. (C) Summary line-plot (measured every 30 sec) shows change in the mean intensity of Ca²⁺ concentration caused by MONNA in 7 similar experiments. (n=7; N=5).

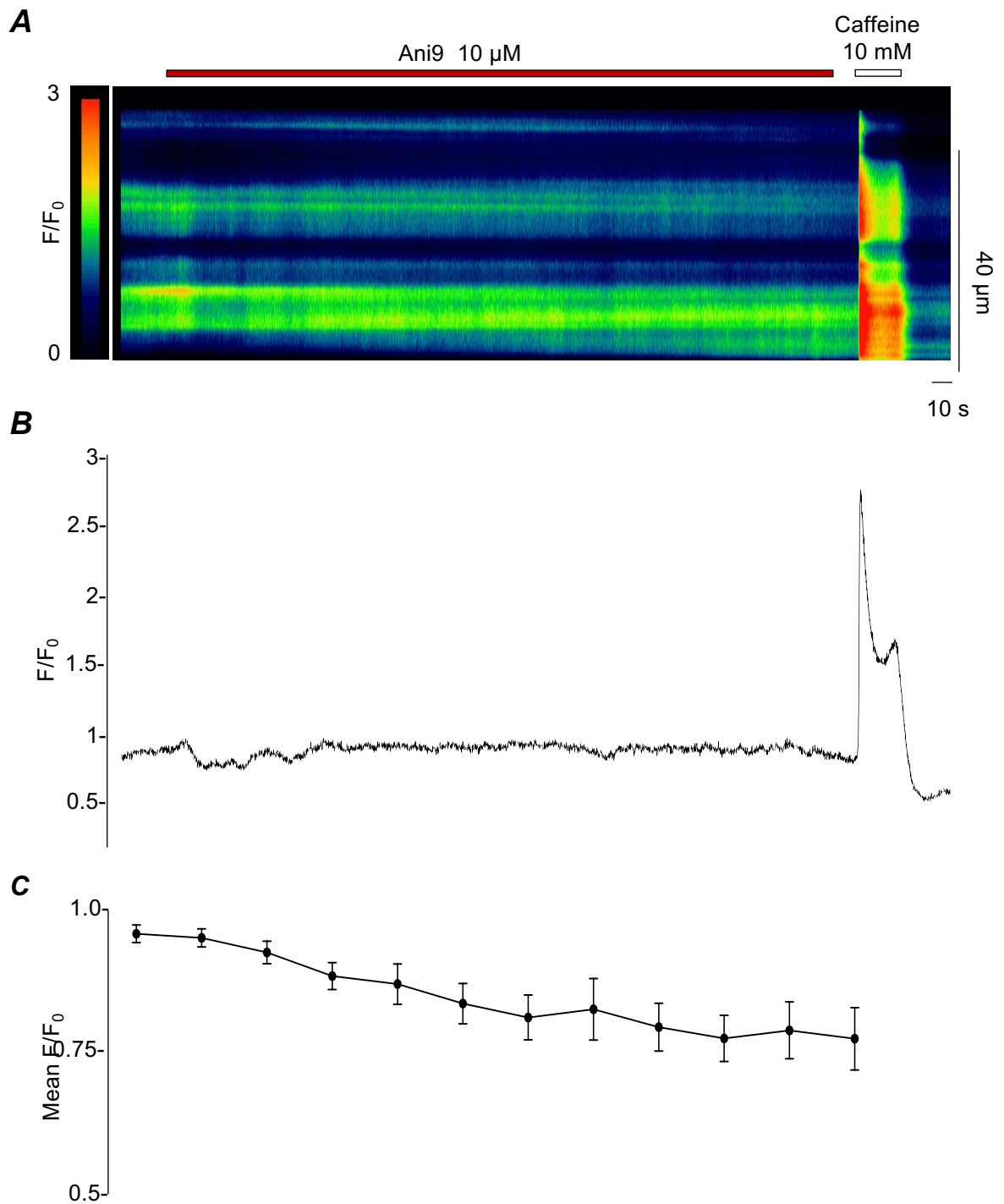


Figure 4.4. Effect of Ani9 on the intracellular Ca²⁺ concentration in freshly isolated ASMCs.

(A) Representative pseudolinescan showing the effects of Ani9 (10 μ M) on basal Ca²⁺ level in ASMCs, and (B) the corresponding intensity profile plot. (C) Summary line-plot (measured every 30 sec) shows change in the mean intensity of Ca²⁺ concentration caused by Ani9 in 8 similar experiments. (n=8; N=4).

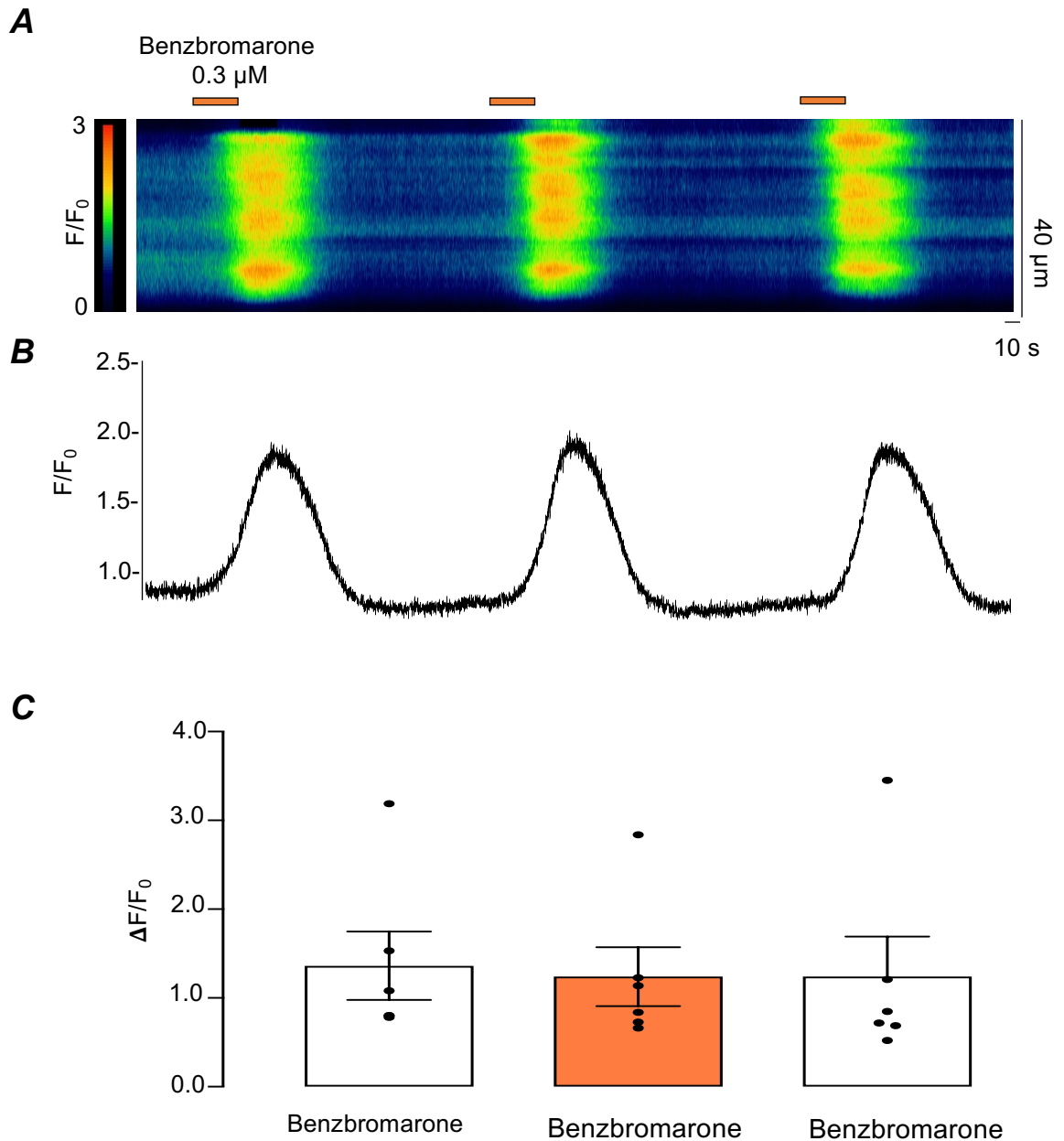


Figure 4.5. Reproducible response of benzbromarone in freshly isolated ASMCs.

Representative pseudoline scan showing the lower concentration of benzbromarone (0.3 μM) producing repeatable response in ASMCs (**A**), and (**B**) the corresponding intensity profile plot. (**C**) Summary bar charts with aligned dot-plot shows no significant change was observed in the mean amplitude of increase in intracellular Ca^{2+} concentration caused by 0.3 μM of benzbromarone in three consecutive applications. $n=6$, $N=5$; $p>0.05$; ANOVA.

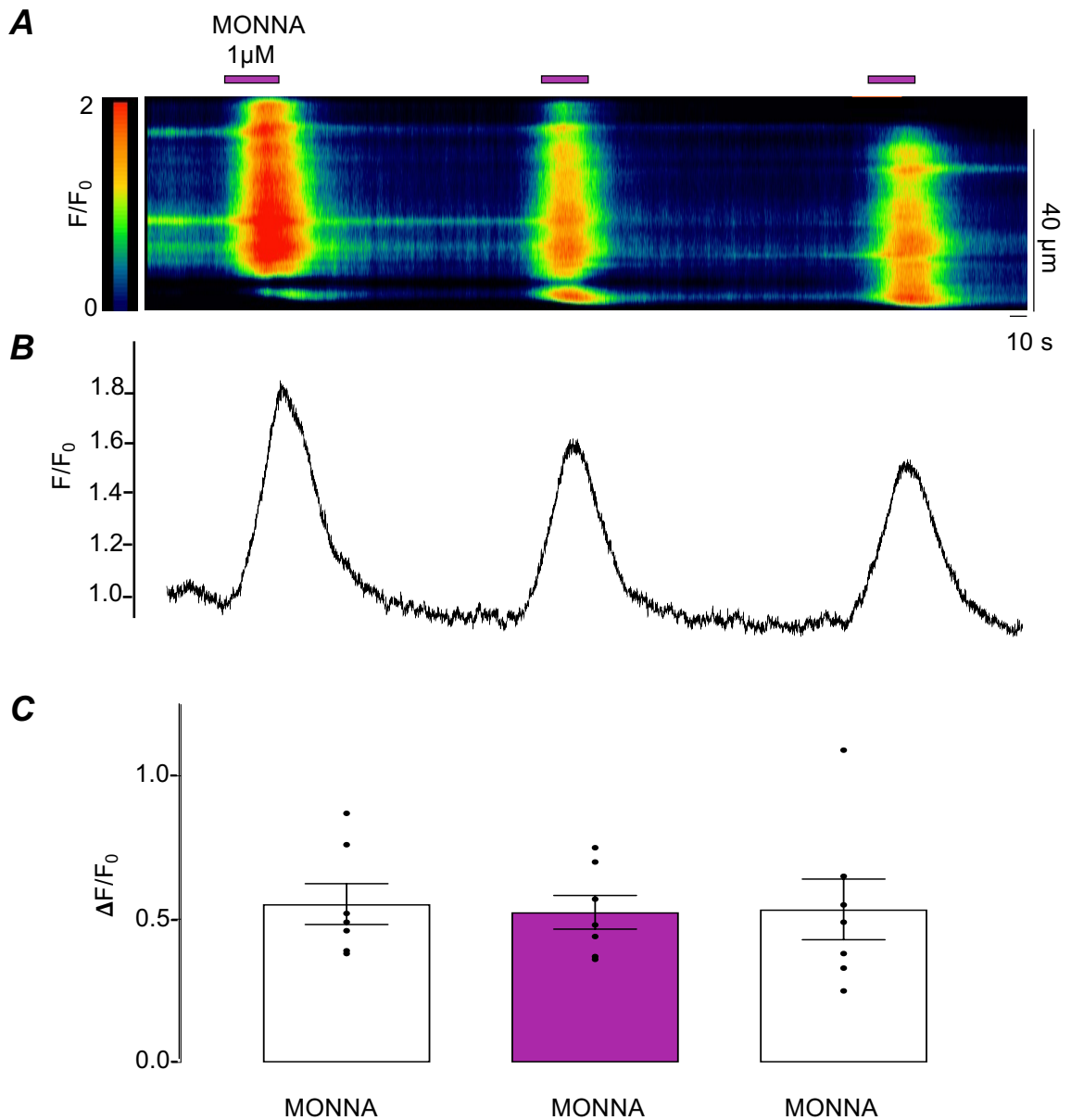


Figure 4.6. Reproducible response of MONNA in freshly isolated ASMCs.

(A) Representative pseudolinescan showing the lower concentration of MONNA (1 μ M) producing repeatable response in ASMCs, and (B) the corresponding intensity profile plot. (C) Summary bar charts with aligned dot-plot shows no significant change in the mean amplitude of increase in intracellular Ca^{2+} levels caused by 1 μ M of MONNA in three consecutive applications. $n=8$, $N=6$; $p>0.05$; ANOVA.

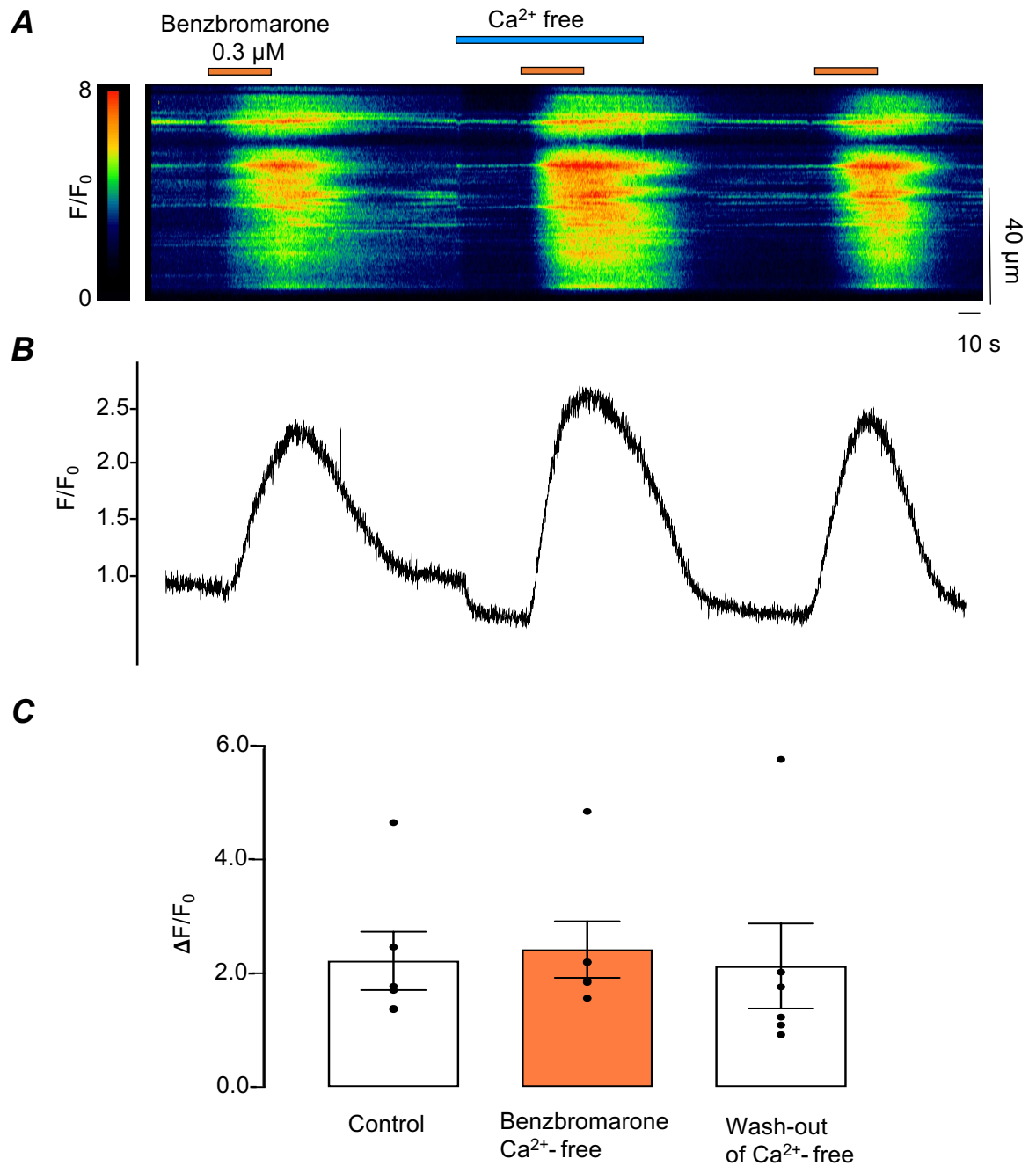


Figure 4.7. Effect of benzbromarone on intracellular Ca^{2+} levels in the absence of extracellular Ca^{2+} in freshly isolated ASMCs.

(A) Representative pseudolinescan showing the effects of benzbromarone (0.3 μM) on the intracellular Ca^{2+} levels in the absence of extracellular Ca^{2+} in ASMCs, and (B) the corresponding intensity profile plot. (C) Summary bar charts with aligned dot-plot shows no significant change in the mean amplitude of calcium levels caused by benzbromarone in Ca^{2+} free conditions. $n=6$, $N=6$; $p>0.05$; ANOVA.

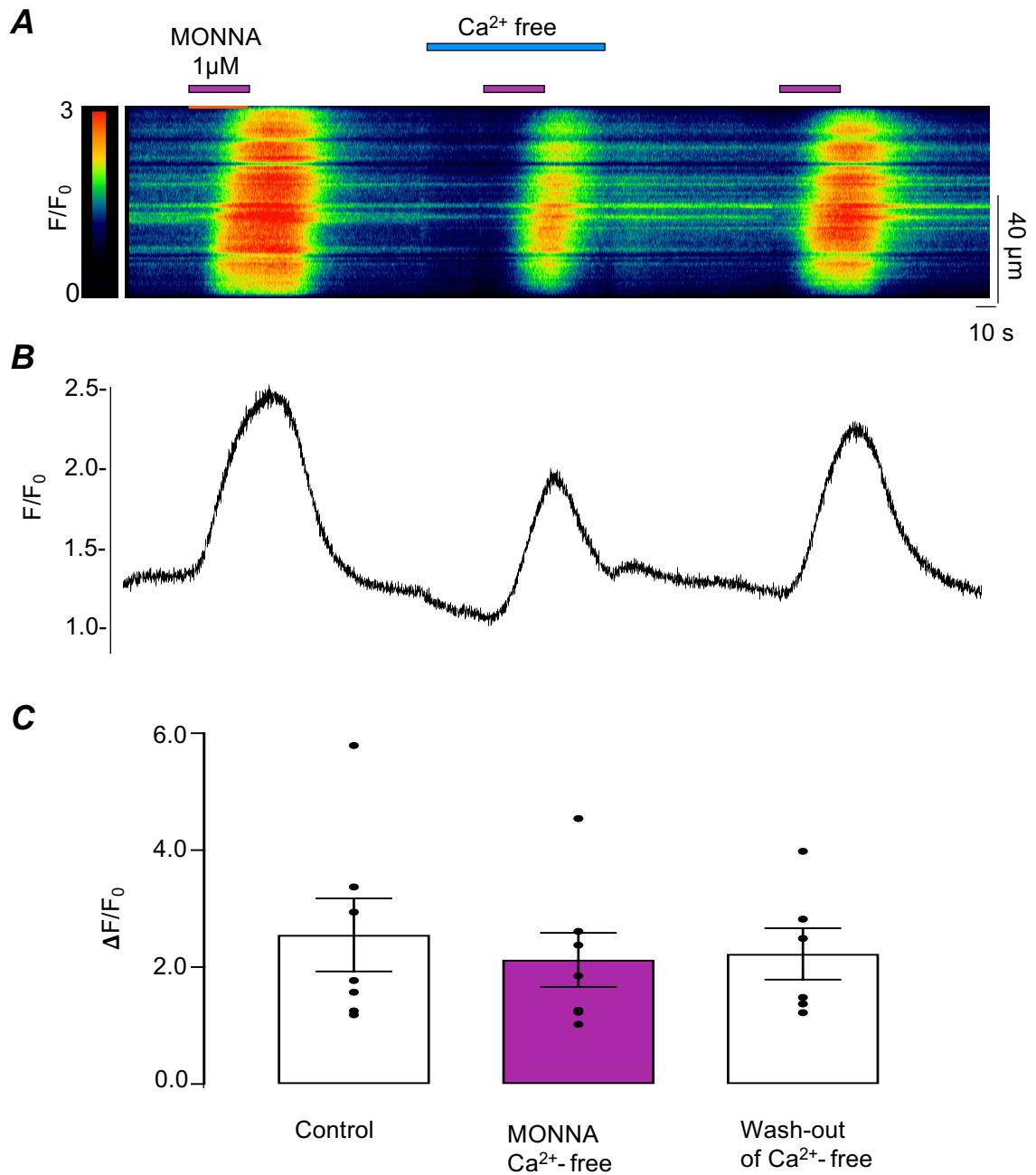


Figure 4.8. Effect of MONNA on intracellular Ca²⁺ levels in the absence of extracellular Ca²⁺ in freshly isolated ASMCs.

(A) Representative pseudolinescan showing the effects of MONNA (1 μ M) on the intracellular Ca²⁺ levels in the absence of extracellular Ca²⁺ in ASMCs, and (B) the corresponding intensity profile plot. (C) Summary bar charts with aligned dot-plot shows no significant change in the mean amplitude of calcium levels caused by MONNA in Ca²⁺ free conditions. n=7, N=6; p>0.05; ANOVA.

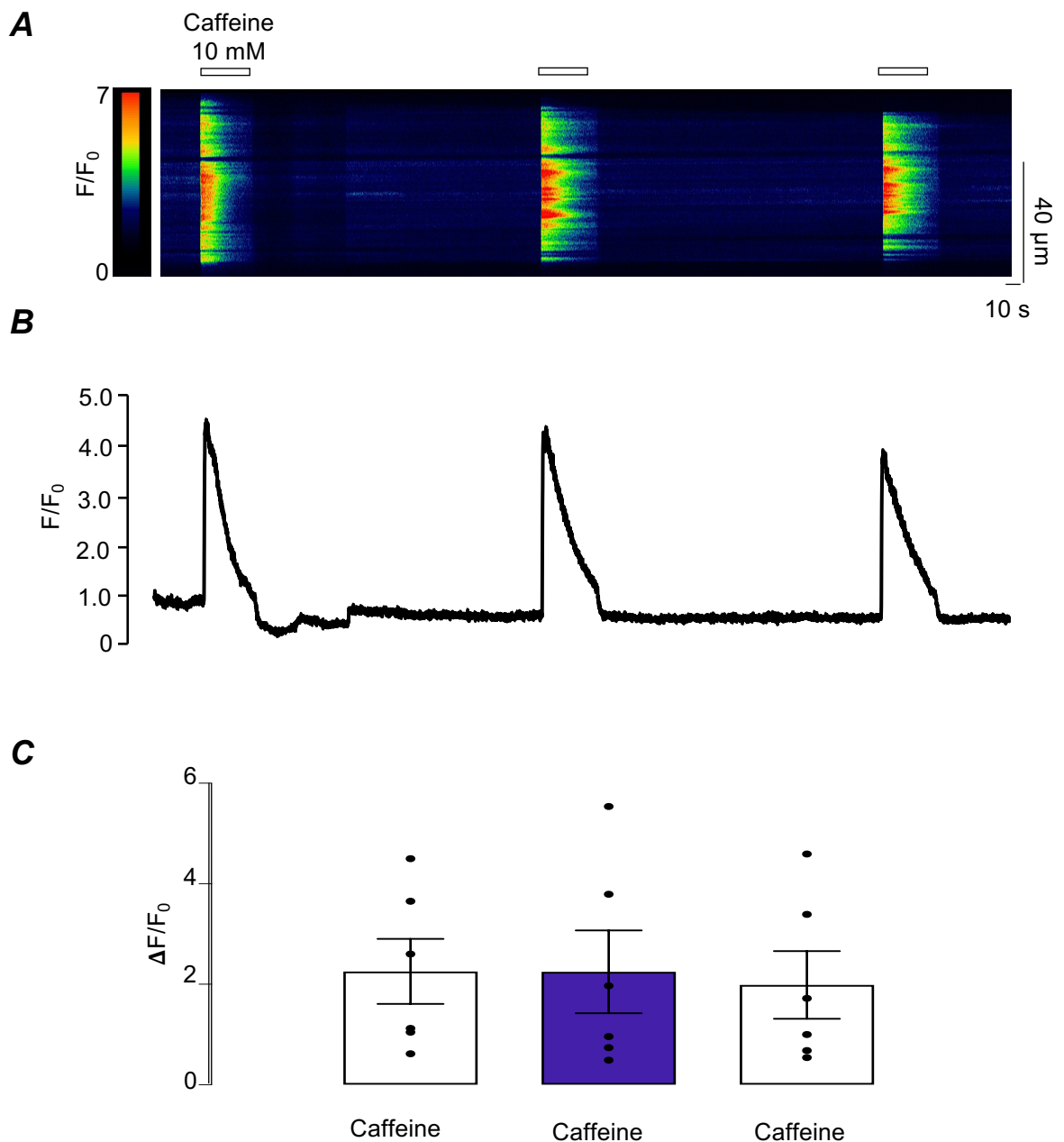


Figure 4.9. Reproducible consistent response of caffeine induced calcium transients in freshly isolated ASMCs.

(A) Representative pseudolinescan showing repetitive additions of 10 mM caffeine evoked calcium transients in murine ASMCs, and (B) the corresponding intensity profile plot. (C) Summary bar charts ($n=6$; $N=5$) with aligned dot-plot shows no significant change in the mean amplitude of calcium release induced by caffeine. $p>0.05$; ANOVA.

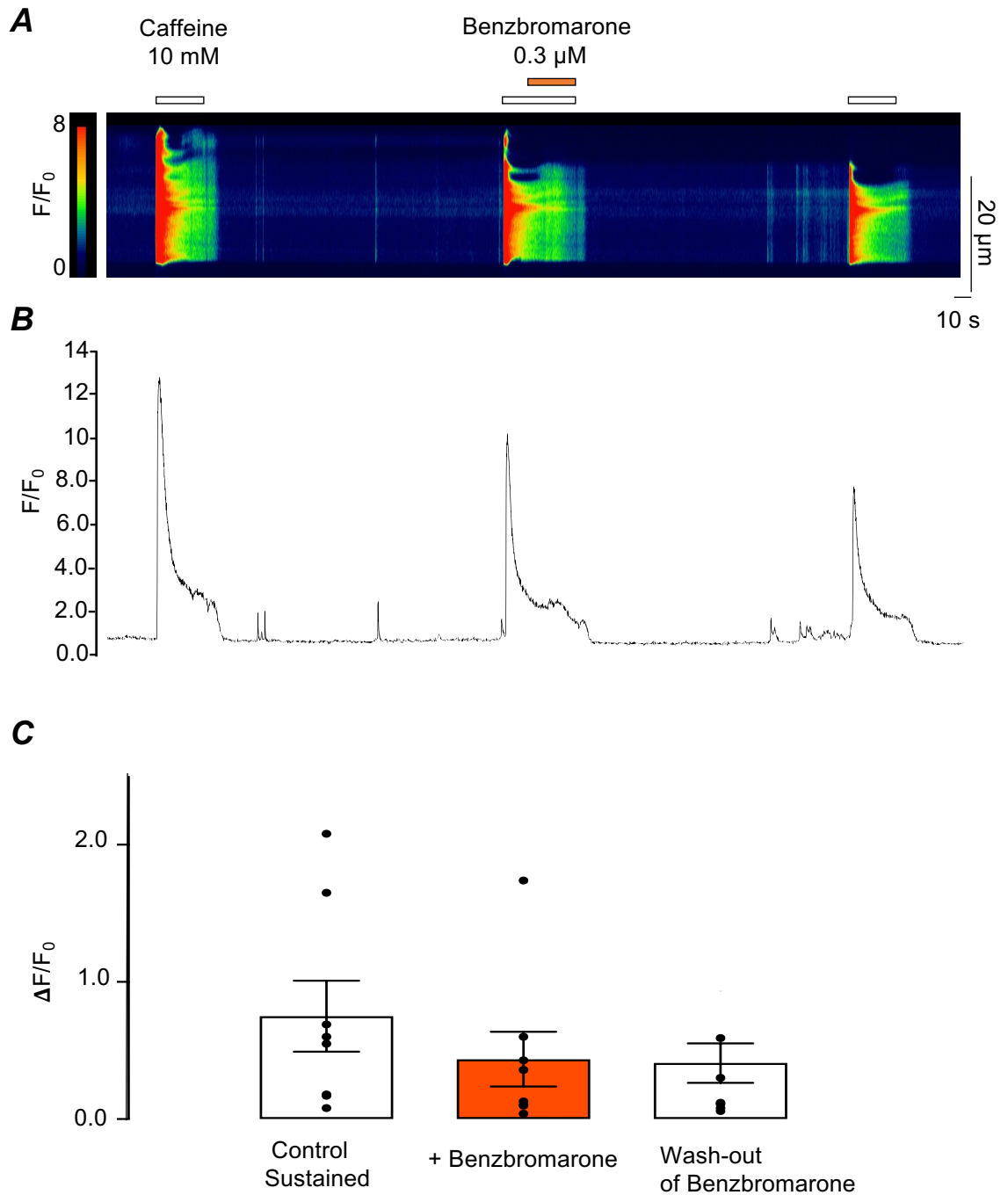


Figure 4.10. Effect of benzbromarone on caffeine induced calcium release in freshly isolated ASMCs.

(A) Representative pseudolinescan showing the effects of benzbromarone (0.3 μ M) on calcium level pre increased by caffeine in ASMCs, and (B) the corresponding intensity profile plot. (C) Summary bar charts with aligned dot-plot shows no significant change caused by benzbromarone in the mean amplitude of calcium release induced by caffeine. $\Delta F/F_0$ was measured at 25th sec after each caffeine application in 6 similar experiments. n=6, N=6; p>0.05; ANOVA.

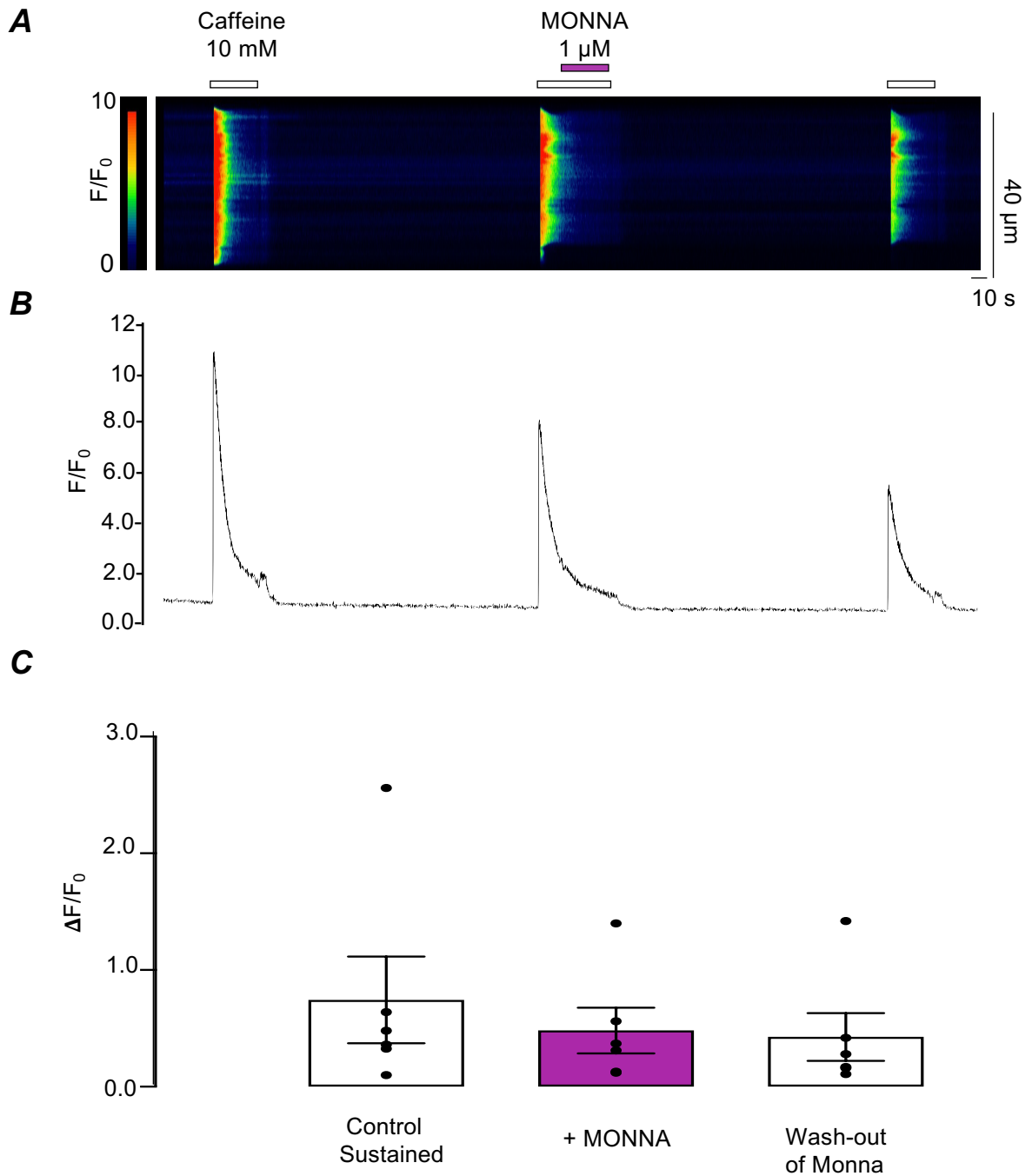


Figure 4.11. Effect of MONNA on caffeine induced calcium release in freshly isolated ASMCs.

(A) Representative pseudolinescan showing the effects of MONNA (1 μ M) on calcium level pre increased by caffeine in ASMCs, and (B) the corresponding intensity profile plot. (C) Summary bar charts with aligned dot-plot of 6 similar experiments shows no significant change caused by MONNA in the mean amplitude of calcium release induced by caffeine. $\Delta F/F_0$ was measured at 25th sec after each caffeine application. n=6, N=5; p>0.05; ANOVA.

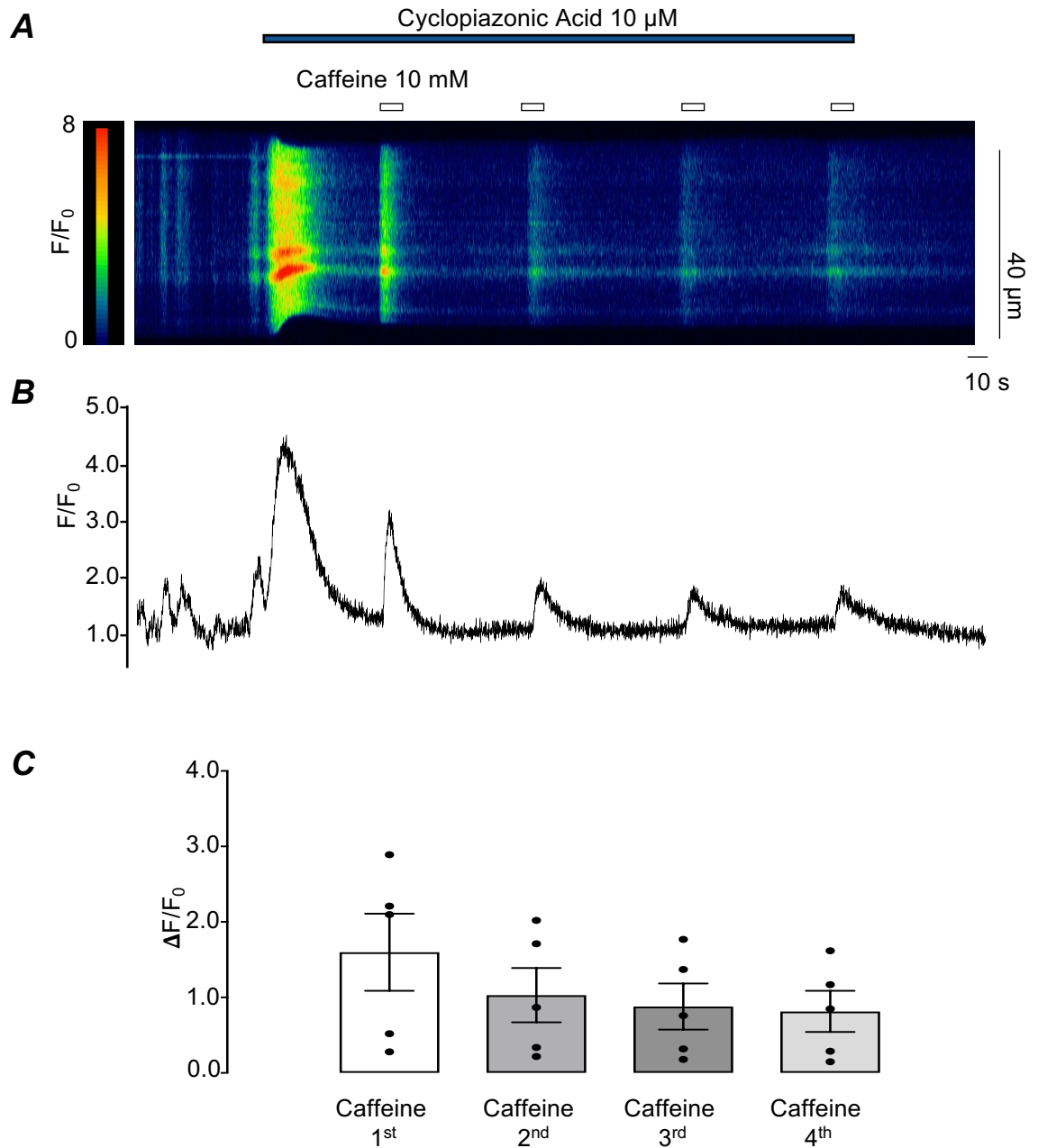


Figure 4.12. Effect of caffeine on intracellular Ca^{2+} levels in the presence of cyclopiazonic acid in freshly isolated ASMCs.

(A) Representative pseudolinescan showing caffeine (10 mM) response on the intracellular Ca^{2+} levels in the presence of SERCA pump blocker, cyclopiazonic acid (10 μ M) in ASMCs, and (B) the corresponding intensity profile plot. (C) Summary bar charts with aligned dot-plot shows no significant change in the mean amplitude of calcium levels increased by caffeine in the presence of cyclopiazonic acid.

$n=5$, $N=4$; $p>0.05$; ANOVA.

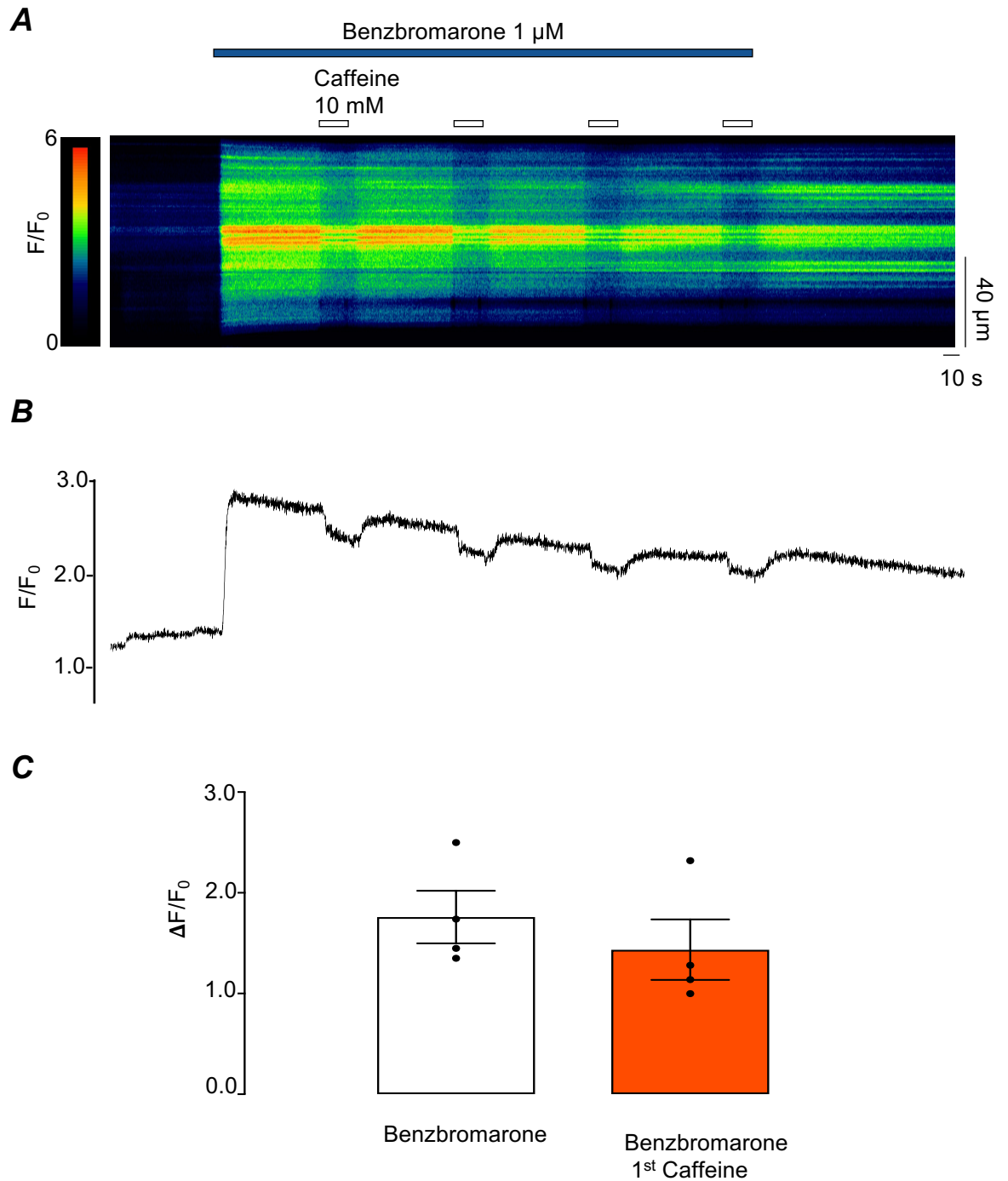


Figure 4.13. Effect of caffeine on intracellular Ca^{2+} levels increased by benzbromarone in freshly isolated ASMCs.

(A) Representative pseudolinescan showing the effect of caffeine (10 mM) on intracellular Ca^{2+} levels increased by benzbromarone (1 μM) in ASMCs, and (B) the corresponding intensity profile plot. (C) Summary bar charts with aligned dot-plot shows no significant change in the mean amplitude of the calcium levels caused by 1st application of caffeine in the presence of benzbromarone. $n=4$, $N=3$; $p>0.05$; paired t-test.

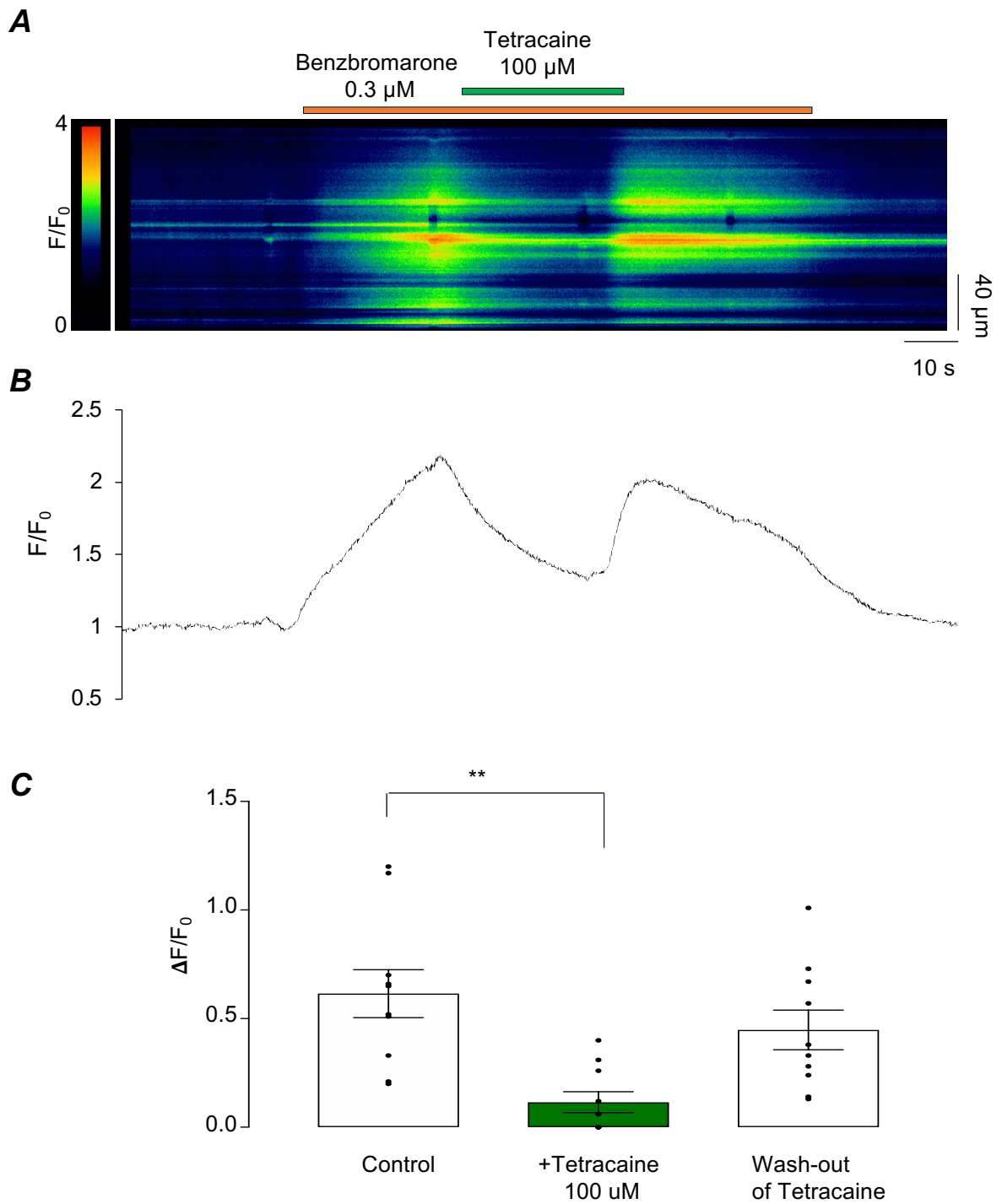


Figure 4.14. Effect of tetracaine on benzbromarone-induced calcium release in freshly isolated ASMCs.

(A) Representative pseudolinescan showing the effects of tetracaine (100 μ M) on benzbromarone (0.3 μ M) - induced calcium release in ASMCs, and (B) the corresponding intensity profile plot. (C) Summary bar charts (n=10; N=6) with aligned dot-plot shows the change in mean amplitude of calcium release caused by benzbromarone in the presence of tetracaine. **p<0.005; ANOVA.

4.3 Discussion

In this chapter, non-specific effects of benzbromarone, CaCC_{inh}-A01 and MONNA on cholinergic contractions highlighted in the previous chapter were investigated. Using the live cell Ca²⁺- imaging technique, we examined the effects of the blockers on cytosolic Ca²⁺ signals. Unexpectedly, we observed that all three TMEM16A blockers increased intracellular Ca²⁺ levels in ASMCs. This was interesting and novel, since, to the best of our knowledge, no other study has reported cytosolic Ca²⁺ increases caused by these blockers.

The next step was to investigate whether this increase in cytosolic Ca²⁺ levels was due to Ca²⁺ influx across the plasma membrane or Ca²⁺ release from the SR. We observed that both benzbromarone and MONNA still caused an increase in cytosolic Ca²⁺ levels in the absence of extracellular Ca²⁺, consistent with the idea that they are causing Ca²⁺ release from stores. To investigate this further, we examined their effects in the presence of caffeine. Caffeine itself increases cytoplasmic Ca²⁺ levels by causing Ca²⁺ release through RyR. We observed that both blockers did not caused any further increase in cytoplasmic Ca²⁺ levels in the presence of caffeine, consistent with the idea that they could be causing Ca²⁺ release through RyR. Furthermore, tetracaine, a RyR inhibitor, reduced the cytosolic Ca²⁺ level after it had been elevated by benzbromarone, again consistent with the idea that the latter might have been opening RyR.

However, an another possibility is that these drugs acted by hindering Ca²⁺ movements across the SR membrane in both directions by blocking SR Cl⁻ channels. Over the last two decades, there have been number of studies done to identify biophysical properties of SR Cl⁻ channels (Takeshima *et al.* 2015). They have shown wide-ranging gating and conductance properties; either they were pH regulated or ATP regulated or voltage sensitive or Ca²⁺ dependent. Although the molecular identity of Cl⁻ channel present on SR membrane is still under debate, their physiological role is assumed to be that they provide charge compensation during Ca²⁺ release and uptake from SR, although this has never been conclusively proved (Takeshima *et al.* 2015).

Pollock *et al.* (1998) were first to suggest that Cl⁻ channels might be important in smooth muscle SR, using permeabilized SMCs isolated from rabbit stomach.

Permeabilized SMCs were used to measure ATP-dependent Ca^{2+} uptake rate by SR. They have found that two Cl^- channel blockers, NPPB {(5-nitro-2-(3-phenylpropylamino) benzoic acid)} and indanyloxyacetic acid 94 derivative (R(+)-IAA-94), inhibited SR Ca^{2+} uptake in a dose -dependent manner. Interestingly, these blockers at maximum concentration, did not inhibit Ca^{2+} uptake by SR in cardiac muscle cells. Moreover, Cl^- channel blockers like niflumic acid and DNDS (4,4' -Dinitrostilbene- 2,2'-disulfonic acid) and replacing Cl^- with I^- and Br^- in the uptake buffer did not alter the rate of Ca^{2+} uptake. However, when Cl^- was substituted with SO_4^{2-} in the uptake buffer, Ca^{2+} uptake by smooth muscle SR was partially inhibited. Overall their study supports the idea that sarcolemmal Cl^- channels play a role in the rate of Ca^{2+} uptake by SR in smooth muscle cells.

Later, Hirota *et al.* (2006) also suggested that Cl^- flux across SR membrane plays a role in movement of Ca^{2+} across the SR membrane in tracheal smooth muscle isolated from cows and pigs. Using NPPB and Ca^{2+} fluorimetry, they showed that Ca^{2+} transients evoked by caffeine were significantly reduced in the presence of NPPB. The representative trace in the paper also showed shows a slight increase in the basal Ca^{2+} levels on the application of NPPB, which they thought was due to inhibition of Ca^{2+} uptake into the SR. However, when a similar experiment was performed in the absence of extracellular Cl^- , there was no increase in the basal Ca^{2+} level, which is inconsistent with their experiment with NPPB.

In the present study, experiments using caffeine in the presence of either CPA or benzbramarone would seem to rule out the possibility of TMEM16A blockers raising the intracellular Ca^{2+} level either by blocking the SERCA pump directly or by hindering Ca^{2+} uptake by blocking SR Cl^- channels. Caffeine caused a drop in the Ca^{2+} levels raised by benzbramarone, which was opposite to its effect in the presence of CPA, where it could still cause Ca^{2+} release (at least over the timecourse of the experiment). This Ca^{2+} lowering effect of caffeine could be because it is also a well-known phosphodiesterase inhibitor, which results in elevated intracellular cAMP (Sato *et al.* 1988). Cyclic AMP activates PKA resulting in phosphorylating phospholamban (PLN), a small transmembrane protein located on the SR. Depending on its phosphorylation state it regulates SERCA pump activity (MacLennan & Kranias, 2003). In the dephosphorylated state, PLN binds to SERCA pump and inhibits its activity. However, in the

phosphorylated state it unbinds from SERCA pump, which results in Ca^{2+} uptake through the pump. It would be interesting to test this idea further, by examining other ways of elevating cAMP, such as 8-bromo-cAMP, forskolin (stimulates adenylate cyclase) and other known inhibitors of phosphodiesterase 3, or activators of PKA such as 6-MB-cAMP.

In contrast to the present study, Danielsson *et al.* revealed that, benzbromarone was able to inhibit increases in cytosolic Ca^{2+} induced by histamine and bradykinin in cultured human ASMC (Danielsson *et al.* 2014). They found that pretreatment of cells with benzbromarone at concentrations of 10 μM , 50 μM and 100 μM reduced the increase in the intracellular Ca^{2+} levels caused by both histamine and bradykinin, with the degree of attenuation increased with the dose of benzbromarone. Importantly, similar experiments were then performed after removing extracellular Ca^{2+} concentration and it was found that the higher concentrations of benzbromarone (50 μM and 100 μM) still attenuated the responses to bradykinin and histamine. This suggested that benzbromarone, at high concentrations, could inhibit Ca^{2+} -release from the SR. To confirm this idea, they used mag-fluo-4 AM (to detect SR Ca^{2+}), along with fura-2 AM (to detect cytosolic Ca^{2+}) and found that pretreatment with either with benzbromarone (10 μM) or MONNA (10 μM) reduced the decrease in mag-fluo-4 fluorescence and the increase in fura-2 fluorescence in response to bradykinin. Similar observations were made when experiments were carried out with ACh. Danielsson *et al.* (2014) suggested that benzbromarone may block TMEM16A on the SR (although they had no evidence that it was expressed there), but accepted that it might have been blocking a different SR Cl^- channel, or having a completely unrelated off target effect. It should be noted that the concentrations of the TMEM16A blockers used in the present study were generally much lower than those used by Danielsson *et al.* with Ca^{2+} elevating effects in Ca^{2+} -free conditions evident at 0.3 μM benzbromarone and 1 μM MONNA, while the effects of benzbromarone on cytosolic Ca^{2+} in Ca^{2+} free conditions were only seen by Danielsson at 50 μM and 100 μM , though the effects on the mag-fluo-4 signal were observed at 10 μM of benzbromarone and MONNA.

Although the findings in this chapter are interesting, yet it raises the thought-provoking question of why we did not observe any contractions caused by these

TMEM16A blockers in organ bath experiments, when they increased cytosolic Ca^{2+} levels in isolated ASMCs. One possible reason behind this could be the concentration used in the study. TMEM16A blockers at micromolar concentrations might not be high enough to increase basal tone of bronchial rings in whole tissue experiments. We observed in initial imaging experiments that they caused a maximum 1.5 F/F_0 increase in cytosolic Ca^{2+} levels, compared to an average 5 F/F_0 increase by 10 mM caffeine. We found that 10 mM caffeine caused basal contraction with average amplitude of just 0.5 mN (data not shown). We can work on this hypothesis by two approach either by a) testing 10 mM or higher TMEM16A blockers concentration on organ bath experiments and observe whether they also cause basal contraction like caffeine or b) using micromolar concentrations of caffeine in organ bath experiments with CCh and see if caffeine like, the TMEM16A blockers might reduce cholinergic responses. If caffeine has an inhibitory effect on CCh induced contractile activity, we can suggest that at low concentrations RyR activators are also able to inhibit CCh-induced contractions.

In conclusion, benzbromarone, $\text{CaCC}_{\text{inh}}\text{-A01}$ and MONNA are not good pharmacological blockers to study plasmalemmal TMEM16A in ASMCs. Ani9 on other hand did not cause any increase in intracellular Ca^{2+} level, suggesting that it might be a better blocker to study plasmalemmal TMEM16A channels. The effects on benzbromarone in elevating intracellular Ca^{2+} are novel and would be worth investigating further to see if can activate RyR.

5. Effect of blocking SOCE on cholinergic activity of mouse bronchi smooth muscles

5.1 Introduction

Store operated calcium entry (SOCE) is a major pathway in Ca^{2+} signalling which is activated upon depletion of Ca^{2+} from the SR during excitation-contraction coupling. Over a decade ago, the molecular basis for SOCE, consisting STIM (Ca^{2+} sensors) on the SR membrane and Orai (Ca^{2+} selective) channels on the plasma membrane were discovered (Lewis, 2007). There is evidence that suggests that SOCE are involved in contractile activity of ASMCs, leading it to be a pathway of interest as a possible target for treating bronchoconstriction. Synta66, a potent CRAC channel blocker, significantly reduced bronchoconstriction-induced by grass allergen in human bronchial smooth muscle (Ashmole *et al.* 2012), but the same study reported that blocker failed to inhibit contractions induced by 10 μM of methacholine indicating the channel is not involved in cholinergic contractions. Interestingly, a recent study by Chen and Sanderson (2017) suggested that SOCE are actively involved in airway constrictions and underlie Ca^{2+} oscillations induced by methacholine, which they showed were inhibited by GSK-7975A, a SOCE blocker. In another study, the same group developed a mathematical model of Ca^{2+} oscillations in ASM, where they proposed that the CRAC pathway could compensate for blocked L-type Ca^{2+} channels (Boie *et al.* 2017). This was based on the idea that if the L-type Ca^{2+} channels were blocked the initial reduction in Ca^{2+} entry would result in increased store depletion and consequently increased CRAC activation. However, if CRAC channels were blocked, there was no mechanism whereby the L-type Ca^{2+} channels could compensate for them (Boie *et al.* 2017). Consequently, these authors attributed little role for L-type Ca^{2+} channels (and, by extension TMEM16A) as a depolarizing stimulus.

Indeed, involvement of L-type Ca^{2+} channels in the contractile activity in ASM has been under debate for a long time (Hirota & Janssen, 2007). CCh 10 nM induced contractions were abolished by nifedipine, however it completely failed to block the effect of CCh 10 μM (Janssen, 2002). In contrast, in pig tracheal smooth muscle, a much greater effect of nifedipine was reported, where 10 μM of nifedipine reduced the contraction evoked by 1 μM of CCh by 50% (Vannier *et al.* 1995). Byron *et al.* (2014) in using precision cut lung slices in rat, where the small airways can be observed, found that that 10 μM of verapamil (L-type Ca^{2+}

channel blocker) relaxed airway constriction induced by 230 nM of methacholine but not by 10 μ M of methacholine (Bryon *et al.* 2014). In the present study, experiments in chapter 3 showed that nifedipine substantially reduced contractions induced by all concentrations of CCh, though the effect was greater at lower CCh concentrations.

Apart from store refilling channels and L-type Ca^{2+} channels, a role in cholinergic activity for Ca^{2+} release channels on the SR has also been reported. Ca^{2+} release from SR in the smooth muscle occurs through IP_3 Rs and RyRs (Kotlikoff & Wang, 1998). Upon stimulation with cholinergic agonists, initial cytosolic Ca^{2+} increase is through IP_3 Rs which causes Ca^{2+} release from SR stores upon binding of IP_3 (Boie *et al.* 2017). RyR are believed to be involved in the subsequent prolonged increase of intracellular Ca^{2+} as they require Ca^{2+} to trigger Ca^{2+} release from SR through Ca^{2+} induced Ca^{2+} release (CICR). Several studies have confirmed the expression of RyRs in ASM (Du *et al.* 2005; Du *et al.* 2006; Hyvelin *et al.* 2000; Tazzeo *et al.* 2008). Du *et al.* (2005) found all three RYR isoforms in mouse bronchi, while RyR1 and RyR3 are expressed in the ASMCS. They investigated the involvement of RyR in bronchoconstriction using two different blockers of RyR, dantrolene and ryanodine. Our interest in studying RyR in whole tissue experiments arose following the observation made in chapter 4, where we showed that benzbramarone might be causing an increase in cytosolic Ca^{2+} levels by Ca^{2+} release through RyR.

There are a few points which made us question findings reported to date regarding the channels discussed above. i) Only high concentrations of CRAC blockers were used (Chen and Sanderson, 2017), ii) most studies have failed to supply details about how the experiments were performed, for example not being explicit as to how long the agonists were applied or time variation in agonists application (e.g. Vannier *et al.* 1995; Hirota & Janssen, 2007; Du *et al.* 2005), iii) investigating the inhibitory effects on one concentration of agonist (e.g. Chen and Sanderson, 2017), iv) missing traces of the experiments (only providing summarized data) (e.g. Tazzeo *et al.* 2008; Janssen, 2002). These are important details, as evidenced by the fact that in chapter 3 the blocking effects of drugs like benzbramarone and nifedipine were not uniform across the concentration range of agonist, and/or over the time course of a contraction. Hence, in the

present study, we have reexamined the effects of blocking CRAC channels, L-type Ca^{2+} channels and RyR on different concentrations of CCh-induced contractions (0.1-10 μM) in mouse bronchus smooth muscle. Each concentration was applied for 10 minutes and we examined the effects of blockers on both initial and sustained responses. The Ca^{2+} imaging experiments presented in this chapter were done using GCaMP8.1 mice (see Results section). These genetically encoded Ca^{2+} indicator (GECI) mice have several advantages over cells loaded with Fluo-4AM, including reduced photobleaching, even distribution of fluorescent indicator throughout the cell, and the ability to perform longer experiments since the fluorescent indicator does not leave the cells.

5.2 Results

5.2.1 Effect of CRAC channels antagonist on CCh-induced contractions

The selective blocker of CRAC channels, GSK-7975A (10 μM) was used in this study. Most of the blockers of CRAC channel such as SKF96365, BTP2 have been reported to have some off target effects (Liang *et al.* 2021). GSK-7975A is one of the most potent blockers on the channel with IC_{50} of 4.5 μM for cell studies (Derler *et al.* 2013). All the isometric tension experiments presented in this chapter were carried out in the presence of indomethacin (COX 1/2 inhibitor) to prevent spontaneous relaxations caused by the release of endogenous prostaglandins from epithelial cells. GSK-7975A had significant effects on cholinergic contractions induced by CCh concentrations in the range of 0.1-10 μM . As shown in panel A and B of *figure 5.1*, the CRAC channel blocker had more effect on higher CCh concentrations as compared to lower concentrations. The effect of inhibiting the channel was slightly greater on the sustained component of the contraction than the initial component. At 0.1 μM , the lowest concentration of carbachol, the mean amplitude of the initial component of contraction was reduced from 3.2 ± 0.8 mN to 2.2 ± 0.6 mN and at the highest CCh concentration of 10 μM mean amplitude was reduced from 4.8 ± 0.9 mN to 2.5 ± 0.6 mN. For the sustained component, the amplitude reduction at 0.1 μM was from 3.0 ± 0.8 mN to 2.4 ± 0.7 mN and at 10 μM it was from 5.6 ± 1.0 mN to 2.2 ± 0.6 mN.

Next, we investigated the effect of CRAC inhibitor on high K^+ contractures in an attempt to determine whether it is having non-specific effect on cholinergic contractions by blocking L-type Ca^{2+} channels. The CRAC inhibitor reversibly inhibited the amplitude of both the initial and sustained components of high K^+ -induced contractions by approximately 60% as represented in *figure 5.2A*. Summarized data is shown as a bar-graph with aligned dot-plot in panel B & C of *figure 5.2*. This blocking effect of the GSK-7975A suggests that its effect on cholinergic contractions might be through blocking of both CRAC and L-type Ca^{2+} channels.

High K^+ is hypothesized to depolarize the SMC membrane and opens L-type Ca^{2+} channels, resulting in Ca^{2+} influx and thus activates contractile activity. Because

GSK-7975A blocked a component of the contracture, it was decided to check the effect of an L-type Ca^{2+} channel blocker on high K^+ contractions. *Figure 5.3.* shows that incubation with 1 μM of nifedipine for 20 min completely inhibited high K^+ induced contractions.

5.2.2 Effect of blocking both L-type Ca^{2+} channels and CRAC channels on cholinergic-induced contractions

The experiments described in *figure 5.1* suggest that CRAC channels are important in mediating cholinergic contractions in mouse bronchial smooth muscle. Data presented in Chapter 3 (*figure 3.14*) also suggest that L-type Ca^{2+} channels are involved. In the next experiment, the effect of blocking CRAC channels was investigated after blocking L-type Ca^{2+} channels similar to the experiments done with TMEM16A blockers and nifedipine in chapter 3.

In *figure 5.4*, a recording from an experiment is presented where A is the control recording, B is in the presence of nifedipine (1 μM) and C was recorded in both nifedipine and GSK-7975A (10 μM). On treating with nifedipine, the inhibitory effect was similar to that observed in the experiments discussed earlier (*figure 3.14*). However when GSK-7975A was applied in the presence of nifedipine, contractions at all CCh concentrations were almost completely abolished. This was confirmed in a total of 6 experiments summarized in panels D & E. This result indicated that the effect of GSK-7975A on cholinergic contractions was not through blocking of L-type Ca^{2+} channels. It also suggests that when the L-type Ca^{2+} channels are blocked, the CRAC pathway mediates nearly all of the contractile response.

In the next experiment, the drugs were applied in reverse order with GSK-7975A applied first followed by nifedipine in the presence of GSK-7975A as shown in *figure 5.5*. Again, panel A is control, B is GSK-7975A alone and C is GSK-7975A plus nifedipine. On treating with GSK-7975A, the effect on cholinergic contractions was similar to results presented in *figure 5.1*, with the exception that a burst of phasic contractions occurred in response to 0.1 μM CCh. When nifedipine was applied in the presence of GSK-7975A, contractions induced by all concentrations of CCh were again almost abolished. This result was confirmed in 6 experiments summarized in panels D & E. This result would seem to

contradict the idea of Boie *et al.* (2017), that L-type Ca^{2+} channels are unable to compensate for absence of SOCE channels.

5.2.3 Effect of Ani9 on cholinergic contractions after blocking CRAC channels

The previous experiment suggested that when SOCE is blocked, the entire cholinergic contractile activity in ASM is driven by Ca^{2+} influx through L-type Ca^{2+} channel. This raised an interesting query about TMEM16A activation and involvement in membrane depolarization under these conditions to open L-type Ca^{2+} channels and cause Ca^{2+} influx. Hence, in the next experiment, the effect of inhibiting TMEM16A using Ani9 on cholinergic contractions after blocking CRAC channel by GSK-7975A was examined. In *figure 5.6*, panel A, B and C shows a recording of the experiment where A is control, B is GSK-7975A and C is GSK-7975A plus Ani9. On treating with GSK-7975A, the amplitudes of all the CCh-induced contractions were significantly reduced. However, when Ani9 was applied in the presence of GSK-7975A the CCh-induced contractions were all further reduced and, in this example, phasic contractions were observed at the two lowest concentrations of CCh. This effect of Ani9 was significant as shown in the summary data in panels D & E. However, unlike nifedipine with GSK-795A, there is still CCh contractions left after blocking of both CRAC and CaCC channels. This indicates there is another pathway which causes membrane depolarization and activation of L-type Ca^{2+} channels in ASM.

5.2.4 Effect of inhibiting Ca^{2+} -induced Ca^{2+} release on cholinergic contractions

In the previous chapter, the data suggested that benzbrumarone could be possibly causing Ca^{2+} release through RyR, as it was sensitive to tetracaine. As discussed in chapter 4, benzbrumarone might be inhibiting cholinergic contractions by depleting the store through its action on RyR. Consequently, it was decided to explore whether Ca^{2+} -induced Ca^{2+} release through RyR contributed to cholinergic contractions by examining the effect of dantrolene (100 μM), a commercially available RyR antagonist. As shown in panel A and B of *figure 5.7*, this RyR blocker reduced contractions in response to all concentrations of CCh and had more effect on the sustained components

compared to the initial components of contraction. The inhibitory pattern was similar to that of benzbromarone. In both cases the inhibitory effect of the blocker was significant (panels C & D).

Interestingly, dantrolene also reversibly inhibited the amplitude of high K^+ -induced contractions (*figure 5.8*). In this case, it reduced the sustained component of high K^+ -induced contractions more than the peak (panels B & C). To confirm the effect of blocking RyR on high K^+ contractures, tetracaine was also tested. 100 μM of tetracaine also reversibly reduced high K^+ contractures as shown in *figure 5.9*. In this case, there was only a slight preference for the sustained versus initial component.

Next, we examined the effect of blocking through L-type Ca^{2+} channel on cholinergic contractions when RyR are already blocked. In *figure 5.10*, panel A, B and C represents a recording of an experiment where A is control, B is dantrolene and C is dantrolene plus nifedipine. On treating with dantrolene, the inhibitory effect of the blocker was the same as observed earlier (*figure 5.7*). However, when nifedipine was added the contractions were further reduced. Overall, nifedipine under these conditions had more effect at lower concentrations of CCh and more effect on the initial components compared to the sustained components of contraction. For instance initial response of CCh at 1 μM was further reduced by 55% after addition of nifedipine in the presence of dantrolene. However, at the same CCh concentration, no further reduction was observed in sustained response as shown in panels B & C. Both of these observations were confirmed in the summary data in panels D & E. This experiment result indicates that apart from involvement of RyR and L-type Ca^{2+} channels, there is another Ca^{2+} -release pathway involved in initial cholinergic responses to CCh > 0.3 μM .

We speculated whether the initial response by cholinergic agonist is more through Ca^{2+} release by IP_3Rs than RyR. Thus the next experiment aimed to study the effect of inhibiting both Ca^{2+} release channels on SR on cholinergic contractions. IP_3Rs was inhibited using 100 μM of 2-APB. In *figure 5.11*, panel A, B and C shows a trace from an experiment where A is control, B is dantrolene and C is dantrolene and 2-APB. On treating with dantrolene, the inhibitory effect

was the same as seen in previous experiments. However, when 2-APB was introduced it almost completely abolished all of the remaining contractions. Care is required in interpreting this result as 2-APB can also block CRAC currents (Wei *et al.* 2016).

Results from experiments presented in *figures* 5.10 & 5.11 hints three key points; i) RyR are more involved in maintaining the sustained component of cholinergic activity, ii) IP₃Rs are more involved in the transient component of cholinergic activity, and iii) in the presence of dantrolene, cholinergic contractions induced by lower CCh (< 1 μ M) concentrations are sensitive to both nifedipine and 2-APB.

5.2.5 Effect of benzbromarone after inhibition of cholinergic contractions with dantrolene

Because of the similarity of the effects of dantrolene (*figures* 5.7, 5.10 & 5.11) to the effects of benzbromarone described in Chapter 3 (*figure* 3.4), it was speculated that, in the whole tissue experiments, benzbromarone might act like dantrolene in blocking RyR. If true, it was postulated that benzbromarone should have little effect if applied in the presence of dantrolene. *Figure* 5.12 shows an experiment where this was done. Initially, dantrolene had its usual effect in reducing the contractions overall, while leaving the initial components relatively untouched (compare panels A & B) but, addition of benzbromarone abolished all of the remaining contractions. This suggests that benzbromarone was not acting merely as a RyR opener, unless it could overcome the blocking of RyR by dantrolene.

5.2.6 Effect of 0.3 μ M CCh on cytosolic Ca²⁺ levels in ASMCs

A final series of experiments were conducted to examine, separately and together, the effects of nifedipine and GSK-7975A on CCh evoked cytosolic Ca²⁺ levels. As these experiments were conducted on bronchial ASM cells isolated from GCaMP8.1 mice, rather than on fluo 4-AM loaded cells from WT mice which were used to perform experiments in chapter 4, some control experiments were performed first to examine the effects of CCh. *Figure* 5.13 shows that 20 sec applications of 0.3 μ M CCh were able to evoke consistent and reversible elevations in Ca²⁺. Morgan *et al.* (2022) had observed 1 μ M CCh generated Ca²⁺

oscillations in isolated ASMCs, however in the present study we observed a uniform rise in intracellular Ca^{2+} by 0.3 μM CCh and no Ca^{2+} oscillations were observed. In the summary bar chart and aligned dot-plot for 9 cells, the mean amplitude of peak at each response was ($\Delta\text{F}/\text{F}_0$): 1.97 \pm 0.4 for the 1st, 1.98 \pm 0.4 for the 2nd and 1.93 \pm 0.3 for the 3rd responses.

In the next set of experiments CCh of 0.3 μM was applied for 120 sec to see if the responses were sustained. An example is shown in panels A & B where it is clear that the Ca^{2+} remained elevated for the duration of the CCh application. This was confirmed in 9 cells, as shown in panel C of *figure 5.14*, where the mean F/F_0 was calculated at every 10 seconds and plotted as a line graph.

5.2.7 Effect of CRAC channels blockers and L-type Ca^{2+} channels blocker on 0.3 μM CCh

The next experiment investigated the effect of GSK-7975A on the CCh-induced Ca^{2+} elevation. Following 20 sec application of CCh, the CRAC channel blocker was applied for 90 sec. Then in the presence of GSK-7975A, CCh was re-applied as shown in the *figure 5.15A*. The response was reduced by 75% and this effect reversed on wash out of GSK-7975A. In 8 cells, $\Delta\text{F}/\text{F}_0$ was significantly reduced from 2.16 \pm 0.44 to 0.53 \pm 0.22 and wash out was almost complete (panel C).

A similar experiment was performed with nifedipine (*figure 5.16*). After application of a control CCh, nifedipine was applied for 60 s before CCh was re-applied. The amplitude of the Ca^{2+} elevation appeared to be significantly reduced in the presence of nifedipine (see panel B) and this effect of nifedipine appeared to wash out. In the summary data in panel C, $\Delta\text{F}/\text{F}_0$ was significantly reduced from 0.92 \pm 0.14 in control to 0.56 \pm 0.14 in nifedipine and this effect was partially reversible within the time course of the experiment.

In the next experiment, CCh was applied for 50 sec, followed by application of GSK-7975A in the presence of CCh for 40 sec as shown *figure 5.17*. GSK-7975A significantly reduced amplitude of Ca^{2+} elevated by CCh by about 85%. After 40 sec application of GSK-7975A, the drug was removed but application of CCh remained there for another 40 sec. The inhibitory effect of GSK-7975A was reversible similar to the previous experiment shown in *figure 5.15*. In the

summary data of 7 cells shown in panel C, $\Delta F/F_0$ was significantly reduced from 0.96 ± 0.26 in control to 0.13 ± 0.09 in GSK-7975A.

A similar experiment was performed with nifedipine. A 40 sec application of nifedipine significantly reduced amplitude of Ca^{2+} elevated by CCh. As shown in *figure 5.18*, there was partial wash-out of nifedipine. This can be confirmed from the summarized data of 8 cells presented in panel C. $\Delta F/F_0$ was significantly reduced from 0.8 ± 0.2 in control to 0.22 ± 0.11 in nifedipine.

5.2.8 Effect of blocking of L-type Ca^{2+} channels and CRAC channels on CCh-induced Ca^{2+} signals

A final set of experiments were carried out to investigate the effect of blocking both CRAC channels and L-type Ca^{2+} channels together on CCh-induced Ca^{2+} elevation in the ASMCs. These experiments were similar to the tension experiments presented in *figures 5.5* and *5.6*.

In the experiment, following 20 sec application of CCh, nifedipine was applied for 60 sec. Then in the presence of nifedipine, CCh was re-applied for 20 sec as shown in *figure 5.19A*. L-type Ca^{2+} blocker slightly reduced the amplitude of the Ca^{2+} elevation similar to previous experiment shown in *figure 5.15*. Next in the presence of nifedipine, GSK-7975A was applied for 90 sec and CCh was re-applied as shown in panel A. The response was further reduced by 84% and this effect was reversible. In 8 cells, $\Delta F/F_0$ was reduced from 1.36 ± 0.2 (nifedipine) to 0.22 ± 0.08 (nifedipine + GSK-7975A). The summarized bar chart with aligned dot-plot in panel C confirmed the observation.

In the next experiment, the drugs were applied in reverse order with GSK-7975A applied first followed by nifedipine in the presence of GSK-7975A as shown in *figure 5.20*. CCh was applied for 20 sec followed by application of GSK-7975A for 90 sec. Similar to the previous experiment (*figure 5.15*) the amplitude of Ca^{2+} elevation was significantly reduced by GSK-7975A. Following the 2nd application of CCh, nifedipine was applied in the presence of CRAC blocker for 60 sec. On re-application of CCh, Ca^{2+} signals were further reduced by 92%. This effect was reversible as confirmed by the summary data in panel C.

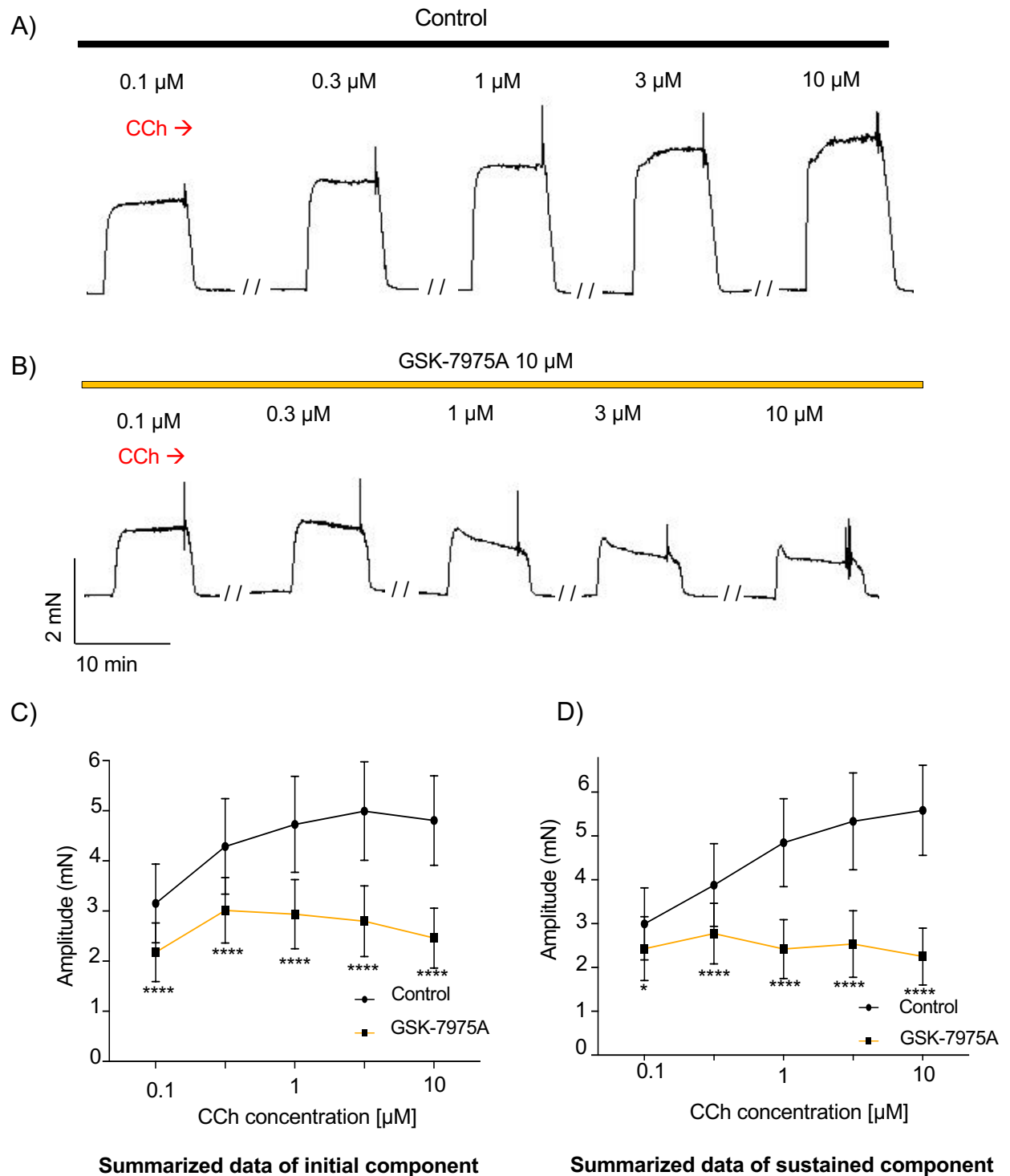
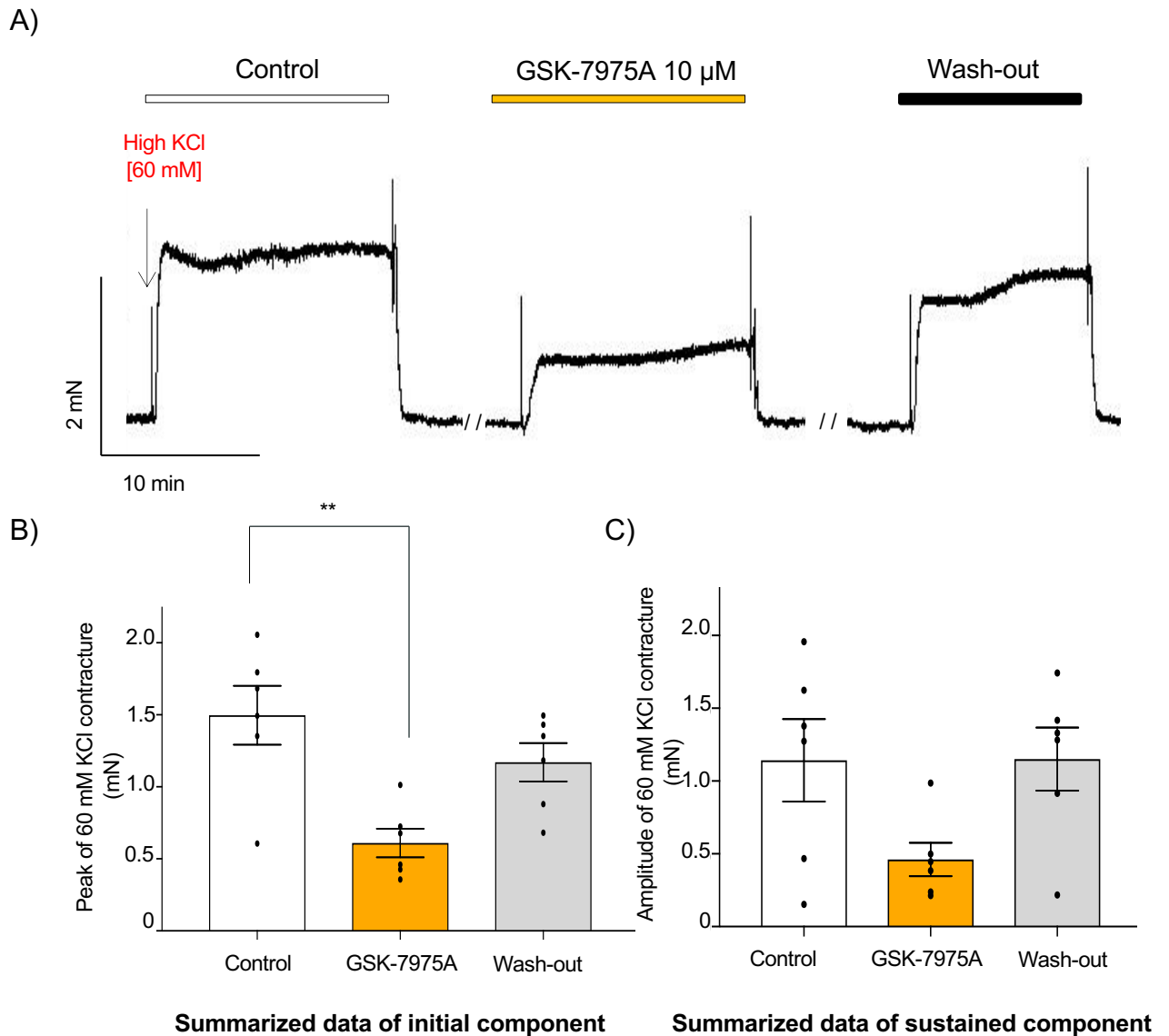


Figure 5.1. Effect of GSK-7975A on carbachol-induced contractions in mouse bronchial rings.

Representative tension recording showing the effect of CRAC channel blocker GSK-7975A (10 μM) on CCh-induced contractions (0.1, 0.3, 1, 3, 10 μM) separately. Panel A and B represents before and after treatment of bronchial rings with GSK-7975A respectively. Summarized data represented as line graph (n=8; N=6) of mean amplitude of initial and sustained response in panel C and D respectively for each CCh concentration.

ANOVA, *p<0.05, ****p<0.0001 comparing GSK-7975A vs Control.

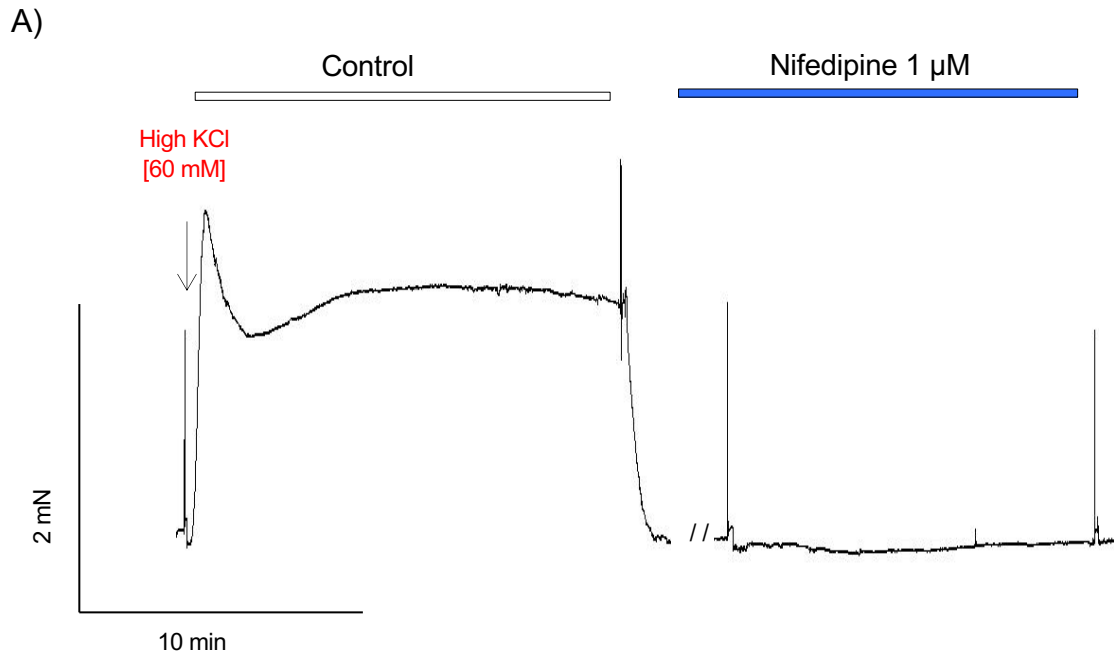


(Indomethacin 10 μ M and Atropine 1 μ M is present throughout the experiment)

Figure 5.2. Effect of GSK-7975A on KCl [60 mM]- induced contraction of mouse bronchial smooth muscle.

Panel A represents an isometric tension recording showing the time-control and effect of GSK-7975A (10 μ M) on KCl [60 mM] contractions in the presence of indomethacin 10 μ M and atropine 1 μ M, respectively. Summary bar chart with aligned dot plot (n=6; N=6) in panel B represents peak amplitude and panel C sustained amplitude of KCl [60 mM] contracture before and after treatment with GSK-7975A.

Paired t-test, ** p<0.05; comparing GSK-7975A vs Control.



(Indomethacin 10 μ M and Atropine 1 μ M is present throughout the experiment)

Figure 5.3. Effect of nifedipine on KCl [60 mM]- induced contraction of mouse bronchial smooth muscle.

Panel A represents an isometric tension recording showing the time-control and effect of nifedipine (1 μ M) on KCl [60 mM] contractions in the presence of indomethacin 10 μ M and atropine 1 μ M, respectively.

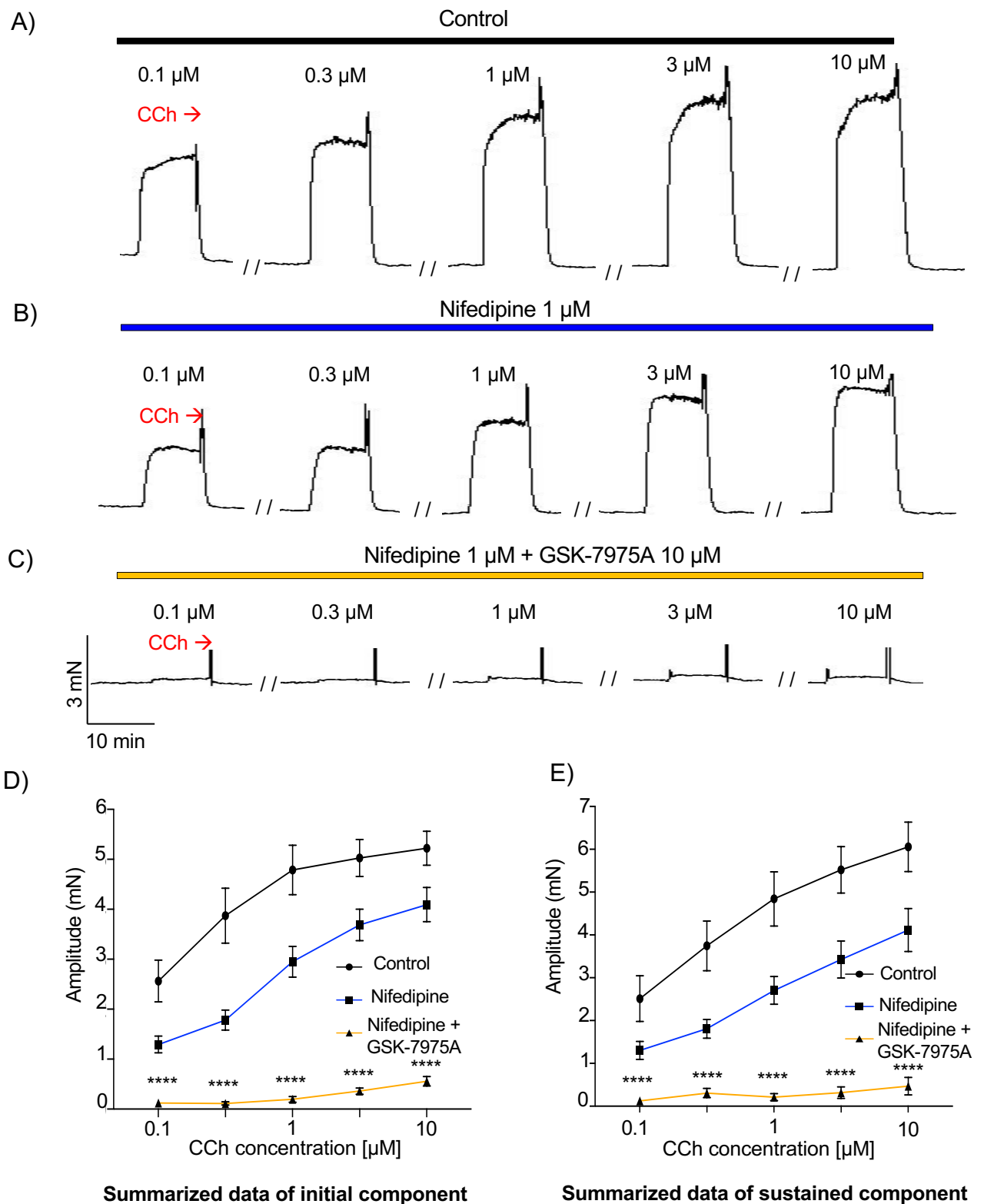


Figure 5.4. Effect of GSK-7975A on carbachol-induced contractions in presence of nifedipine in mouse bronchial rings.

Representative tension recording showing the effect of CRAC channel blocker GSK-7975A (10 μM) in presence of nifedipine (1 μM) on CCh-induced contraction (0.1, 0.3, 1, 3, 10 μM). Panel (A) control, (B) nifedipine (1 μM), (C) nifedipine (1 μM) with GSK-7975A (10 μM). Summarized data represented as line graph (n=6; N=6) of mean amplitude of initial (D) and sustained CCh responses (E) of all three sets; which were measured within 2nd and at 10th minute for each CCh contractions, respectively.

ANOVA, ****p<0.0001; comparing Nifedipine + GSK-7975A vs Nifedipine.

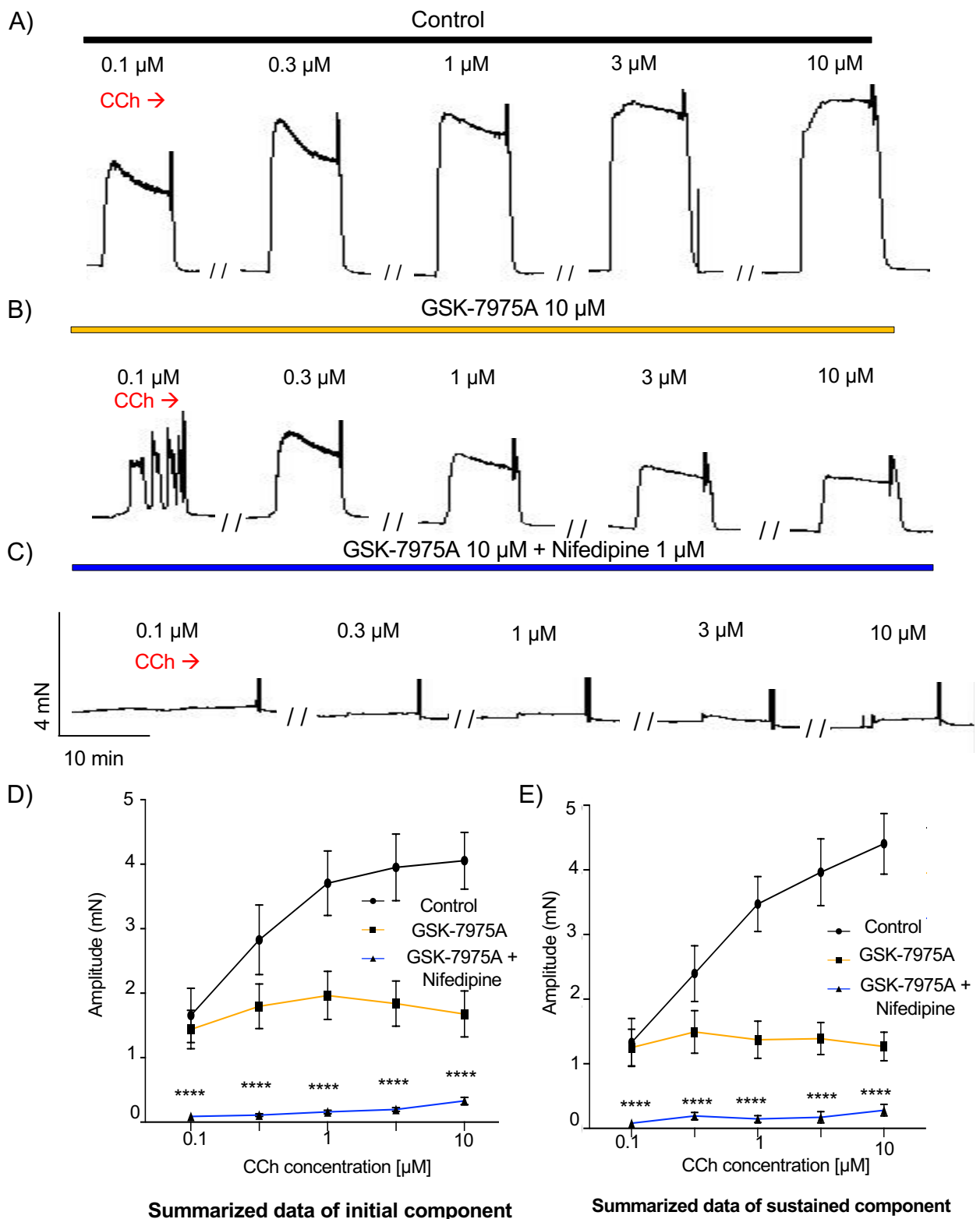


Figure 5.5. Effect of nifedipine on carbachol-induced contractions in presence of GSK-7975A in mouse bronchial rings.

Representative tension recording showing the effect of L-type Ca^{2+} channel blocker nifedipine (1 μM) in presence of GSK-7975A (10 μM) on CCh-induced contraction (0.1, 0.3, 1, 3, 10 μM). Panel (A) control, (B) GSK-7975A (10 μM), (C) GSK-7975A (10 μM) with nifedipine (1 μM). Summarized data represented as line graph (n=6; N=6) of mean amplitude of initial (D) and sustained CCh responses (E) of all three sets; which were measured within 2nd and at 10th minute for each CCh contractions, respectively.

ANOVA, ****p<0.0001; comparing GSK-7975A + Nifedipine vs GSK-7975A.

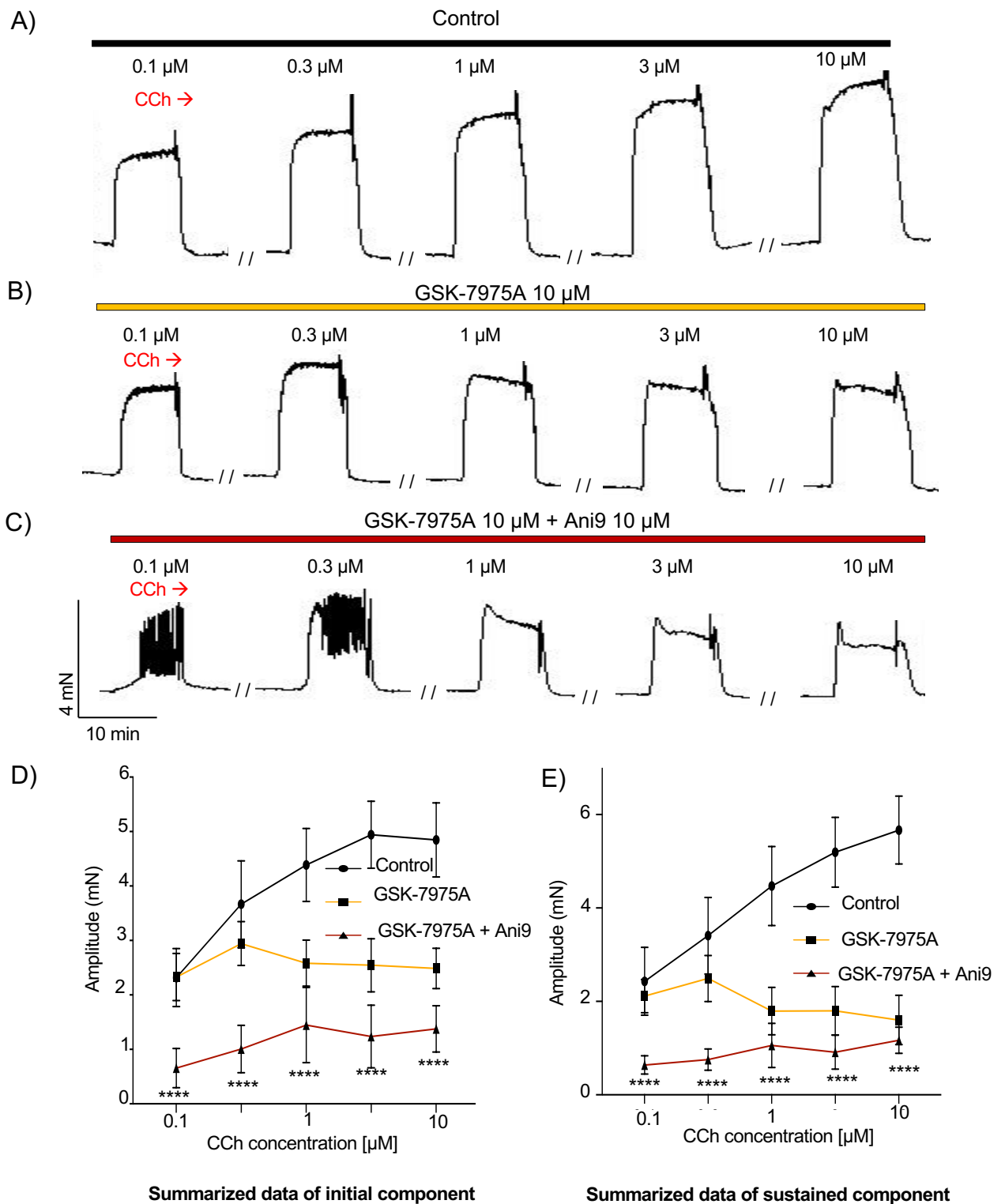


Figure 5.6. Effect of Ani9 on carbachol-induced contractions in presence of GSK-7975A in mouse bronchial rings.

Representative tension recording showing the effect of TMEM16A blocker Ani9 (10 μM) in presence of GSK-7975A (10 μM) on CCh-induced contraction (0.1, 0.3, 1, 3, 10 μM). Panel (A) control, (B) GSK-7975A (10 μM), (C) GSK-7975A (10 μM) with Ani9 (10 μM). Summarized data represented as line graph (n=6; N=6) of mean amplitude of initial (D) and sustained CCh responses (E) of all three sets; which were measured within 2nd and at 10th minute for each CCh contractions, respectively.

ANOVA, ****p<0.0001; comparing GSK-7975A + Ani9 vs GSK-7975A.

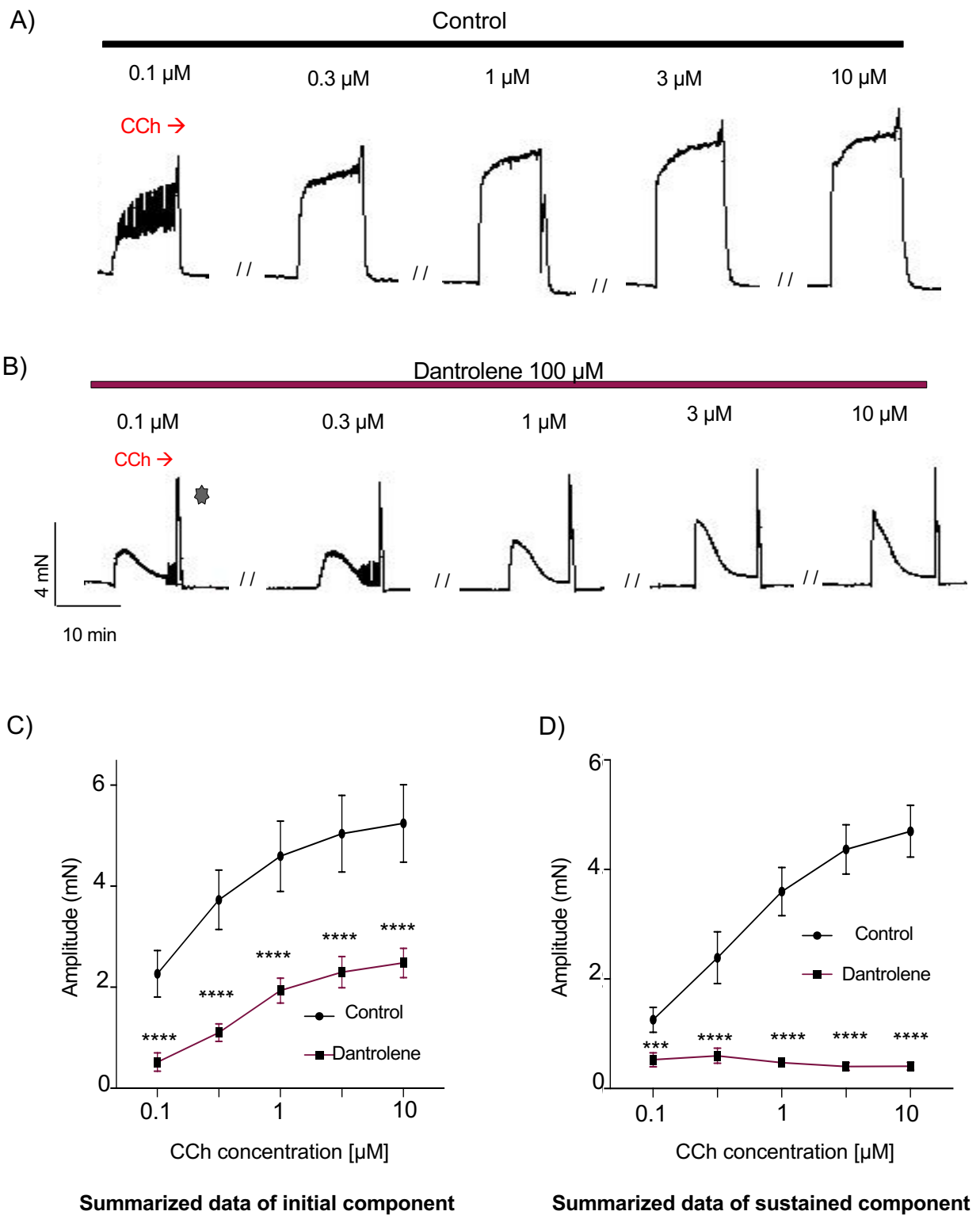
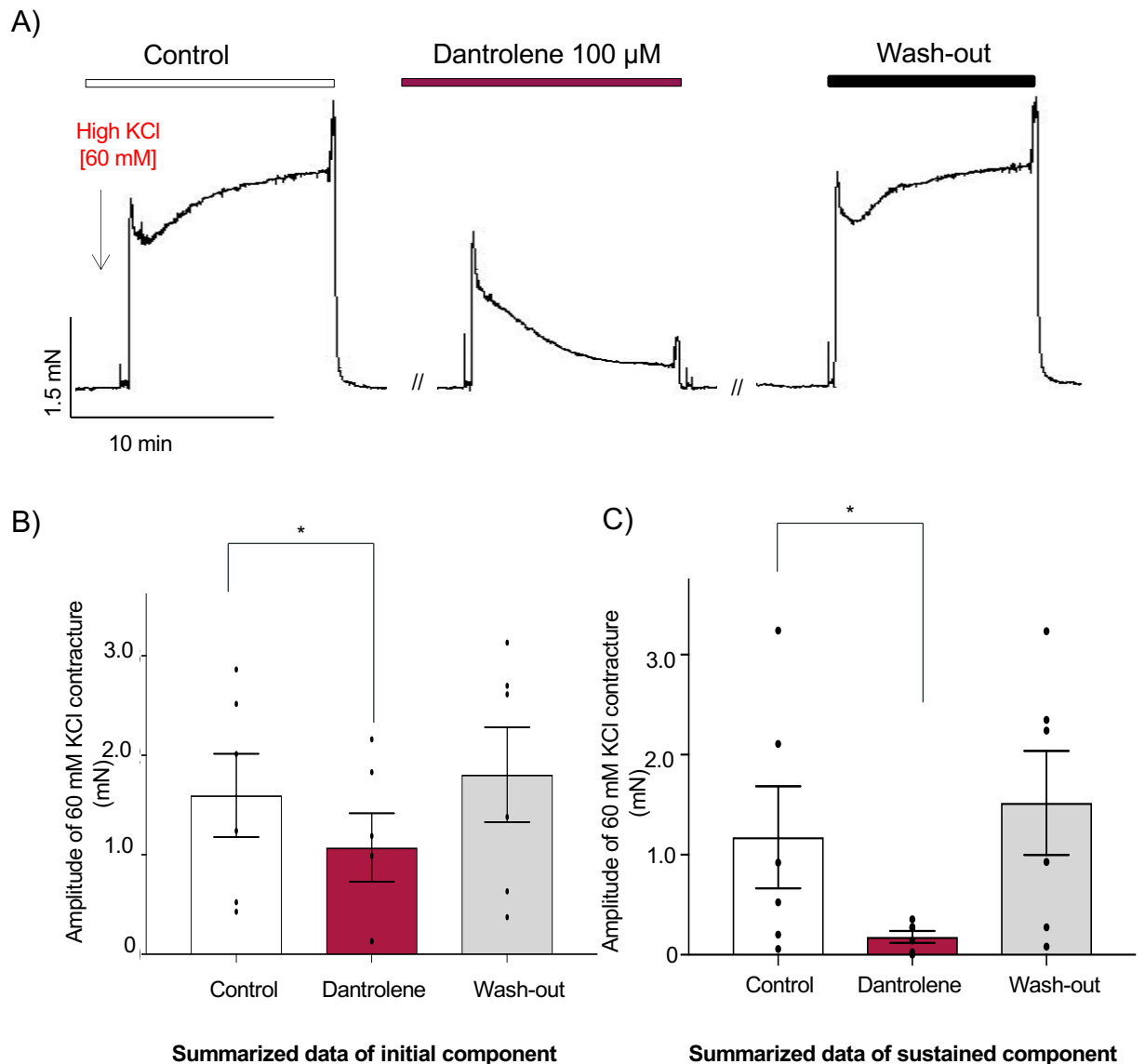


Figure 5.7. Effect of dantrolene on carbachol-induced contractions in mouse bronchial rings.

Representative tension recording showing the effect of RYR blocker dantrolene (100 μM) on CCh-induced contractions (0.1, 0.3, 1, 3, 10 μM) separately. Panel A and B represents before and after treatment of bronchial rings with dantrolene respectively. Summarized data represented as line graph (n=6; N=6) of mean amplitude of initial and sustained response in panel C and D respectively for each CCh concentration.

ANOVA, ****p<0.0001; comparing Dantrolene vs Control.

★ Recording artefacts during wash-out

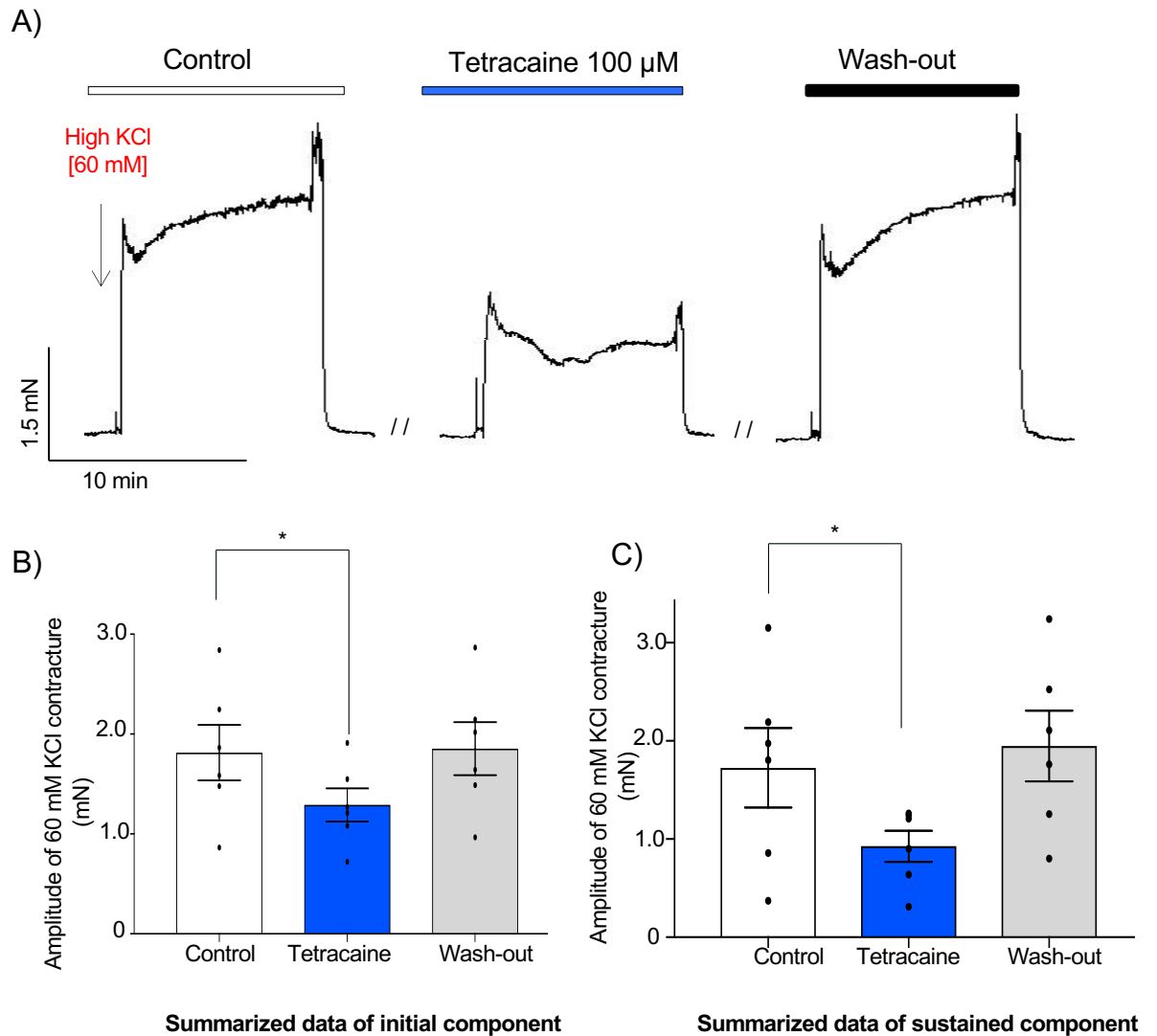


(Indomethacin 10 μ M and Atropine 1 μ M is present throughout the experiment)

Figure 5.8. Effect of dantrolene on KCl [60 mM]- induced contraction of mouse bronchial smooth muscle.

Panel A represents an isometric tension recording showing the time-control and relaxing effect of dantrolene (100 μ M) on KCl [60 mM] contractions in presence of indomethacin 10 μ M and atropine 1 μ M respectively. Summary bar chart with aligned dot plot (n=6; N=6) in panel B represents peak amplitude and panel C sustained amplitude of KCl [60 mM] contracture before and after treatment with dantrolene.

Paired t-test, * p<0.05; comparing Dantrolene vs Control.



(Indomethacin 10 μ M and Atropine 1 μ M is present throughout the experiment)

Figure 5.9. Effect of tetracaine on KCl [60 mM]- induced contraction of mouse bronchial smooth muscle.

Panel A represents an isometric tension recording showing the time-control and relaxing effect of tetracaine (100 μ M) on KCl [60 mM] contractions in presence of indomethacin 10 μ M and atropine 1 μ M respectively. Summary bar chart with aligned dot plot (n=6; N=6) in panel B represents peak amplitude and panel C sustained amplitude of KCl [60 mM] contracture before and after treatment with tetracaine.

Paired t-test, * p<0.05; comparing Tetracaine vs Control.

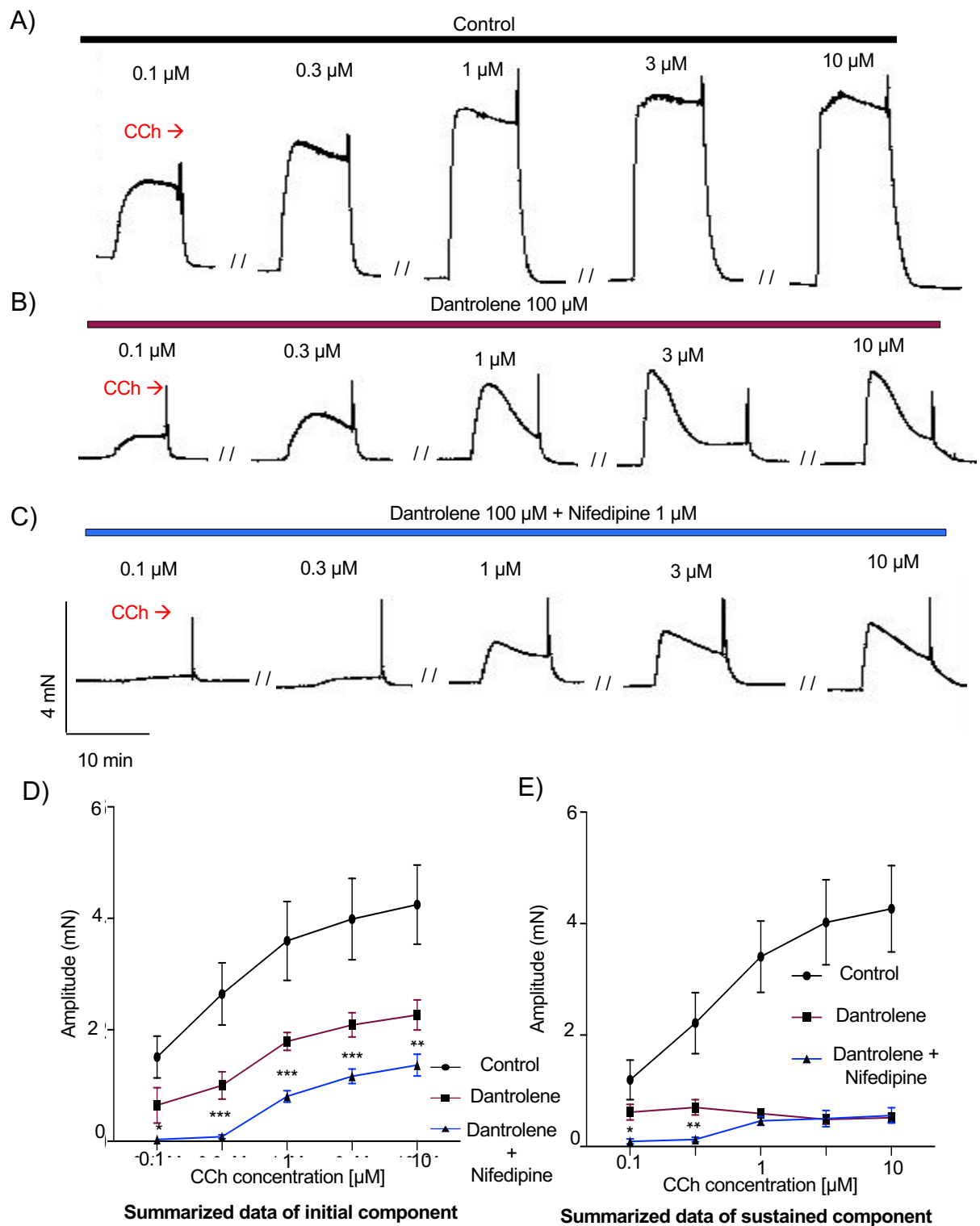


Figure 5.10. Effect of nifedipine on carbachol-induced contractions in presence of dantrolene in mouse bronchial rings.

Representative tension recording showing the effect of L-type Ca^{2+} channel blocker nifedipine (1 μM) in presence of dantrolene (100 μM) on CCh-induced contraction (0.1, 0.3, 1, 3, 10 μM). Panel (A) control, (B) dantrolene (100 μM), (C) dantrolene (100 μM) with nifedipine (1 μM). Summarized data represented as line graph (n=6; N=6) of mean amplitude of initial (D) and sustained CCh responses (E) of all three sets; which were measured within 2nd and at 10th minute for each CCh contractions, respectively.

ANOVA, *p<0.05, **p<0.01, ***p<0.001; comparing Dantrolene + Nifedipine vs Dantrolene.

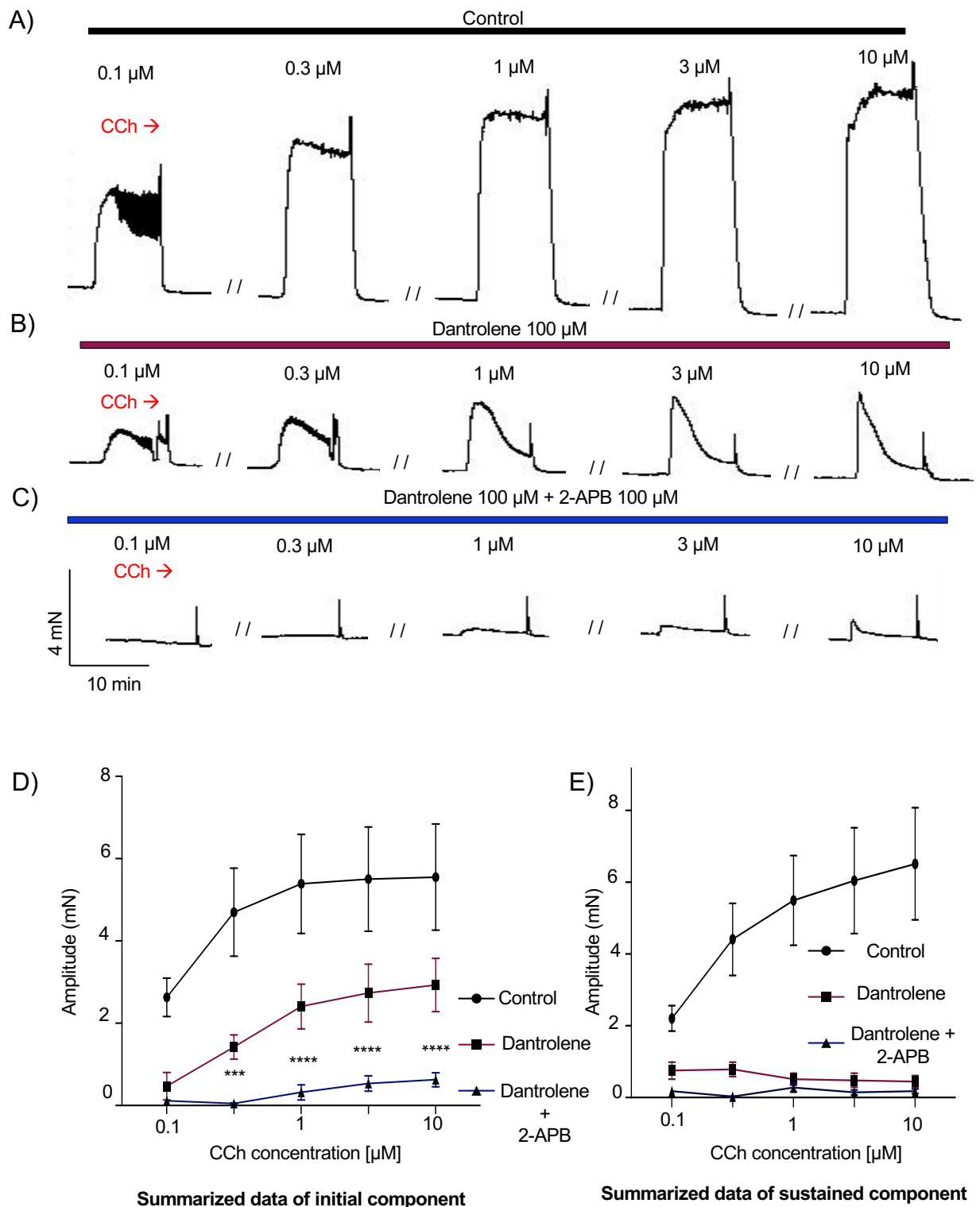


Figure 5.11. Effect of 2-APB on carbachol-induced contractions in presence of dantrolene in mouse bronchial rings.

Representative tension recording showing the effect of IP₃ blocker 2-APB (100 μM) in presence of dantrolene (100 μM) on CCh-induced contraction (0.1, 0.3, 1, 3, 10 μM). Panel (A) control, (B) dantrolene (100 μM), (C) dantrolene (100 μM) with 2-APB (100 μM). Summarized data represented as line graph (n=5; N=5) of mean amplitude of initial (D) and sustained CCh responses (E) of all three sets; which were measured within 2nd and at 10th minute for each CCh contractions, respectively.

ANOVA, ***p<0.001, ****p<0.0001; comparing Dantrolene + 2-APB vs Dantrolene.

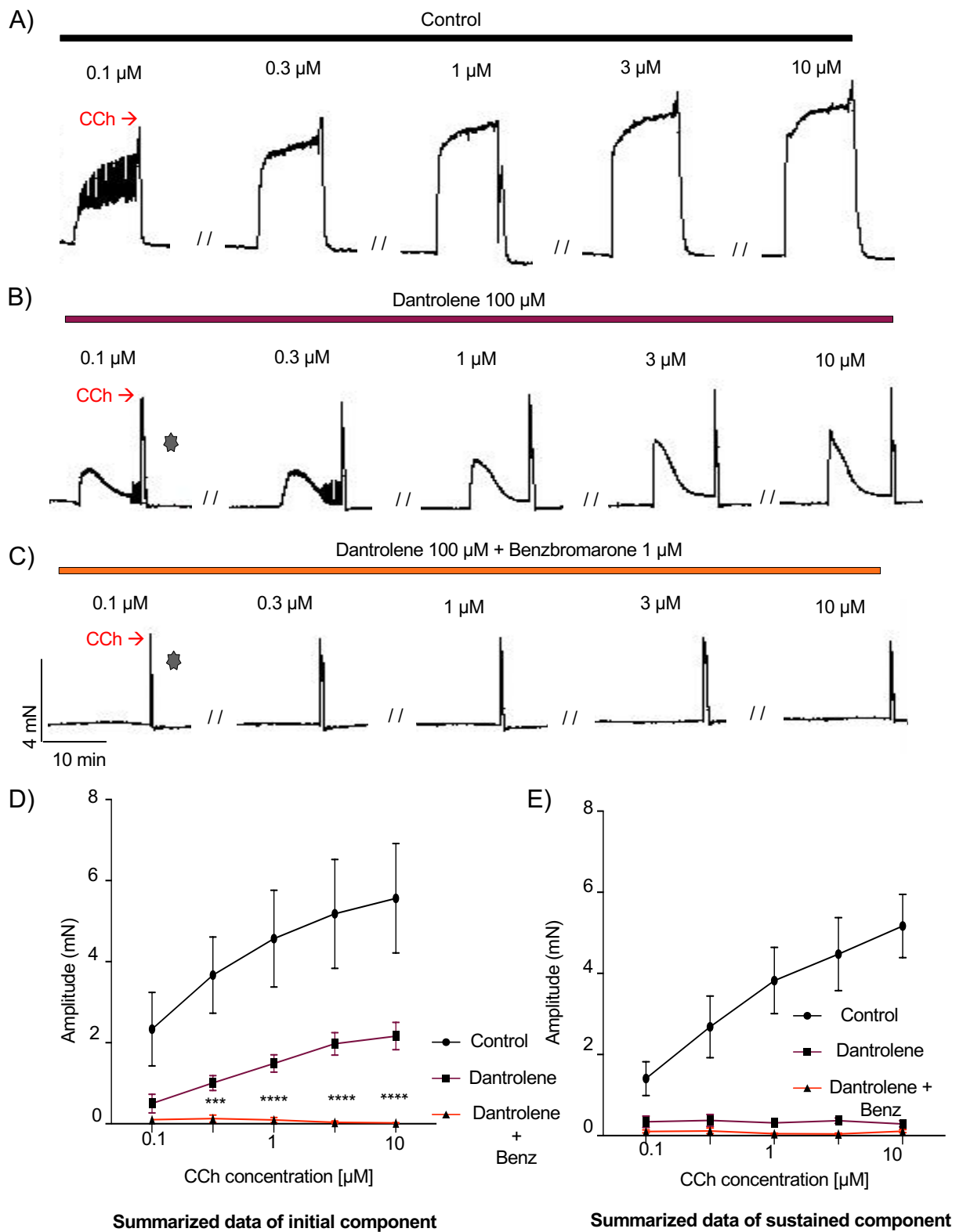


Figure 5.12. Effect of benzbromarone (Benz) on carbachol-induced contractions in presence of dantrolene in mouse bronchial rings.

Representative tension recording showing the effect of TMEM16A blocker benzbromarone (1 μM) in presence of dantrolene (100 μM) on CCh-induced contraction (0.1, 0.3, 1, 3, 10 μM). Panel (A) control, (B) dantrolene (100 μM), (C) dantrolene (100 μM) with benzbromarone (1 μM). Summarized data represented as line graph (n=6; N=6) of mean amplitude of initial (D) and sustained CCh responses (E) of all three sets; which were measured within 2nd and at 10th minute for each CCh contractions, respectively.

ANOVA, ***p<0.001, ****p<0.0001; comparing Dantrolene + Benz vs Dantrolene.

★ Recording artefacts during wash-out

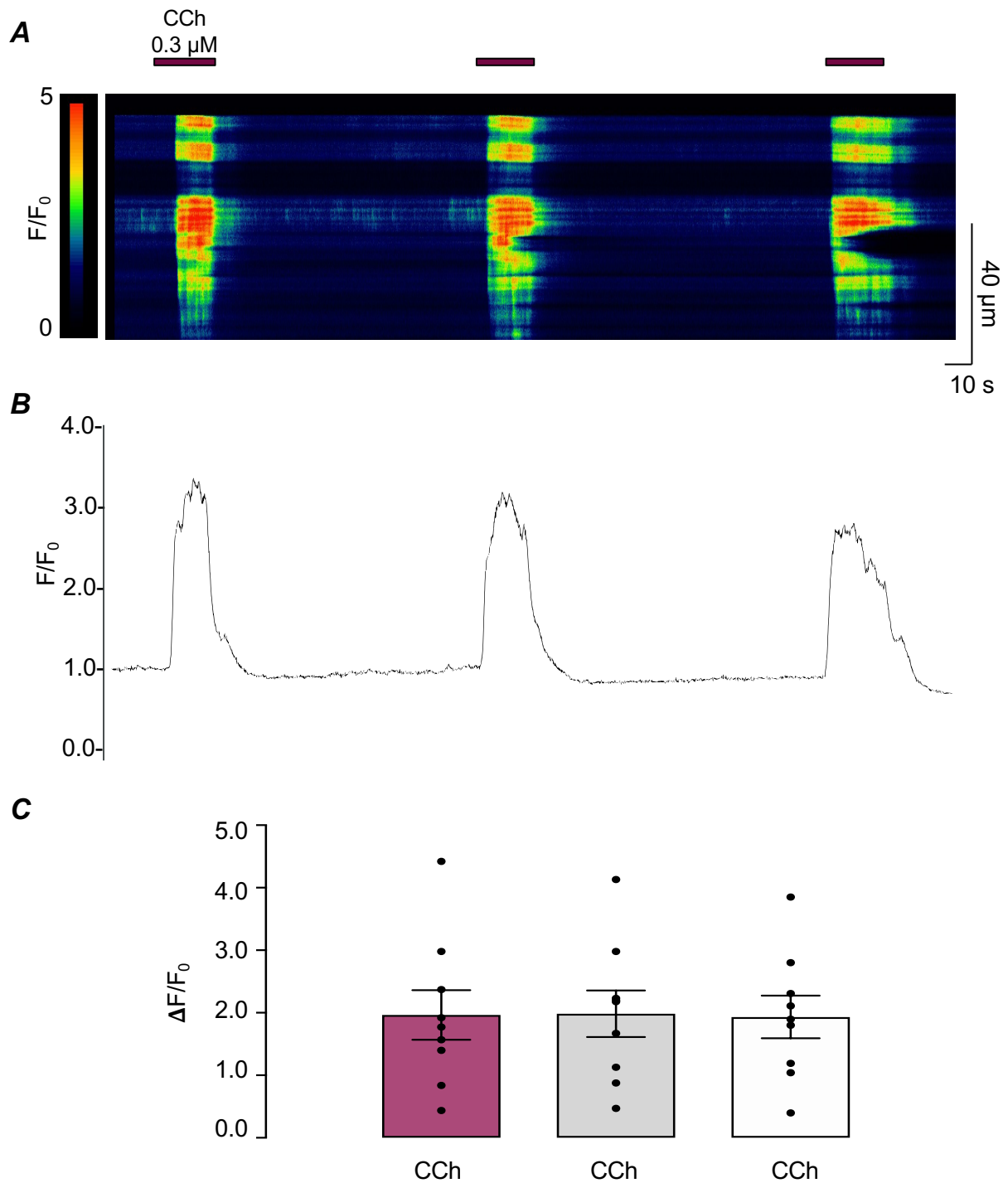


Figure 5.13. Successive applications of CCh-induced Ca²⁺ influx in freshly isolated ASMCs.

(A) Representative pseudolinescan showing three consecutive CCh (0.3 μ M)-induced calcium signals in ASMCs, and (B) the corresponding intensity profile plot. Summary bar charts with aligned dot plot as shown in panel (C) shows mean amplitude ($\Delta F/F_0$) of initial transient Ca²⁺ signals of 9 similar experiments. No significant change was observed between transients. (n=9, N=6; ANOVA).

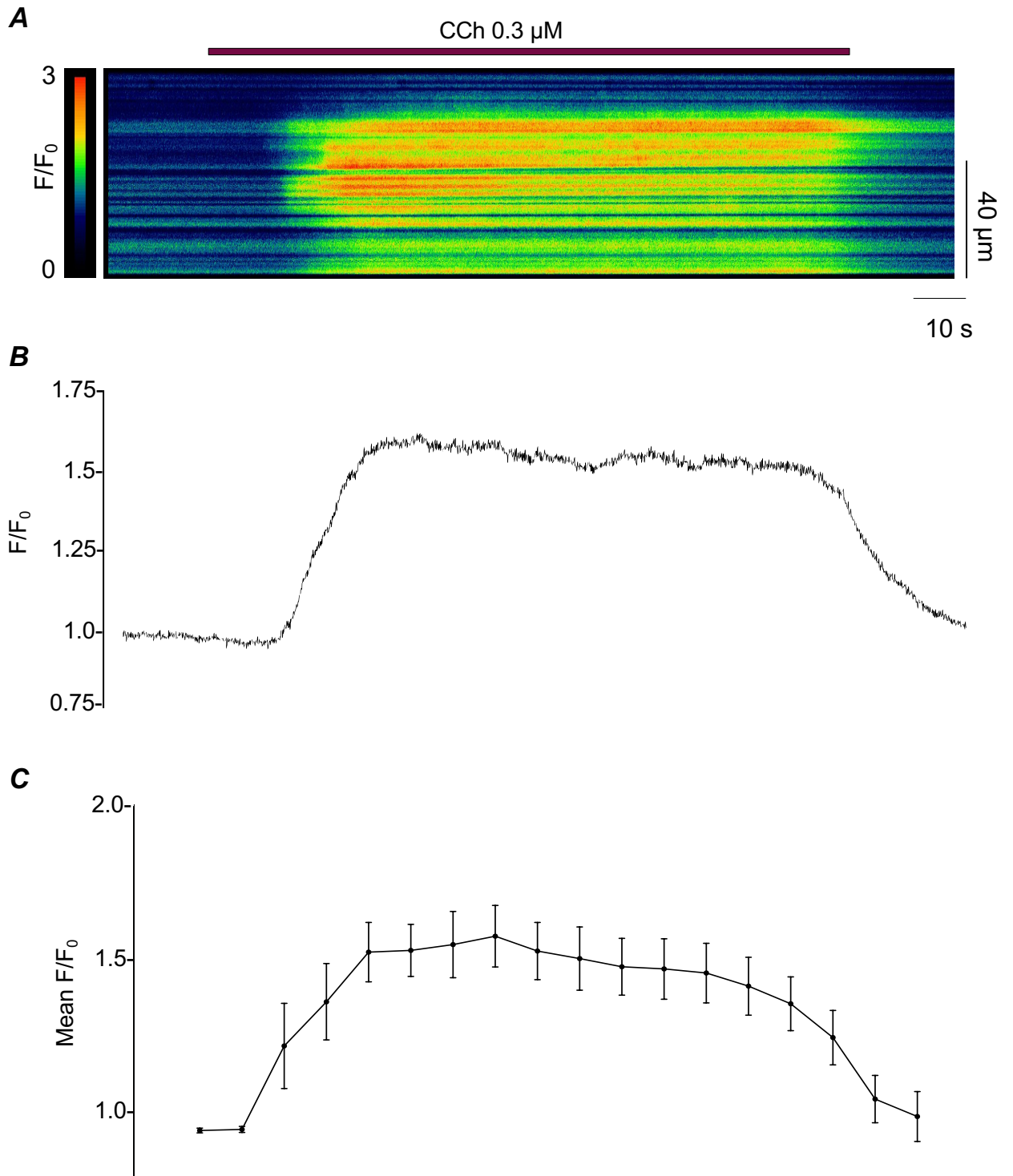


Figure 5.14. Successive application of CCh-induced Ca^{2+} influx in freshly isolated ASMCs.

(A) Representative pseudolinescan showing CCh (0.3 μ M)-induced calcium signals in ASMCs, and (B) the corresponding intensity profile plot. Summary bar charts with aligned dot plot as shown in panel (C) shows mean amplitude ($\Delta F/F_0$) of Ca^{2+} signals of 9 similar experiments measured every 10 sec. ($n=9$, $N=6$).

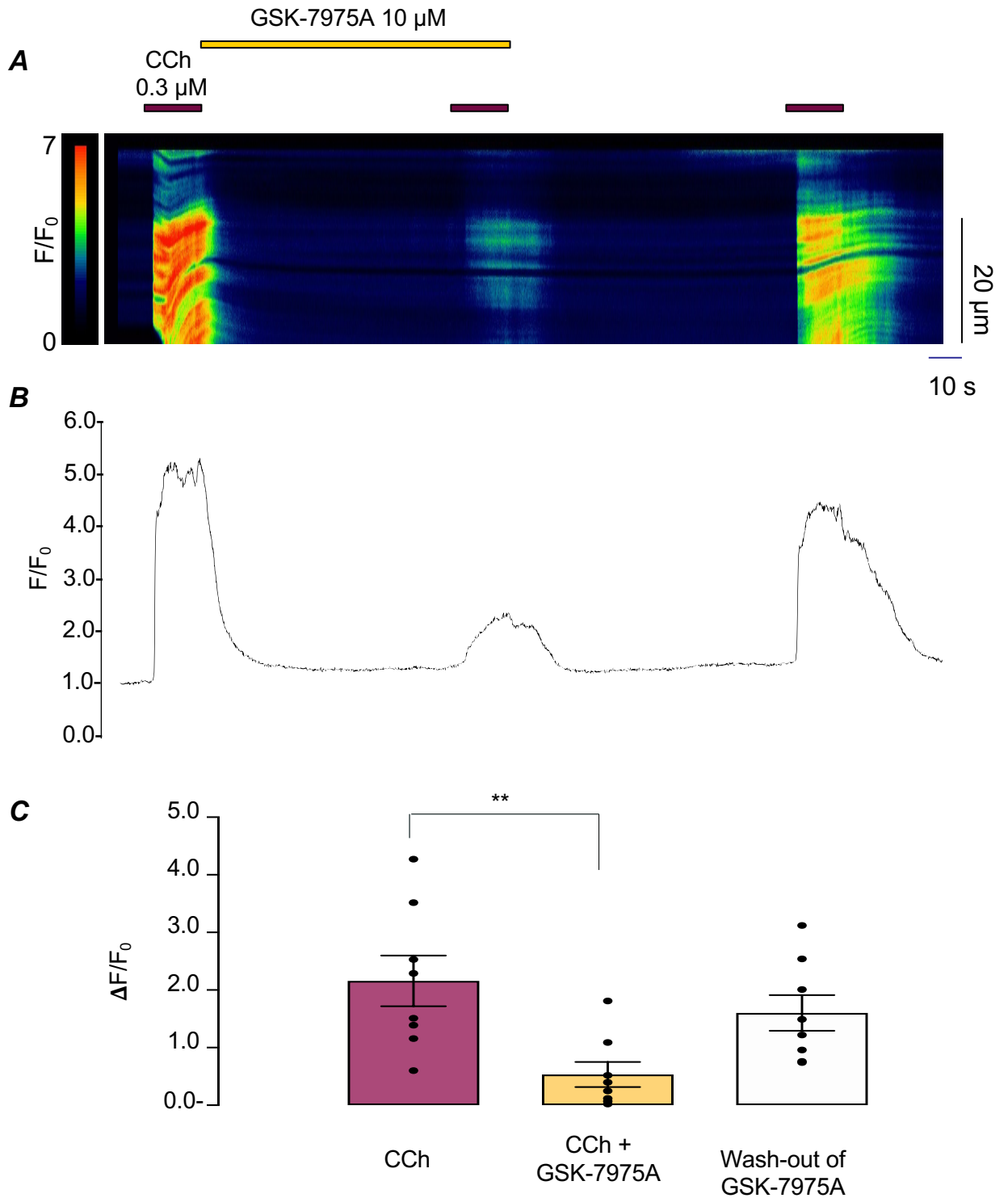


Figure 5.15. Effect of GSK-7975A on CCh-induced calcium transients in freshly isolated ASMCs.

(A) Representative pseudolinescan showing the effects of GSK-7975A (10 μ M) on CCh (0.3 μ M)-induced calcium transients in ASMCs, and (B) the corresponding intensity profile plot. Summary bar charts with aligned dot-plot shown in the panel (C) plot mean amplitude of calcium transients in the absence and presence of GSK-7975A (n=8, N=6; **p<0.005; ANOVA).

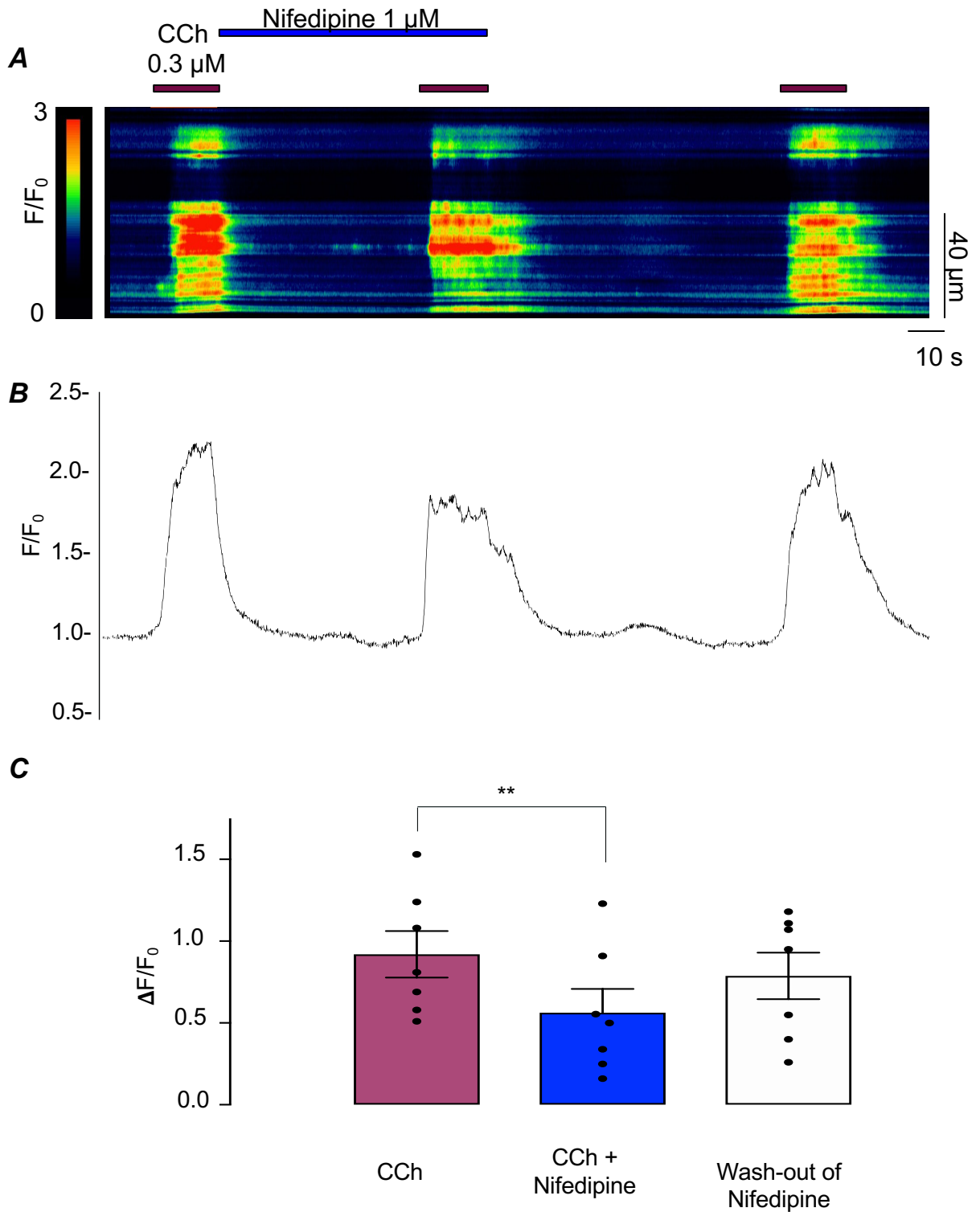


Figure 5.16. Effect of nifedipine on CCh-induced calcium transients in freshly isolated ASMCs.

(A) Representative pseudolinescan showing the effects of nifedipine (1 μ M) on CCh (0.3 μ M)-induced calcium transients in ASMCs, and (B) the corresponding intensity profile plot. Summary bar charts with aligned dot-plot shown in the panel (C) plot mean amplitude of calcium transients in the absence and presence of nifedipine (n=7, N=6; **p<0.005; ANOVA).

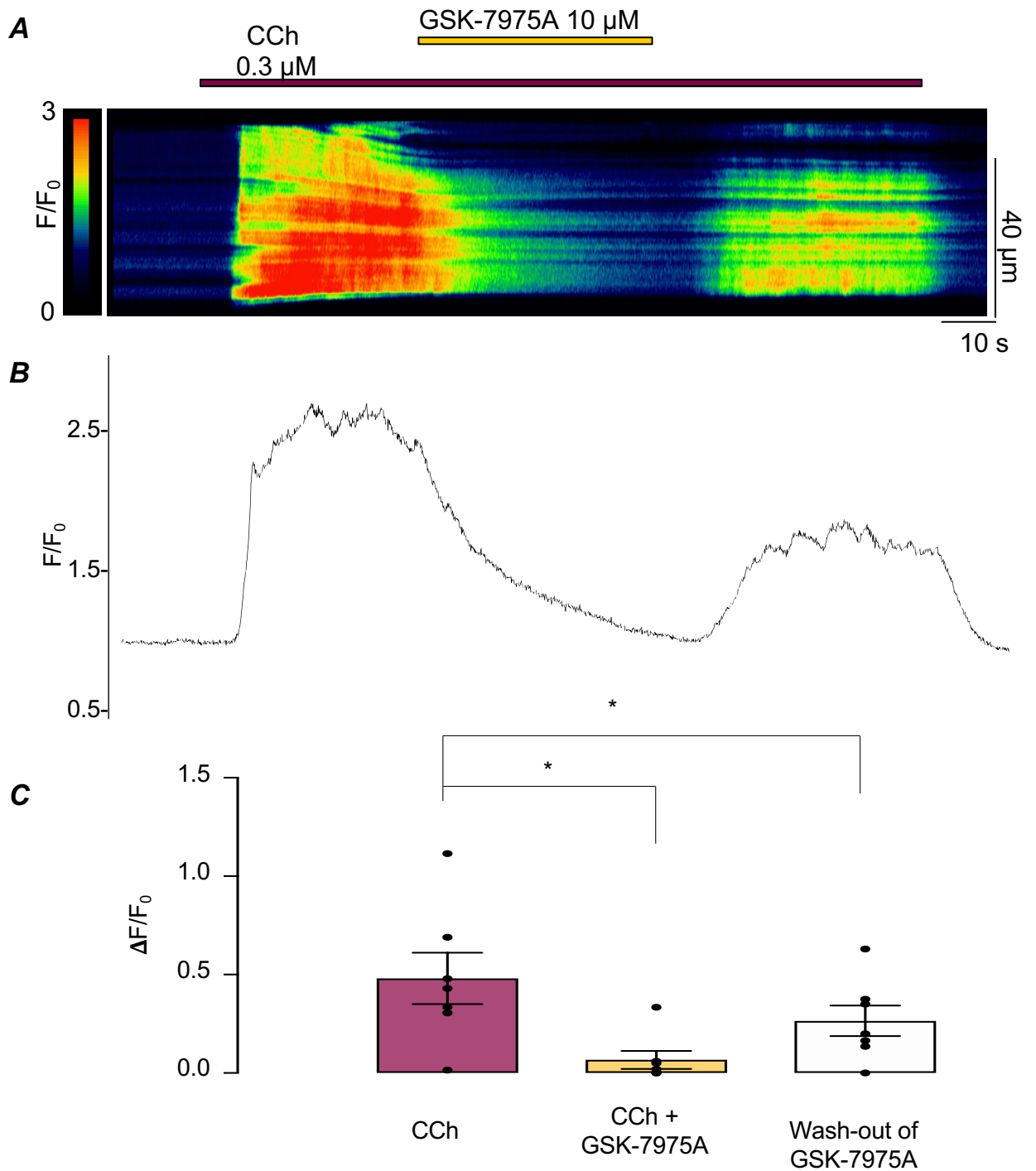


Figure 5.17. Effect of GSK-7975A on CCh evoked Ca^{2+} signals in freshly isolated ASMCs.

(A) Representative pseudolinescan showing inhibitory effect of GSK-7975A (10 μM) on CCh (0.3 μM)-induced calcium signals in ASMCs, and (B) the corresponding intensity profile plot. Summary bar charts with aligned dot-plot shown in the panel (C) plot change in mean amplitude of calcium signals before the addition of GSK-7975A and after adding GSK-7975A in the presence of CCh (n=7, N=6; *p<0.005; ANOVA).

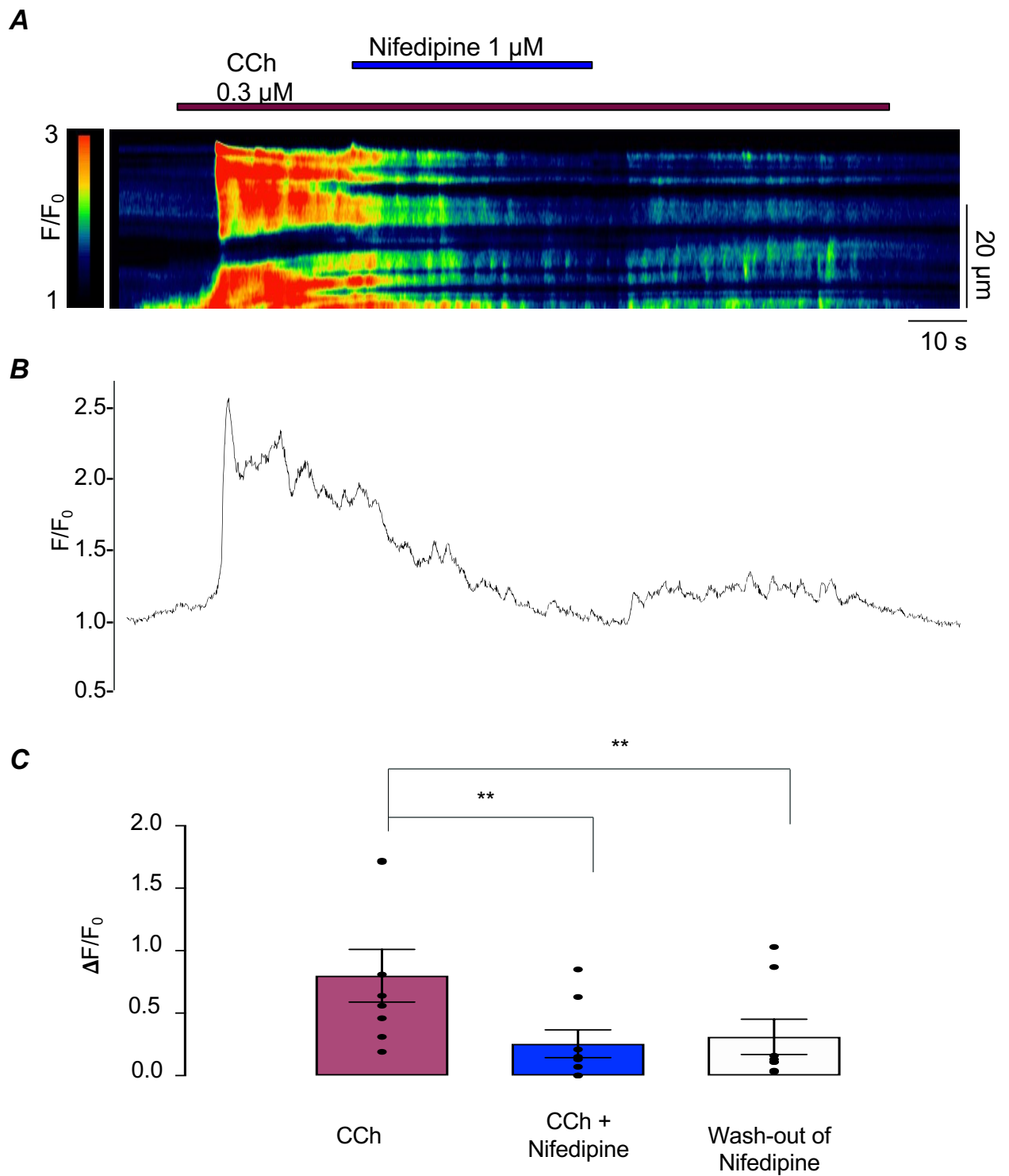


Figure 5.18. Effect of nifedipine on CCh evoked Ca^{2+} signals in freshly isolated ASMCs.

(A) Representative pseudolinescan showing the inhibitory effect of nifedipine (1 μ M) on CCh (0.3 μ M)-induced calcium signals in ASMCs, and (B) the corresponding intensity profile plot. Summary bar charts with aligned dot-plot shown in the panel (C) plot change in mean amplitude of calcium signals before the addition of nifedipine and after adding nifedipine in the presence of CCh (n=8, N=6; **p<0.005; ANOVA).

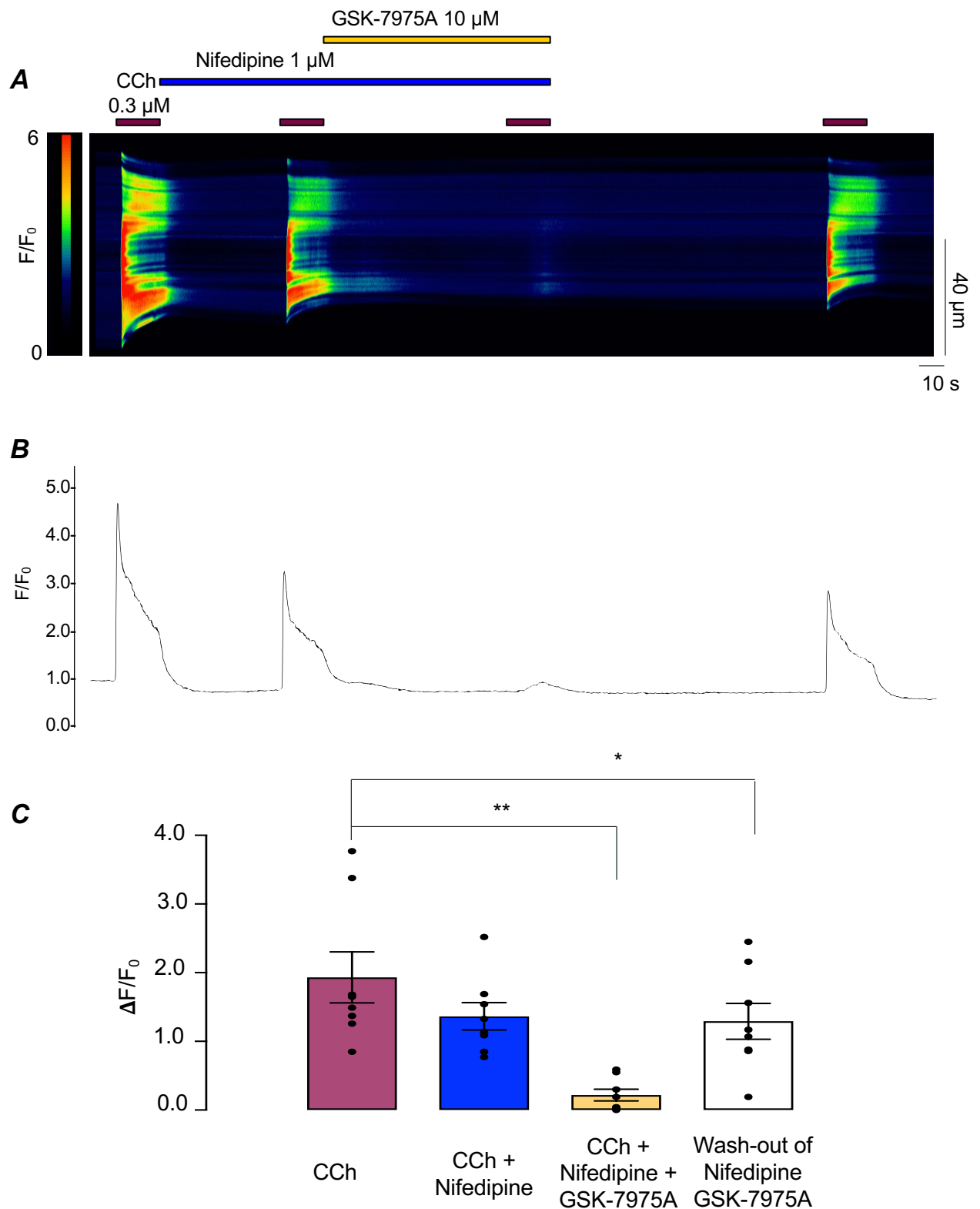


Figure 5.19. Inhibitory effect of GSK-7975A on CCh-induced Ca^{2+} transients in the presence of nifedipine in freshly isolated ASMCs.

(A) Representative pseudolinescan showing the inhibitory effect of GSK-7975A on CCh (0.3 μ M)-induced calcium signals in ASMCs after inhibiting L-type Ca^{2+} channel using nifedipine (1 μ M), and (B) the corresponding intensity profile plot. Summary bar charts shown with aligned dot-plot in the panel (C) plot change in mean amplitude of calcium signals after incubation with nifedipine and after incubation with GSK-7975A in the presence of nifedipine (n=8, N=7; *p<0.05, **p<0.005; ANOVA).

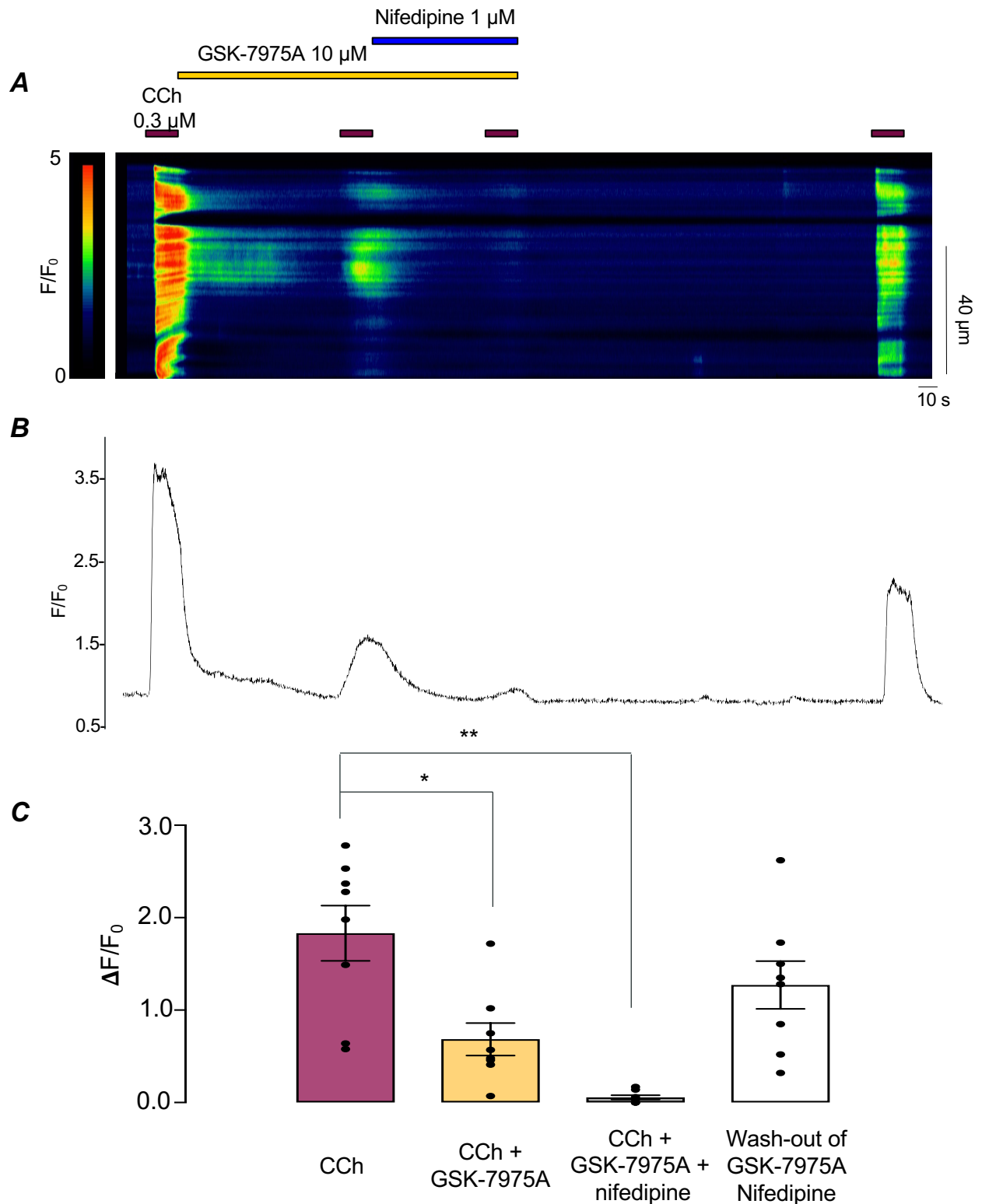


Figure 5.20. Inhibitory effect of nifedipine on CCh-induced Ca²⁺ transients in the presence of GSK-7975A in freshly isolated ASMCs

(A) Representative pseudolinescan showing the inhibitory effect of nifedipine (1 μ M) on CCh (0.3 μ M)-induced calcium signals in ASMCs after inhibiting CRAC channel using GSK-7975A (10 μ M), and (B) the corresponding intensity profile plot. Summary bar charts with aligned dot-plot shown in the panel (C) plot change in mean amplitude of calcium signals after incubation with GSK-7975A and after incubation with nifedipine in the presence of GSK-7975A (n=8, N=6; *p<0.05, **p<0.005; ANOVA).

5.3 Discussion

In 1986, Putney was first to describe the depletion of internal Ca^{2+} stores controls Ca^{2+} influx through plasma membrane. Initially it was named Capacitative Ca^{2+} Entry (CCE) as it was proposed that influx Ca^{2+} ions can be directly taken up by SR (Putney, 1986). However, it was later named Store-Operated Ca^{2+} Entry (SOCE) as Kwan and colleagues showed that the store refilling process occurred by successive Ca^{2+} influx into the cytoplasm followed by uptake into the stores by the SERCA pump (Kwan *et al.* 1990). SOCE was first characterized in non-excitabile cells (Putney, 1986; Thomas *et al.* 1996) but has increasingly been acknowledged as an important Ca^{2+} influx pathway in a range of excitable cells (Gibson *et al.* 1998; Trebak & Putney, 2017), including SMC from the vascular system (Trebak, 2012; Trebak *et al.* 2013), lower urinary tract (Drumm *et al.* 2018; Rembetski *et al.* 2020) and GI interstitial cells (Drumm *et al.* 2019b; Drumm *et al.* 2020; Zheng *et al.* 2018).

There is evidence which suggests that when SOCE is increased, it can lead to proliferation of ASMCs (hyperplasia), hypercontractile activity of ASMCs, leading to airway hyperresponsiveness in conditions of inflammation or asthma. In cultured ASMC from the ovalbumin challenged asthmatic mouse model, STIM and Orai1 expressions were upregulated (Spinelli *et al.* 2012). Patch-clamp experiments on cultured ASMC showed that the pro-inflammatory mediator platelet-derived-growth-factor (PDGF; secreted by epithelial cells and inflammatory cells from asthmatic airways), activated a small inward current that was reduced when either STIM1 or Orai1 was knocked down by siRNA (Spinelli *et al.* 2012). This finding was confirmed in cultured human ASMC with Ca^{2+} imaging, where PDGFR induced a SOCE Ca^{2+} overshoot that was resistant to nifedipine (Suganuma *et al.* 2012). The importance of SOCE in ASMC Ca^{2+} signalling has also been proposed from mathematical modelling, which indicates that SOCE is critical for ASMC Ca^{2+} oscillations and can sustain SR Ca^{2+} release even in the absence of other influx pathways (Croisier *et al.* 2013; Boie *et al.* 2017). A recent study by Johnson *et al.* (2022) provided a novel insight into how STIM1 and SOCE promote airway remodelling and airway hyperresponsiveness during asthma. They showed that ASM STIM1 protein expression increased in chronic house dust mite (HDM) challenged asthmatic mice and also STIM1 protein is

necessary for airway remodelling through the activation of nuclear factor of activated T cells 4 (NFAT4). They are the first to report STIM1 is crucial for the development of airway remodelling during asthma. ASM hypertrophy and fibrosis in response to HDM was significantly reduced in SMC – specific STIM1 knockout (*STIM1-smKO*) mice, thus, indicating STIM1 could be potential target for asthma therapy.

Chen and Sanderson's (2017) study on Ca^{2+} signals in mouse ASMCs suggested SOCE is a major Ca^{2+} entry pathway to sustain contractile activity. They suggested that CRAC channels are more involved in cholinergic agonist induced contractions and Ca^{2+} oscillations than L-type Ca^{2+} channels. However, they used 100 μ M of GSK blockers to fully relax the contraction induced by 0.4 μ M of methacholine. This concentration seems excessive, since Derler *et al.* (2013) work on HEK293 cells suggested that 10 μ M of GSK-7975A blocker is enough to completely abolish CRAC currents. Same study has also shown that 10 μ M of GSK-7975A completely inhibited TRPV6 currents. However, as per our knowledge TRPV6 expression has not been reported in bronchial smooth muscle.

Thus, we aimed at reinvestigating the interaction of CRAC and L-type Ca^{2+} channels involvement in bronchial tissues and ASMCs. The present study differs from Chen and Sanderson's in three ways: 1) we have used a much lower concentration of GSK-7975A (10 μ M) and nifedipine (1 μ M); 2) we examined the effect of blocking both channels, CRAC and L-type Ca^{2+} channels on 5 different concentrations of cholinergic agonist, 3) we have investigated the inhibitory effects on both initial and sustained components of cholinergic activity.

In preliminary experiments, we confirmed the observation of Chen & Sanderson (2017) that 100 μ M GSK-7975A completely abolished the cholinergic contractions induced by all concentrations of CCh (data not shown). In the Chen and Sanderson (2017) study, 10 μ M of GSK-7975A reversed about 50% airway constriction caused by MCh (0.4 μ M) and in present study, the same concentration of the blocker reduced 50% of contraction evoked by 1 μ M CCh. However, the data presented in this chapter also showed that 10 μ M GSK-7975A, followed by 1 μ M nifedipine, abolished the CCh-mediated contractions at all concentrations of CCh. This is consistent with 10 μ M GSK-7975A being sufficient to block all of the CRAC-dependent response and nifedipine

blocking a remaining component dependent on L-type Ca^{2+} current. Preliminary experiments in our laboratory also showed that 10 μM of GSK-7975A reduced L-type Ca^{2+} current by 20% in ASM (Srikanth Dudem, personal communication), hence it is possible that the high concentrations used by Chen & Sanderson completely blocked both the CRAC current and the L-type Ca^{2+} current. If so, this would invalidate their conclusion that the L-type Ca^{2+} current cannot compensate when CRAC is blocked, as this was based on the finding that contractions were completely blocked only by the higher concentrations of GSK-7975A. In contrast, it is unlikely that blocking of L-type Ca^{2+} channels could account to the effects of 10 μM GSK-7975A in the present study, as this concentration abolished contractions where all of the L-type current had been already blocked with nifedipine (see *figure 5.4*).

We observed that blocking both channels in any order almost completely abolished cholinergic contractions induced by all CCh concentrations. The inhibitory effect of nifedipine in absence of SOCE, suggests that L-type Ca^{2+} channels act as a safety factor in regulating Ca^{2+} influx in ASMC. When either of the channels are blocked, the other channel can maintain the integrity of the SR and sustain Ca^{2+} signalling in response to cholinergic stimulation, therefore the tissue can continue contracting. This suggests that both L-type Ca^{2+} channels and CRAC channels play a vital role in maintaining cholinergic activity in ASM. It was reported in chapter 3 that blocking of TMEM16A in CCh-induced contraction by Ani9 had almost no effect on the amplitude of contractions of CCh concentrations. However, in the present chapter we observed that after blocking CRAC channels, Ani9 had further inhibitory effects on cholinergic contractions. This suggests that when the CRAC current was blocked the TMEM16A channels can contribute to cholinergic contractions, thus it appears that they provide an additional safety factor that is normally masked by more powerful mechanisms. However, there were still CCh contractions left after blocking of both CRAC and CaCC channels. This indicates there is another pathway which causes membrane depolarization and activation of L-type Ca^{2+} channels in ASM. Most likely this is the non-specific cation current first reported by Janssen & Sims (1992), the molecular identity of which may be TRPC3 (Wang *et al.* 2011). Unfortunately, no effective small molecule inhibitors of TRPC3 have been developed to date, so it was not possible to test this further in the present study. However, it would have been interesting to block TRPC3 after blocking CRAC.

Lastly, it was found that blocking of CRAC channels using GSK-7975A significantly reduced both the initial and sustained component of cholinergic contractions induced by CCh of concentrations 0.1, 0.3, 1, 3 and 10 μM . However, blocking the channels had more effect on contractions induced by higher CCh concentrations. The latter effect is opposite to that of nifedipine, which blocks the effects of lower concentrations of CCh more effectively than higher concentrations. This may suggest that electro-mechanical coupling is more involved in responses to lower concentrations, while responses to higher concentrations depend more on pharmaco-mechanical coupling.

The role of L-type Ca^{2+} channels in facilitating ASMC Ca^{2+} oscillations and contractions is still debated, with researchers using different experimental methodologies across several species coming to very different and often conflicting conclusions. It was initially proposed that VDCC were involved in refilling ASMC SR Ca^{2+} stores based on experiments with dog airway. In patch clamp experiments on dog bronchi, native ASMC exhibited L-type Ca^{2+} current that was abolished by nifedipine, and T-type Ca^{2+} current that was reduced by Ni^{2+} , and it was suggested that VDCC were involved in refilling SR stores (Janssen, 1997). 5-HT (1 μM) and ACh (1 μM) induced repetitive Ca^{2+} oscillations in ASMC mouse lung slices that were insensitive to nifedipine but decreased in frequency by 1 μM Ni^{2+} , which also decreased agonist and caffeine induced contractions, implicating T-type Ca^{2+} channels in SR Ca^{2+} store refilling (Perez & Sanderson, 2005). In contractile recordings of guinea-pig trachea strips, nifedipine only blocked histamine induced contractions and not contractions induced by ACh (Matyas *et al.* 1995). However, in pig trachea and human bronchi strips, reproducible Ca^{2+} waves and contractile tone evoked by ACh (3 μM) were decreased by 40% by 10 μM nifedipine (Dai *et al.* 2006; Dai *et al.* 2007). 0.3 μM of ACh induced reproducible contractions of bovine tracheal strips that were decreased by 50 % by 1 μM nifedipine (Hirota & Janssen, 2007).

In our study we used 1 μM of nifedipine to inhibit L-type Ca^{2+} channels. Several studies have shown that 1 μM of dihydropyridine blocker is sufficient to abolish L-type Ca^{2+} currents in smooth muscle cells isolated from different species and organs (Hollywood *et al.* 2003; Cotton *et al.* 1997; Large *et al.* 2012). As discussed in chapter 3, the inhibitory effect of nifedipine did not differentiate between the initial and sustained

response to CCh contractions, although its inhibitory effect on bronchial contractions decreased with increasing concentration of CCh, maximum blocking effect of 70% at 0.1 μM CCh and about 30% relaxation for CCh $\geq 1 \mu\text{M}$.

We have further investigated the effect of GSK-7975A and nifedipine on CCh-evoked cytosolic Ca^{2+} levels in the freshly isolated ASMCs. Johnson *et al.* (2022) have shown ASMCs isolated from HDM-challenged mice produced Ca^{2+} oscillations with increased frequency and amplitude compared to the control ASMCs, thus elucidating a possible mechanism for airway hyperresponsiveness in asthmatic subjects. Johnson *et al.* (2022) have also shown that ASMCs from HDM-challenged *STIM1-smKO* mice have fewer Ca^{2+} oscillations compared to HDM-challenged *Myh11 Cre* (tamoxifen-inducible smooth muscle Cre) mice. Both observations indicate that STIM1 are actively involved in Ca^{2+} oscillations in ASMCs. In the current study, we found that both GSK-7975A and nifedipine individually significantly reduced Ca^{2+} levels elevated by CCh, but the inhibitory effect of GSK-7975A was greater than nifedipine. Furthermore, we carried out similar experiments to the isometric tension ones where both CRAC channels and L-type Ca^{2+} channels were blocked together to study the effects on CCh-induced Ca^{2+} elevation in the ASMCs. We observed that, like in tension experiments, cytosolic Ca^{2+} elevations evoked by CCh in ASMCs were completely eliminated when cells were treated with both GSK-7975A and nifedipine.

In chapter 4, we showed that benzbrumarone could be increasing intracellular Ca^{2+} concentration by causing Ca^{2+} release, probably through RyR. Thus, we speculated that these TMEM16A blockers might have little further effect if the RyRs were blocked, thus eliminating their contribution. To further examine this idea, we used dantrolene, a benchmark blocker of RyR (specifically for RyR1 and RyR3), to study involvement of the receptor in the cholinergic activity. In our study, dantrolene of 100 μM significantly reduced both the initial and sustained components of all CCh concentrations induced contractions, however the effect was greater on the sustained component than on the initial component and this was more evident at higher concentrations of CCh. This is similar to the observation of Du *et al.* (2005), that dantrolene reduced CCh-induced contractions more at concentrations of 2 μM and 3 μM as compared to lower concentrations $< 1\mu\text{M}$. In the present study, the pattern of

inhibition by dantrolene was strikingly similar to the effect that of benzbromarone. However, we observed that after blocking of RyR, benzbromarone completely abolished leftover contractions at all CCh concentrations, thus, suggesting that the effect of benzbromarone was not solely mediated by acting on RyR.

According to the literature, high K^+ -induced contractions in SMCs are a result of activation of voltage-dependent Ca^{2+} channels caused by cell membrane depolarization. However, there have been doubts about whether it is entirely depolarization induced contractile activity. In the skeletal muscle, depolarization induced the Ca^{2+} -release mechanism known to be important for excitation-contraction coupling. This mechanism relies on a mechanical linkage between RyR1 and $Ca_v1.1$ (Kraner *et al.* 2011). A similar coupling complex could be possible in smooth muscle also, although it is more likely to rely on CICR than mechanical coupling. Du *et al.* (2006) have shown that RyR1 may co-localize with $Ca_v1.1$ in ASM and 200 μM of ryanodine partially relaxed bronchial rings pre-contracted using high K^+ [80 mM]. In the present study, we have shown that the other two blockers of RyR, dantrolene and tetracaine, reversibly reduce high K^+ contractions. Du *et al.* and our findings suggests that Ca^{2+} release through RyR are involved in high K^+ -induced contractile activity in ASM. However, as nifedipine abolished all the high K^+ -induced contractions, it can be speculated that the store-mediated component was entirely dependent on Ca^{2+} -influx via L-type channels. It was interesting that dantrolene blocked the sustained component of the high K^+ contracture much more than the initial component, suggesting that the sustained component was maintained partly by recycling of Ca^{2+} from stores as well as perhaps some sustained L-type Ca^{2+} current. This pattern, however, was less obvious in the case of tetracaine, and GSK-7975A, seemed to reduce both components of the high K^+ contraction to a similar extent. The most likely explanation for the effect of GSK-7975A on K^+ contractures is that following membrane depolarization and opening of VGCCs causing an increase in intracellular Ca^{2+} , CICR releases further Ca^{2+} into the cytoplasm from stores through RyR. The CRAC channels are then activated upon sensing low Ca^{2+} in the stores and thus maintains Ca^{2+} level in the cell during high K^+ -induced contraction. Thus we suggest that along with VGCC and Ca^{2+} induced Ca^{2+} release through RyR, CRAC channels are also involved in high KCl induced contractile activity in ASM.

We can conclude from the results of this chapter that CRAC channels, L-type Ca^{2+} channels and Ca^{2+} release through RyR all play a role in maintaining cholinergic contractions in airway smooth muscle. These channels also all participate in mediating depolarization induced contractions by high KCl.

6. General discussion & Future prospects

6.1 General discussion

This study has reassessed the role of CaCC in cholinergic activity elicited in mouse bronchial smooth muscle. We have also evaluated the contribution of store operated Ca^{2+} channels in ASM contractile activity. Previous studies examined the inhibitory effects of ion channel blockers on tissues precontracted with a single concentration of a cholinergic agonist. Moreover, they solely focused on the transient, not the sustained component of cholinergic contractions. In the current study, we evaluated the effects of inhibiting various ion channels on increasing concentrations of CCh while taking the effects on the sustained and transient components of the cholinergic contractions into consideration.

TMEM16A is one of the most extensively studied Cl^- channels in ASM. The channel expression has been shown to be upregulated in asthmatic models and patients. Previous research has shown that benchmark blockers of this channel had successfully inhibited or reduced the contractile activity induced by various agonists in ASM. In the current study, the effects of $CaCC_{inh}$ -A01, benzbramarone and MONNA were more prominent on the sustained component of CCh contractions compared to the transient component. According to the literature, upon activation of TMEM16A, Cl^- efflux occurs and causes membrane depolarization and activation of L-type Ca^{2+} channels. In this scenario, addition of these blockers following blockade of VDCC should not have any further effects on cholinergic contractions. Therefore, the effects of TMEM16A blockers were tested in the presence of VDCC blocker nifedipine. We observed that nifedipine reduced the effects of all concentrations of CCh, however, the TMEM16A inhibitors further reduced these responses in the presence of nifedipine, suggesting off target effects over and above any tendency of these blockers to block L-type Ca^{2+} channels. Through further experimentation, using live Ca^{2+} imaging, we found that these blockers caused Ca^{2+} release, possibly through RyRs, which has not been previously reported to our knowledge. Unlike caffeine, the Ca^{2+} release caused by these TMEM16A blockers was slow and sustained throughout the applications

Ani9 is one of the novel selective blockers of TMEM16A. Yet, our results also showed that Ani9 had no effect on the CCh-induced contractions, unlike the other three TMEM16A antagonists. A previous study by Wang *et al.* (2017) on TMEM16A^{-/-} airways suggested an involvement of TMEM16A in contractions induced by thromboxane agonist, U-46619, but not by methacholine. In the present study, we found that 3 μ M of Ani9 significantly reduced phasic contractions induced by U-46619. Hence our observations are in agreement with the work of Wang *et al.* (2017). Also, the fact that Ani9 blocked the responses to U-46619 in whole tissue experiments suggests that it is not broken down by airway tissues, making it a suitable blocker to study airway plasmalemmal TMEM16A channels in future experiments.

Another interesting finding in this thesis is that Ani9 significantly reduced cholinergic contractions following blockade of CRAC channels using the GSK-7975A compound. However, this block was incomplete, suggesting that apart from TMEM16A, there is another pathway to activate L-type Ca²⁺ channels. One possibility could be membrane depolarization and activation of voltage dependent Ca²⁺ channels caused by muscarinic cation current widely known as ml_{CAT} . This idea was previously proposed by Wang *et al.* (2011) who proposed that ml_{CAT} is mediated by TRPC3 channels in murine ASMCs. Unfortunately, due to lack of selective TRPC3 antagonists available it is difficult to test this idea using the available techniques. Another potential pathway leading to activation of L-type Ca²⁺ current in airways is through activation of PKC (Mukherjee *et al.* 2013). PKC is well known to phosphorylate L-type Ca²⁺ channels and increase their open probability (Shistik *et al.* 1998). Mukherjee *et al.* showed that PMA (Phorbol 12-myristate 13-acetate), a PKC activator, induced Ca²⁺ oscillations and twitch contractions in small airways of mouse lung slices that were completely blocked by nifedipine, hence implying that PKC activation alone was enough to stimulate Ca²⁺ influx via L-type Ca²⁺ channels. This effect was completely reversed by, GF-109203X, a PKC inhibitor. It would be interesting, therefore, to investigate the effect of a PKC inhibitor on cholinergic contractions and cytosolic Ca²⁺ when SOCE was blocked by GSK-7975A.

Over a decade ago, STIM and Orai were recognised as the molecular basis for store operated Ca²⁺ channels widely known as Ca²⁺ released activated Ca²⁺ (CRAC) channels. STIM and Orai proteins have been shown to be expressed in ASM (Peel *et*

al. 2006, 2008) and their expression levels were reported to be upregulated in ovalbumin- challenged asthmatic airways (Spinelli *et al.* 2012). Chen and Sanderson (2017) suggested that the contribution of CRAC channels in cholinergic activity induced by 0.4 μM CCh is more prominent than that of L-type Ca^{2+} channels in ASM. In the current study, we confirmed the importance of CRAC and showed that inhibition of CRAC channels using GSK-7975A, was more effective on higher concentrations ($\geq 1 \mu\text{M}$) than lower concentrations of CCh. However, the difference in the Chen & Sanderson study and the present study is the concentration of GSK-7975A used. In their study, they used 100 μM of GSK-7975A to completely relax the airways, whereas we used 10 μM . During preliminary experimentations, we observed that with high concentration of GSK-7975A (100 μM), the blocker completely abolished cholinergic contractions induced by all concentrations of CCh. We have also tested the effects of GSK-7975A (10 μM) on L-type Ca^{2+} currents in native ASMCs and found that it caused a 20% reduction in the current. Moreover, Derler *et al.* (2013) showed that the IC_{50} of GSK-7975A is 4.5 μM . Therefore, in our study, we avoided using GSK-7975A ($> 10 \mu\text{M}$) as it may have off target effects on L-type Ca^{2+} channels. Our finding also proposes that CRAC channels are more involved in the sustained component vs the initial component of CCh-induced contractions and overall, in resting state more involved in cholinergic contractions than L-type Ca^{2+} channels. Another intriguing finding showed that following blockade of both L-type Ca^{2+} channels and CRAC channels in any order, cholinergic contractions induced by CCh of all concentrations applied are completely abolished. Similar effects of both blockers were observed on Ca^{2+} signals evoked by CCh in freshly isolated ASMCs. As discussed in earlier (see chapter 5) the inhibitory effect of L-type Ca^{2+} channels blocker in the absence of CRAC channels, suggests that the dihydropyridine sensitive channels act as safety factor in controlling Ca^{2+} influx in ASM. When either of the channels are blocked the other channel can maintain the integrity of the SR and sustain Ca^{2+} signalling in response to cholinergic stimulation, therefore the tissue can continue contracting. Thus, our findings suggest that both L-type Ca^{2+} channels and CRAC channels are equally essential in maintaining cholinergic activity in ASM.

Apart from SOCE, Ca^{2+} release through RyR is another major Ca^{2+} channel located at the SR. Although, limited evidence of their involvement in the cholinergic activity in the ASM exists, yet the literature suggests that they are activated following Ca^{2+} influx

through L-type Ca^{2+} channels and lead to Ca^{2+} release from stores into the cytoplasm. Hence, they are referred as Ca^{2+} induced Ca^{2+} release channels. In the present study, inhibitory effects of dantrolene on contractile activity of ASM suggests that RyR are majorly involved in maintaining the sustained component of the cholinergic response. Following blockade of RyR, nifedipine had no further inhibitory effects on the sustained component of CCh induced responses ($\geq 1 \mu\text{M}$) suggesting that RyR are more involved in contractile activity induced by higher CCh concentrations. However, nifedipine effectively blocked the effect of lower concentrations of CCh in the presence of dantrolene and blocked some of the initial response at higher concentrations. This suggests that the Ca^{2+} influx through the L-type Ca^{2+} channels are sufficient under these conditions to activate the contractile process without the need for amplification through CICR. We have also confirmed the findings reported by Du *et al.* (2006) which suggests that Ca^{2+} release through RyR is involved in high KCl induced contractions. Our data proposed that store refilling through CRAC channels is also involved in the high KCl induced activity in ASM.

Overall, the results presented in this thesis suggest that involvement of ion channels varies depending on the state of the smooth muscle cells (*figure 6.1*). In the normal state, SOCE and Ca^{2+} release through RyR majorly controls the contractile activity. L-type Ca^{2+} channels can be activated in the absence of CaCC, thus suggesting CaCC might not be only pathway or major pathway to cause membrane depolarization in ASM. Interestingly, the situation changes when CRAC channels are blocked. We found that nifedipine completely abolishes cholinergic contractions in absence of SOCE, suggesting that L-type Ca^{2+} channels act as safety factor in controlling Ca^{2+} influx in ASM. Our findings through organ bath experiments and Ca^{2+} imaging experiments suggest that when either of the channels are blocked the other channel can retain the integrity of the SR and sustain Ca^{2+} signalling in response to cholinergic stimulation, hence contractile activity of ASM continues. From the literature, it is expected that Ca^{2+} -release from IP_3R are also involved, although we did not investigate this, apart from applying 2-APB in the presence of dantrolene. Although it blocked almost all of the responses, it was difficult to interpret this result, as 2-APB also blocks SOCE.

To summarize, the present study suggests that TMEM16A might not be involved in cholinergic contractions in murine bronchial rings under normal conditions, although it seems to be able to play a compensatory role when SOCE is blocked. However, it is well established that this channel is upregulated in airway disease model and it would be a suitable target to investigate in contractile activity induced in the asthmatic or COPD airway smooth muscle. Additionally, SOCE and RyR were shown to be majorly involved in cholinergic activity and can be approached as potential therapeutic targets for hypercontractile activity in ASM.

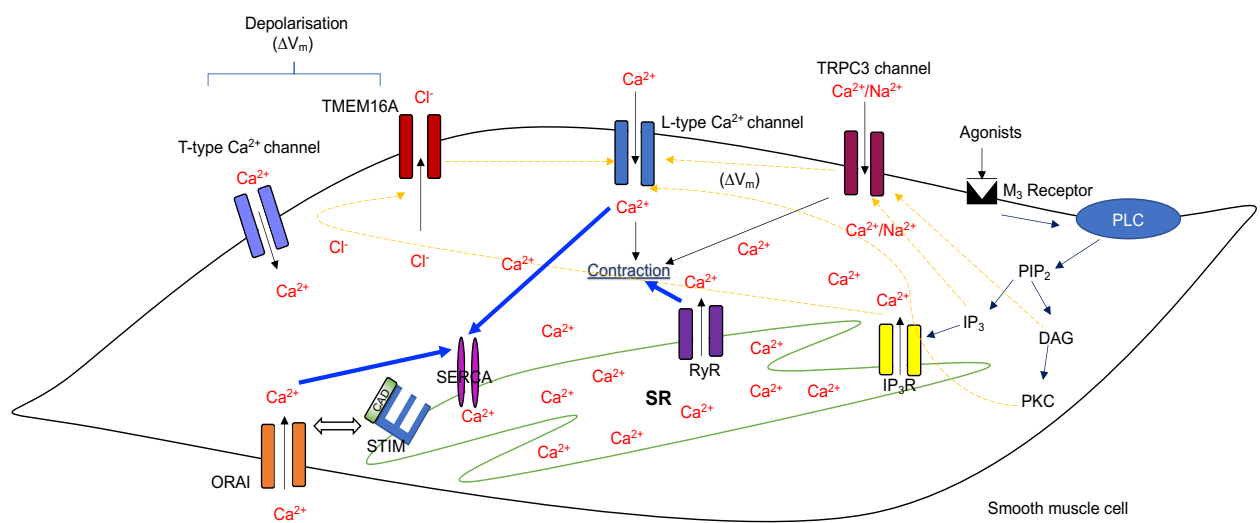


Figure 6.1: Illustrative figure of Ca²⁺ signalling in mouse bronchial smooth muscle.
This project contribution to the signalling pathway is highlighted with blue arrow (→).

6.2 Future prospects

- ➔ Non-selective cation channels have been reported to be involved in ASM contractile activity. Studies have suggested that the TRPC3 are the molecular identity of these channels involved in airway cholinergic contractions. No highly selective blocker of this channels is available at present, however, PYR3 has been shown to block these channels in high concentration. Preliminary experiments (not presented) in the present study failed to show any effect of PYR3 on cholinergic contractions. However, it would be interesting to repeat these experiments in combination with Ani9, as both TRPC3 and TMEM16A may be capable of providing the initial depolarising stimulus necessary to activate L-type Ca^{2+} channels. As we showed Ani9 was only effective after block of SOCE, it would be interesting to perform similar experiments by applying PYR3 after GSK-7975A. TRPC3 KO mice should also be considered to study the contribution of this channel to ASM contractility. Several blockers of TRPC3 and TRPC6 have been described in a single publication in the literature, so these compounds would be worth testing (Seo *et al.* 2014).

- ➔ Studies have also shown that TRPC6 contributes to allergic airway inflammation and mucus secretion making TRPC6 a potential therapeutic target for COPD and asthma. We therefore should investigate the involvement of TRPC6 in cholinergic contractions using TRPC6 inhibitor, BI 749327 on isometric tension.

- ➔ The possibility that Cl^- channels on SR membrane contribute to Ca^{2+} fluxes across the SR membrane requires further investigation. Using immunohistochemical staining we should determine if TMEM16A channels are in fact expressed on the SR of bronchial smooth muscle cells. Following this we should examine the effects of Cl^- replacement on Ca^{2+} release by CCh in single cell Ca^{2+} experiments. Alternatively, experiments could be performed on skinned cells from GCaMP mice where Ca^{2+} release in response to caffeine and IP_3 is measured while examining the effects of replacing Cl^- and a range Cl^- channel blockers.

- ➔ Studies have suggested that TMEM16A is upregulated in asthmatic ASM. It will be interesting to investigate the effect of blocking TMEM16A in airway disease models.
- ➔ We should also examine the effect of using a PKC inhibitor on CCh-induced increases in Ca^{2+} after blocking CRAC channels using GSK-7975A. If it blocks the remaining Ca^{2+} response, it suggests that PKC can cause activation of the L-type Ca^{2+} channels without the need for a further depolarising current. The current clamp configuration of the patch clamp technique could be used to determine if activation of PKC causes membrane depolarization.
- ➔ It is puzzling that TMEM16A channels appear to contribute little to cholinergic contractions, yet they appear to contribute substantially to the responses to other agonists, such as 5-HT, histamine and U46619 (Wang *et al.* 2017; results of the present study). It is possible that cholinergic stimulation involves activation of TRPC channels (which can therefore compensate for block or lack of TMEM16A) and the other agonists do not. This possibility and the other possible differences between the activation mechanisms of a range of agonists should be thoroughly investigated.
- ➔ To confirm the observation that benzbrumarone is causing Ca^{2+} release through RyR, the effect of ryanodine (RyR blocker) on Ca^{2+} responses generated by benzbrumarone should be investigated. We also observed that caffeine reduced Ca^{2+} elevations generated by benzbrumarone, possibly by acting as a phosphodiesterase inhibitor. It would be interesting to test this idea further, by examining other ways of elevating cAMP, by using 8-bromo-cAMP, forskolin (to stimulates adenylate cyclase) and other known inhibitors of phosphodiesterase 3, or activators of PKA such as 6-MB-cAMP.
- ➔ Curtis and Scholfield (2001) had shown through their work on rabbit arteriolar smooth muscle that nifedipine blocks store refilling. The effect of different L-type Ca^{2+} channel blockers (verapamil and diltiazem) should be investigated on cholinergic activity after blocking SOCE using GSK-7975A to confirm inhibiting L-type Ca^{2+} channels are not blocking store refilling in ASM.

7. References

- Abramowitz, J. and Birnbaumer, L. (2009). Physiology and pathophysiology of canonical transient receptor potential channels. *FASEB Journal*, 23(2), pp. 297-328.
- Adda, S., Fleischmann, B. K., Freedman, B. D., Yu, M., Hay, D. W., and Kotlikoff, M. I. (1996). Expression and function of voltage-dependent potassium channel genes in human airway smooth muscle. *The Journal of biological chemistry*, 271(22), pp. 13239–13243.
- Adams, P. R., Constanti, A., Brown, D. A. and Clark, R. B. (1982). Intracellular Ca^{2+} -activates a fast voltage-sensitive K^+ current in vertebrate sympathetic neurones. *Nature*, 296(5859), pp. 746–749.
- Alexander, S. P. H., Mathie, A. and Peters, J.A. (2009). *Guide to Receptors and Channels (GRAC)*, 4th edition. British Journal of Pharmacology.
- Alkawadri, T., McGarvey, L. P., Mullins, N. D., Hollywood, M. A., Thornbury, K. D. and Sergeant, G. P. (2021). Contribution of Postjunctional M2 Muscarinic Receptors to Cholinergic Nerve-Mediated Contractions of Murine Airway Smooth Muscle. *Function*, 3(1), zqab053.
- Altieri, R.J., Szarek, J.L. and Diamond, L. (1985). Neurally mediated non-adrenergic relaxation in cat airway occurs independent of cholinergic mechanisms. *Journal of Pharmacology and Experimental Therapeutics*, 234(3), pp. 590-597.
- Altorki, N.K., Markowitz, G.J., Gao, D., Port, J.L., Saxena, A., Stiles, B., McGraw, T. and Mittal, V. (2019). The lung microenvironment: an important regulator of tumour growth and metastasis. *Nature Reviews Cancer*, 19(1), pp. 9-31.
- Alvarez, D.F., King, J.A., Weber, D., Addison, E., Liedtke, W. and Townsley, M.I. (2006). Transient receptor potential vanilloid 4-mediated disruption of the alveolar septal barrier: a novel mechanism of acute lung injury. *Circulation Research*, 99(9), pp. 988-995.
- Ashmole, I., Duffy, S. M., Leyland, M. L., Morrison, V. S., Begg, M., and Bradding, P. (2012). CRACM/Orai ion channel expression and function in human lung mast cells. *The Journal of allergy and clinical immunology*, 129(6), pp. 1628–35.
- Askew Page, H.R., Dalsgaard, T., Baldwin, S.N., Jepps, T.A., Povstyan, O., Olesen, S.P. and Greenwood, I.A. (2019). TMEM16A is implicated in the regulation of coronary flow and is altered in hypertension. *British journal of pharmacology*, 176(11), pp.1635-1648.
- Avila-Medina, J., Mayoral-Gonzalez, I., Dominguez-Rodriguez, A., Gallardo-Castillo, I., Ribas, J., Ordoñez, A., Rosado, J. A., and Smani, T. (2018). The Complex Role of Store Operated Calcium Entry Pathways and Related Proteins

in the Function of Cardiac, Skeletal and Vascular Smooth Muscle Cells. *Frontiers in physiology*, 9, 257.

Ay, B., Prakash, Y.S., Pabelick, C.M. and Sieck, G.C. (2004). Store-operated Ca^{2+} entry in porcine airway smooth muscle. *American Journal of Physiology-Lung Cellular and Molecular Physiology*, 286(5), pp.L909-L917.

Bai, T.R., Mak, J.C. and Barnes, P.J. (1992). A comparison of beta-adrenergic receptors and *in-vitro* relaxant responses to isoproterenol in asthmatic airway smooth muscle. *American Journal of Respiratory Cell and Molecular Biology*, 6(6), pp. 647-651.

Bai, Y. and Sanderson, M.J. (2006). Airway smooth muscle relaxation results from a reduction in the frequency of Ca^{2+} oscillations induced by a cAMP-mediated inhibition of the IP_3 receptor. *Respiratory Research*, 7(1), 34.

Bao, R., Lifshitz, L. M., Tuft, R. A., Bellvé, K., Fogarty, K. E., and ZhuGe, R. (2008). A close association of RyRs with highly dense clusters of Ca^{2+} -activated Cl^- channels underlies the activation of STICs by Ca^{2+} sparks in mouse airway smooth muscle. *The Journal of general physiology*, 132(1), pp.145–160.

Bara, I., Ozier, A., Tunon de Lara, J.M., Marthan, R. and Berger, P. (2010). Pathophysiology of bronchial smooth muscle remodelling in asthma. *European Respiratory Journal*, 36(5), pp. 1174-1184.

Barish, M.E. (1983). A transient calcium-dependent chloride current in the immature *exnopus* oocyte. *The Journal of Physiology*, 342, pp. 309-325.

Barnes, N. C., Piper, P. J. and Costello, J. F. (1984). Comparative effects of inhaled leukotriene C₄, leukotriene D₄, and histamine in normal human subjects. *Thorax*, 39(7), pp. 500–504.

Barnes, P. J. (1998). Pharmacology of airway smooth muscle. *American journal of respiratory and critical care medicine*, 158(5 Pt 3), pp. S123–S132.

Barnes, P.J. (1988). Neuropeptides and airway smooth muscle. *Pharmacology & Therapeutics*, 36(1), pp. 119-129.

Barnes, P.J., Baraniuk J.N. and Belvisi, M.G. (1991). Neuropeptides in the respiratory tract. Part I. *The American Review of Respiratory Disease*, 144(5), pp. 1187-1198.

Barnes, P.J., Baraniuk J.N. and Belvisi, M.G. (1991). Neuropeptides in the respiratory tract. Part II. *The American Review of Respiratory Disease*, 144(5), pp. 1391-1399.

Belvisi, M.G., Miura, M., Stretton, D. and Barnes, P.J. (1993). Endogenous vasoactive intestinal peptide and nitric oxide modulate cholinergic

neurotransmission in guinea-pig trachea. *European Journal of Pharmacology*, 231, pp. 97-102.

Benayoun, L., Druilhe, A., Dombret, M.C., Aubier, M. and Pretolani, M. (2003). Airway structural alterations selectively associated with severe asthma. *Am J Respir Crit Care Med*, 167(10), pp. 1360–1368.

Benedetto, R., Schreiber, R. and Kunzelmann, K. (2018). TMEM16A is indispensable for basal mucus secretion in airways and intestine. *The FASEB Journal*, 33(3), pp. 4502-4512.

Benham, C.D., Davis, J.B. and Randall, A.D. (2002). Vanilloid and TRP channels: a family of lipid-gated cation channels. *Neuropharmacology*, 42(7), pp. 873-888.

Berkefeld, H., Fakler, B. and Schulte, U. (2010). Ca²⁺-activated K⁺ channels: from protein complexes to function. *Physiological reviews*, 90(4), pp. 1437–1459.

Berridge, M. J. (1997). Elementary and global aspects of calcium signalling. *The Journal of experimental biology*, 200(Pt 2), pp. 315–319.

Berridge, M. J., Lipp, P. and Bootman, M. D. (2000). The versatility and universality of calcium signalling. *Nature reviews. Molecular cell biology*, 1(1), pp. 11–21.

Blatter L. A. (2017). Tissue Specificity: SOCE: Implications for Ca²⁺ Handling in Endothelial Cells. *Advances in experimental medicine and biology*, 993, pp. 343–361.

Boedtkjer, D.M., Kim, S., Jensen, A.B., Matchkov, V.M. and Andersson, K.E. (2015). New selective inhibitors of calcium-activated chloride channels - T16A_{inh}-A01, CaCC_{inh}-A01 and MONNA - what do they inhibit? *British Journal of Pharmacology*, 172, pp. 4158-4172.

Boie, S., Chen, J., Sanderson, M. J., and Sneyd, J. (2017). The relative contributions of store-operated and voltage-gated Ca²⁺ channels to the control of Ca²⁺ oscillations in airway smooth muscle. *The Journal of physiology*, 595(10), pp. 3129–3141.

Bonvini, S., Birrell, M., Dubuis, E., Adcock, J., Jones, V., Flajolet, P., Poushpas, S., Wang, M., Duffy, S.M., Bradding, P., Langley, K. and Belvisi, M. (2015). Activation of TRPV4 triggers ATP release and mast cell dependent contraction of airway smooth muscle (ASM). *European Respiratory Journal*, 46(59), p.OA3253.

Bourreau, J. P., Abela, A. P., Kwan, C. Y. and Daniel, E. E. (1991). Acetylcholine Ca²⁺ stores refilling directly involves a dihydropyridine-sensitive channel in dog trachea. *The American journal of physiology*, 261(3 Pt 1), pp. C497–C505.

- Bradley, E., Fedigan, S., Webb, T., Hollywood, M.A., Thornbury, K.D., McHale, N.G. and Sergeant, G.P. (2014). Pharmacological characterization of TMEM16A currents. *Channels (Austin)*, 8(4), pp. 308-320
- Bradley, E., Large, R.J., Bihun, V.V., Mullins, N.D., Hollywood, M.A., Sergeant, G.P. and Thornbury, K.D. (2018). Inhibitory effects of openers of large-conductance Ca²⁺-activated K⁺ channels on agonist-induced phasic contractions in rabbit and mouse bronchial smooth muscle. *American Journal of Physiology-Cell Physiology*, 315(6), pp. C818-C829.
- Breeze, R. and Turk, M. (1984). Cellular Structure, Function and Organization in the Lower Respiratory Tract. *Environment Health Perspectives*, 55, pp. 3-24.
- Brozovich, F. V., Nicholson, C. J., Degen, C. V., Gao, Y. Z., Aggarwal, M., and Morgan, K. G. (2016). Mechanisms of Vascular Smooth Muscle Contraction and the Basis for Pharmacologic Treatment of Smooth Muscle Disorders. *Pharmacological reviews*, 68(2), pp. 476–532.
- Brueggemann, L.I., Kakad, P.P., Love, R.B., Solway, J., Dowell, M.L., Cribbs, L.L. and Byron K.L. (2012). Kv7 potassium channels in airway smooth muscle cells: signal transduction intermediates and pharmacological targets for bronchodilator therapy, *American Journal of Physiology-Lung Cellular and Molecular Physiology*, 302 (1), pp. L120-L132.
- Brunner, J.D., Lim, N.K., Schenck, S., Duerst, A. and Dutzler, R. (2014). X-ray structure of a calcium-activated TMEM16 lipid scramblase. *Nature*, 516(7530), pp. 207-212.
- Bulley, S. and Jaggar, J.H. (2014). Cl⁻ channels in smooth muscle cells. *Pflügers Archiv European Journal of Physiology*, 466(5), pp. 861-872.
- Burnstock, G. (1969). Evolution of the autonomic innervation of visceral and cardiovascular systems in vertebrates. *Pharmacological Reviews*, 21(4), pp. 247-324.
- Burnstock, G. and Holman, M.E. (1963). Smooth Muscle: Autonomic Nerve Transmission. *Annual Review of Physiology*, 25(1), pp.61-90.
- Byron, K.L., Brueggemann, L.I., Kakad, P.P. and Haick, J.M. (2014). Kv7 (KCNQ) potassium channels and L-type calcium channels in the regulation of airway diameter. In: *Calcium Signaling in Airway Smooth Muscle Cells*, edited by Wang Y.-X., editor. *New York: Springer*, pp. 21–33.
- Cadieux, A., Benchekroun, M.T., St-Pierre, S. and Fournier, A. (1989). Bronchoconstrictor action of neuropeptide Y (NPY) in isolated guinea pig airways. *Neuropeptides*, 13, pp. 215-219.

- Campos-Bedolla, P., Vargas, M. H., Segura, P., Carbajal, V., Calixto, E., Figueroa, A., Flores-Soto, E., Barajas-López, C., Mendoza-Patiño, N., and Montaña, L. M. (2008). Airway smooth muscle relaxation induced by 5-HT_{2A} receptors: role of Na⁺/K⁺-ATPase pump and Ca²⁺-activated K⁺ channels. *Life sciences*, 83(11-12), pp. 438–446.
- Canning, B.J. and Undem, B.J. (1993). Evidence that distinct neural pathways mediate parasympathetic contractions and relaxations of guinea-pig trachealis. *The Journal of Physiology*, 471, pp. 25-40.
- Caputo, A., Caci, E., Ferrera, L., Pedemonte, N., Barsanti, C., Sondo, E., Pfeiffer, U., Ravazzolo, R., Zegarra-Moran, O. and Galletta, L.J. (2008). TMEM16A, a membrane protein associated with calcium-dependent chloride channel activity. *Science*, 322(5901), pp. 590-594.
- Cardell, L.O., Uddman, R. and Edvinsson, L. (1994). Low plasma concentrations of VIP and elevated levels of other neuropeptides during exacerbations of asthma. *European Respiratory Journal*, 7(12), pp. 2169-2173.
- Catterall W. A. (2011). Voltage-gated calcium channels. *Cold Spring Harbor perspectives in biology*, 3(8), a003947.
- Cerrina, J., Le Roy Ladurie, M., Labat, C., Raffestin, B., Bayol, A. and Brink, C. (1986). Comparison of human bronchial muscle responses to histamine *in-vivo* with histamine and isoproterenol agonists *in-vitro*. *The American Review of Respiratory Disease*, 134, pp. 57-61.
- Chen, J. and Sanderson, M. J. (2017). Store-operated calcium entry is required for sustained contraction and Ca²⁺ oscillations of airway smooth muscle. *The Journal of physiology*, 595(10), pp. 3203–3218.
- Chen, X., Zhang, J., Pan, B., Ren, H., Feng, X., Wang, J. and Xiao, J. (2016). Cell Calcium TRPC3-mediated Ca²⁺ entry contributes to mouse airway smooth muscle cell proliferation induced by lipopolysaccharide. *Cell Calcium*, 60(4), pp. 273-281.
- Chen, X., Zhang, J., Pan, B., Ren, H., Feng, X., Wang, J. and Xiao, J. (2017). Role of canonical transient receptor potential channel-3 in acetylcholine- induced mouse airway smooth muscle cell proliferation. *Life Sciences*, 187(8), pp. 64-73.
- Clapham, D.E. (2003). TRP channels as cellular sensors. *Nature*, 426, pp. 517-524.
- Clapham, D.E., Runnels, L.W. and Strubing, C. (2001). The TRP ion channel family. *Nature reviews. Neuroscience*, 2(6), pp. 387-396.

- Coleridge, J.C. and Coleridge, H.M. (1984). Afferent vagal C fibre innervation of the lungs and airways and its functional significance. *Reviews of Physiology Biochemistry and Pharmacology*, 99, pp. 1-110.
- Contet, C., Goulding, S. P., Kuljis, D. A. and Barth, A. L. (2016). BK Channels in the Central Nervous System. *International review of neurobiology*, 128, pp. 281–342.
- Copland, I.B., Reynaud, D., Pace-Asciak, C. and Post, M. (2006). Mechanotransduction of stretch-induced prostanoid release by fetal lung epithelial cells. *American Journal of Physiology-Lung Cellular and Molecular Physiology*, 291(3), pp. L487-L495.
- Corteling, R.L., Li, S., Giddings, J., Westwick, J., Poll, C. and Hall, I.P. (2004). Expression of transient receptor potential C6 and related transient receptor potential family members in human airway smooth muscle and lung tissue. *American Journal of Respiratory Cell and Molecular Biology*, 30, pp. 145-154.
- Cotton, K. D., Hollywood, M. A., McHale, N. G., and Thornbury, K. D. (1997). Ca²⁺ current and Ca(2+)-activated chloride current in isolated smooth muscle cells of the sheep urethra. *The Journal of physiology*, 505 (Pt 1), pp. 121–131.
- Cox, G., Thomson, N., Rubin, A., Niven, R., Corris, P., Siersted, H., Olivenstein, R., Pavord, I., McCormack, D., Chaudhuri, R., Miller, J. and Laviolette, M. (2007). Asthma Control during the Year after Bronchial Thermoplasty. *New England Journal of Medicine*, 356(13), pp. 1327-1337.
- Criado, P. R., Criado, R. F., Maruta, C. W., and Machado Filho, C.D. (2010). Histamine, histamine receptors and antihistamines: new concepts. *Anais brasileiros de dermatologia*, 85(2), pp. 195–210.
- Croisier, H., Tan, X., Perez-Zoghbi, J. F., Sanderson, M. J., Sneyd, J., and Brook, B. S. (2013). Activation of store-operated calcium entry in airway smooth muscle cells: insight from a mathematical model. *PloS one*, 8(7), e69598.
- Crottès, D., and Jan, L. Y. (2019). The multifaceted role of TMEM16A in cancer. *Cell calcium*, 82, 102050.
- Cunningham, S.A., Awayda, M.S., Bubien, J.K., Ismailov, I.I., Arrate, M.P., Berdiev, B.K., Benos, D.J. and Fuller, C.M. (1995). Cloning of an epithelial chloride channel from bovine trachea. *Journal of Biological Chemistry*, 270(52), pp. 31016-31026.
- Curtis, T. M. and Scholfield, C. N. (2001). Nifedipine blocks Ca²⁺ store refilling through a pathway not involving L-type Ca²⁺ channels in rabbit arteriolar smooth muscle. *The Journal of physiology*, 532(Pt 3), pp. 609–623.

- Curry J. J. (1946). The effect of antihistamine substances and other drugs on histamine bronchoconstriction in asthmatic subjects. *The Journal of clinical investigation*, 25(6), pp. 792–799.
- Dai, J. M., Kuo, K. H., Leo, J. M., Paré, P. D., van Breemen, C., and Lee, C. H. (2007). Acetylcholine-induced asynchronous calcium waves in intact human bronchial muscle bundle. *American journal of respiratory cell and molecular biology*, 36(5), pp. 600–608.
- Dai, J. M., Kuo, K. H., Leo, J. M., van Breemen, C., and Lee, C. H. (2006). Mechanism of ACh-induced asynchronous calcium waves and tonic contraction in porcine tracheal muscle bundle. *American journal of physiology. Lung cellular and molecular physiology*, 290(3), pp. L459–L469.
- Dale, P., Head, V., Dowling, M. R. and Taylor, C. W. (2018). Selective inhibition of histamine-evoked Ca^{2+} signals by compartmentalized cAMP in human bronchial airway smooth muscle cells. *Cell calcium*, 71, pp. 53–64.
- Daniel, E.E., Kannan, M.S., Davis, C. and Posey-Daniel, V. (1986). Ultrastructural studies on the neuromuscular control of human tracheal and bronchial muscle. *Respiration Physiology*, 63, pp. 109-128.
- Danielsson, J., Perez-Zoghbi, J., Bernstein, K., Barajas, M.B., Zhang, Y., Kumar, S., Sharma, P.K., Gallos, G. and Emala, C.W. (2015). Antagonists of the TMEM16A Calcium-activated Chloride Channel Modulate Airway Smooth Muscle Tone and Intracellular Calcium. *Anesthesiology*, 123, pp. 569-581.
- Davis, A. J., Shi, J., Pritchard, H. A., Chadha, P. S., Leblanc, N., Vasilikostas, G., Yao, Z., Verkman, A. S., Albert, A. P., and Greenwood, I. A. (2013). Potent vasorelaxant activity of the TMEM16A inhibitor T16A(inh) -A01. *British journal of pharmacology*, 168(3), pp. 773–784.
- Davis, C., Kannan, M.S., Jones, T.R. and Daniel, E.E. (1982). Control of human airway smooth muscle: *In-vitro* studies. *Journal of Applied Physiology*, 53, pp. 1080 -1087.
- de Jongste, J.C., Mons, H., Bonta, I.L. and Kerrebijn, K.F. (1987). *In-vitro* responses of airways from an asthmatic patient. *European Journal of Respiratory Diseases*, 71, pp. 23-29
- Derler, I., Schindl, R., Fritsch, R., Heftberger, P., Riedl, M. C., Begg, M., House, D., and Romanin, C. (2013). The action of selective CRAC channel blockers is affected by the Orai pore geometry. *Cell calcium*, 53(2), pp. 139–151.
- Diercks, B.P. and Guse, A.H. (2020). Unexpected players for local calcium signals: STIM and Orai proteins. *Current Opinion in Physiology*, 17, pp. 17-24.

Dietrich, A. (2019). Modulators of Transient Receptor Potential (TRP) Channels as Therapeutic Options in Lung Disease. *Pharmaceuticals*, 12(1), 23.

Dietrich, A., Chubanov, V., Kalwa, H., Rost, B.R. and Gudermann, T. (2006). Cation channels of the transient receptor potential superfamily: their role in physiological and pathophysiological processes of smooth muscle cells. *Pharmacology & therapeutics*, 112(3), pp. 744-760.

Dogné, J. M., de Leval, X., Benoit, P., Delarge, J. and Masereel, B. (2002). Thromboxane A₂ inhibition: therapeutic potential in bronchial asthma. *American journal of respiratory medicine : drugs, devices, and other interventions*, 1(1), pp. 11–17.

Doidge, J.M. and Satchell, D.G. (1982). Adrenergic and non-adrenergic inhibitory nerves in mammalian airways. *Journal of the Autonomic Nervous System*, 5, pp. 83-99.

Dong, X.P., Wang, X. and Xu, H. (2010). TRP channels of intracellular membranes. *Journal of neurochemistry*, 113(2), pp. 313-328.

Drazen, J. M., Fanta, C. H. and Lacouture, P. G. (1983). Effect of nifedipine on constriction of human tracheal strips *in-vitro*. *British journal of pharmacology*, 78(4), pp. 687–691.

Drumm, B. T., Hannigan, K. I., Lee, J. Y., Rembetski, B. E., Baker, S. A., Koh, S. D., Cobine, C. A., and Sanders, K. M. (2022). Ca²⁺ signalling in interstitial cells of Cajal contributes to generation and maintenance of tone in mouse and monkey lower oesophageal sphincters. *The Journal of physiology*, 10.1113/JP282570.

Drumm, B. T., Rembetski, B. E., Baker, S. A., and Sanders, K. M. (2019b). Tonic inhibition of murine proximal colon is due to nitroergic suppression of Ca²⁺ signaling in interstitial cells of Cajal. *Scientific reports*, 9(1), 4402.

Drumm, B. T., Rembetski, B. E., Cobine, C. A., Baker, S. A., Sergeant, G. P., Hollywood, M. A., Thornbury, K. D., and Sanders, K. M. (2018). Ca²⁺ signalling in mouse urethral smooth muscle in situ: role of Ca²⁺ stores and Ca²⁺ influx mechanisms. *The Journal of physiology*, 596(8), pp.1433–1466.

Drumm, B. T., Rembetski, B. E., Messersmith, K., Manierka, M. S., Baker, S. A., and Sanders, K. M. (2020). Pacemaker function and neural responsiveness of subserosal interstitial cells of Cajal in the mouse colon. *The Journal of physiology*, 598(4), pp. 651–681.

Drumm, B.T., Rembetski, B.E., Baker, S.A. and Sanders, K.M. (2019). Tonic inhibition of murine proximal colon is due to nitroergic suppression of Ca²⁺ signaling in interstitial cells of Cajal. *Scientific Reports*, 9(1), pp. 4402-4416.

- Du, W., McMahon, T. J., Zhang, Z. S., Stiber, J. A., Meissner, G. and Eu, J. P. (2006). Excitation-contraction coupling in airway smooth muscle. *The Journal of biological chemistry*, 281(40), pp. 30143–30151.
- Du, W., Stiber, J. A., Rosenberg, P. B., Meissner, G. and Eu, J. P. (2005). Ryanodine receptors in muscarinic receptor-mediated bronchoconstriction. *The Journal of biological chemistry*, 280(28), pp. 26287–26294.
- Dunlap, K., Luebke, J.I. and Turner, T.J. (1995). Exocytotic calcium channels in mammalian central neurons. *Trends Neurosci*, 18, pp. 89–98.
- Duran, C., Qu, Z., Osunkoya, A.O., Cui, Y. and Hartzell, H.C. (2012). ANOs 3-7 in the anoctamin/Tmem16 Cl⁻ channel family are intracellular proteins. *American Journal of Physiology- Cell Physiology*, 302, pp. C482-C493.
- Ebina, M., Takahashi, T., Chiba, T. and Motomiya, M. (1993). Cellular hypertrophy and hyperplasia of airway smooth muscles underlying bronchial asthma. A 3-D morphometric study. *The American Review of Respiratory Disease*, 148(3), pp. 720-760.
- Ebina, M., Yaegashi, H., Chiba, R., Takahashi, T., Motomiya, M. and Tanemura, M. (1990). Hyperreactive Site in the Airway Tree of Asthmatic Patients Revealed by Thickening of Bronchial Muscles: A Morphometric Study. *American Review of Respiratory Disease*, 141(5 Pt 1), pp.1327-1332.
- Eglen, R. M., Hegde, S. S. and Watson, N. (1996). Muscarinic receptor subtypes and smooth muscle function. *Pharmacology Review*, 48, pp. 531-565.
- Ehlert, F.J. (2003). Contractile role of M₂ and M₃ muscarinic receptors in gastrointestinal, airway and urinary bladder smooth muscle. *Life Science*, 74, pp. 355-366.
- Endo, M. (1983). Excitation-contraction coupling in smooth muscle. *Japanese Journal of Pharmacology*, 33(Supp. 1), 4.
- Erle, D. J. and Zhen, G. (2006). The asthma channel? Stay tuned. *American journal of respiratory and critical care medicine*, 173(11), pp. 1181–1182.
- Ertel, E.A., Campbell, K.P., Harpold, M.M., Hofmann, F., Mori, Y., Perez-Reyes, E., Schwartz, A., Snutch, T.P., Tanabe, T., Birnbaumer, L., Tsien, R.W. and Catterall, W.A. (2000). Nomenclature of voltage-gated calcium channels. *Neuron*, 25, pp. 533–535.
- Farley, J. M. and Miles, P. R. (1978). The sources of calcium for acetylcholine-induced contractions of dog tracheal smooth muscle. *The Journal of pharmacology and experimental therapeutics*, 207(2), pp. 340–346.

- Fatigati, V. and Murphy, R.A. (1984). Actin and tropomyosin variants in smooth muscles. Dependence on tissue type. *Journal of Biological Chemistry*, 259(23), pp. 14383-14391.
- Fedigan, S., Bradley, E., Webb, T., Large, R.J., Hollywood, M.A., Thornbury, K.D., Mchale, N.G. and Sergeant, G.P. (2017). Effects of new-generation TMEM16A inhibitors on calcium-activated chloride currents in rabbit urethral interstitial cells of Cajal. *Pflugers Arch: European Journal of Physiology*, 469(11), pp. 1443-1455.
- Fernandez-Fernandez, J.M., Andrade, Y.N., Arniges, M., Fernandes, J., Plata, C., Rubio-Moscardo, F., Vazquez, E. and Valverde, M.A. (2008). Functional coupling of TRPV4 cationic channel and large conductance, calcium-dependent potassium channel in human bronchial epithelial cell lines. *Pflugers Arch: European Journal of Physiology*, 457, pp. 149-159,
- Ferrera, L., Caputto, A. and Galiotta, L.J.V. (2019). TMEM16A Protein: A new identity for Ca²⁺-dependent Cl⁻ channels. *Physiology*, 25, pp. 357-363
- Finney-Hayward, T.K., Popa, M.O., Bahra, P., Li, S., Poll, C.T., Gosling, M., Nicholson, A.G., Russell, R.E., Kon, O.M., Jarai, G., Westwick, J., Barnes, P.J. and Donnelly, L.E. (2010). Expression of transient receptor potential C6 channels in human lung macrophages. *American Journal of Respiratory Cell and Molecular Biology*, 43(3), pp. 296-304.
- Fryer, A. and Jacoby, D. (1998). Muscarinic receptors and control of airway smooth muscle. *American Journal of Respiratory and Critical Care Medicine*, 158(5 Pt 3), pp. S154- S160.
- Gallos, G., Remy, K. E., Danielsson, J., Funayama, H., Fu, X. W., Chang, H. Y., Yim, P., Xu, D. and Emala, C. W. Sr (2013). Functional expression of the TMEM16 family of calcium-activated chloride channels in airway smooth muscle. *American journal of physiology. Lung cellular and molecular physiology*, 305(9), pp. L625–L634.
- GBD 2019 Diseases and Injuries Collaborators (2020). Global burden of 369 diseases and injuries in 204 countries and territories, 1990-2019: a systematic analysis for the Global Burden of Disease Study 2019. *Lancet (London, England)*, 396(10258), pp. 1204–1222.
- Gibson, A., Lewis, A.P., Affleck, K., Aitken, A.J., Meldrum, E. and Thompson, N. (2005). hCLCA1 and mCLCA3 are secreted non-integral membrane proteins and therefore are not ion channels. *Journal of Biological Chemistry*, 280, pp. 27205-27212.

- Gibson, A., McFadzean, I., Wallace, P. and Wayman, C. P. (1998). Capacitative Ca^{2+} entry and the regulation of smooth muscle tone. *Trends in pharmacological sciences*, 19(7), pp. 266–269.
- Godin, N. and Rousseau, E. (2007). TRPC6 silencing in primary airway smooth muscle cells inhibits protein expression without affecting OAG-induced calcium entry. *Molecular and cellular biochemistry*, 296(1–2), pp. 193-201.
- Goldie, R.G., Spina, D., Henry, P.J., Lulich, K.M. and Paterson, J.W. (1986). *In-vitro* responsiveness of human asthmatic bronchus to carbachol, histamine, beta-adrenoceptor agonists and theophylline. *British Journal of Clinical Pharmacology*, 22(6), pp. 669-676.
- Gombedza, F., Kondeti, V., Al-Azzam, N., Koppes, S., Duah, E., Patil, P., Hexter, M., Philips, D., Thodeti, C.K. and Paruchuri, S. (2017). Mechanosensitive transient receptor potential vanilloid 4 regulates *Dermatophagoides farinae*-induced airway remodeling via 2 distinct pathways modulating matrix synthesis and degradation. *The FASEB Journal*, 31(4), pp. 1556-70.
- Gonzalez-Cobos, J.C. and Trebak, M. (2010). TRPC channels in smooth muscle cells. *Frontiers in bioscience (Landmark edition)*, 15, pp. 1023-1039.
- Graves, S., Dretchen, K. L. and Kruger, G. O. (1978). Dantrolene sodium: effects on smooth muscle. *European journal of pharmacology*, 47(1), pp. 29–35.
- Groot-Kormelink, P.J., Fawcett, L., Wright, P.D., Gosling, M. and Kent, T.C. (2012). Quantitative GPCR and ion channel transcriptomics in primary alveolar macrophages and macrophage surrogates. *BMC immunology*, 13, 57.
- Guerrero-Hernández, A., Gómez-Viquez, L., Guerrero-Serna, G. and Rueda, A. (2002). Ryanodine receptors in smooth muscle. *Frontiers in bioscience : a journal and virtual library*, 7, pp. d1676–d1688.
- Gyobu, S., Miyata, H., Ikawa, M., Yamazaki, D., Takeshima, H., Suzuki, J. and Nagata, S. (2016). A role of TMEM16E carrying a scrambling domain in sperm motility. *Molecular and Cellular Biology*, 36(4), pp. 645-659.
- Hall, A.K., Barnes, P.J., Meldrum, L.A. and MacLagan, J. (1989). Facilitation by tachykinins of neurotransmission in guinea-pig pulmonary parasympathetic nerves. *British Journal of Pharmacology*, 97, pp. 274-280.
- Hall, I.P., Daykin, K. and Widdop, S. (1993). Beta 2-adrenoceptor desensitization in cultured human airway smooth muscle. *Clinical science*, 84(2), pp.151-157.
- Hall, I.P., Widdop, S., Townsend, P. and Daykin, K. (1992). Control of cyclic AMP levels in primary cultures of human tracheal smooth muscle cells. *British journal of pharmacology*, 107(2), pp. 422-428.

- Hamberg, M., Svensson, J. and Samuelsson, B. (1975). Thromboxanes: a new group of biologically active compounds derived from prostaglandin endoperoxides. *Proceedings of the National Academy of Sciences of the United States of America*, 72(8), pp. 2994-2998.
- Hamid, Q.A., Mak, J.C., Sheppard, M.N., Corrin, B., Venter, J.C. and Barnes, P.J. (1991). Localization of beta2-adrenoceptor messenger RNA in human and rat lung using *in-situ* hybridization: Correlation with receptor autoradiography. *European Journal of Pharmacology*, 206, pp.133-138.
- Hannigan, K.I., Griffin, C.S., Large, R.J., Sergeant, G.P., Hollywood, M.A., McHale, N.G. and Thornbury, K.D. (2017). The role of Ca²⁺-activated Cl⁻ current in tone generation in the rabbit corpus cavernosum. *American Journal of Physiology - Cell Physiology*, 313(5), pp. C475-C486.
- Hartzell, C., Putzier, I. and Arreola, J. (2005). Calcium-activated chloride channels. *Annual review of physiology*, 67, pp. 719–758.
- Hernandez, J.M. and Janssen, L.J. (2015). Revisiting the usefulness of thromboxane-A2 modulation in the treatment of bronchoconstriction in asthma. *Canadian Journal of Physiology and Pharmacology*, 93(2), pp. 111-117.
- Higashida, H., Yokoyama, S., Hashii, M., Taketo, M., Higashida, M., Takayasu T., Ohshima, T., Takasawa, S., Okamoto, H. and Noda, M. (1997). Muscarinic receptor-mediated dual regulation of ADP-ribosyl cyclase in NG108-15 neuronal cell membranes. *Journal of Biological Chemistry*, 272(50), pp. 31272-31277.
- Hill-Eubanks, D. C., Werner, M. E., Heppner, T. J. and Nelson, M. T. (2011). Calcium signaling in smooth muscle. *Cold Spring Harbor perspectives in biology*, 3(9), a004549.
- Hille, B. (2001). *Ion Channels of Excitable Membranes* (3rd Edition).
- Himmel, N. J. and Cox, D. N. (2020). Transient receptor potential channels: current perspectives on evolution, structure, function and nomenclature. *Proceedings. Biological sciences*, 287(1933), 1309.
- Hirota, K., Hashiba, E., Yoshioka, H., Kabara, S. and Matsuki, A. (2003). Effects of three different L-type Ca²⁺ entry blockers on airway constriction induced by muscarinic receptor stimulation. *Br J Anaesth*, 90(5), pp. 671-675.
- Hirota, S. and Janssen, L. J. (2007). Store-refilling involves both L-type calcium channels and reverse-mode sodium-calcium exchange in airway smooth muscle. *The European respiratory journal*, 30(2), pp. 269–278.

- Hirota, S., Helli, P. and Janssen, L. J. (2007). Ionic mechanisms and Ca²⁺ handling in airway smooth muscle. *The European respiratory journal*, 30(1), pp. 114–133.
- Hirota, S., Trimble, N., Pertens, E. and Janssen, L.J. (2006). Intracellular Cl⁻ fluxes play a novel role in Ca²⁺ handling in airway smooth muscle. *American Journal of Physiology- Lung Cellular and Molecular Physiology*, 290, pp. L1146-L1153.
- Hogg, J. C., Chu, F., Utokaparch, S., Woods, R., Elliott, W. M., Buzatu, L., Cherniack, R. M., Rogers, R. M., Sciurba, F. C., Coxson, H. O. and Paré, P. D. (2004). The nature of small-airway obstruction in chronic obstructive pulmonary disease. *The New England journal of medicine*, 350(26), pp. 2645–2653.
- Holgate, S. T., Peters-Golden, M., Panettieri, R. A. and Henderson, W. R., Jr (2003). Roles of cysteinyl leukotrienes in airway inflammation, smooth muscle function, and remodeling. *The Journal of allergy and clinical immunology*, 111(1 Suppl), pp. S18–S36.
- Hollywood, M. A., Sergeant, G. P., McHale, N. G. and Thornbury, K. D. (2003). Activation of Ca²⁺-activated Cl⁻ current by depolarizing steps in rabbit urethral interstitial cells. *American journal of physiology. Cell physiology*, 285(2), pp. C327–C333.
- Howarth, P. H., Knox, A. J., Amrani, Y., Tliba, O., Panettieri, R. A. Jr, and Johnson, M. (2004). Synthetic responses in airway smooth muscle. *The Journal of allergy and clinical immunology*, 114(2 Suppl), pp. S32–S50.
- Howarth, P.H., Springall, D.R., Redington, A.E., Djukanovic, R., Holgate, S.T. and Polak, J.M. (1995). Neuropeptide containing nerves in endobronchial biopsies from asthmatic and nonasthmatic subjects. *American Journal of Respiratory Cell and Molecular Biology*, 13, pp. 288-296.
- Huang, F., Rock, J. R., Harfe, B. D., Cheng, T., Huang, X., Jan, Y. N. and Jan, L. Y. (2009). Studies on expression and function of the TMEM16A calcium-activated chloride channel. *Proceedings of the National Academy of Sciences of the United States of America*, 106(50), pp. 21413–21418.
- Huang, F., Zhang, H., Wu, M., Yang, H., Kudo, M., Peters, C. J., Woodruff, P. G., Solberg, O. D., Donne, M. L., Huang, X., Sheppard, D., Fahy, J. V., Wolters, P. J., Hogan, B. L., Finkbeiner, W. E., Li, M., Jan, Y. N., Jan, L. Y. and Rock, J. R. (2012). Calcium-activated chloride channel TMEM16A modulates mucin secretion and airway smooth muscle contraction. *Proceedings of the National Academy of Sciences of the United States of America*, 109(40), pp. 16354–16359.

- Huang, J. S., Ramamurthy, S. K., Lin, X. and Le Breton, G. C. (2004). Cell signalling through thromboxane A₂ receptors. *Cellular signalling*, 16(5), pp. 521–533.
- Hwang, S. J., Basma, N., Sanders, K. M. and Ward, S. M. (2016). Effects of new-generation inhibitors of the calcium-activated chloride channel anoctamin 1 on slow waves in the gastrointestinal tract. *British Journal of Pharmacology*, 173, pp. 1339-1349.
- Hyuga, S., Danielsson, J., Vink, J., Fu, X.W., Wapner, R. and Gallos, G. (2018). Functional comparison of anoctamin 1 antagonists on human uterine smooth muscle contractility and excitability. *Journal of Smooth Muscle Research*, 54(1), pp. 28-42.
- Hyvelin, J.M., Martin, C., Roux, E., Marthan, R. and Savineau, J.P. (2000). Human isolated bronchial smooth muscle contains functional ryanodine/caffeine-sensitive Ca-release channels. *Am J Respir Crit Care Med*, 162(2 Pt 1), pp. 687-694.
- Ind, P.W. (1994). Role of the sympathetic nervous system and endogenous catecholamines in the regulation of airways smooth muscle tone. In *Airways smooth muscle: structure, innervation and neurotransmission*. Edited by Raeburn, D. and Giembycz, M. A., Basel: Birkhäuser Basel, pp. 29-41.
- Inoue, T., Makita, Y., Ito, Y. and Kuriyama, H (1985). Regulations of transmitter release by prostaglandins on vascular and tracheal smooth muscle tissues. *Advances in prostaglandin, thromboxane, and leukotriene research*, 15, pp. 685-688.
- Islam, M.S. (2020). Calcium Signaling: from Basic to Bedside. In M.S. Islam (Ed.), *Calcium Signaling (Advances in Experimental Medicine and Biology, 1131)*, 2nd edition, Springer, pp 1-6.
- Jaggar, J. H., Porter, V. A., Lederer, W. J. and Nelson, M. T. (2000). Calcium sparks in smooth muscle. *Am J Physiol Cell Physiol*, 278(2), pp. C235–C256.
- James, A. and Carroll, N. (2000). Airway smooth muscle in health and disease; methods of measurement and relation to function. *European Respiratory Journal*, 15(4), pp. 782-789.
- Jang, Y. and Oh, U. (2014). Anoctamin 1 in secretory epithelia. *Cell calcium*, 55(6), pp. 355–361.
- Janssen L. J. (2002). Ionic mechanisms and Ca²⁺ regulation in airway smooth muscle contraction: do the data contradict dogma?. *American journal of physiology. Lung cellular and molecular physiology*, 282(6), pp. L1161–L1178.

- Janssen, L.J. (1997). T-type and L-type Ca^{2+} currents in canine bronchial smooth muscle: Characterization and physiological roles. *American Journal of Physiology - Cell Physiology*, 272(6), pp. 41-46.
- Janssen, L.J. (2009). Asthma therapy: how far have we come, why did we fail and where should we go next? *Eur Respir J*, 33(1), pp. 11-20.
- Janssen, L.J. and Sims, S.M. (1992). Acetylcholine activates non-selective cation and chloride conductance in canine and guinea-pig tracheal myocytes. *The Journal of Physiology*, 453, pp.197-218.
- Janssen, L.J. and Sims, S.M. (1995). Ca^{2+} -dependent Cl^{-} current in canine tracheal smooth muscle cells. *American Journal of Physiology*, 269, pp. 163-169.
- Janssen, L.J., Tazzeo, T. and Zuo, J. (2004). Enhanced myosin phosphatase and Ca^{2+} -uptake mediate adrenergic relaxation of airway smooth muscle. *American Journal of Respiratory Cell and Molecular Biology*, 30(4), pp. 548-554.
- Jia, Y., Wang, X., Varty, L.A., Rizzo, C.A., Yang, R., Correll, C.C., Phelps, P.T., Egan, R.W. and Hey, J.A. (2004). Functional TRPV4 channels are expressed in human airway smooth muscle cells. *American Journal of Physiology - Lung Cellular and Molecular Physiology*, 287(2), pp. 272-278.
- Johnson, M. and Trebak, M. (2019). ORAI channels in cellular remodeling of cardiorespiratory disease. *Cell calcium*, 79, pp. 1–10.
- Johnson, M. T., Xin, P., Benson, J. C., Pathak, T., Walter, V., Emrich, S. M., Yoast, R. E., Zhang, X., Cao, G., Panettieri, R. A. Jr, and Trebak, M. (2022). STIM1 is a core trigger of airway smooth muscle remodeling and hyperresponsiveness in asthma. *Proceedings of the National Academy of Sciences of the United States of America*, 119(1), pp. 1-12.
- Jongejan, R.C., de Jongste, J.C., Raatgeep, R.C., Stijnen, T., Bonta, I.L. and Kerrebijn, K.F. (1990). Effects of inflammatory mediators on the responsiveness of isolated human airways to methacholine. *The American Review of Respiratory Disease*, 142, pp. 1129-1132.
- Kanefsky, J., Lenburg, M. and Hai, C.M. (2006). Cholinergic receptor and cyclic stretch-mediated inflammatory gene expression in intact ASM. *American Journal of Respiratory Cell and Molecule Biology*, 34(4), pp. 417-425.
- Kang, J.W., Lee, Y.H., Kang, M.J., Lee, H.J., Oh, R., Min, H.J., Namkung, W., Choi, J.Y., Lee, S.N., Kim, C.-H., Yoon, J.H. and Cho, H.J. (2017). Synergistic mucus secretion by histamine and IL-4 through TMEM16A in airway epithelium. *American Journal of Physiology-Lung Cellular and Molecular Physiology*, 313(3), pp. L466-L476.

- Kaufman, M.P., Coleridge, H.M., Coleridge, J.C. and Baker, D.G.(1980). Bradykinin stimulates afferent vagal C-fibers in intrapulmonary airways of dogs. *Journal of Applied Physiology*, 48(3), pp. 511-517.
- Knight, D. and Holgate, S. (2003). The airway epithelium: Structural and functional properties in health and disease. *Respirology*, 8(4), pp. 432-446.
- Kondo, M., Tsuji, M., Hara, K., Arimura, K., Yagi, O., Tagaya, E., Takeyama, K. and Tamaoki, J. (2017). Chloride ion transport and overexpression of TMEM16A in a guinea-pig asthma model. *Clinical & Experimental Allergy*, 47(6), pp. 795-804.
- Kotlikoff, M. I. and Wang, Y. X. (1998). Calcium release and calcium-activated chloride channels in airway smooth muscle cells. *American journal of respiratory and critical care medicine*, 158(5 Pt 3), pp. S109–S114.
- Kotlikoff, M.I. (1993). Potassium channels in airway smooth muscle: a tale of two channels. *Pharmacol Ther*, 58(1), pp. 1-12.
- Kraner, S. D., Wang, Q., Novak, K. R., Cheng, D., Cool, D. R., Peng, J. and Rich, M. M. (2011). Upregulation of the CaV 1.1-ryanodine receptor complex in a rat model of critical illness myopathy. *American journal of physiology. Regulatory, integrative and comparative physiology*, 300(6), pp. R1384–R1391.
- Kshatri, A. S., Gonzalez-Hernandez, A. and Giraldez, T. (2018). Physiological Roles and Therapeutic Potential of Ca²⁺ Activated Potassium Channels in the Nervous System. *Frontiers in molecular neuroscience*, 11, 258.
- Kuang, Q., Purhonen, P. and Hebert, H. (2015). Structure of potassium channels. *Cell Mol Life Sci*, 72(19), pp. 3677-3693.
- Kume, H., Hall, I.P., Washabau, R.J., Takagi, K. and Kotlikoff, M.I. (1994). β -Adrenergic agonists regulate K_{Ca} channels in airway smooth muscle by cAMP-dependent and -independent mechanisms. *Journal of Clinical Investigation*, 93, pp. 371-379.
- Kume, H., Nishiyama, O., Isoya, T., Higashimoto, Y., Tohda, Y. and Noda, Y. (2018). Involvement of Allosteric Effect and K_{Ca} Channels in Crosstalk between β_2 -Adrenergic and Muscarinic M₂ Receptors in Airway Smooth Muscle. *International journal of molecular sciences*, 19(7), pp. 1-17.
- Kwan, C. Y., Takemura, H., Obie, J. F., Thastrup, O. and Putney, J. W., Jr (1990). Effects of MeCh, thapsigargin, and La³⁺ on plasmalemmal and intracellular Ca²⁺ transport in lacrimal acinar cells. *The American journal of physiology*, 258(6 Pt 1), pp. C1006–C1015.
- Kwong, K. and Carr, M.J. (2015). Voltage-gated sodium channels. *Current Opinion in Pharmacology*, 22, pp. 131-139

- Lacruz, R. S. and Feske, S. (2015). Diseases caused by mutations in ORAI1 and STIM1. *Annals of the New York Academy of Sciences*, 1356(1), pp. 45–79.
- Laitinen, L.A., Laitinen, M.V.A. and Widdicombe, J.G. (1987). Parasympathetic nervous control of tracheal vascular resistance in the dog. *Journal of Physiology*, 385, pp. 135-146.
- Lammers, J.W., Barnes, P.J. and Chung, K.F. (1992). Non-adrenergic, non-cholinergic airway inhibitory nerves. *European Respiratory Journal*, 5, pp. 239-246.
- Lammers, J.W., Minette, P., McCusker, M.T., Chung, K.F. and Barnes, P.J. (1988). Non-adrenergic bronchodilator mechanisms in normal human subjects in-vivo. *Journal of Applied Physiology*, 64, pp. 1817-1822.
- Lanner, J.T., Dimitri, K., Georgiou, A.D., Hamilton, J. and Hamilton, S. (2010). Ryanodine receptors: structure, expression, molecular details, and function in calcium release. *Cold Spring Harbor Perspectives in Biology*, 2(11), a003996.
- Lapie, P., Lory, P., and Fontaine, B. (1997). Hypokalemic periodic paralysis: an autosomal dominant muscle disorder caused by mutations in a voltage-gated calcium channel. *Neuromuscular disorders : NMD*, 7(4), pp. 234–240.
- Large, R. J., Bradley, E., Webb, T., O'Donnell, A. M., Puri, P., Hollywood, M. A., Thornbury, K. D., McHale, N. G. and Sergeant, G. P. (2012). Investigation of L-type Ca^{2+} current in the aganglionic bowel segment in Hirschsprung's disease. *Neurogastroenterology and motility : the official journal of the European Gastrointestinal Motility Society*, 24(12), pp. 1126–e571.
- Lechner, A.J., Matsuchak, M. and Brink, D.S. (2011). Respiratory: An integrated Approach to Disease. *New York: McGraw-Hill Professional*.
- Leff, A. (1982). Pathogenesis of asthma. Neurophysiology and pharmacology of bronchospasm. *Chest*, 81(2), pp. 224–229.
- Leiva-Juárez, M., Kolls, J. and Evans, S. (2017). Lung epithelial cells: therapeutically inducible effectors of antimicrobial defense. *Mucosal Immunology*, 11(1), pp. 21-34.
- Lewis R. S. (2007). The molecular choreography of a store-operated calcium channel. *Nature*, 446(7133), pp. 284–287.
- Li, S., Westwick, J. and Poll, C. (2003). Transient receptor potential (TRP) channels as potential drug targets in respiratory disease. *Cell Calcium*, 33, 551-558.

- Liang, X., Zhang, N., Pan, H., Xie, J., and Han, W. (2021). Development of Store-Operated Calcium Entry-Targeted Compounds in Cancer. *Frontiers in pharmacology*, 12, 688244.
- Lifshitz, L.M., Carmichael, J.D., Lai, F.A., Sorrentino, V., Bellvé, K., Fogarty, K.E. and ZhuGe, R. (2011). Spatial organization of RYRs and BK channels underlying the activation of STOCs by Ca^{2+} sparks in airway myocytes. *J Gen Physiol*, 138(2), pp. 195-209.
- Liu, X. and Farley, J.M. (1996a). Acetylcholine-induced Ca^{++} -dependent chloride current oscillations are mediated by inositol 1,4,5-trisphosphate in tracheal myocytes. *J Pharmacol Exp Ther*, 277, pp. 796-804.
- Liu, X. and Farley, J.M. (1996). Acetylcholine-induced chloride current oscillations in swine tracheal smooth muscle cells. *Journal of Pharmacology and Experimental Therapeutics*, 276, pp. 178-186.
- Lopes-Pacheco, M. (2020). CFTR Modulators: The Changing Face of Cystic Fibrosis in the Era of Precision Medicine. *Frontiers in pharmacology*, 10, 1662.
- Ma, K., Wang, H., Yu, J., Wei, M. and Xiao, Q. (2017). New insights on the regulation of Ca^{2+} -activated chloride channel TMEM16A. *Journal of Cellular Physiology*, 232(4), pp. 707-716.
- Ma, M. M., Gao, M., Guo, K. M., Wang, M., Li, X. Y., Zeng, X.L., Sun, L., Lv, X.F., Du, Y.H., Wang, G.L., Zhou, J.G. and Guan, Y.Y. (2017). TMEM16A contributes to endothelial dysfunction by facilitating Nox2 NADPH oxidase-derived reactive oxygen species generation in hypertension. *Hypertension*, 69(5), pp. 892-901.
- MacLennan, D. H. and Kranias, E. G. (2003). Phospholamban: a crucial regulator of cardiac contractility. *Nature reviews. Molecular cell biology*, 4(7), pp. 566–577.
- Macmillan, S., Sheridan, R. D., Chilvers, E. R. and Patmore, L. (1995). A comparison of the effects of SCA40, NS 004 and NS 1619 on large conductance Ca^{2+} -activated K^{+} channels in bovine tracheal smooth muscle cells in culture. *British journal of pharmacology*, 116(1), pp. 1656–1660.
- Martin-Romero, F. J., Pascual-Caro, C., Lopez- Guerrero, A., Espinosa-Bermejo, N. and Pozo-Guisado, E. (2018). Regulation of Calcium Signaling by STIM1 and ORAI1. In J. N. Buchholz, & E. J. Behringer (Eds.), *Calcium and Signal Transduction*. IntechOpen.
- Martin, G., O'Connell, R. J., Pietrzykowski, A. Z., Treistman, S. N., Ethier, M. F. and Madison, J. M. (2008). Interleukin-4 activates large-conductance, calcium-activated potassium (BK_{Ca}) channels in human airway smooth muscle cells. *Experimental physiology*, 93(7), pp. 908–918.

- Mátyás, S., Pucovský, V. and Bauer, V. (1995). Involvement of different Ca²⁺ sources in changes of responsiveness of guinea-pig trachea to repeated administration of histamine and acetylcholine. *General physiology and biophysics*, 14(1), pp. 51–60.
- McAlexander, M.A., Luttmann, M.A., Hunsberger, G.E. and Undem, B.J. (2014). Transient Receptor Potential Vanilloid 4 Activation Constricts the Human Bronchus via the Release of Cysteinyl Leukotrienes. *Journal of Pharmacology and Experimental Therapeutics*, 349(1), pp.118-125.
- McCann, J. D. and Welsh, M. J. (1986). Calcium-activated potassium channels in canine airway smooth muscle. *The Journal of physiology*, 372, pp. 113–127.
- McDonald, T.F., Pelzer, S., Trautwein, W. and Pelzer, D.J. (1994). Regulation and modulation of calcium channels in cardiac, skeletal, and smooth muscle cells. *Physiol Rev*, 74, pp. 365 – 507.
- Meiss, R.A. (1997). Mechanics of smooth muscle contraction. In: Cellular Aspects of Smooth Muscle Function, edited by Kao, C.Y. and Carsten, M.E. *New York: Cambridge Univ. Press*, 1997, pp. 169 -201.
- Mitzner, W. (2004). Airway smooth muscle: the appendix of the lung. *American journal of respiratory and critical care medicine*, 169(7), pp. 787-790.
- Mondéjar-Parreño, G., Barreira, B., Callejo, M., Morales-Cano, D., Barrese, V., Esquivel-Ruiz, S., Olivencia, M. A., Macías, M., Moreno, L., Greenwood, I. A., Perez-Vizcaino, F. and Cogolludo, A. (2020). Uncovered Contribution of Kv7 Channels to Pulmonary Vascular Tone in Pulmonary Arterial Hypertension. *Hypertension (Dallas, Tex. : 1979)*, 76(4), pp. 1134–1146.
- Morgan, L. M., Martin, S. L., Mullins, N. D., Hollywood, M. A., Thornbury, K. D., and Sergeant, G. P. (2022). Modulation of carbachol-induced Ca²⁺ oscillations in airway smooth muscle cells by PGE₂. *Cell calcium*, 103, 102547.
- Morgan, S.J., Deshpande, D.A., Tiegs, B.C., Misor, A.M., Yan, H., Hershfeld, A.V., Rich, T.C., Panettiera, R.A., An, S.S. and Penn, R.B. (2014). β-agonist-mediated Relaxation of Airway Smooth Muscle Is Protein Kinase A-dependant. *The Journal of Biological Chemistry*, 289(33), pp. 23065-23074.
- Mukherjee, S., Trice, J., Shinde, P., Willis, R. E., Pressley, T. A. and Perez-Zoghbi, J. F. (2013). Ca²⁺ oscillations, Ca²⁺ sensitization, and contraction activated by protein kinase C in small airway smooth muscle. *The Journal of general physiology*, 141(2), pp. 165–178.
- Murray, M. A., Berry, J. L., Cook, S. J., Foster, R. W., Green, K. A. and Small, R. C. (1991). Guinea-pig isolated trachealis: the effects of charybdotoxin on mechanical activity, membrane potential changes and the activity of

plasmalemmal K(+)-channels. *British journal of pharmacology*, 103(3), pp. 1814–1818.

Namkung, W., Phuan, P.W. and Verkman, A.S. (2011). TMEM16A inhibitors reveal TMEM16A as a minor component of calcium-activated chloride channel conductance in airway and intestinal epithelial cells. *Journal of Biological Chemistry*, 286(3), pp. 2365-2374.

Narayanan, D., Adebisi, A. and Jaggar, J.H. (2012). Inositol trisphosphate receptors in smooth muscle cells. *Am J Physiol Heart Circ Physiol*, 302(11), pp. H2190-H2210.

Nilius, B., Owsianik, G., Voets, T. and Peters, J.A. (2007). Transient receptor potential cation channels in disease. *Physiology Review*, 87(1), pp. 165-217.

Nilius, B., Vennekens, R., Prenen, J., Hoenderop, J.G., Bindels, R.J. and Droogmans, G. (2000). Whole-cell and single channel monovalent cation currents through the novel rabbit epithelial Ca²⁺ channel ECaC. *Journal of Physiology*, 527(2), pp. 239-248.

Nilius, B., Vriens, J., Prenen, J., Droogmans, G. and Voets, T. (2004). TRPV4 calcium entry channel: a paradigm for gating diversity. *American journal of physiology-Cell physiology*, 286(2), pp. C195-C205.

Nilius, B., Watanabe, H. and Vriens, J. (2003). The TRPV4 channel: structure-function relationship and promiscuous gating behaviour. *Pflügers Archiv: European journal of physiology*, 446(3), pp. 298-303.

Oh, S. J., Hwang, S. J., Jung, J., Yu, K., Kim, J., Choi, J. Y., Hartzell, H.C., Roh, E.J. and Lee, C. J. (2013). MONNA, a potent and selective blocker for transmembrane protein with unknown function 16/anoctamin-1. *Molecular Pharmacology*, 84(5), pp. 726-735.

Oh, U. and Jung, J. (2016). Cellular functions of TMEM16/anoctamin. *Pflügers Archiv : European journal of physiology*, 468(3), pp. 443–453.

Ong, H.L., Brereton, H.M., Harland, M.L. and Barritt, G.J.(2003). Evidence for the expression of transient receptor potential proteins in guinea pig airway smooth muscle cells. *Respirology*, 8(1), pp. 23-32.

Ong, H.L., Chen, J., Chataway, T., Brereton, H., Zhang, L., Downs, T., Tsiokas, L. and Barritt, G. (2002). Specific detection of the endogenous transient receptor potential (TRP)-1 protein in liver and airway smooth muscle cells using immunoprecipitation and Western-blot analysis. *Biochemical Journal*, 64(3), pp. 641-648.

Ousingsawat, J., Martins, J.R., Schreiber, R., Rock, J.R., Harfe, B.D. and Kunzelmann, K. (2009). Loss of TMEM16A causes a defect in epithelial Ca²⁺-

dependent chloride transport. *Journal of Biological Chemistry*, 284 (42), pp. 28698-28703.

Pack, R.J. and Richardson, P.S. (1984). The aminergic innervation of the human bronchus: a light and electron microscopic study. *Journal of Anatomy*, 138(3), pp. 493-502.

Palmer, J.B.A. and Barnes, P.J. (1987). Neuropeptides and airway smooth muscle function. *The American Review of Respiratory Disease*, 136(6 pt 2), pp. S77-83.

Panettieri, R.A. Jr., Kotlikoff, M.I., Gerthoffer, W.T., Hershenson, M.B., Woodruff, P.G., Hall, I.P. and Banks-Schlegel, S. (2008). Airway smooth muscle in bronchial tone, inflammation, and remodeling: basic knowledge to clinical relevance. *Am J Respir Crit Care Med*, 177(3), pp. 248-252.

Papassotiriou, J., Eggermont, J., Droogmans, G. and Nilius, B. (2001). Ca²⁺-activated Cl⁻ channels in Ehrlich ascites tumor cells are distinct from mCLCA1, 2 and 3. *Pflugers Archiv. European Journal of Physiology*, 442, pp. 273-79

Partiseti, M., Le Deist, F., Hivroz, C., Fischer, A., Korn, H. and Choquet, D. (1994). The calcium current activated by T cell receptor and store depletion in human lymphocytes is absent in a primary immunodeficiency. *The Journal of biological chemistry*, 269(51), pp. 32327–32335.

Peatfield, A.C., Barnes, P.J., Bratcher, C., Nadel, J.A. and Davis, B. (1983). Vasoactive intestinal peptide stimulates tracheal submucosal gland secretion in ferret. *American Review of Respiratory Disease*, 128(1), pp. 89-93.

Peel, S. E., Liu, B. and Hall, I. P. (2006). A key role for STIM1 in store operated calcium channel activation in airway smooth muscle. *Respiratory research*, 7(1), 119.

Peel, S. E., Liu, B. and Hall, I. P. (2008). ORAI and store-operated calcium influx in human airway smooth muscle cells. *American journal of respiratory cell and molecular biology*, 38(6), pp. 744–749.

Pelaia, G., Renda, T., Gallelli, L., Vatrella, A., Teresa, M., Agati, S., Caputi, M., Cazzola, M., Maselli, R. and Marsico, S.A. (2008). Molecular mechanisms underlying airway smooth muscle contraction and proliferation : Implications for asthma. *Respiratory Medicines*, 102(8), pp. 1173-1181.

Perez-Reyes E. (2003). Molecular physiology of low-voltage-activated t-type calcium channels. *Physiological reviews*, 83(1), pp. 117–161.

Perez-Zoghbi, J.F., Karner, C., Ito, S., Shepherd, M., Alrashdan, Y. and Sanderson, M.J. (2009). Ion channel regulation of intracellular calcium and

airway smooth muscle function. *Pulmonary pharmacology & therapeutics*, 22(5), pp. 388–397.

Perez, J. F. and Sanderson, M. J. (2005). The frequency of calcium oscillations induced by 5-HT, ACH, and KCl determine the contraction of smooth muscle cells of intrapulmonary bronchioles. *The Journal of general physiology*, 125(6), pp. 535–553.

Philteos, G. S., Davis, B. E., Cockcroft, D. W. and Marciniuk, D. D. (2005). Role of leukotriene receptor antagonists in the treatment of exercise-induced bronchoconstriction: a review. *Allergy, asthma, and clinical immunology : official journal of the Canadian Society of Allergy and Clinical Immunology*, 1(2), pp. 60–64.

Pollock, N. S., Kargacin, M. E. and Kargacin, G. J. (1998). Chloride channel blockers inhibit Ca^{2+} uptake by the smooth muscle sarcoplasmic reticulum. *Biophysical journal*, 75(4), pp. 1759–1766.

Putney J. W. (2018). Forms and functions of store-operated calcium entry mediators, STIM and Orai. *Advances in biological regulation*, 68, pp. 88–96.

Putney J. W. Jr (1986). A model for receptor-regulated calcium entry. *Cell calcium*, 7(1), pp. 1–12.

Rahaman, S.O., Grove, L.M., Paruchuri, S., Southern, B.D., Abraham, S., Niese, K.A., Scheraga, R.G., Ghosh, S., Thodeti, C.K., Zhang, D.X., Moran, M.M., Schilling W.P., Tschumperlin, D.J. and Oلمان, M.A. (2014). TRPV4 mediates myofibroblast differentiation and pulmonary fibrosis in mice. *Journal of Clinical Investigation*, 124(12), pp. 5225 - 5238.

Rehman, R., Bhat, Y.A., Panda, L. and Mabalirajan, U. (2013). TRPV1 inhibition attenuates IL-13 mediated asthma features in mice by reducing airway epithelial injury. *International Immunopharmacology*, 15(3), pp. 597-605.

Rembetski, B. E., Sanders, K. M. and Drumm, B. T. (2020). Contribution of $\text{Ca}_v1.2$ Ca^{2+} channels and store-operated Ca^{2+} entry to pig urethral smooth muscle contraction. *American journal of physiology. Renal physiology*, 318(2), pp. F496–F505.

Reyes-García, J., Flores-Soto, E., Carbajal-García, A., Sommer, B. and Montañó, L. M. (2018). Maintenance of intracellular Ca^{2+} basal concentration in airway smooth muscle. *International journal of molecular medicine*, 42(6), pp. 2998–3008.

Riccio, A., Li, Y., Tsvetkov, E., Gapon, S., Yao, G.L., Smith, K.S., Engin, E., Rudolph, U., Bolshakov, V.Y. and Clapham, D.E. (2014). Decreased Anxiety-Like

- Behavior and $G_{aq/11}$ -Dependent Responses in the Amygdala of Mice Lacking TRPC4 Channels. *The Journal of Neuroscience*, 34(10), pp. 3653-3667.
- Richardson, J. and Beland, J. (1976). Nonadrenergic inhibitory nervous system in human airways. *Journal of Applied Physiology*, 41(5), pp. 764-771.
- Richardson, J.B. (1979). Nerve supply to the lungs. *American Review of Respiratory Disease*, 119(5), pp. 785-802.
- Richter, J.M., Schaefer, M. and Hill, K. (2014). Clemizole hydrochloride is a novel and potent inhibitor of transient receptor potential channel TRPC5. *Molecular Pharmacology*, 86, pp. 514-521.
- Riordan, J.R. (2008). CFTR function and prospects for therapy. *Annual Review of Biochemistry*, 77, pp. 701-726.
- Robinson, C., Hardy, C.C. and Holgate, S.T. (1985). Pulmonary synthesis, release, and metabolism of prostaglandins. *The Journal of Allergy and Clinical Immunology*, 76(2), pp. 265-271.
- Rock, J.R., Futtner, C.R. and Harfe, B.D. (2008). The transmembrane protein TMEM16A is required for normal development of the murine trachea. *Developmental Biology*, 321(1), pp. 141-149.
- Rock, J.R., O'Neal, W.K., Gabriel, S.E., Randell, S.H., Harfe, B.D., Boucher, R.C. and Grubb, B.R. (2009). Transmembrane protein 16A (TMEM16A) is a Ca^{2+} -regulated Cl^- secretory channel in mouse airways. *Journal of Biological Chemistry*, 284(22), pp. 14875–14880.
- Roffel, A.F., Elzinga, C.R. and Zaagsma, J. (1990). Muscarinic M3 receptors mediate contraction of human central and peripheral airway smooth muscle. *Pulmonary Pharmacology and Therapeutics*, 3(1), pp. 47-51.
- Roffel, A.F., Elzinga, C.R., Van Amsterdam, R.G., De Zeeuw, R.A. and Zaagsma, J. (1988). Muscarinic M2 receptors in bovine tracheal smooth muscle: discrepancies between binding and function. *European Journal of Pharmacology*, 153(1), pp. 73-82.
- Romanenko, V.G., Catalan, M.A., Brown, D.A., Putzier, I., Hartzell, H.C., Marmorstein, A.D., Gonzalez-Begne, M., Rock, J.R., Harfe, B.D. and Melvin, J.E. (2010). TMEM16A encodes the Ca^{2+} -activated Cl^- channel in mouse submandibular salivary gland acinar cells. *Journal of Biological Chemistry*, 285(17), pp. 12990-3001.
- Saleem, H., Tovey, S.C., Molinski, T.F. and Taylor, C.W. (2014). Interactions of antagonists with subtypes of inositol 1,4,5-trisphosphate (IP3) receptor. *Br J Pharmacol*, 171(13), pp. 3298-3312.

- Sanders, K. M., Zhu, M. H., Britton, F., Koh, S. D. and Ward, S. M. (2012). Anoctamins and gastrointestinal smooth muscle excitability. *Experimental physiology*, 97(2), pp. 200–206.
- Sato, K., Ozaki, H. and Karaki, H. (1988). Changes in cytosolic calcium level in vascular smooth muscle strip measured simultaneously with contraction using fluorescent calcium indicator fura 2. *The Journal of pharmacology and experimental therapeutics*, 246(1), pp. 294–300.
- Saunders, H. M. and Farley, J. M. (1991). Spontaneous transient outward currents and Ca(++)-activated K⁺ channels in swine tracheal smooth muscle cells. *The Journal of pharmacology and experimental therapeutics*, 257(3), pp. 1114–1120.
- Schreiber, R., Uliyakina, I., Kongsuphol, P., Warth, R., Mirza, M., Martins, J.R. and Kunzelmann, K. (2010). Expression and function of epithelial anoctamins. *Journal of Biological Chemistry*, 285(10), pp. 7838-7845.
- Schroeder, B.C., Cheng, T., Jan, Y.N. and Jan, L.Y. (2008). Expression cloning of TMEM16A as a calcium-activated chloride channel subunit. *Cell*, 134(6), pp. 1019-1029.
- Secondo, A., Bagetta, G. and Amantea, D. (2018). On the Role of Store-Operated Calcium Entry in Acute and Chronic Neurodegenerative Diseases. *Frontiers in molecular neuroscience*, 11, 87.
- Sel, S., Rost, B.R., Yildirim, A.O., Sel, B., Kalwa, H., Fehrenbach, H., Renz, H., Gudermann, T. and Dietrich, A. (2008). Loss of classical transient receptor potential 6 channel reduces allergic airway response. *Clinical and experimental allergy: journal of the British Society for Allergy and Clinical Immunology*, 38(9), pp.1548-1558.
- Seo, K., Rainer, P. P., Shalkey Hahn, V., Lee, D. I., Jo, S. H., Andersen, A., Liu, T., Xu, X., Willette, R. N., Lepore, J. J., Marino, J. P., Jr, Birnbaumer, L., Schnackenberg, C. G., and Kass, D. A. (2014). Combined TRPC3 and TRPC6 blockade by selective small-molecule or genetic deletion inhibits pathological cardiac hypertrophy. *Proceedings of the National Academy of Sciences of the United States of America*, 111(4), pp. 1551–1556.
- Seo, Y., Kim, J., Chang, J., Kim, S.S., Namkung, W. and Kim, I. (2018). Synthesis and biological evaluation of novel Ani9 derivatives as potent and selective ANO1 inhibitors. *Eur. J. Med. Chem.* 160, pp. 245–255.
- Seo, Y., Lee, H.K., Park, J., Jeon, D.K., Jo, S., Jo, M. and Namkung, W. (2016). Ani9, A Novel Potent Small-Molecule ANO1 Inhibitor with Negligible Effect on ANO2. *PLoS ONE*, 11, e0155771.

- Shen, S., Huang, Y. and Bourreau, J. P. (2000). Efficacy of muscarinic stimulation and mode of excitation-contraction coupling in bovine trachealis muscle. *Life sciences*, 67(15), pp. 1833–1846.
- Shimura, S., Andoh, Y., Haraguchi, M. and Shirato, K. (1996). Continuity of airway goblet cells and intraluminal mucus in the airways of patients with bronchial asthma. *The European respiratory journal*, 9(7), pp. 1395-1401.
- Shistik, E., Ivanina, T., Blumenstein, Y. and Dascal, N. (1998). Crucial role of N terminus in function of cardiac L-type Ca²⁺ channel and its modulation by protein kinase C. *The Journal of biological chemistry*, 273(28), pp. 17901–17909.
- Spinelli, A. M. and Trebak, M. (2016). Orai channel-mediated Ca²⁺ signals in vascular and airway smooth muscle. *American journal of physiology. Cell physiology*, 310(6), pp. C402–C413.
- Spinelli, A. M., González-Cobos, J. C., Zhang, X., Motiani, R. K., Rowan, S., Zhang, W., Garrett, J., Vincent, P. A., Matrougui, K., Singer, H. A. and Trebak, M. (2012). Airway smooth muscle STIM1 and Orai1 are upregulated in asthmatic mice and mediate PDGF-activated SOCE, CRAC currents, proliferation, and migration. *Pflugers Archiv : European journal of physiology*, 464(5), pp. 481–492.
- Struckmann, N., Schwering, S., Wiegand, S., Gschnell, A., Yamada, M., Kummer, W., Wess, J. and Haberberger, R.V. (2003). Role of muscarinic receptor subtypes in the constriction of peripheral airways: studies on receptor-deficient mice. *Molecular Pharmacology*, 64(6), pp. 1444-1451.
- Suganuma, N., Ito, S., Aso, H., Kondo, M., Sato, M., Sokabe, M. and Hasegawa, Y. (2012). STIM1 regulates platelet-derived growth factor-induced migration and Ca²⁺ influx in human airway smooth muscle cells. *PloS one*, 7(9), e45056.
- Sun, H., Tsunenari, T., Yau, K.W. and Nathans, J. (2002). The vitelliform macular dystrophy protein defines a new family of chloride channels. *Proceedings of the National Academy of Sciences of the United States of America*, 99(6), pp. 4008-4013.
- Suzuki, J., Fujii, T., Imao, T., Ishihara, K., Kuba, H. and Nagata, S. (2013). Calcium-dependent Phospholipid Scramblase Activity of TMEM16 Family Members. *Journal of Biological Chemistry*, 288(19), pp.13305-13316.
- Suzuki, M. (2006). The Drosophila tweety family : molecular candidates for large-conductance Ca²⁺-activated Cl⁻ channels. *Experimental Physiology*, 91(1), pp.141-147.
- Sweeney, M., McDaniel, S.S., Platoshyn, O., Zhang, S., Yu, Y., Lapp, B.R., Zhao, Y., Thistlewaite, P.A. and Yuan, J.X. (2002). Role of capacitative Ca²⁺ entry in

bronchial contraction and remodeling. *Journal of Applied Physiology*, 92(4), pp. 1594-1602.

Takahashi, T., Ward, J. K., Tadjkarimi, S., Yacoub, M. H., Barnes, P. J. and Belvisi, M. G. (1995). 5-Hydroxytryptamine facilitates cholinergic bronchoconstriction in human and guinea pig airways. *American journal of respiratory and critical care medicine*, 152(1), pp. 377–380.

Takeshima H. (1993). Primary structure and expression from cDNAs of the ryanodine receptor. *Annals of the New York Academy of Sciences*, 707, pp. 165–177.

Takeshima, H., Venturi, E. and Sitsapesan, R. (2015). New and notable ion-channels in the sarcoplasmic/endoplasmic reticulum: do they support the process of intracellular Ca^{2+} release?. *The Journal of physiology*, 593(15), pp. 3241–3251.

Tao, F.C., Tolloczko, B., Mitchell, C.A., Powell, W.S. and Martin, J.G. (2000). Inositol (1,4,5) trisphosphate metabolism and enhanced calcium mobilization in airway smooth muscle of hyperresponsive rats. *Am J Respir Cell Mol Biol*, (23), pp. 514– 520.

Tao, L., Huang, Y.U. and Bourreau, J. (2000). Control of the mode of excitation-contraction coupling by Ca^{2+} stores in bovine trachealis muscle. *Am J Physiol Lung Cell Mol Physiol*, 279(4), pp. L722-L732.

Taylor, S.M., Pare, P.D. and Schellenberg, R.R. (1984). Cholinergic and non-adrenergic mechanisms in human and guinea pig airways. *Journal of Applied Physiology*, 56(4), pp. 958-965.

Tazzeo, T., Zhang, Y., Keshavjee, S. and Janssen, L. J. (2008). Ryanodine receptors deplete internal Ca^{2+} store in human and bovine airway smooth muscle. *The European respiratory journal*, 32(2), pp. 275–284.

Ten Berge, R.E.J., Santing, R.E., Hamstra, J.J., Roffel, A.F. and Zaagsma, J. (1995). Dysfunction of muscarinic M_2 receptors after the early allergic reaction: Possible contribution to bronchial hyperresponsiveness in allergic guinea-pigs. *British Journal of Pharmacology*, 114(4), pp. 881-887.

Thakore, P. and Earley, S. (2022). STIM1 is the key that unlocks airway smooth muscle remodeling and hyperresponsiveness during asthma. *Cell calcium*, 104, 102589.

The top 10 causes of death. (2020, December 9). The Top 10 Causes of Death. <https://www.who.int/news-room/fact-sheets/detail/the-top-10-causes-of-death>

Thomas, A. P., Bird, G. S., Hajnóczky, G., Robb-Gaspers, L. D. and Putney, J. W., Jr (1996). Spatial and temporal aspects of cellular calcium signaling. *FASEB*

journal: official publication of the Federation of American Societies for Experimental Biology, 10(13), pp. 1505–1517.

Thomas, K.C., Sabnis, A.S., Johansen, M.E., Lanza, D.L., Moos, P.J., Yost, G.S. and Reilly, C.A. (2007). Transient receptor potential vanilloid 1 agonists cause endoplasmic reticulum stress and cell death in human lung cells. *Journal of Pharmacology and Experimental Therapeutics*, 321(3), pp. 830-838.

Tian, C., Du, L., Zhou, Y. and Li, M. (2016). Store-operated CRAC channel inhibitors: opportunities and challenges. *Future medicinal chemistry*, 8(7), pp. 817–832.

Tian, Y., Schreiber, R. and Kunzelmann, K. (2012). Anoctamins are a family of Ca²⁺-activated Cl⁻ channels. *Journal of Cell Science*, 125(21), pp. 4991-4998.

Tliba, O. and Panettieri, R. A. (2009). Noncontractile Functions of Airway Smooth Muscle Cells in Asthma. *Annual Review of Physiology*, 71, pp. 509-535.

Trebak M. (2012). STIM/Orai signalling complexes in vascular smooth muscle. *The Journal of physiology*, 590(17), pp. 4201–4208.

Trebak, M. and Putney, J. W., Jr (2017). ORAI Calcium Channels. *Physiology (Bethesda, Md.)*, 32(4), pp. 332–342.

Trebak, M., Zhang, W., Ruhle, B., Henkel, M. M., González-Cobos, J. C., Motiani, R. K., Stolwijk, J. A., Newton, R. L. and Zhang, X. (2013). What role for store-operated Ca²⁺ entry in muscle?. *Microcirculation (New York, N.Y. : 1994)*, 20(4), pp. 330–336.

Tsvilovskyy, V.V., Zholos, A.V., Aberle, T., Philipp, S.E., Dietrich, A., Zhu, M.X., Birnbaumer, L., Freichel, M. and Flockerzi, V. (2009). Deletion of TRPC4 and TRPC6 in mice impairs smooth muscle contraction and intestinal motility *in-vivo*. *Gastroenterology*, 137, pp. 1415-1424.

Tu, J., Inthavong, K. and Ahmadi, G. (2012). Computational Fluid and Particle Dynamics (CFPD): An Introduction. *Computational Fluid and Particle Dynamics in the Human Respiratory System*, pp. 1–18.

Vannier, B., Peyton, M., Boulay, G., Brown, D., Qin, N., Jiang, M., Zhu, X. and Birnbaumer, L. (1999). Mouse *trp2*, the homologue of the human *trpc2* pseudogene, encodes mTrp2, a store depletion-activated capacitative Ca²⁺ entry channel. *Proceedings of the National Academy of Sciences of the United States of America*, 96(5), pp. 2060-2064.

Vannier, C., Croxton, T.L., Farley, L.S. and Hirshman, C.A. (1995). Inhibition of dihydropyridine-sensitive calcium entry in hypoxic relaxation of airway smooth muscle. *Am J Physiol*, 68(2 Pt 1), pp. L201-L206.

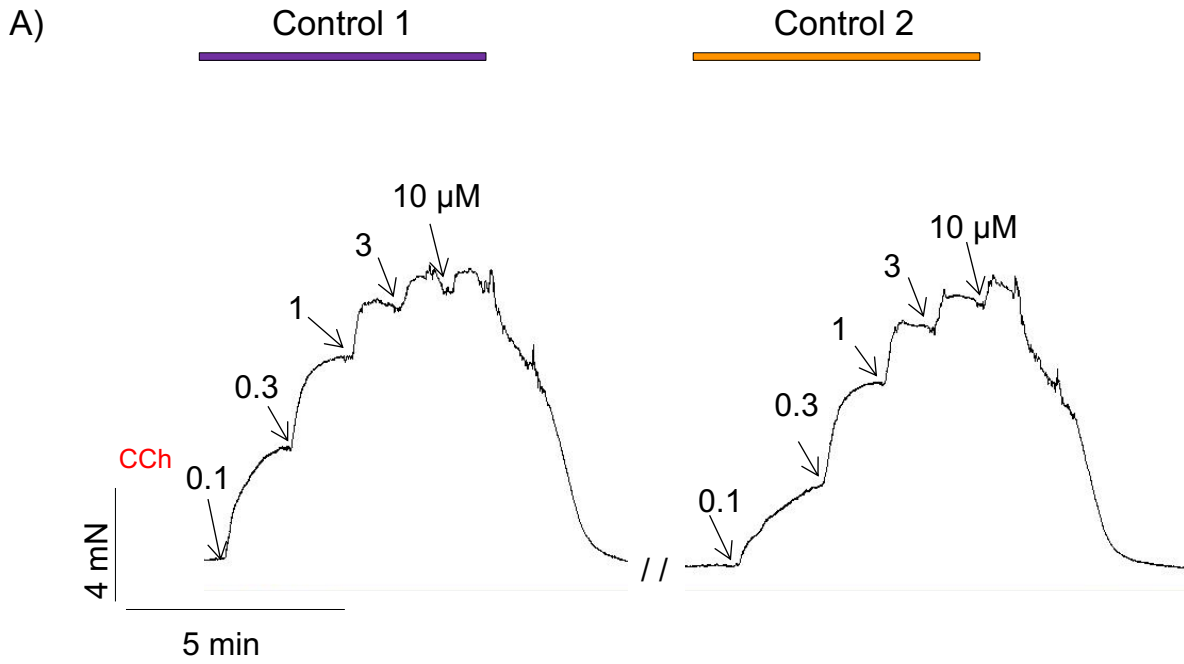
- Vennekens, R., Hoenderop, J.G., Prenen, J., Stuiver, M., Willems, P.H., Droogmans, G., Nilius, B. and Bindels, R.J. (2000). Permeation and gating properties of the novel epithelial Ca²⁺ channel. *Journal of Biological Chemistry*, 275(6), pp. 3963-3969.
- Vennekens, R., Owsianik, G. and Nilius, B. (2008). Vanilloid transient receptor potential cation channels: an overview. *Current pharmaceutical design*, 14(1), pp. 18-31.
- Vennekens, R., Voets, T., Bindels, R.J.M., Droogmans, G. and Nilius, B. (2002). Current understanding of mammalian TRP homologues. *Cell calcium*, 31(6), pp. 253-264.
- Verkman, A.S. and Galiotta, L.J. V. (2009). Chloride channels as drug targets. *Nature reviews. Drug discovery*, 8(2), pp.1 53–171.
- Wang, P., Zhao, W., Sun, J., Tao, T., Chen, X., Zheng, Y., Zhang, C.H., Chen, Z., Gao, Y.Q., She, F., Li, Y.Q., Wei, L.S., Lu, P., Chen, C.P., Zhou, J., Wang, D.Q., Chen, L., Shi, X.H., Deng, L., ZhuGe, R., Chen, H.Q. and Zhu, M.S. (2017). Inflammatory mediators mediate airway smooth muscle contraction through a G protein-coupled receptor-transmembrane protein 16A-voltage-dependent Ca²⁺ channel axis and contribute to bronchial hyperresponsiveness in asthma. *Journal of Allergy and Clinical Immunology*, 141(4), pp. 1259-1268.
- Wang, Y., Sun, J., Jin, R., Liang, Y., Liu, Y. Y., Yin, L. M., and Xu, Y. D. (2012). Influence of acupuncture on expression of T-type calcium channel protein in airway smooth muscle cell in airway remodeling rats with asthma. *Chinese acupuncture & moxibustion*, 32(6), pp. 534–540
- Wang, Y. X. and Zheng, Y. M. (2011). Molecular expression and functional role of canonical transient receptor potential channels in airway smooth muscle cells. *Advances in experimental medicine and biology*, 704, pp. 731–747.
- Wang, Y.X. and Kotlikoff, M.I. (1997). Inactivation of calcium-activated chloride channels in smooth muscle by calcium/calmodulin-dependent protein kinase. *Proceedings of the National Academy of Sciences of the United States of America*, 94(26), pp. 14918-14923
- Wang, Y.X., Zheng, Y.M., Mei, Q.B., Wang, Q.S., Collier, M.L., Fleischer, S., Xin, H.B. and Kotlikoff, M.I. (2004). FKBP12 . 6 and cADPR regulation of Ca²⁺ release in smooth muscle cells. *Am J Physiol Cell Physiol*, 286, pp. C538–C546.
- Ward, J.K., Barnes, P.J., Springall, D.R., Abelli, L., Tad-jkarimi, S., Yacoub, M.H., Polak, J.M. and Belvisi, M.G. (1995). Distribution of human i-NANC bronchodilator and nitric oxide-immunoreactive nerves. *American Journal of Respiratory Cell and Molecule Biology*, 13, pp. 175-184.

- Watanabe, N., Horie, S., Michael, G.J., Keir, S., Spina, D., Page, C.P. and Priestley, J.V. (2006). Immunohistochemical co-localization of transient receptor potential vanilloid (TRPV)1 and sensory neuropeptides in the guinea-pig respiratory system. *Neuroscience*, 141(3), pp. 1533-1543.
- Watanabe, N., Horie, S., Spina, D., Michael, G.J., Page, C.P. and Priestley, J.V. (2008). Immunohistochemical localization of transient receptor potential vanilloid subtype 1 in the trachea of ovalbumin-sensitized Guinea pigs. *International Archives of Allergy and Immunology*, 2008, 146(1), pp. 28-32.
- Webb, R.C. (2003). Smooth Muscle Contraction and Relaxation. *Advances in Physiology Education*, 27(4), pp. 201-206.
- Wei, M., Zhou, Y., Sun, A., Ma, G., He, L., Zhou, L., Zhang, S., Liu, J., Zhang, S. L., Gill, D. L. and Wang, Y. (2016). Molecular mechanisms underlying inhibition of STIM1-Orai1-mediated Ca^{2+} entry induced by 2-aminoethoxydiphenyl borate. *Pflugers Archiv : European journal of physiology*, 468(11-12), pp. 2061–2074.
- White, E.S. (2015). Lung Extracellular Matrix and Fibroblast Function. *Annual American Thoracic Society*, 12(1), pp. S30-S33.
- White, M.V. (1995). Muscarinic receptors in human airways. *Journal of Allergy and Clinical Immunology*, 95(5), pp. 1065-1068.
- White, T.A., Xue, A., Chini, E.N., Thompson, M., Sieck, G.C. and Wylam, M.E (2006). Role of transient receptor potential C3 in TNF- α -enhanced calcium influx in human airway myocytes. *American Journal of Respiratory Cell and Molecule Biology*, 35(2), pp. 243-251.
- Widdicombe, J.G. and Wells, U.M., 1994. Vagal reflexes. In: Raeburn, D., Gymbiec, M.A. (Eds.), *Airway Smooth Muscle: Structure, Innervation and Neurotransmission*. Birkhäuser Verlag, Basel, pp. 279–307.
- Woolcock, A. J., Anderson, S. D., Peat, J. K., Du Toit, J. I., Zhang, Y. G., Smith, C. M., and Salome, C. M. (1991). Characteristics of bronchial hyperresponsiveness in chronic obstructive pulmonary disease and in asthma. *The American review of respiratory disease*, 143(6), pp. 1438–1443.
- Wray, S., Prendergast, C. and Arrowsmith, S. (2021). Calcium-Activated Chloride Channels in Myometrial and Vascular Smooth Muscle. *Frontiers in physiology*, 12, 751008.
- Xiao, J.H., Zheng, Y.M., Liao, B. and Wang, Y.X. (2010). Functional role of canonical transient receptor potential 1 and canonical transient receptor potential 3 in normal and asthmatic airway smooth muscle cells. *American Journal of Respiratory Cell and Molecule Biology*, 43(1), pp. 17-25.

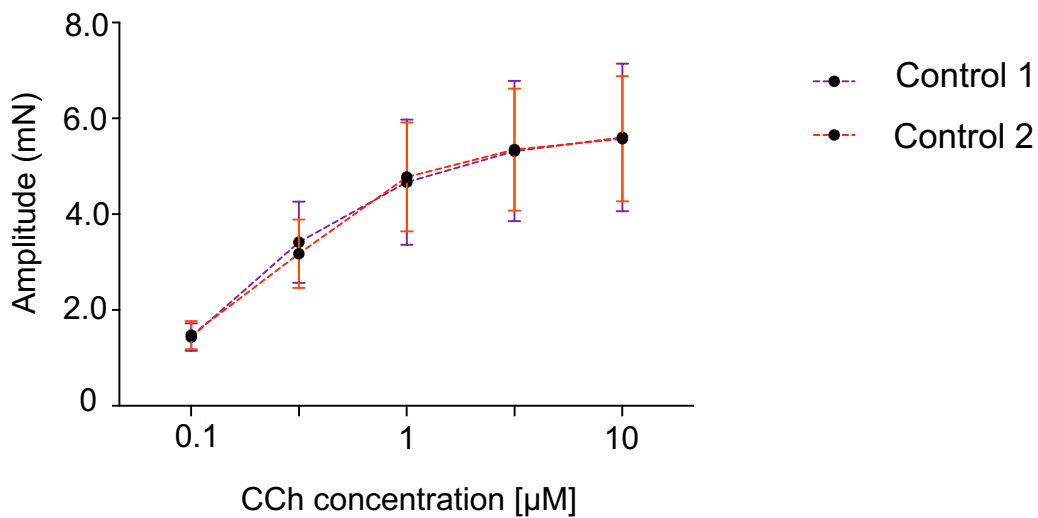
- Xu, B.M., Zhang, J.H., Wang, J.L. and Xiao, J.H. (2018). TRPC3 overexpression and intervention in airway smooth muscle of ovalbumin-induced hyperresponsiveness and remodeling. *Cell biology international*, 42(8), pp. 1021-1029.
- Yamauchi, K. and Ogasawara, M. (2019). The Role of Histamine in the Pathophysiology of Asthma and the Clinical Efficacy of Antihistamines in Asthma Therapy. *International journal of molecular sciences*, 20(7), 1733.
- Yang, C.M., Chou, S.P. and Sung, T.C. (1991). Muscarinic receptor subtypes coupled to generation of different second messengers in isolated tracheal smooth muscle cells. *British Journal of Pharmacology*, 104(3), pp. 613-618.
- Yang, X.R., Lin, M.J., McIntosh, L.S. and Sham, J.S. (2006). Functional expression of transient receptor potential melastatin- and vanilloid-related channels in pulmonary arterial and aortic smooth muscle. *American Journal of Physiology-Lung Cell and Molecule Physiology*, 290(6), pp. L1267-L1276.
- Yang, Y.D., Cho, H., Koo, J.Y., Tak, M.H., Cho, Y., Shim, W.S., Park, S.P., Lee, J., Lee, B., Kim, B.M., Raouf, R., Shin, Y.K. and Oh, U. (2008). TMEM16A confers receptor-activated calcium-dependent chloride conductance. *Nature*, 455(7217), pp. 1210-1215.
- Zaagsma, J., van Amsterdam R.G., Brouwer, F., van der Heijden, P.J., van der Schaar, M.W., Verwey, W.M. and Veenstra, V. (1987). Adrenergic control of airway function. *American Review of Respiratory Disease*, 136(4 Pt 2), pp. S45-S50.
- Zaidman, N. A., Panoskaltis-Mortari, A. and O'Grady, S. M. (2017). Large-conductance Ca^{2+} -activated K^{+} channel activation by apical P2Y receptor agonists requires hydrocortisone in differentiated airway epithelium. *The Journal of physiology*, 595(14), pp. 4631–4645.
- Zhang, C.H., Li, Y., Zhao, W., Lifshitz, L.M., Li, H., Harfe, B.D., Zhu, M.S. and ZhuGe, R. (2013). The transmembrane protein 16A Ca^{2+} -activated Cl^{-} channel in airway smooth muscle contributes to airway hyperresponsiveness. *American Journal of Respiratory and Critical Care Medicine*, 187(4), pp. 374-381.
- Zhang, S.L., Yu, Y., Roos, J., Kozak, J.A., Deerinck, T.J., Ellisman, M.H., Stauderman, K.A. and Cahalan, M.D. (2005). STIM1 is a Ca^{2+} sensor that activates CRAC channels and migrates from the Ca^{2+} store to the plasma membrane. *Nature*, 437(7060), pp. 902-905.
- Zhang, T., Luo, X., Sai, W., Yu, M., Li, W., Ma, Y., Chen, W., Zhai, K., Qin, G., Guo, D., Zheng, Y., Wang, Y., Shen, J., Ji, G. and Liu, Q. (2014). Non-Selective Cation Channels Mediate Chloroquine- Induced Relaxation in Precontracted Mouse Airway Smooth Muscle. *PLoS One*, 9(7), pp. 7-12.

- Zhao, J.F., Ching, L.C., Kou, Y.R., Lin, S.J., Wei, J., Shyue, S.K. and Lee, T.S. (2013). Activation of TRPV1 prevents OxLDL-induced lipid accumulation and TNF-alpha-induced inflammation in macrophages: role of liver X receptor alpha. *Mediators of inflammation*, p.925171.
- Zhao, L., Sullivan, M.N., Chase, M., Gonzales, A.L. and Earley, S. (2014). Calcineurin/nuclear factor of activated T cells-coupled vanilloid transient receptor potential channel 4 Ca^{2+} sparklets stimulate airway smooth muscle cell proliferation. *American Journal of Respiratory Cell and Molecular Biology*, 50(6), pp. 1064–1075.
- Zheng, H., Drumm, B. T., Earley, S., Sung, T. S., Koh, S. D. and Sanders, K. M. (2018). SOCE mediated by STIM and Orai is essential for pacemaker activity in the interstitial cells of Cajal in the gastrointestinal tract. *Science signaling*, 11(534), eaaq0918.
- Zhu, Z., Yu, T., Liu, H., Jin, J. and He, J. (2018). SOCE induced calcium overload regulates autophagy in acute pancreatitis via calcineurin activation. *Cell death and disease*, 9(2), 50.
- Zhuge, R., Bao, R., Fogarty, K. E. and Lifshitz, L. M. (2010). Ca^{2+} sparks act as potent regulators of excitation-contraction coupling in airway smooth muscle. *The Journal of biological chemistry*, 285(3), pp. 2203–2210.
- ZhuGe, R., Sims, S.M., Tuft, R.A., Fogarty, K.E. and Walsh, J.V. (1998). Ca^{2+} sparks activate K^+ and Cl^- channels, resulting in spontaneous transient currents in guinea-pig tracheal myocytes. *The Journal of Physiology*, 513(3), pp. 711-718.

8. Appendix

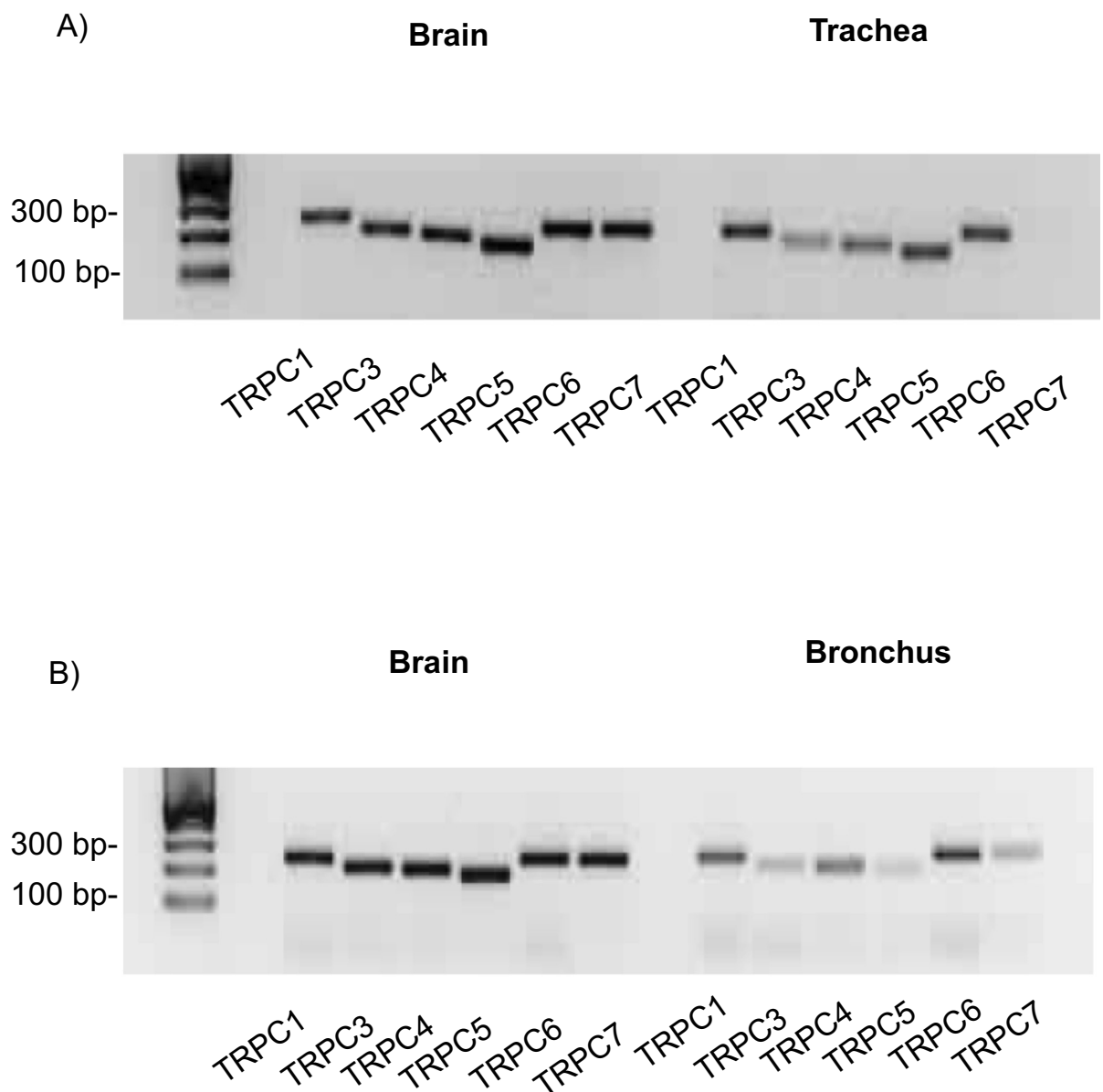


B)



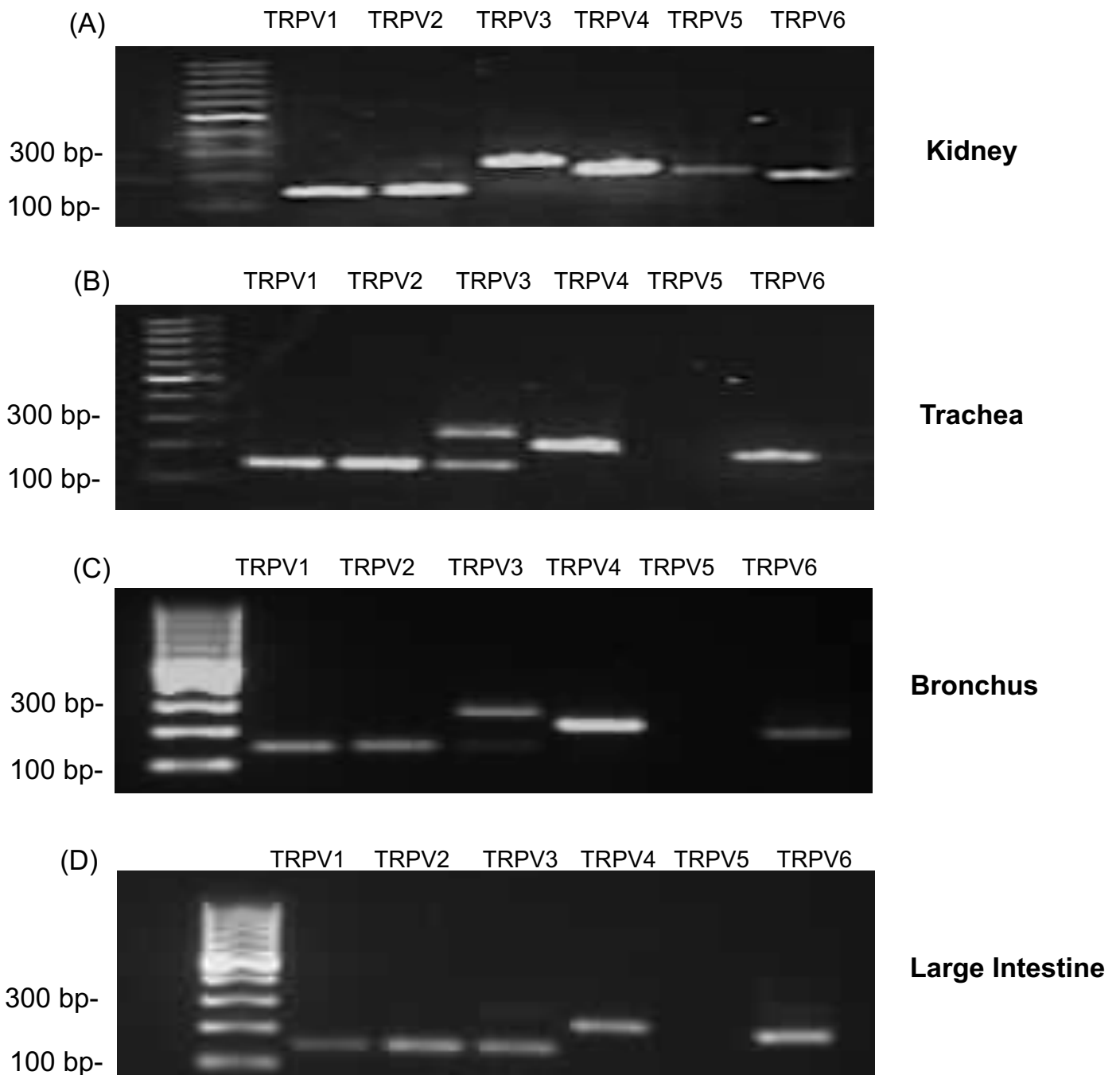
Appendix A :- Reproducible application of CCh concentration 0.1- 10 μ M.

Panel A shows isometric tension recording of two consecutive “initial component” or 2 minutes application of each CCh concentration ranging from 0.1 – 10 μ M. Panel B shows summary line graph of both controls. n=6; N=6.



Appendix B:- Transcriptional Expression profile of TRPC1,C3-7 in murine airway

Agarose gel images showing the transcriptional expression of TRPC1, C3-C7 subtypes in cDNA synthesized from total RNA extracted from murine (A) trachea (B) bronchus tissue with brain as positive control. Amplicons were separated by electrophoresis on a 2% agarose gel.



Appendix C :- Transcriptional Expression profile of TRPV1-V6 in murine airway

Agarose gel images showing the transcriptional expression of TRPV1 – V6 subtypes in cDNA synthesized from total RNA extracted from murine (A) kidney tissue (positive control), (B) trachea tissue (C) bronchus tissue (D) large intestine tissue. Amplicons were separated by electrophoresis on a 2% agarose gel.